The Impact of Size and Location of Pool Fires on Compartment Fire Behaviour

---

A thesis
submitted in partial fulfilment
of the requirements for the Degree
of
Doctor of Philosophy in Fire Engineering
at the
University of Canterbury,
Christchurch,
New Zealand.

---

by
Anthony Richard Parkes
2009

TABLE OF CONTENTS

Table of Contents

INDEX OF FIGURES

Index of Figures

Index of Figures

INDEX OF TABLES

Index of Tables

NOMENCLATURE

A	=	Area [m²]
D	=	Diameter [m]
g	=	acceleration of gravity, [kg/s² m]
Gr	=	Grashof number, [--]
H	=	Height of the compartment [m]
Δh_c	=	Heat of Combustion [MJ/kg]
Δh_g	=	Heat of Gasification [J/kg]
k	=	Absorption-extinction coefficient of the flame [m^{-1}]
$\dot{Q}$	=	Heat Release Rate [kW]
L	=	Characteristic Length, [m]
m	=	Mass of species [kg]
$\dot{m}$	=	Mass flow rate [kg/s]
$\dot{m}''_\infty$	=	Mass loss rate for an infinite diameter pool [kg/m^2 s]
M	=	Molecular weight [kg/kmol]
n	=	Number of moles [--]
Nu	=	Nusselt Number, [--]
P	=	Pressure [Pa]
Pr	=	Prandtl Number, [--]
r	=	Stoichiometric air/mass ratio [--]
R	=	Ideal gas constant [J/(K mol)]
Ra	=	Rayleigh Number, [--]
t	=	Time, [s]
T	=	Temperature [K]
T_f	=	Film Temperature, [K]
V	=	Volume flow rate [m/s]
X	=	Mole fraction [--]

Nomenclature

Greek Symbols

χ	=	Combustion efficiency [--]
ϕ	=	Equivalence Ratio [--]
σ	=	Stefan-Boltzmann constant (W m^{-2} K^{-4})
β	=	Mean-beam-length corrector [--]
ε	=	Gas emissivity [--]

Superscripts

i	=	Refer to concentrations prior to experiment
o	=	Refer to incoming flow at ambient

Subscripts

a	=	incoming air
f	=	fuel
i	=	species
o	=	opening
p	=	pool
v	=	vent opening

Abbreviations

CFD	=	Computational Fluid Dynamics
HRR	=	Heat Release Rate
ER	=	Equivalence Ratio
GER	=	Global Equivalence Ratio
MLR	=	Mass Loss Rate
ODC	=	Oxygen Depletion Calorimetry
TC	=	Thermocouple
TCP	=	Thermocouple Plate
TTC	=	Time Temperature Curve
UDL	=	Universal Data Logging system developed at the University of Canterbury
UOC	=	University of Canterbury

Specific Terms

Full = Fully open geometry 2.4m wide x 1.2m high (Unrestricted)

Soffit = 2.4m wide x 1.0m high (0.2m downstand), ($A_v\sqrt{H_v} = 2.4$).

Door = 0.4 m wide by 1.0 m high, ($A_v\sqrt{H_v} = 0.4$).

Window = 0.8 m wide by 0.6 m high (0.2m Sill), ($A_v\sqrt{H_v} = 0.372$).

Small Window = 0.4 m wide by 0.6 m high (0.2m Sill), ($A_v\sqrt{H_v} = 0.186$).

x2 pan = a pan having the equivalent area to that of two 200mm square pans. This pan has dimensions of 283mm x 283mm square.

x3 pan = a pan having the equivalent area to that of three 200mm square pans. This pan has dimensions of 346mm x 346mm square.

Front = The pan in the front location position was located 3000mm from the rear compartment wall.

Centre = The pan in the centre location position was located 1800mm from the rear compartment wall.

Rear = The pan in the rear position is located 600mm from the rear compartment wall.

Nomenclature

ABSTRACT

An understanding of compartment fire behaviour is important for fire protection engineers. For design purposes, whether to use a prescriptive code or performance based design, life safety and property protection issues are required to be assessed. The use of design fires in computer modelling is the general method to determine fire safety. However these computer models are generally limited to the input of one design fire, with consideration of the complex interaction between fuel packages and the compartment environment being simplified. Of particular interest is the Heat Release Rate, HRR, as this is the commonly prescribed design parameter for fire modelling. If the HRR is not accurate then it can be subsequently argued that the design scenario may be flawed. Therefore the selection of the most appropriate fire design scenario is critical, and an increased level of understanding of compartment behaviour is an invaluable aid to fire engineering assumptions.

This thesis details an experimental study to enhance the understanding of the impact and interaction that the size and location of pool fires within an enclosure have upon the compartment fire behaviour. Thirty four experiments were conducted in a reduced scale compartment (½ height) with dimensions of 3.6m long by 2.4m wide by 1.2m high using five typical ventilation geometries (fully open, soffit, door, window and small window). Heptane pool fires were used, located in permutations of three evenly distributed locations within the compartment (rear, centre and front) as well as larger equivalent area pans located only in the centre. This thesis describes the experimental development, setup and results of the experimental study. To assist in the classification of compartment fire behaviour during the experiments, a 'phi' meter was developed to measure the time dependent equivalence ratio. The phi meter was developed and configured to measure O_2, CO_2 and CO. The background development, calibration, and experimental results are reported. A review of compartment fire modelling using Fire Dynamics Simulator, has also been completed and the results discussed.

Abstract

The results of this experimental study were found to have significant implications for Fire Safety Engineering in that the size of the fire is not as significant as the location of the fire. The effect of a fire near the vent opening was found to have a significant impact on compartment fire behaviour with the vent located fuel source increasing the total compartment heat release rate by a factor of 1.7 to that of a centrally placed pool fire of the same total fuel area. The assumption that a fire located in the centre of the room provides for the highest heat release rate is not valid for post-flashover compartment fires. The phi meter was found to provide good agreement with the equivalence ratio calculated from total compartment mass loss rates, and the results of FDS modelling indicate that the use of the model in its current form can not be applied to complex pool fire geometries.

ACKNOWLEDGEMENTS

"I have no special gifts. I am just passionately curious"

Albert Einstein (1879-1955)

First, and foremost, I would like to thank my wife Sonja, and my beautiful children Oscar & Eloise for their continuous support during my extended study. It has not been easy and I could not have done it without your love and encouragement.

I would like to acknowledge the financial support provided by the New Zealand Fire Service Commission and the Foundation of Research Science and Technology (FRST). Fire research undertaken at the University of Canterbury is providing a valuable contribution globally and the funding for this work is greatly appreciated.

To Charley Fleischmann, I thank you for your patience, support, and belief in me. I also wish to thank Andy Buchanan and Michael Spearpoint for their discussion and encouragement during my experimental study.

Thanks to all technicians involved during the project. A special mention goes to Grant Dunlop whose amazing work and skill was invaluable.

Finally, thanks to family and friends for their support.

Acknowledgements

Chapter 1: Introduction

1.1 Impetus for Research

The practicing fire engineer in today's performance based environment evaluates the life safety risk to occupants with respect to the fire conditions developing within a room. They may also evaluate any potential impact upon a building(s) structure whether this be to their clients own property or to any other adjacent property. The use of deterministic fire modelling is often employed to evaluate the fire conditions in conjunction with the fire protection features provided in a building. The results from these fire models can then be used to evaluate the time required for occupants evacuate by the use of egress models. Although these models do have limitations it is not uncommon to see them being misused.

The fire resistance performance requirements of the building or individual elements can also be designed. Generally fire resistance is quantified by subjecting a specimen of the element to a standard fire resistance test [1,2] in which the test specimen is exposed to a prescribed standard fire curve. The effective time of resistance is taken at that point when the element fails stability, integrity or insulation criteria. Computer models may also be use to evaluate the performance requirements for fire resisting structures and elements such as walls, floor, beams and columns. Therefore it is with these life safety and property considerations in mind that the use of experimental data to verify the accuracy of computer models is important.

As with all engineering designs, the use of computer models should be cautioned as the models used are only as accurate as their limitations and the input data provided by the design engineer. With the advancement of computer resources and computational fire modelling, current computer models are expected to be able to provide greater accuracy with which a fire scenario can be simulated. However, this increase in computational analysis also requires an increased level of understanding of the requirements of the

input parameters, the subsequent the evaluation of the modelling results, and our understanding of compartment fire behaviour.

There are two types of deterministic fire models, zone models, and field models (Computational Fluid Dynamic, CFD). Zone models divide an enclosure into two distinct regions and assume a uniform hot upper zone and a uniform cold lower zone. Each zone is solved for the conservation equations of mass, energy and species, and empirical correlations are used to describe characteristics such as entrainment into the fire plume. The advantages of zone models are that they are easy to run, require little computational time, and are relatively inexpensive. However the disadvantages relate to the complexity of the scenarios able to be analysed due to the limitations of the models empirical correlations. The use of the model outside of these limitations can result in results that are inaccurate, whether this is conservative or non-conservative.

Field models on the other hand divide the volume to be simulated into a three-dimensional grid of cells and solve the conservation mass momentum, energy and species in each cell. They consist generally of a set of three-dimensional, time dependant, non-linear partial differential equations, referred to as the Navier Stokes equations. The advantages of field models are that they rely minimally on empirical correlations, so are capable of simulating scenarios without the limitations associated with empirical correlations used in the zone model. The main disadvantage is that they need significant computer resources.

Of these models, the zone model is most commonly used by the practising engineer. This is predominantly due to their low cost, availability and ease of use. Computational Fluid Dynamic (CFD) models are less commonly used due to their cost and time consuming use, yet there is a general trend leading towards their use. Due to the computational complexity over that of zone models the results from CFD models can provide significant advantages, although the model will still be bound by the user input and general scenarios as mentioned above.

All computer models rely on the user to input an expected fire scenario. By default this scenario is generally located in the centre of the input room geometry, and is based upon a time dependent fire growth rate which may be selected based upon design guides,

literature, or engineering judgement. Typically the fire growth rate is based upon idealised t^2 fire growth rates and the output of this analysis is regarded as a '*credible design fire scenario*'.

The factors that influence the development of a fire in an enclosure are: fuel type and size, and enclosure geometry including ventilation. The location of the fire can also have a distinct effect on the fire development, and in particular this specifically relates to wall and corner fires. Typically if a fuel package is located away from the bounding walls, air is able to be entrained into the plume from all directions. Generally, in fire engineering design, corner and wall fire scenarios are neglected and other locations within the room are not expected to result in significantly different behaviour to that of the centrally located fire. Hence location of the fire source is not deemed important and is not accounted for. Therefore as noted, credible design fire scenarios may be developed considering a fire located in the centre of an enclosure.

Many computer models are also limited to evaluating single prescribed burning items, and the behaviour of a multi-packaged fuel source within a compartment cannot be accurately determined This is because objects will burn at different rates due to interaction between objects and the surrounding environment. As the accurate prediction of fire behaviour in buildings is not possible unless the heat release rate of the fire is known, research into the behaviour of multi-packaged fuel sources is required. The heat release rate of a design fire is the key characteristic that describes quantitatively how "big" a fire is and in fire engineering design the heat release rate is considered the most important variable in evaluating the fire hazard. Therefore research to improve the understanding of these compartment fire variables can be invaluable.

The University of Canterbury Fire Engineering program has conducted research to investigate the reduction of fire deaths within New Zealand residential buildings. As part of the residential fire safety research program, the understanding of compartment fires has been investigated. This research study also proposes to advance the understanding of compartment fires through the continuation of research by the Author which started in 1996 [3,4]. This previous experimental research was conducted to determine the effects that ventilation (in particular low-ventilation) had on compartment fires. The results found that the ventilation characteristics and radiation feedback had a

significant impact on the mass loss rate of burning fuels in a compartment. The study also found that although compartment fires are generally defined by two zones (an upper hot layer and a lower cold layer), represented by an inflow (of ambient air) and outflow (of combustion products), this may not always be the case. Low ventilation can lead to a compartment displaying one-zone properties as is common in post flashover fires.

1.2 Aim of Research

Results from previous research and other studies have shown a need for further investigation into the size of a fire (including multiple fuel packages) and the location of a fire within a compartment. The accuracy with which we are able to model and predict burning compartment items (such as furniture) requires an understanding of not only the individual items but also how individual burning items interact with each other.

1. The principle aim of this research is to investigate and enhance our understanding of the impact that size and location of pool fires within an enclosure have upon the compartment fire behaviour. This study attempts to investigate the interaction of these characteristics to improve the understanding of the severity and behaviour of burning items in a compartment. Although information for predicting the heat release rate for single items in a building is available, the behaviour of fires with multiple burning items is a more complex problem and such information is not readily available. This study investigates the effect of single and multiple fires located throughout a compartment. The assumption that a credible design fire scenario can consist of one centrally located non-wall bounded fire will be investigated by review of the interaction of multiple fires in relation to a centrally located fire of equivalent size. The issue of fire spread to other fuel packages is not investigated.

2. In conjunction with this study it is also aimed to develop and calibrate a new experimental apparatus as an aid to classifying the compartment behaviour of the pool fire experiments undertaken. The aim of the apparatus is to successfully

measure the time dependent equivalence ratio which is a parameter that describes the ventilation conditions during a compartment fire.

3. This research also aims to simulate the fire experiments with a computational fluid dynamic model, FDS, and compare the computational results with the experimental measurements to determine accuracy of the pool fire and radiative predictions within the model.

1.3 Method of Research

The method of research undertaken is experimental rather than an analytical. This experimental research investigates compartment fires in detail and the effect that the ventilation characteristics, size and location of fires within an enclosure have upon the mass loss rate and rate of heat release.

The experimental fire enclosure used in this study has dimensions more appropriate to that found in typical building spaces in which the bounding walls are located at a greater distance from the fire than the ceiling e.g. the room is typically wider than its height. Subsequently, in this study the fire experiments were conducted in a reduced scale ISO test room compartment (½ height) with dimensions of 3.6m long by 2.4m wide by 1.2m high using five typical ventilation geometries (fully open, soffit, door, window and small window), and heptane pool fires located in three evenly distributed locations within the compartment (rear, centre and front).

1.4 Thesis structure

Chapter two provides a general background behind compartment pool fire behaviour. The general development of compartment fires through ignition/incipient, growth, pre-flashover, flashover, fully developed, and decay phases are discussed in the context of this experimental study and fire engineering designs. Mass loss rate, heat release rate,

and equivalence ratio terms are also discussed followed by a summary of pool fire characteristics both free-burning and compartment enhanced behaviour. Previous experimental studies of compartment fire behaviour associated with the theme of this research study are also discussed.

Chapter three details the experimental method and apparatus setup used in this experimental study. Details of the construction of the experimental enclosure, including the location of instrumentation is provided as well as data reduction methods. The chapter begins with a schematic exploded sketch of the completed compartment showing the installed compartment instrumentation and photographs showing the left and right hand sides of the compartment. This is shown as prelude and visual aid to the detailed description of the construction and instrumentation of the experimental apparatus in the remainder of the chapter. The detailed description of the size and construction of the compartment is then provided along with the ventilation geometries used in the experiments, the location of windows and video cameras, and details on the pool fire and delivery system used. Instrumentation description and location follow and details the acquisition systems used, temperature, heat flux, velocity, mass loss, heat release rate and combustion species measurements. Finally the experimental matrix is tabled and the operation procedure noted.

Chapter four is presented in the form of a paper submitted to a peer reviewed Journal describing the development, calibration, and experimental use of an enhanced Equivalence Ratio apparatus, 'Phi Meter'. The phi meter was developed to measure the time dependent equivalence ratio from enclosure fire experiments undertaken in conjunction with this research study as an aid to the classification of compartment fire behaviour. This enhanced phi meter was developed and configured on the principle of measuring O_2, CO_2 and CO combustion species and details of the formulation and derivation of the equivalence ratio equations is presented. A description of the apparatus and its calibration with propane and methane is detailed. The use of the phi meter in practical fire situations is also discussed along with practical considerations for continued use and future development.

Chapter five details the results from an experimental series using a single 200mm square heptane pan in three independent locations within the experimental compartment and five ventilation geometries. This chapter is presented in the form of the paper published and presented at the Eighth International Symposium, International Association for Fire Safety Science, Beijing China titled "*The Impact of Location and Ventilation on Pool Fire in a Compartment*". The paper has been modified from the original paper to include results not able to be included at the time of submission. It provides an introduction and brief background on pool fires and a general overview of the experimental apparatus and instrumentation. The results are presented, including heat release rate, heat flux, compartment temperatures and vent velocities along with a discussion of visual observations.

Chapter six details the results from the experimental series using multiple 200mm square heptane pans in various permutations of three pan locations (rear, centre and front) within the experimental compartment. This series of experiments used the five different ventilation geometries of fully open, soffit, door, window, and small window. The chapter is presented in the form of the paper submitted to Fire & Materials. The paper is divided into two sections detailing the experimental results from:

- Double multiple pan experiments in which two 200mm square pans are located in combination within the enclosure. Results from the x2 pan e.g. a pan having the equivalent area to that of two 200mm square pans (283mm square) located in the centre of the room are also detailed.
- Triple multiple pan experiments in which three 200mm square pans are located in simultaneously in the enclosure. Results from the x3 pan e.g. a pan having the equivalent area to that of three 200mm square pans (346mm square) located in the centre of the room are also detailed.

The paper provides an introduction and brief background on pool fires and a general overview of the experimental apparatus and instrumentation. Results of measurements recorded during the experiments are presented, including heat release rate, heat flux, compartment temperatures, and vent velocities.

Chapter seven provides further detail of the experimental results from both the single pan and multiple pan experiments to help quantify the observed and recorded compartment behaviour. As the rate of burning in the enclosure fire is assume proportional to the ventilation factor, the observed and measured results of Flame Behaviour and Vent Flows, Heat Release Rate, Mass Loss Rate, Equivalence Ratio, Combustion Efficiency, Compartment Temperatures, and Heat Flux are analysed in terms of the ventilation geometry.

Chapter eight provides some background information and evaluation work completed using Fire Dynamics Simulator, FDS, to model the compartment fire experiments presented in this study.

Chapter nine summarises and concludes the experimental compartment fire study. The conclusions and recommendations from the aim of the research are presented and divided into three categories; Equivalence Ratio 'Phi' Meter, Experimental Compartment Fire Behaviour, and Computer Modelling.

It is noted that the thesis includes three chapters; Chapter 4, Chapter 5 and Chapter 6; that have been published in part or submitted to peer-reviewed journals and/or peer-reviewed conference proceedings. As these chapters are based upon the published or submitted papers, it is acknowledged that several references appear in two or more of the papers and that some of the content within the chapters may be shared with the other chapters. It is also noted that these chapters may contain additional work not presented in the papers. The papers previously published or submitted are noted at the beginning or each chapter. References for each chapter are noted at the end of each section, and each section is individually number based upon the chapter numbering.

Appendix A details the compartment instrumentation list and Appendix B details the visual observations for each of the 34 compartment experiments completed. Critical observations and details of the flame/combustion structure both internal and externally to the experimental enclosure is noted based upon the ventilation geometry in the

following order; fully open, soffit, door, window and small window, and each of the pan locations series; single pan, double pan, triple pan, and equivalent pan locations and not based on the chronological order in which the experiments were completed.

1.5 References

1 ISO 9705:1993, Fire Tests – Full Scale Room Test for Surface Products, International Organisation for Standardization, 1993.

2 ASTM "Standard Test Methods ofr Fire Tests of Building Constrcution and Meaterials". E119-88. American Society for Testing and Materials, 1988.

3 Parkes, A R., "Under-Ventilated Compartment Fires – A Precursor to Smoke Explosions" Fire Engineering Research Report 96/5, December 1996.

4 Fleischmann, C. M., and Parkes, A. R., "Effects of Ventialtion on the Compartment Enhanced Mass Loss Rate" Proceedings of the Fifth International Symposium on Fire Safety Science, pp. 415-426, 1997.

Chapter 2: Background

This chapter provides a general background behind compartment pool fire behaviour. General classifications for the development of compartment fires from an ignition/incipient phase to the final decay phase are discussed. Considerations in the context of this experimental study and with fire engineering design are also noted and the term *flashover* is defined for future reference. The mass loss rate and heat release rate terms and their impact on fire severity are discussed, along with a brief theoretical background. This is followed by an evaluation of stoichiometric combustion and the use of the term equivalence ratio for classification of compartment fire behaviour. A summary of pool fire characteristics both free-burning and compartment affected behaviour is then presented with a final summary discussing previous experimental studies of compartment fire behaviour associated with the theme of this research study.

2.1 Enclosure Fires

There is a considerable amount of data available in the fire engineering community regarding compartment fires and the behaviour of compartment fires with both cellulosic and thermoplastic materials. The classical development of a compartment fire exhibits the following phases;

- Ignition/Incipient
- Growth/Pre-flashover
- Flashover
- Fully Developed/Post-flashover
- Decay

2.1.1 Ignition and Incipient Phase

The ignition/incipient phase of a fire is considered an exothermic reaction which causes an increase in temperature, followed by either smouldering or flaming combustion. In the context of this experimental study the ignition stage occurs as a result of piloted spark ignition which causes flaming ignition of the liquid pool fire.

2.1.2 Growth and Pre-Flashover Phase

As the fire grows, it produces combustion products and releases energy. These early stages are difficult to predict, as there is generally sufficient air available for combustion, and the fire will burn at a rate controlled by its own properties. Depending upon these parameters the growth rate of the fire can be extremely variable. It is during the early stages of this growth phase when the fire is at its most easy to control or extinguish. For the growth to continue, there are a number of dependent factors including, fuel type, fuel size, fuel location, and the ventilation into the enclosure.

For fire engineering design purposes, the growth phase of a fire is usually generalised as a t^2 fire, which assumes that the energy release rate increases as the square of the time. The t^2 fire growth rates are divided to provide four categories of growth time, slow, medium, fast and ultra fast; with each factor representing the time function to attain a heat output of 1.055 MW.

As the fire continues to grow, the fire plume will entrain air and an upper hot smoke layer will develop at the ceiling. Below this hot layer will be area consisting of a clear cooler lower layer. This phase of the development is referred to as the pre-flashover phase and is generally identified by localised behaviour within the compartment. Initially, this fire can be considered as a freely burning, unconfined fire until such a time when radiative feedback or a reduction in oxygen in the compartment becomes significant. As the temperatures within the compartment increase the fire will further develop to the point when temperatures within the space will cause all combustible material to spontaneously ignite, a condition referred to as Flashover.

2.1.3 Flashover

Flashover is the transition between the growth phase and the fully developed phase. It is commonly defined as [1];

1. The transition from a localised fire to the general conflagration within the compartment when all fuel surfaces are burning;
2. The transition from a fuel controlled fire to a ventilation controlled fire.

There have been numerous studies investigating flashover, but it is typically noted that flashover behaviour is defined by the temperature of about 600 °C (1,112 °F) and a received heat flux at the floor of 20kW/m² [2] sufficient to cause spontaneous ignition of most combustibles in a compartment. The occurrence of flashover is of importance for designers for two reasons;

1. *Life Safety*: Flashover represents untenable enclosure conditions in the room of origin, however occupants in close proximity to the fire may also be at risk from its effects due to smoke and fire spread. The failure of structural elements can endanger life safety as a direct result of collapse or by failing to prevent fire spread to other parts of the building.
2. *Property Protection*: Flashover represents the point in time at which the fire has developed to its most severe stage, and this will begin to have a critical impact upon the behaviour of passive fire protection methods within the building and also the buildings' structural elements. Structural failure can cause unacceptable building or content damage.
3. *Threat to Adjacent Property*: After the point of flashover the threat of fire spread and damage to adjacent property increases as a result of radiation through compartment openings and the potential for ignition of adjoining buildings, and the failure of structural fire resisting elements designed to prevent fire spread to other property.

2.1.4 Fully Developed Post-Flashover Phase

After the occurrence of flashover and assuming an unlimited supply of fuel; such that the decay phase can be ignored; the fully developed 'post-flashover' fire will involve all combustibles within the area of origin and be limited by the available oxygen. This means that more fuel will pyrolyse than can be burned by the available oxygen; a term

referred to as ventilation limited. Typically the unburned fuel will leave with the compartment gas flow and may burn outside the compartment. The compartment environment will continue to affect the increased pyrolysis rate and subsequently the rate of heat release will depend upon the amount of oxygen available.

The post flashover stage indicates the following for designers;

1. *Life Safety*: Post-flashover fire life safety considerations related to prescriptive or performance based code are generally ignored as it is assumed that occupants likely to be affected by the fire will have made their escape and are no longer at further risk, or if they have not escaped could not reasonably be expected to survive.
2. *Property*: The post-flashover fire represents the point in time where the design and impact on the structural and passive fire protection elements become critical. The temperatures with the post flashover compartment will be high, and are assumed to be continuous over the vertical profile indicating the occurrence of a well mixed single zone combustion reaction. The duration of this phase and the maximum temperatures achieved will be of paramount importance as this will impact upon the radiation through openings and failure of structural elements.

The compartment temperature is of interest in the study of compartment fire as it is governed by the ventilation and the fire characteristics. The peak fire temperatures are generally noted to form a wide frequency distribution [3], however the maximum value is around 1,200°C (2,192°F). The typical post-flashover room fire will more commonly have a peak temperature of 900 to 1,000°C (about 1,650 to 1,850°F).

The practical consideration for designers is that the time-temperature curve (TTC) for the standard fire endurance test both ASTM E119 and ISO 834 do not even reach 1,200°C (2,192°F) in 4 hours. The New Zealand Building Code compliance document [4] does not specify a fire endurance periods of more than 4 hours.

It is recognised that the time-temperature curves used by standard test methods do not represent the actual time-temperature curve of a real compartment fire. Therefore there is no direct relationship available for designers to use of standard tests methods to determine the actual resistance of construction elements when subjected to a real fire.

Continued experimental study will improve the understanding of compartment fires and fire severity.

2.1.5 Decay and extinction

Fires will decay and eventually burn out after a period of time as a result of a depletion of fuel load, lack of ventilation, or manual or automatic fire suppression systems extinguishing the fire. As this experimental study reviews quasi-steady state burning, a decay phase has been ignored.

2.2 Mass Loss Rates and Heat Release Rate

The burning rate or mass loss rate is the term used to describe the mass rate at which a fuel source is vaporised and is measured in units of kg/s [5]. The term heat release rate (HRR) is also often used for this burning rate and is the rate at which the combustion reactions produce heat, measured in kilowatts (kW). In its simplest form when sufficient oxygen is available and the temperature of the surrounding environment does not rise significantly, the energy generated by a fire can be described as;

$$\dot{Q} = \dot{m}_f \cdot \Delta h_c \qquad \textbf{(2.2-1)}$$

Where h_c is the fuel heat of combustion (MJ kg^{-1}) and $\dot{m}_f$ is the mass loss rate of the fuel (kg s^{-1}).

The heat release rate, HRR, is commonly considered the most significant and important factor in predicting the severity of a fire [6]. The most common method to measure the HRR is known as “oxygen consumption calorimetry” (ASTM E1354). The basis of this method is that a constant net amount of heat is released per unit mass of oxygen consumed for complete combustion. This constant has been found to be 13,100 kJ/kg of oxygen consumed and is considered to be accurate within ±5 percent for most hydrocarbon fuels including cellulosic fuels and plastics [7].

Experimentally the method of determining the HRR of a pool fire is taken from the measurement of the mass loss rate of the pool. Once the mass loss rate has been determined the estimation of the HRR then requires knowledge of the heat of combustion. The heat of combustion is a constant material property, and represents the total amount of energy released by a unit mass of a material (kJ/g) when undergoing complete combustion. Typically the 'total' or 'net' heat of combustion value is calculated using an oxygen bomb calorimeter. This forces all the material to combust at a temperature in a pure oxygen environment whist the mass loss of the specimen is measured. For this experimental study the total heat release rate is measured by oxygen consumption calorimetry. Therefore this measurement enables an 'effective' heat of combustion to be calculated by dividing the heat release rate by the total mass loss of the pool fire(s). The effective heat of combustion is the expected value considering the combustion behaviour in a compartment and will take into account incomplete combustion.

2.3 Pool Fires

Pool fires are generally used in experiments as they are one of the simplest geometry's that can be used for a non-premixed flame where the radiation feedback can govern the burning rate. An enormous number of studies have been conducted where pool fire burning rates have been considered theoretically or measured empirically. The earliest study was by two Russian researchers, Blinov and Khudiakov and by Hottel [8].

The common hydrocarbon fuel Heptane (C_7H_{16}) was used in this experimental pool fire study as it has consistent properties. Pool fire burning also can be applied to a significant number of domestic, residential, commercial and industrial situations. Although pool fires are typically identified as a liquid, at room temperature they can be solid, in the form of many of the manufactured thermoplastic materials and products available in today's modern environment. We are surrounded by an enormous amount of hydrocarbon polymer based products including plastics and foams. When these products are on fire they can behave not to dissimilar to that of pool fires. It is noted

that the HRR of upholstered furniture is normally the highest of any goods found in residential applications. Experiments conducted at the University of Canterbury have found that the heat release rates from modern furniture in New Zealand can provide a significant risk to occupants in residential buildings [9,10]. The results from this experimental study may therefore be related back to practical situations such as residential fires.

The pool fire (in the open) is typically described as a horizontal plane circular bed, displaying a buoyant non-premixed flame. One of the aims of this study was to simulate the fire experiments with the Computational Fluid Dynamic model, FDS. This computer model divides a space into a 3 dimensional grid of rectangular cells. Therefore the pool fire pan was designed to be square to allow for an easier comparison between experimental and computational results.

When a pool fire is place within the bounded confines of an enclosure, the behaviour and structure of the fire can be varied as a result of the radiation from the surrounding boundaries, and ventilation. Therefore this research study focuses of the structure and behaviour of enclosure pool fires both in singular and multiple locations in quasi-steady state conditions.

2.3.1 Free Burning Pool Fires

In the context of this experimental study the terminology "pool fire" relates to a bounded liquid heptane pan fire, however this form of burning is typically associated with free open liquid fuel tanks or liquids spills. Burning liquid fires have been studied extensively, and it has long been known that the burning rate of these pool fires is controlled by the heat transfer back to the pool. Hottel analysed pool burning data and related it to heat transfer principles. The equation for the conservation of energy for liquid is [11]:

$$\dot{m}''_p \Delta h_c = \dot{q}''_r + \dot{q}''_c - \dot{q}''_{rr} - \dot{q}''_{misc} \qquad \textbf{(2.3-1)}$$

Where;

$\dot{m}''_p$ is the mass loss rate per unit area,

Δh_c is the heat of combustion,

$\dot{q}''_r$ is the radiant flux absorbed by the pool,

$\dot{q}''_c$ is the heat received convectively,

$\dot{q}''_{rr}$ is the re-radiation heat loss, and

$\dot{q}''_{misc}$ is the lumped wall conduction losses and non-steady terms.

Although pool fire experiments with diameters less than 0.2m in diameter have often been studied, fires of this size do not typically yield burning rates large enough to be significant in the context of building fires [12]. Therefore the pool fire size of interest to fire engineers is a diameter greater than 0.2 m where the heat transfer is governed by the radiation back to the surface. For pools fire with diameters between 0.2m and 1m the flame is considered to be optically thin, whereas for pools fire greater than 1m in diameter the flame is optically thick [13, 14]. Babrauskas distinguishes four burning modes of pool fires defined by size;

- <0.05m Convective, laminar
- <0.2m Convective, turbulent
- 0.2m to 1.0m Radiative, optically thin
- >1.0m Radiative, optically thick

For most fuels the following semi-theoretical expression can be used to represent the burning rate of an open pool fire of diameter greater than 0.2m;

$$\dot{m} = \dot{m}''_{\infty} \left(1 - \exp\left(-k\beta D_p\right)\right) A_p \qquad \textbf{(2.3-2)}$$

Where;

$\dot{m}''_{\infty}$ is the mass loss rate for an infinite diameter pool (kg/m²s),

k is the absorption-extinction coefficient of the flame (m^{-1}),

β is the mean-beam-length corrector; D is the pool diameter, and

A_p is the pool area (m²).

This expression is based upon the following assumptions;

1. The pool fire is burning in the open and is characterised by the instantaneous and complete involvement of the liquid

2. There is no fire growth period subsequently the maximum heat release rate is reached instantaneously.

The heat release rate can then be estimated by;

$$\dot{q} = \Delta h_c \cdot \dot{m}'' \cdot A_p \qquad \textbf{(2.3-3)}$$

For heptane in a 0.2m square pan the free burning heat release rate is expected to be 100kW using typical values for heptane ($\dot{m}''_\infty = 0.101$ kg/s.m², $\kappa\beta$=1.1m^{-1}, Δh_c=44.6MW) taken from reference [13].

This expression is an idealised predication of the heat release rate and it is noted that in practice a number of physical conditions may impact upon this prediction. The best known of these physical conditions are;

a. *Boiling spill over* in which the boiling of the liquid can overflow the sides of the pool fire pan. This is not to be mistaken for 'boil-over' which is a violent ejection of flammable liquid from its container caused by vaporisation of a water layer beneath the body of a liquid [15].

b. *Transient effects* in which the pool does not burn in quasi-steady state manner due to changing bounding conditions. This is generally the behaviour of the typical pool fire. As the fire develops, temperatures at the pan walls and base increase impacting upon the burning rate of the pool fire. In this experimental study the pool fire experiments are continued until quasi-steady conditions are reached. With the added insulation of the pan bounding surfaces, any transient effects are ignored.

c. *Lip height* which is noted as the height from the top of the liquid to the top of the pan. The selection of this height is determine in conjunction with preventing the boiling spill over as well as mitigating the impact that the heated lip height will have on the fire plume behaviour and any radiation feedback to the fuel.

d. *Wind effects* which are a generally associated with outdoor combustion. Considering this internal experimental study any wind effects on fire behaviour can be neglected. However the impact of air velocity over the pool fire due to the ventilation opening is recognised and when considering vent flows it has been noted by Emmons [16] that the a fire near the vent has effects that are at present unknown.

The above expressions are only applicable for the free burning pool fire burning regime in which the temperatures of the surrounding environment does not rise significantly. Once the pool fire is introduced to an enclosure this presents a significantly different scenario as the effects from the enclosure boundaries have a considerable effect upon the burning behaviour of the pool fire. The free burning expression (eq. (2.3-2)) is however appropriate to use in enclosure fires up to the point of flashover [12].

2.3.2 Enclosure Effects

When a pool fire is placed inside an enclosure, the two main factors that influence the fire growth are the energy released and the mass loss rate of the fuel.

For pre-flashover fires the burning rate will increase as a function of time due to the accumulation of smoke and hot gases at the compartment ceiling, and the heating of the physical compartment boundaries (walls and ceiling). The heated layer and compartment boundaries will subsequently increase the amount of radiated heat back to the fuel surface, and this will increase slightly as the fire grows and the upper layer temperature increases.

For post-flashover fires the radiation feedback is significantly increased and can drive the mass loss rate to several times that attained in the open air free burning case [17,18]. In this instance the effect of ventilation plays an increasing role, as the compartment openings (doors, windows, and other leakage areas) may restrict the availability of oxygen needed for combustion to occur within the enclosure. If the ventilation opening is small, the limited availability of oxygen causes incomplete combustion, thereby decreasing the HRR. Subsequently compartment gas temperatures and heat transfer to the fuel surface is reduced, while the fuel continues to release volatile gases at a similar

or lower rate. The effect of ventilation is the easiest form of controlling the energy released in a fire and has been studied previously [17,18] to determine the effects upon a single pool fire in a small compartment. Although the reduction in oxygen may reduce the burning rate, a reduction in the ventilation opening may not significantly limit the amount of oxygen that reaches the fire. Unburnt combustion products will continue to burn outside of the compartment as an external flame and in doing so this may help induce the onset of flashover.

The pool fire geometry represents a worse case in terms of a radiation enhanced mass loss rate. The entire fuel surface sees the hot upper layer and bounding surfaces. More complex fuels such as furniture or wood cribs will be partially shielded from the compartment environment and therefore less radiation will reach the fuel surface.

The significant work by Kawagoe [19] with wood cribs and by Thomas [20] and Rockett [21] found the correlation that the mass loss rate of heat released by the fire was proportional to the ventilation factor of the compartment opening. The ventilation factor is defined as the area of the opening multiplied by the square root of the height $A_v\sqrt{H_v}$. It has further been identified that with liquid and thermoplastic materials, a greater pyrolysis rate than that of cellulosic materials is achieved. The burning of liquid pool fires has been extensively studied, and it has long been known that the burning rate is controlled by the amount of heat transfer back to the surface of the pool fire. Therefore the relationship between the ventilation factor $A_v\sqrt{H_v}$ and the pool area A_p has been shown to be the dominant variable in predicting the behaviour of thermoplastic pool fires in a compartment [22].

Therefore the theoretical pyrolysis rate (g/s) for a thermally thick radiative pool based upon the inflow of air into the compartment is considered to be approximated by;

$$\dot{m}_{air} \approx 0.5\, A_v\sqrt{H_v} \qquad \textbf{(2.3-4)}$$

where A_v is the area of the opening (m²) and H_v is the height of the opening (m)

It has long been observed that pool fires can burn in a high fuel rich manner. Babrauskas [22] has also shown that the ventilation limited stoichiometric fuel pyrolysis rate can be estimated as;

$$\dot{m}_p(st) = \frac{0.5}{r} A_v \sqrt{H_v} \qquad \textbf{(2.3-5)}$$

Where r = the stoichiometric air/mass ratio (15.1 for heptane); A_v is the vent area (m²); and H_v is the vent height (m).

Previous work in small scale enclosure pool fire behaviour has shown that burning rates with liquid pool fires in enclosures can be six to seven times that of the free burning rate [18,23]. The mass loss rate as governed by these post flashover compartment temperatures has the following form:

$$\dot{m}_p = A_p \frac{\varepsilon\sigma(T_f^4 - T_b^4)}{\Delta h_g} \qquad \textbf{(2.3-6)}$$

where A_p is the pool area (m²); σ is the Stefan-Boltzmann constant (5.67×10^{-8} $Wm^{-2}K^{-4}$); T_f is the fire gases temperature (K); T_b is the boiling point temperature (K); and Δh_g is the heat of gasification (J/kg).

This requires the solution for the compartment temperature, and to date the behaviour of multi-fuelled compartment fires has yet to be accurately modelled. No simple formulas exist for computing the enhanced burning rates when an object receives significant radiation feedback from a compartment. Babrauskas and Wickström and the computer program COMPF2 [24] have been used in the case when post-flashover compartment fire temperatures are required. However the past evaluation of post flashover models is that they over estimate the compartment fire temperatures. Ee Yii [25] developed a model to predict the temperatures in post flashover fires. This model uses the energy balance approach and the post-flashover compartment fire temperatures are calculated based on the conservation of energy and has shown to provide satisfactory results.

The expected heat release rate within an enclosure sufficient to cause flashover can be calculated using the following expression based upon theoretical work derived by Babrauskas [26]

$$\dot{Q} = 600\, A_v \sqrt{H_v} \qquad \textbf{(2.3-7)}$$

For the different ventilation geometries represented in this study the predicted heat release rates for flashover for each geometry are;

1. *Full*: 2.4m wide x 1.2m high (1893kW).
2. *Soffit*: 2.4m wide x 1.0m high (1440kW).
3. *Door*: 0.4m wide x 1.0m high (240kW).
4. *Window*: 0.8m wide x 0.6m high (223kW).
5. *Small Window*: 0.4m wide x 0.6m high (112kW).

2.4 Equivalence Ratio

The quantity of fuel and the availability of the oxygen (air) supply within a compartment fire have a considerable effect on the production and composition of compartment fire gases. They also impact upon the energy released within the enclosure. Therefore it is important to not only measure the degree of ventilation within an enclosure but also to quantify the ventilation with respect to the fire loading and combustion behaviour.

This can be particularly important in enclosure fires where the amount of oxygen available for combustion is low i.e. under-ventilated fires. Partial combustion as a result of insufficient ventilation means that the reaction between oxygen in the incoming air flow and the products of combustion remains incomplete. This results in the release of hazardous gases such as carbon monoxide. The hazard to life and property is generally due to fires which occur in enclosed spaces, such as buildings, and one of the principle life safety concerns is that gaseous carbon monoxide is preferentially taken up by the human body and is mainly responsible for deaths in fires [27,28].

When the amount of available fuel is exactly balanced with the oxygen available, then complete combustion occurs and there is neither unburned fuel nor unused air remaining. This burning is referred to as stoichiometric, and the ratio of fuel to air is a called the stoichiometric fuel to oxygen ratio.

The amount of fuel with respect to the ventilation can then be defined as the actual mass flow of fuel to oxygen ratio compared with the stoichiometric fuel to oxygen ratio;

$$\phi = \frac{\left(\dot{m}_{fuel} / \dot{m}_{oxygen} \right)_{actual}}{\left(\dot{m}_{fuel} / \dot{m}_{oxygen} \right)_{Stoichiometry}}$$

This ratio is called the Equivalence Ratio, ER, (ϕ), and at stoichiometry is equal to unity. When the overall combustion process is studied, the ratio is usually called the Global Equivalence Ratio, GER.

If there is excess air provided the ER term is often referred to as 'oxygen rich' or 'fuel lean' combustion, as the equivalence ratio is less than one. If there is not enough air provided then the ER is referred to as "oxygen lean' or 'fuel rich' combustion, as the equivalence ratio is greater than one. In the oxygen rich $\phi<1$ situation most of the burning is expected to take place within the enclosure and therefore the burning is associated with pre-flashover compartment behaviour. When the fuel rich $\phi>1$ situation occurs there is not enough oxygen available for complete combustion and burning is noted to take place in front of the enclosure, which is commonly associated with post-flashover behaviour.

The equivalence ratio can also be obtained by the evaluation of the stoichiometric mass loss rate [29]. The relationship between the stoichiometric mass loss rate and air consumption can be expressed as;

$$\left(\dot{m}_f\right)_{Stoichiometry} = \frac{1}{r}\left(\dot{m}_{air}\right)_{Stoichiometry} \quad \textbf{(2.4-1)}$$

Where *r* is the dimensionless stoichiometric air/fuel mass ratio of 15.1 for heptane. This means any mixture less than 15.1 to 1 is considered to be a rich mixture, any more than 15.1 to 1 is a lean mixture.

The equivalence ratio can then be expressed as;

$$\phi = \frac{\dot{m}_f}{\left(\dot{m}_f\right)_{Stoichiometry}} \quad \textbf{(2.4-2)}$$

As noted in equation (2.3-4) the induced mass inflow of air into a fire compartment is a function of the ventilation factor and can be approximated as;

$$\dot{m}_{air} \approx 0.5\, A_v \sqrt{h_v}$$

Therefore the equivalence ratio in a compartment is;

$$\phi = \left(\frac{r}{0.5\, A_v \sqrt{H_v}} \right) \dot{m}_f \quad \textbf{(2.4-3)}$$

The evaluation above is the ER defined by the ratio between the mass-loss rate of the fuel and the mass flow of the air entering the entire room, normalized by the stoichiometric air to fuel mass ratio. Therefore it is defined as the ER for the total combustion process and is considered an approximation of the Global Equivalence Ratio, GER.

Previous research by the author [17,18] showed that the global equivalence ratio was approximately 1.7 over a range of opening factors for vent with a $H_o/W_o<8$. The experiments also tended to show that for $H_o/W_o<12$ the global equivalence ratio is closer to 3.

2.5 Previous Work

Previous work by the author [17,18] has shown that the ventilation plays an important part in the behaviour of enclosure pool fires. Thomas, I. R [30,31] studied large pool fires in a deep narrow compartment with different opening geometries. In these studies, the entire floor of the compartment was covered with fuel pans. The results from these studies have shown that the burning rate of fires in a deep enclosure is strongly influenced by the ventilation geometry.

More complex wood cribs fuels in large narrow enclosures have been studied at British Research Establishment, BRE [32,33]. In the BRE, study, wood cribs were placed over the entire floor of a long narrow compartment with a single vent at the opposite end of the enclosure. The importance of the fire location relative to the opening was also identified in this work as the fire ignited in the rear, spread quickly to the front of the enclosure and then spread more slowly into the compartment as the fuel was consumed, thus demonstrating the importance of the fire location relative to the ventilation opening.

The experimental study by Marshall [34] also looked at the effect of location of a fire within a compartment. The study was carried out in a 1/10th scale model enclosure to examine the effect of different fire locations within a compartment, on the mass flow rate of gases toward a compartment opening. Four different fire locations were studied; back, centre, side and corner of the compartment; using industrial methylated spirits. The study noted that behaviour of the fires at each location, with particular attention to the 'hugging' of the rear pan location to the rear wall, and the flame structure leaning toward the rear of the compartment for the centre pan. A fire located in the centre of the compartment produced the largest mass flow rate of hot gases towards the opening and it was quoted by Marshall as representing the "worst case" for practical design.

Ventilation opening flows have previously been noted to be the greatest with a fire located just inside a compartment opening and decrease as the fire is moved to the rear of the compartment. This behaviour was reported by Quintiere [35] as 'wind effect' due to the fire plume entrainment being increased as the plume is blown over by the door jet flow. Quintiere and Hansell [36] examined the effect of leaning fire plumes

and demonstrated that the quantity of air entrained into a leaning fire plume can be double the amount expected for an upright plume.

Steckler [37] also conducted steady state experiments to study the flow induced by a simulated pool fire in a compartment. If a fire is located in close enough proximity to a wall then the leaning effect may have other consequences. The resulting interaction with a wall will distort the fire plume and result in restricting air entrainment will have a significant effect on fire growth and spread. The reduction in entrainment lengthens flames will cause the fire to lean and spread vertically up the wall. This effect is due to the fire having limited air entrainment and is similar to the mechanism called "the trench effect" studied by Smith [38]. However this does not necessarily imply that the fire entrains more air since its effective fire perimeter is limited by the wall and may entrain less air.

In the above studies the magnitude of the air velocity into the fire compartment was determined to be the governing behaviour of the fire plume. As the ventilation geometries decrease in size this will of course generate larger incoming air velocities at the opening and this will affect the leaning angle of the fire plume. The location of the opening with respect to the fire will also alter the fire behaviour. In all these cases the size of the fire and its proximity to the opening will determine the degree of distortion from the ideal upright fire plume. Emmons [39] notes that a fire near the vent has effects that are at present unknown as this has not been studied.

2.6 References

1 Drysdale, D, An Introduction to Fire Dynamics, 2nd Edition, John Wiley & Sons, New York, 1998.

2 Peacock, R. D., Reneke, P. A. Bukowski, R. W. And Babrauskaus, V., ”Defining Flashover for Fire Hazard Calculations”, Fire Safety Journal, Volume 32, Issue 4, June 1999, pages 331-345.

3 Babrauskas, V., and R.B. Williamson, “Post-Flashover Compartment Fires,” Fire and Materials, Volume 2, pp. 39–53: 1978, and Volume 3, pp. 1–7, 1979.

4 Compliance Document for New Zealand Buidling Code Clauses C1, C2 C3, C4, Fire Safety, Department of Building and Housing, Wellingon New Zealand.

5 Karlsson, B., and J.G. Quintiere, “Enclosure Fire Dynamics. CRC Press LLC, New York, 1999.

6 Babrauskas, V., and Peacock, R. D., Heat Release Rate: The Single Most Important Variable in Fire Hazard, Fire Safety J. 18, 255-272 (1992).

7 Janssens, M. L. “Measuring Rate of Heat Release by Oxygen Consumption” Fire Technology, August 1991, pp234-249

8 Hottel, H.C., Review Certain Laws Governing Diffusive Burning of Liquids, by V. I. Blinov and G. N. Khudiakov, Fire Research Abstracts and Reviews 1, 41-44 (1958).

9 Girgis, N, “Full-Scale Compartment Fire Experiments on Upholstered Furniture”, Fire Engineering Reseasrch Report 2000/5, University of Canterbury

10 Enright, P.A “Heat Release and the Combustion Behaviour of Upholstered Furniture” Fire Engineering Reseasrch Report 99/17, University of Canterbury.

11 A Hamis, S.J. Fischer and T. Kashiwagi, "Heat Feedback To The Fuel Surface In Pool Fires" Combustion Science and Technology, Vol. 97, No 1-3, pp37-62, 1994

12 Babrauskas, V., "Free-Burning Fires," Fire Safety Journal, Volume, 11, Nos. 1 & 2, pp. 33–51, July/September 1986.

13 Babrauskas, V, "Heat Release Rates", The SFPE Handbook of Fire Protection Engineering, Section 3/Chapter 1, 3rd edition, 2002.

14 Babrauskas, V., Estimating Large Pool Fire Burning Rates, Fire Technology 19, 251-261 (1983).

15 NFPA Fire Protection Handbook, 2003

16 Emmons, H. W., Vent Flows, The SFPE Handbook of Fire Protection Engineering, Third Editon, Section 2/Chapter 3, 2002.

17 Parkes, A. R. "Under-Ventilated Comaprtment Fires –A Precuser to Smoke Explosions" Fire Engineering Reseasrch Report 96/5, University of Canterbury, 1996

18 C.M. Fleischmann and A.R Parkes, "Effect of Ventilation on the Compartment Enhanced Mass Loss Rate, Fire Saftey Science – Procedings of the Fifth International Symposium, pp. 415-426

19 Kawagoe, K "Fire Behaviour in Rooms", Report No 27, Building Research Insitute, Toyko, Japan, 1958.

20 Thomas, P. H., Heselden, A. J. M., and Law, M. (1967). "Fully developed compartment fires: two kinds of behaviour." Fire Research Technical Paper No. 18, HMSO, London.

21 J. A. Rockett, “Fire Induced Gas Flow in an Enclosure”, Combustion Science and Technology, Vol. 12, (1976), pp 165-175.

22 Babrauskas, V., and Wickström, U. G., Thermoplastic Pool Compartment Fires, Combustion and Flame 34, pp. 195-201 (1979).

23 Bullen, M. L., and Thomas, P. H. (1979). “Compartment fires with non-cellulosic fuels.” 17th Symposium (International) on Combustion. pp. 1139-1148. The Combustion Institute, Pittsburgh.

24 Babrauskas, V., COMPF2-A Program for Calculating Post-Flashover Fire Temperatures (Tech Note 991). [U. S.] Natl. Bur. Stand. (1979).

25 Yii, E “Modelling the Effects of Fuel Types and Ventilation Openings on Post-Flashover Compartment Fires” PhD Thesis, University of Canterbury, 2002.

26 Walton, W.D and Thomas, P. H, “Estimating Temperatures in Compartment Fires”, The SFPE Handbook of Fire Protection Engineering, Section 3/Chapter 6, 3rd edition, 2002

27 Pitts, W. M., “The Global Equivalence Ratio Concept and the Prediction of Carbon Monoxide Formation in Enclosure Fires”, National Institute of Standards and Technology Monograph 179, Gaithersburg, MD, 1994, p 171.

28 Babrauskas, V., Parker, W. J, Mullholland, G., and Twilley, W. H, “The phi meter: A simple, fuel-independent instrument for monitoring combustion equivalence ratio” Rev. Sci. Instrum. Vol 65, No 7, pp. 2367-2375, July 1994.

29 Babrauskas, V, “A Closed-form Approximation for Post-flashover Compartment Fire Temperatures”, Fire Safety Journal, 4, pp 63-73, 1981.

30 Thomas, I. R., and Bennetts, I D., "Fires in Enclosures with Single Ventilation Openings – Comparison of Long and Wide Enclosures", Fire Safety Science – Proceedings of the Sixth International Symposium, 941-952, 1999.

31 Thomas, I. R., Moinuddin, K., and Bennetts, I., "Fire Development in a Deep Enclousure", Fire Safety Science – Proceedings of the Eigth International Symposium, 1277-1288, 2005.

32 Kirby, B. R., Wainman, D. E., Tomlinson, L. N., Kay, T. R. and Peacock, B. N., Natural Fires in Large Scale Compartments, A British Steel Technical, Fire Research Station Collaborative Project, BSC, 1994.

33 Cooke, G. M. E., "Tests to Determine the Behaviour of Fully Developed Natural Fires in a Large Compartment", Fire Note 4, BRE, 1998.

34 Marshall, N. R., "A model scale study of the effect of the location of a fire within a compartment" Building Research Establishment. Fire Research Station, 1997

35 Quintiere, J. G, Rinkinen, W. J. And Jones, W. W., "The Effect of Room Openings on Fire Plume Entrainment", Combustion Science and Technology26, 193, 1981.

36 G O Hansell, Heat and mass transfer process affecting smoke control in atrium buildings. PhD Thesis, London South Bank University, 1993.

37 Steckler, K. D., Quintiere, J. G., and Rinkinen, W. J., "Flow induced by fire in a compartment. Nineteenth Symposium (International) on Combustion." The Combustion Institute, 1982, pp. 913-920.

38 D Smith, Measurements of flame length and flame angle in an inclined trench. Fire Safety Journal 18 (1992) 231-244.

39 Emmons, H. W., Vent Flows, The SFPE Handbook of Fire Protection Engineering, Third Editon, Section 2/Chapter 3, 2002.

Chapter 3: Experimental Setup and Procedure

This chapter details the experimental method and apparatus setup used in this research study. Details of the construction of the experimental enclosure, including the location of instrumentation is provided as well as data reduction methods. In total 215 channels of data were continuously logged during this experimental study.

The chapter begins with a schematic exploded sketch of the completed compartment showing the installed compartment instrumentation and photographs showing the left and right hand sides of the compartment. This is shown as prelude and visual aid to the detailed description of the construction and instrumentation of the experimental apparatus in the remainder of the chapter.

The detailed description of the size and construction of the compartment is then provided along with the ventilation geometries used in the experiments, the location of windows and video cameras, and details on the pool fire and delivery system used. Instrumentation description and location follow and details the acquisition systems used, temperature, heat flux, velocity, mass loss, heat release rate and combustion species measurements. Lastly the experimental matrix is tabled and the operational procedures noted.

3.1 Completed Layout Summary

The experimental layout showing all instrumentation is detailed the exploded box layout below in Figure 3.1.

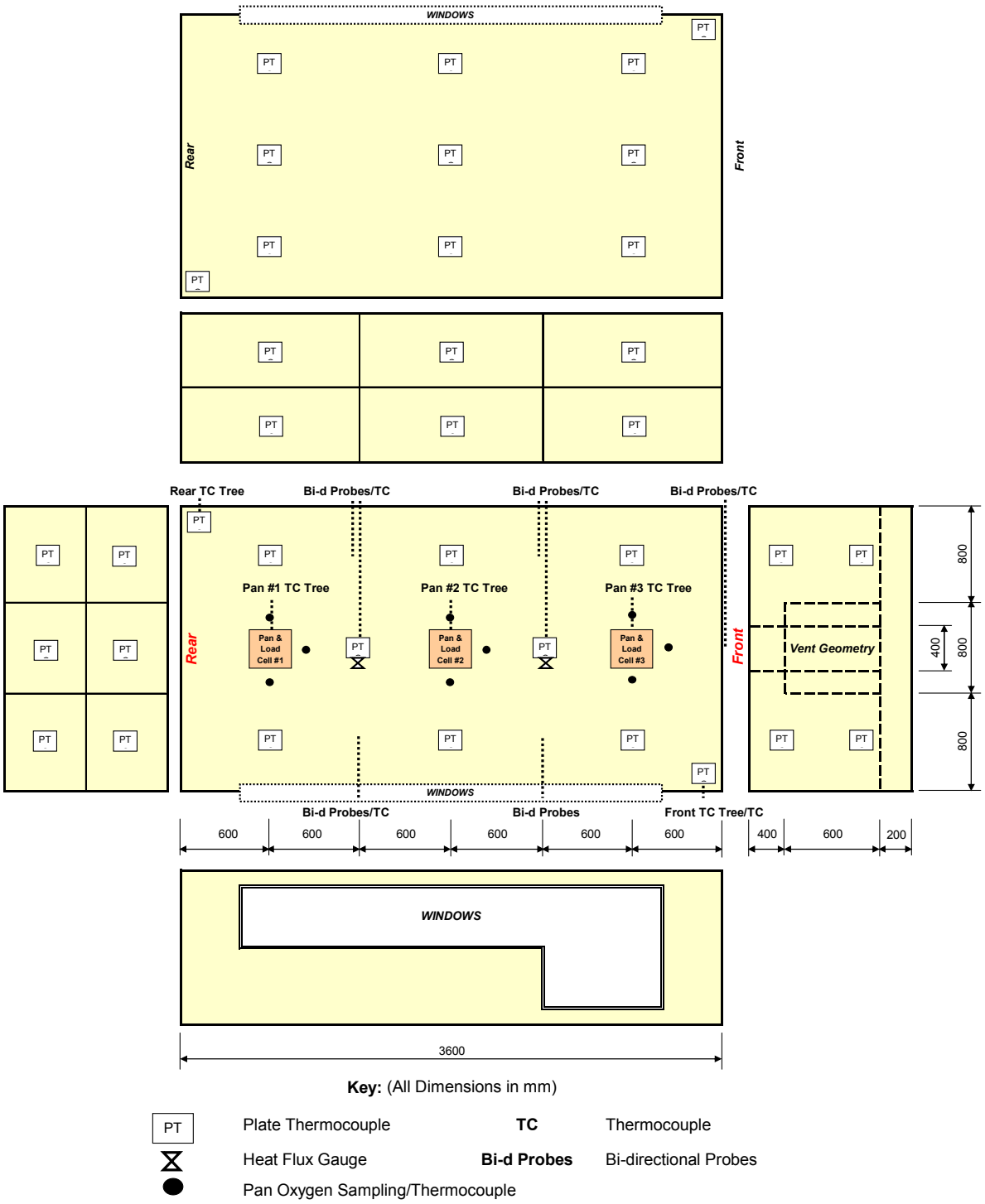

Figure 3.1: Exploded box sketch of the completed compartment detailing all instrumentation locations

The photograph in Figure 3.2 shows the left hand side of the experimental enclosure. Fire rated windows can be seen along the left hand wall, with three pan locations noted along the centreline of the compartment and thermocouple trees located above each pan. Bi-directional probes and thermocouples can also be identified in the vent opening which is configured in the fully open geometry.

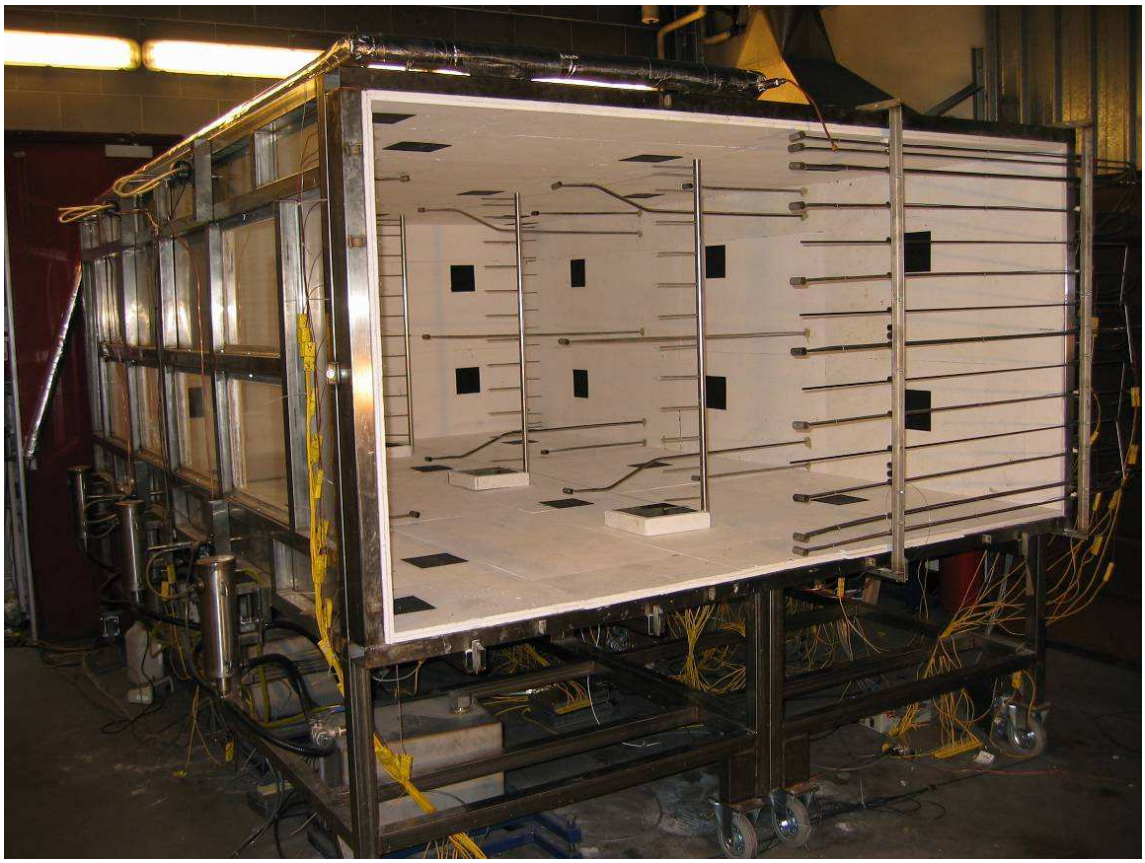

Figure 3.2: Photograph of the completed enclosure as viewed from the left hand side with the full ventilation opening showing fire rated windows, three pan locations, thermocouple trees, and bi-directional probes

The photograph in Figure 3.3 shows the left and right hand side of the completed enclosure. A thermocouple tree can be seen to the left of the photograph at the front of the room and the pressure transducer and aspirated thermocouple lines can be identified on the outside of the right hand wall.

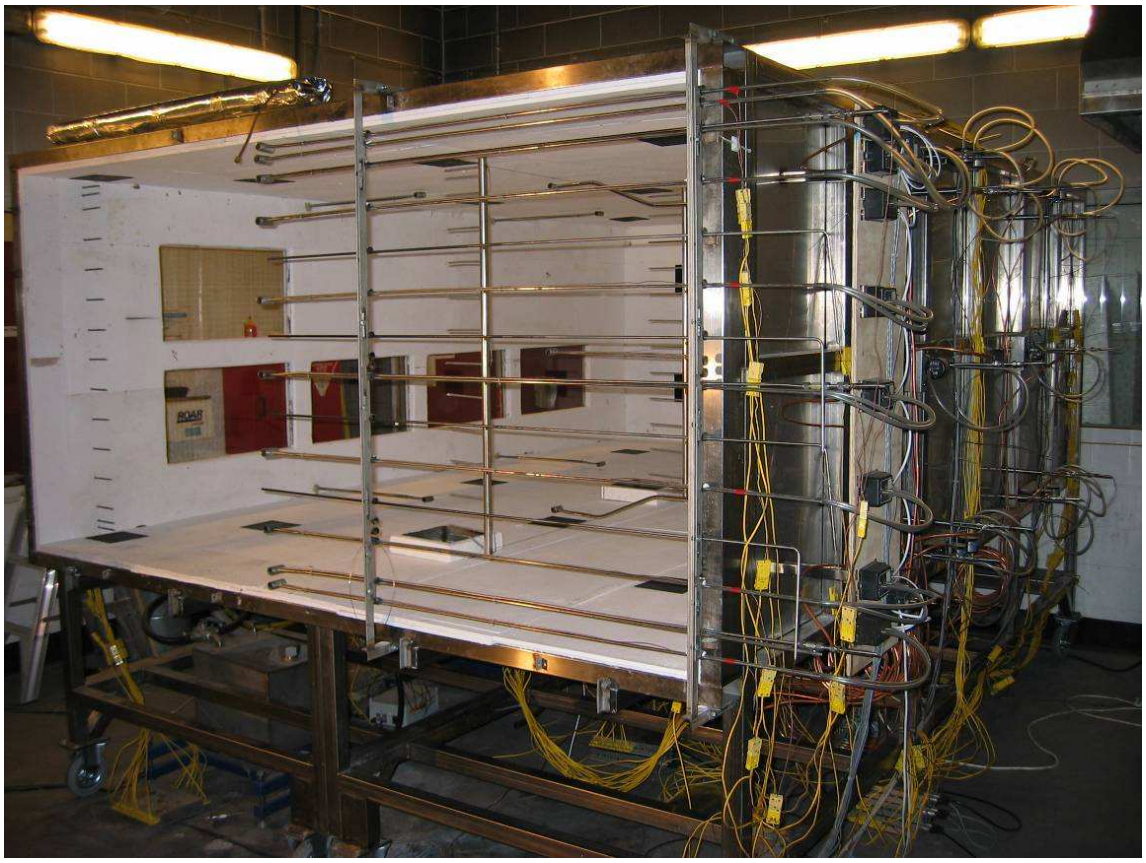

Figure 3.3: Photograph of the completed enclosure as view from the right hand side with the full ventilation opening showing five fire rated windows, thermocouple trees, bi-directional probes and pressure transducer and aspirated thermocouple lines on the outside wall

3.2 Experimental Enclosure

The standard size of an enclosure used to perform fire experiments is typically based upon the scaling of an ISO 9705 test geometry [1]. This is a full scale test method that simulates fires with a single open doorway in order to evaluate the contribution to fire growth provided by surface products. The ISO room corner test is used in a number of countries for classification of surface materials by determining the fire performance characteristics of products with respect to the quantity of heat released, the rate at which

it is released, and the time to flashover which is generally regarded as the most significant result. It should however be noted that the type, position and heat output of the ignition source will considerably influence the fire growth.

The ISO 9705 test method enclosure has dimensions of 3.66m long by 2.44m wide by 2.44m high. This of course provides an equal height to width ratio. Fires within enclosures of this size are therefore exposed to radiation from walls that are located the same characteristic distance from the fire as the ceiling. This geometry is not representative of typical rooms in general buildings.

It was proposed in this experimental study to provide an enclosure with dimensions more appropriate to that of a typical building space. The bounding walls are located at a greater distance from the fire than the ceiling e.g. the room is wider than its height. Subsequently, in this study the fire experiments were conducted in a reduced scale compartment (½ height scaled ISO 9705) with dimensions of 3.6m long by 2.4m wide by 1.2m high as shown in Figure 3.4 below.

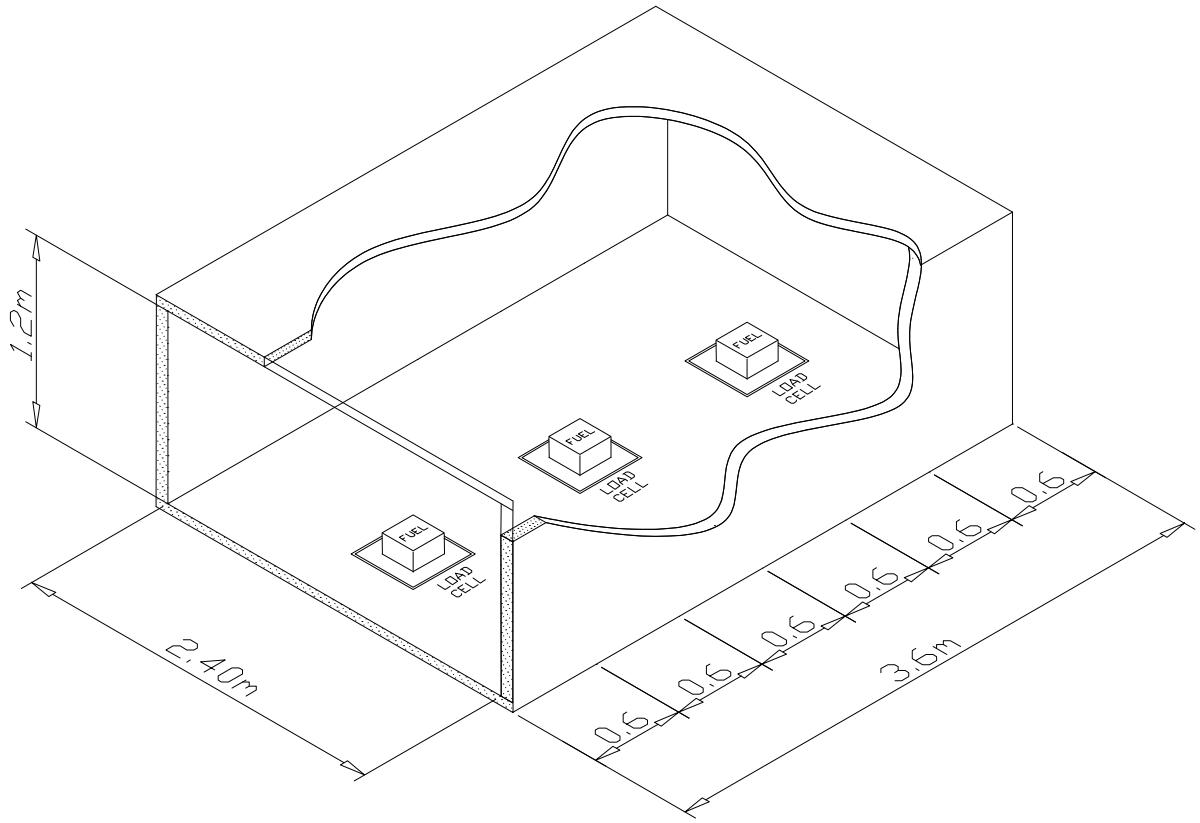

Figure 3.4: Sketch showing the dimensions of the experimental compartment and pan locations

The primary objective of this experimental study was to investigate the behaviour of compartment fires in relation to the ventilation and the fire source (size and location). The compartment was therefore constructed to allow the front 1.2m high and 2.4m wide vent opening to be modified (refer to 3.2.2 for further details on the vent openings). The pan locations are also able to be varied to investigate the impact upon the size and location of fires within a compartment.

3.2.1 Construction

The experimental compartment for this study was purpose built and fabricated with finished internal dimensions of 3.6m long by 2.4m wide by 1.2m high. The compartment was constructed from grade 305 stainless steel with main supporting structural members consisting of 50mm x 50mm rectangular hollow sections (RHS) at approximately 500mm centres. The enclosure wall lining consisted of 3mm thick stainless steel, welded to the inside of the main frame. The enclosure was constructed in two halves to allow access into the fire laboratory doors (1670mm total width). The two halves were then bolted and welded together.

The walls, ceiling and floor of the compartment were lined with two layers of 10mm Kaowool ceramic fibre vacuum board (manufactured by Thermal Ceramics). Each layer of Kaowool was positioned to overlap adjacent jointing sheets to ensure no direct exposure to the stainless steel lining behind. The Kaowool vacuum board was fixed to both the stainless steel lining and inter-sheet by a high temperature adhesive; Kaogrip cement.

During the experimental series the kaogrip adhesive was found not to provide sufficient board to board adhesion. Subsequently the roof and wall linings suffered damage and collapsed in places. Relining of the walls and ceiling was required and support to the new and existing lining was achieved by the use of metal supporting plates bolted to the stainless steel structure.

3.2.2 Ventilation Openings

The aim of this research was to investigate fire behaviour with respect to the variables of location and ventilation. Therefore the ventilation into the compartment was designed to be adapted by the use of removable panels to enable the ventilation geometry to be modified.

Nine individual ventilation panels were designed as shown in Figure 3.5. When installed either separately or in combination, the compartment ventilation was able to be modified from fully unrestricted to a small window. These panels were lined with two overlapping layers of 10mm ceramic fibre board and fixed with kaogrip cement. The panels were bolted together with hinges attached to the main structure. This allowed each the side panel to be un-bolted from the soffit panel allowing the side vents to swing open providing easy access.

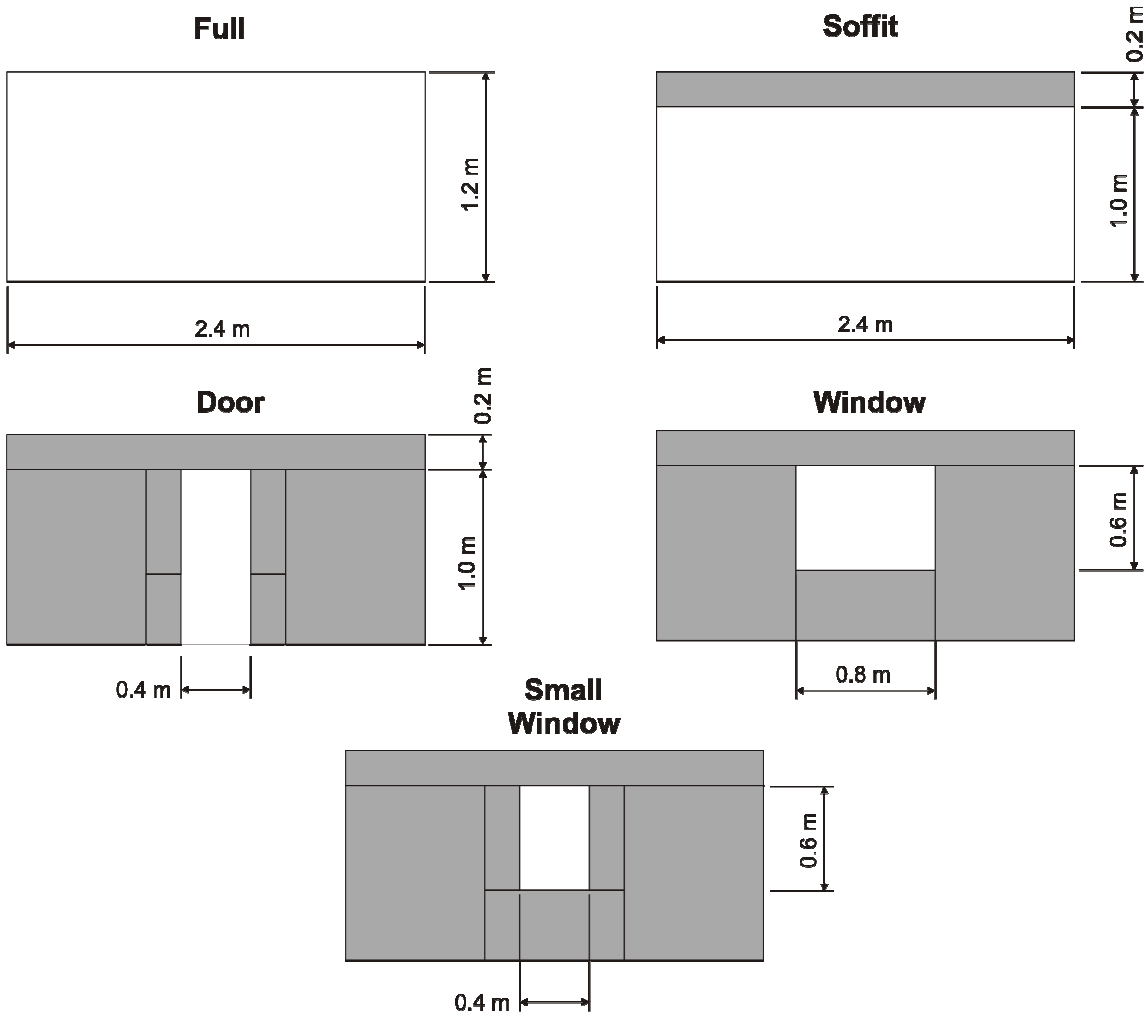

Figure 3.5: Sketch detailing the five ventilation geometries used in the experimental study and the eight removable panel locations.

The dimensions of the various ventilation geometries and ventilation factors [2] are detailed below:

1. *Full*: Unrestricted opening; 2.4m wide x 1.2m high ($A_v\sqrt{H_v} = 3.155$).
2. *Soffit*: 0.2m downstand; opening 2.4m wide x 1.0m high ($A_v\sqrt{H_v} = 2.4$).
3. *Door*: 0.4m wide x 1.0m high ($A_v\sqrt{H_v} = 0.4$).
4. *Window*: 0.8m wide x 0.6m high ($A_v\sqrt{H_v} = 0.372$).
5. *Small-window*: 0.4m wide x 0.6m high ($A_v\sqrt{H_v} = 0.186$).

3.2.3 Observations

To allow visual observations to be taken during the compartment experiments, five fire integrity-only rated windows were located along the left hand side of the compartment as shown in the photograph in Figure 3.6. Four of the windows were located at lower half of the compartment with the fifth located at the upper level near the vent opening. The glazing used consisted of 5mm FireLite® ceramic glass (tinted).

During the initial experiments, the windows consisted of a single pane of FireLite® glass installed within a fixed bolted steel frame system. The windows were installed with a spacing tolerance of fire rated felt between the steel frame and the glass. However, during these initial experiments, all the lower window glass cracked as a result of the high temperatures and thermal movement of the compartment frame. Subsequently the window system was modified to provide a double glazed system.

The revised window framing system provided a toggle clamping system as shown in the insert diagram in Figure 3.6. 10mm Kaowool rope was used as the separating buffer between each sheet of glass to allow for movement. The resulting double glazing system provided no further issues for the reminder of the experiments. It should be noted that the internal panes of glass on all the lower windows cracked, however integrity was maintained.

The affect of the windows on the boundary conditions was not investigated.

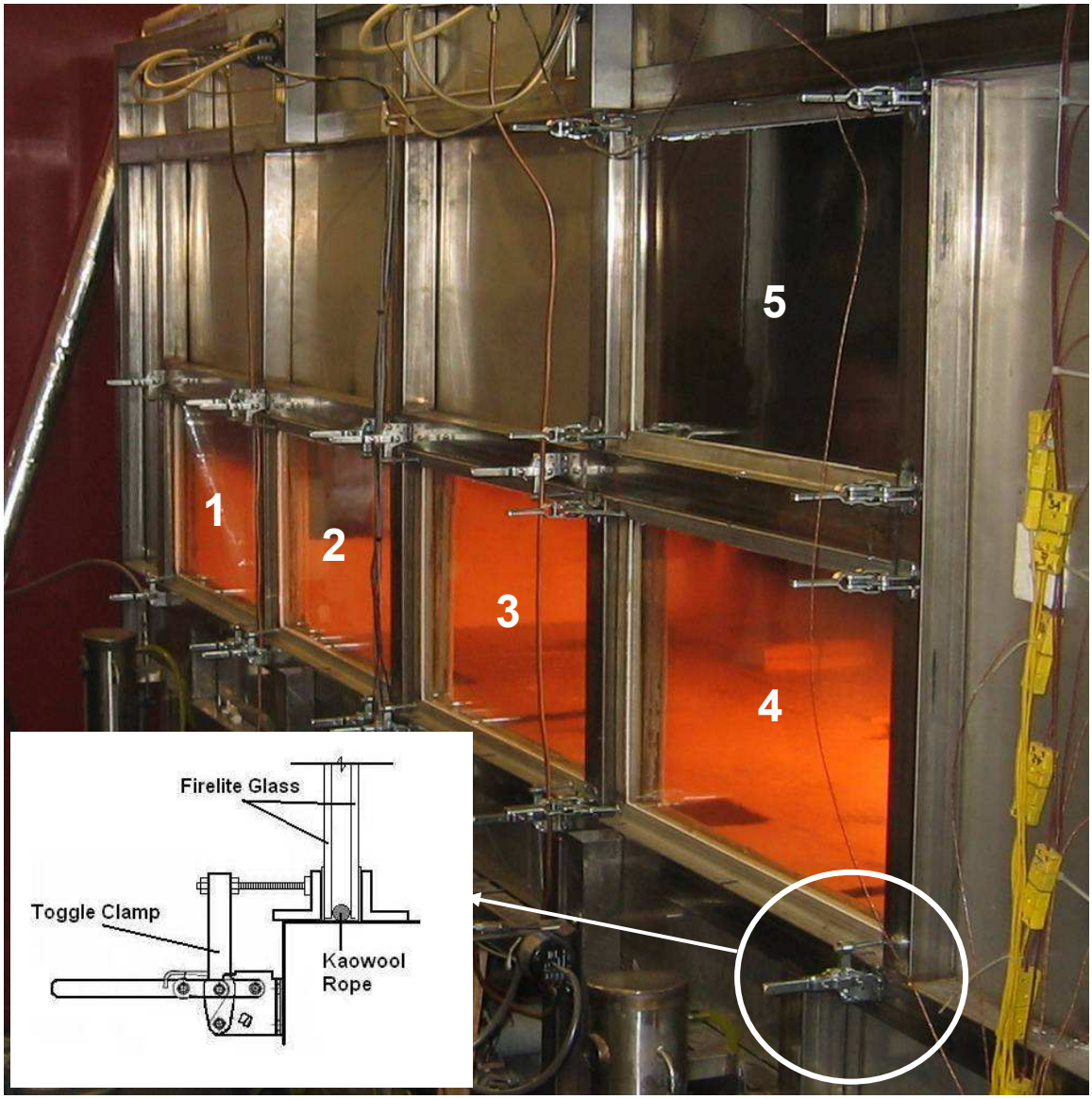

Figure 3.6: Photograph showing the double glazed window system and toggle framing clamp detail (insert)

Video cameras were used to record the full duration of each experiment. One camera was initially located at the front of the enclosure to record the fire behaviour within the compartment. This however was only of use during the fully open and soffit ventilation case in which the openings provided unrestricted views. For the door, window and small window vents the camera was located perpendicular to the ventilation opening to capture the flame extension. The other camera was located at an angled view along the face of the fire rated windows.

3.2.4 Fire Type, Location, and Delivery System

Heptane pool fires were used in this experimental study as they are one of the simplest methods to provide a non-premixed flame, and have the advantage of providing easy repeatability. Heptane (C_7H_{16}) has consistent properties for repeated testing and the pool fire geometry burns similar to situations presented by melting thermoplastics which are commonly widespread in furniture manufactured today. It is therefore considered that these experimental results can be related to practical fire design situations such as residential and office applications. Also as this research study is looking at compartment effects, radiation is considered to be a major factor with pool fires. Therefore the chemical composition of heptane with a high carbon content, ensures a high level of soot production during the experiments such that radiation is expected to be the dominant form of heat transfer within the enclosure. The use of heptane was also consistent with previous small scale pool fire experiments in a 1m wide x 1m high x 1.5m deep compartment by Parkes [3] and Yii [4].

All of the fuel pans were located along the centreline of the compartment and ventilation opening; e.g. 1.2m from each of the side walls. It is not the intention of this work to investigate the behaviour of multiple fires located offset from the centreline. Some experimental studies reviewing this behaviour are noted by Thomas [5, 6].

3.2.4.a) Pan Size

Typical pool fires are considered thermally thick once over a diameter of 200mm. Diameters of 200mm and over mean that radiation from the flame becomes the dominant form of heat transfer. This was used as the basis for minimum size of the proposed pool geometry. As the experimental results may be investigated in the future within CFD models, the single pan used in all the experiments was not circular but square. Single pan dimensions used were 200mm x 200mm square with a depth of 50 mm.

One aim of the experimental study was to also look at the impact of multiple fires within an enclosure. This behaviour would then be reviewed against the general assumption that a credible design fire modelling scenario is located in the centre of a

room. Therefore a large pan was made to provide an equivalent area comparison with two 200mm square pans. A larger pan was also made to compare three 200mm pans. These equivalent area pans are designated as follows;

- ***x2 pan*** - a pan having the equivalent area to that of two 200mm square pans. This pan has dimensions of 283mm x 283mm square.
- ***x3 pan*** - a pan having the equivalent area to that of three 200mm square pans. This pan has dimensions of 346mm x 346mm square.

All of the pans were fabricated from 3mm thick Stainless steel with the outside edge insulated with 20mm of Kaowool vacuum board to reduced edge effects to the fuel source through conduction into the pan. A photograph of a typical pan is shown in Figure 3.7 and shows the heptane fuel inlet at the base of the base pan and the insulation lining.

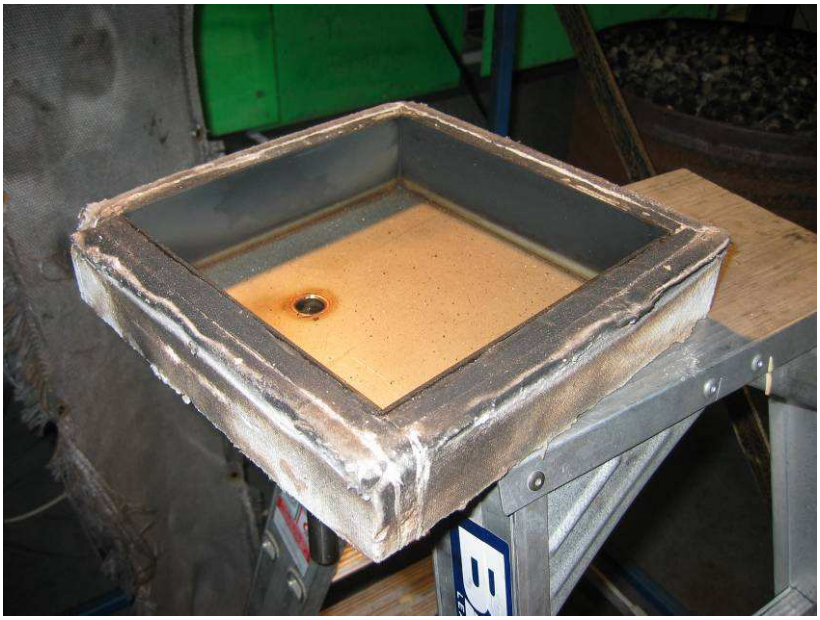

Figure 3.7: Photograph of a typical pool fire pan used showing inlet at the base of the pan and the insulation lining on all edges

3.2.4.b) Pan Locations

The pans were able to be positioned in three different locations within the room as shown in Figure 3.4. The three pan locations are noted based upon pan centreline dimensions;

a) ***Front***: The pan in the front location position was located 3000mm from the rear compartment wall.
b) ***Centre***: The pan in the centre location position was located 1800mm from the rear compartment wall.
c) ***Rear***: The pan in the rear position is located 600mm from the rear compartment wall.

The experiments evaluated pool fires in single locations as well as multiple locations. The locations used are detailed in Figure 3.8 and are;

a. *Single pan experiments*; rear, centre and front.
b. *Multiple pan experiments*; rear-centre, rear-front, centre-front and rear-centre-front.
c. *Equivalent area pan experiments*; x2 and x3 sized pans in the centre.

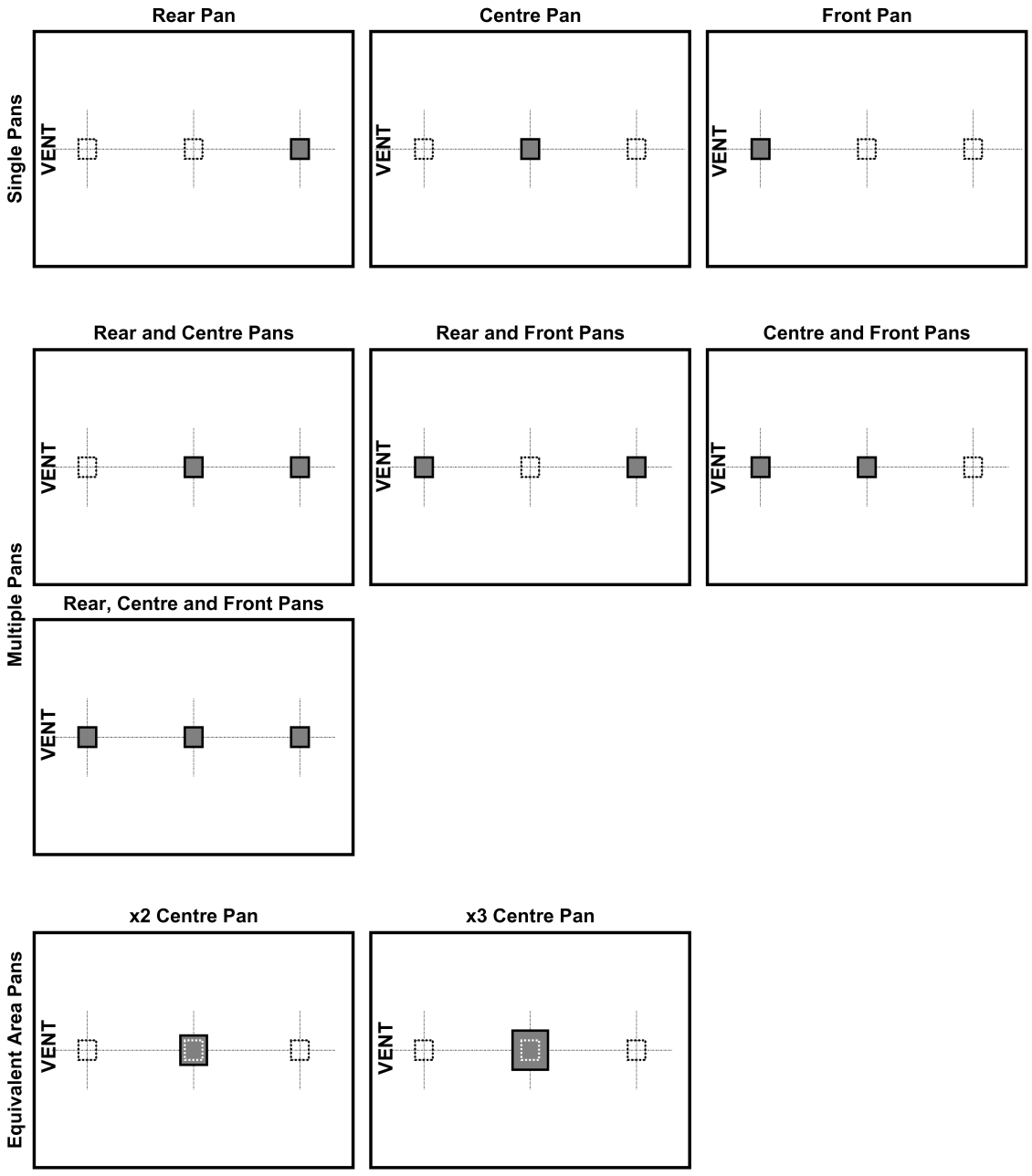

Figure 3.8: Sketch detailing the pan locations for the single, multiple and equivalent area compartment pool fire experiments.

Those pans not used in experiments remain empty in the enclosure and are not removed.

3.2.4.c) Fuel System Operation

Fuel was supplied to each of the compartment pans via constant head system. Heptane was pumped from three 40-litre pre fabricated stainless steel fuel tanks located underneath the compartment using a Masterflex tubing pump connected to three individual header tanks (one header tank per pan). Figure 3.9 shows a photograph of

the completed layout of the fuel system used in the experiments detailing the front, centre and rear header tanks, the tubing pump used to supply the fuel, and the rear fuel tank located on a load cell.

Each of the pool fire pan(s) were gravity fed from the individual header tanks through tubing connected to a pipe at the bottom of the pool fire pan. Each header tank allowed a constant head of heptane to flow to the pan with the overflow draining back to the fuel tank. The constant head was regulated by the speed of the tubing pump, and observation windows in the header tank allowed the flow to be monitored to ensure appropriate supply was maintained at all times. A schematic representation of the fuel system operation is shown in Figure 3.10 and shows fuel supply to the header tank, which is gravity feed to the pan, with excess fuel and drainage provided back to the fuel tank.

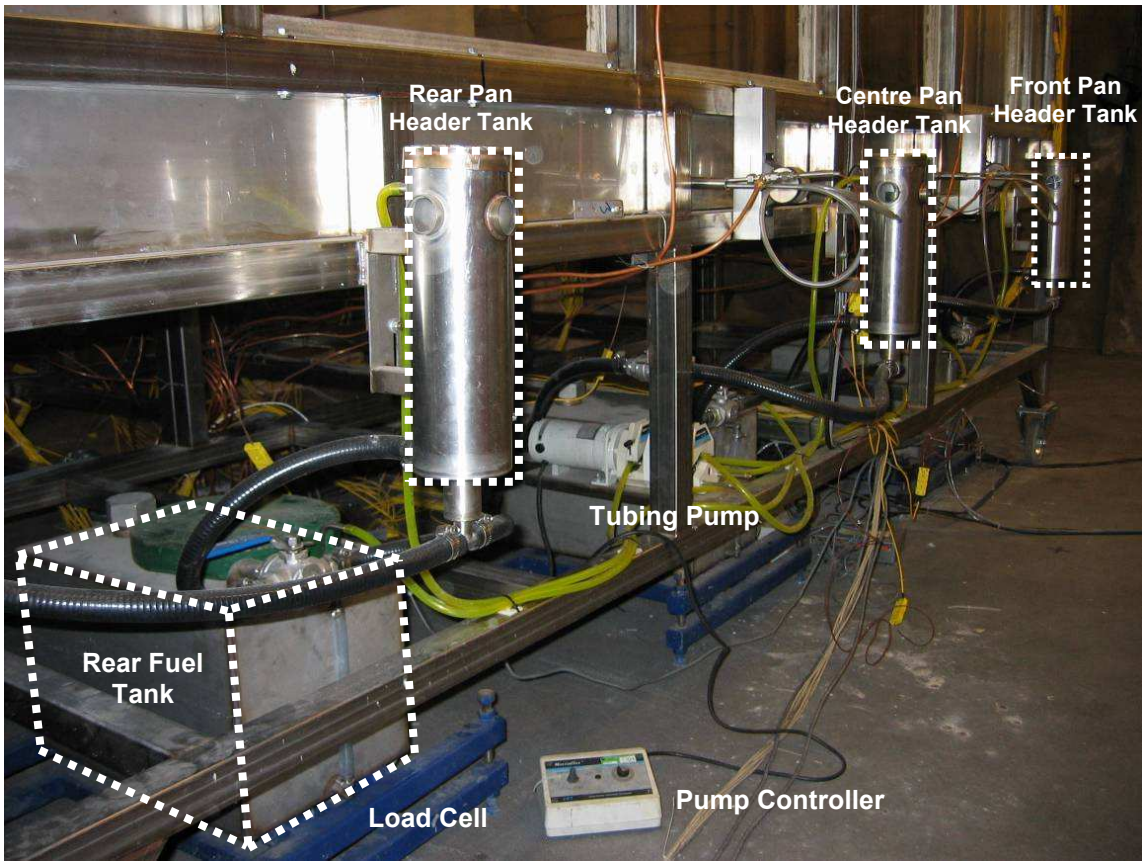

Figure 3.9: Photograph of the completed fuel system layout, showing the front, centre and rear header tanks, the tubing pump used to supply the fuel, and the rear fuel tank located on its load cell.

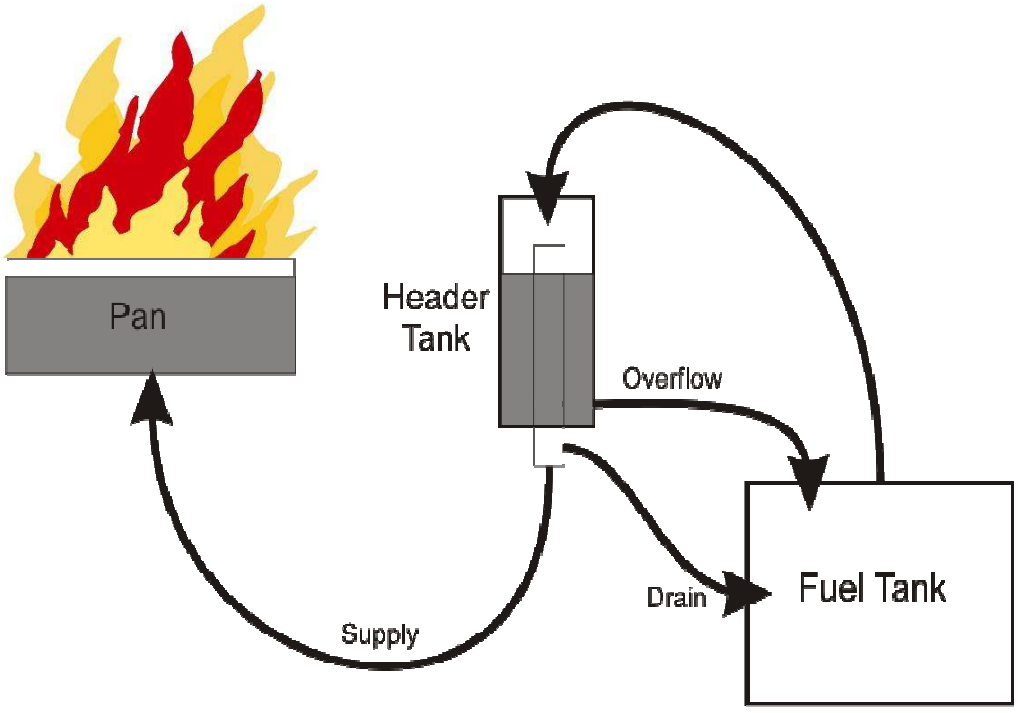

Figure 3.10: Schematic diagram showing the fuel system operation with the fuel supply to the header tank, which is gravity feed to the pan, with excess fuel and drainage provided back to the fuel tank.

The fuel level within the pans was keep at a height of approximately 5-10mm from the top of the pan in order to minimise the impact of edge effects from the pan. The fuel supply could be stopped in an emergency by inter-connected valves on the supply tanks. This allowed all supply to the pans to be stopped simultaneously if required.

3.2.4.d) Ignition

The heptane pans were ignited by a series of spark electrodes connected to two 15000 Volt transformers. The electrode formed an arc between the lip of the pan and the electrode sufficient to initiate ignition of the heptane.

3.3 Instrumentation

In total 215 channels of data were continuously logged during this experimental study. A spreadsheet detailing the instrumentation is provided in Appendix A with each of the measurements described in the following sections.

3.3.1 Data Acquisition

A Universal Data Logging, UDL, system developed at the University of Canterbury was used to log the experimental measurements. The system logs voltages from a wide range of devices including thermocouples, load cells, pressure transducers, and gas analysis, and consists of a combination of both software and hardware interfaces.

The hardware consists of a serial box for each type different sensing device which was then calibrated within the UDL programme using associated calibration and offset factors. For this experimental compartment 13 serial boxes were used to measure 215 channels. The logging was performed on a Pentium 4 computer running Windows XP Professional and the sample interval was 1 sample per second.

Experiments were run until a quasi-steady state was attained which meant running times of between 45 minutes to 120 minutes.

3.3.2 Temperature Measurements

Temperatures were monitored both inside and outside of the experimental enclosure. To measure the compartment gas temperatures, vertical thermocouple trees were installed at a number of locations. Typically 1.6 mm diameter type K stainless steel clad thermocouples were used although a number of aspirated thermocouples were also used as they reduce the magnitude of the errors in the upper and lower layers of a room fire and reduce the likelihood that large errors will occur in the lower layer [7, 8]

Aspirated thermocouples were made in accordance with Blevein and Pitts [9] using chromel-alumel thermocouples. In accordance with the ASTM, 1998 [10] which recommends that the gas velocity within aspirated thermocouples be maintained near 5 m/s, stating that this is "sufficiently high to allow accurate temperature measurement based on thermocouple voltage alone, even within flame zones". A reverse air blower was used to provide suction through the aspirated thermocouples and the corresponding air flow was tested using a wet test meter. The velocity was confirmed to be no less than 6m/s which was considered acceptable. The aspirated thermocouples were suctioned though copper lines, and it was noted that the copper lines were not water

cooled as natural convection provided sufficient cooling of the gas temperatures to the blower unit.

3.3.2.a) Corner Compartment Temperatures

To measure the compartment gas temperatures, vertical thermocouple trees were installed at the front and rear of the enclosure as thermocouples located in these regions are considered to provide a reasonable representation of temperatures within the compartment. Figure 3.11 shows a sketch of the experimental compartment showing the rear and front corner thermocouple tree locations.

Two sets of 15, 1.6 mm diameter type K thermocouples were used and positioned at a spacing of 100 mm vertically between the floor and ceiling. To avoid effects from the boundary layer, the thermocouples were installed 150 mm off the rear wall, 100mm of the side walls. The lowest thermocouple was located 25mm above the floor, then 50mm above the floor, with a subsequent spacing of 100mm. The highest thermocouples were located 25mm below the ceiling, then 50mm below the ceiling. The thermocouples were installed within 6mm stainless steel tubing for protection.

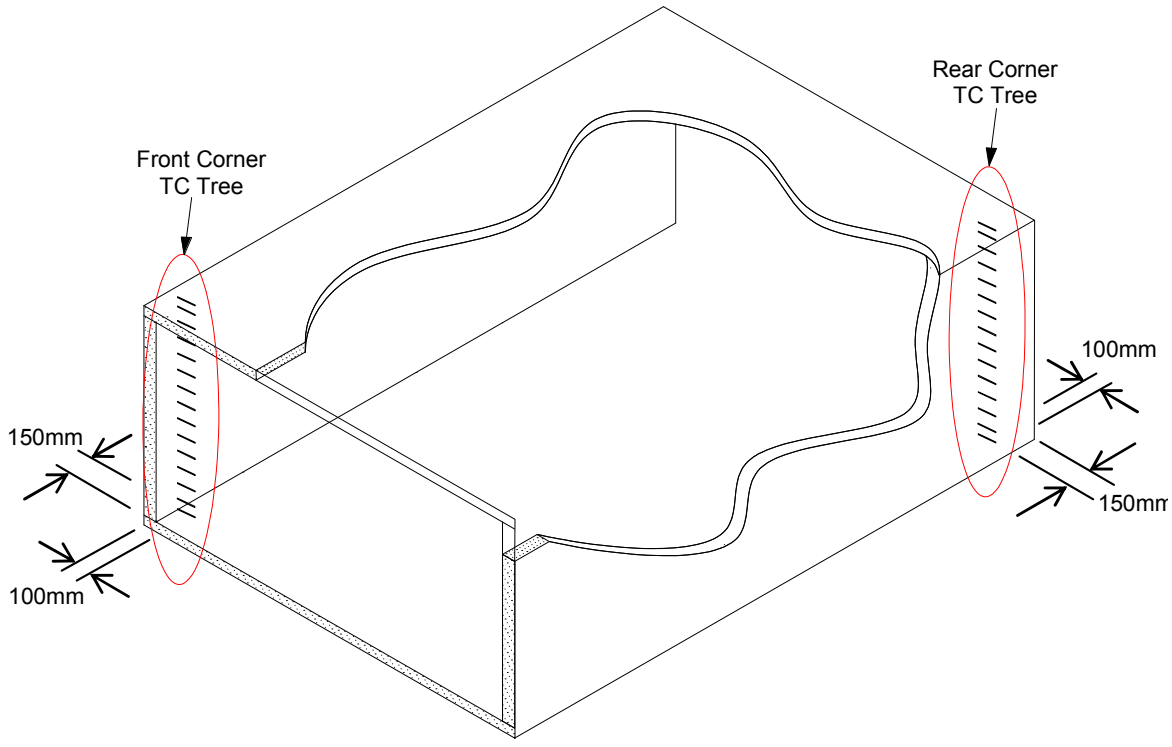

Figure 3.11: Sketch of the experimental compartment showing the rear and front corner thermocouple tree locations

3.3.2.b) Vent Temperatures

A thermocouple tree was installed along the centreline of the ventilation openings to record the vent flow temperatures in conjunction with the analysis of vent mass flows measurements. The fully open (11), soffit and door geometry experiments provided 13, 1.6 mm diameter type K thermocouples within the vent opening. The thermocouples were located within a stainless sheath for protection. The highest thermocouple was located 25mm below the top of the ventilation opening, then at 50mm below the top of the ventilation opening, with a subsequent spacing of 100mm. The lowest thermocouple was located 50mm above the bottom of the ventilation opening. Figure 3.12 shows a sketch of the experimental compartment showing the location of the vent thermocouple tree. Specific details on the location are given in section 3.3.4 Velocity Flow Measurements/Temperatures and in Figure 3.15.

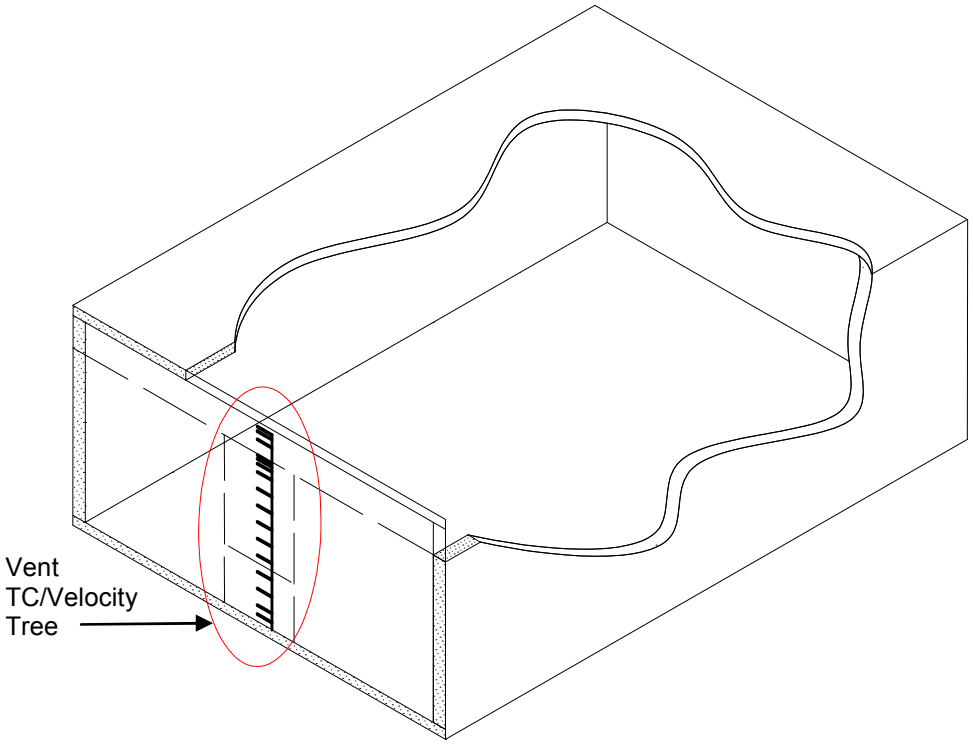

Figure 3.12: Sketch of the experimental compartment showing the location of the vent thermocouple tree and bi-directional probes

3.3.2.c) Centreline/Pan Temperatures

Three thermocouple trees were position along the centreline of the enclosure above each of the pool fire pan locations, front, centre and rear as detailed in Figure 3.13. 14, 1.6 mm diameter type K stainless steel clad thermocouples were positioned above each

plan. The highest thermocouple was located 25mm below the ceiling, then at 50mm below the ceiling, with a subsequent spacing of 100mm. A single thermocouple was also installed 50 mm above the centre of the fuel pan to measure the temperature above the pool fire.

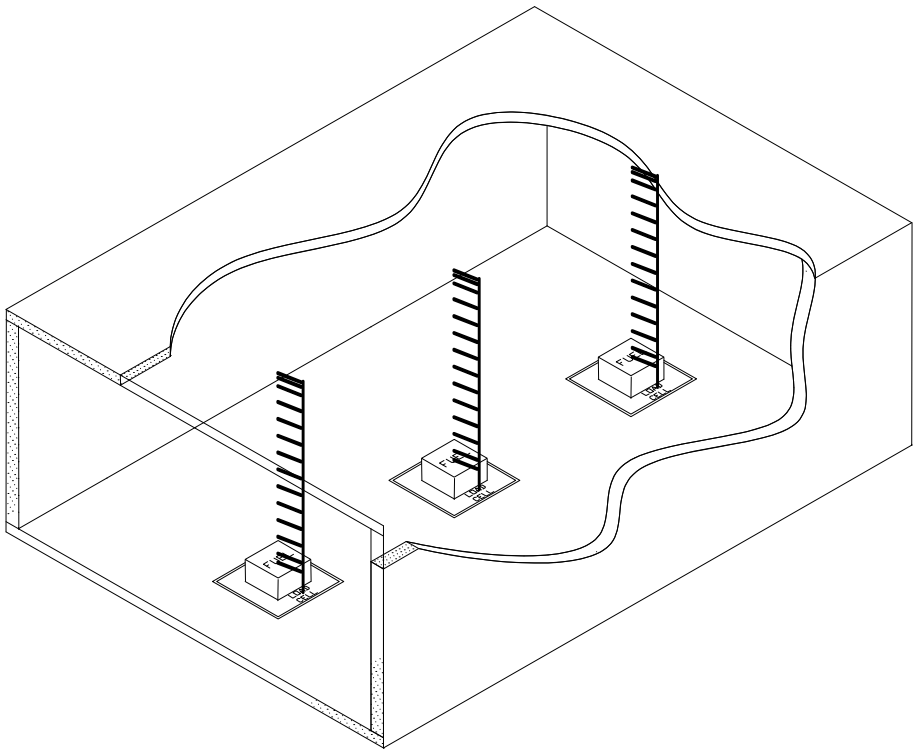

Figure 3.13: Sketch of the experimental compartment showing the centreline and pan thermocouple tree locations

3.3.2.d) External Wall Temperatures

As the experiments continued the compartment temperatures reached were considered high enough that they may impact the compartment structure so thermocouples were installed in a number of locations on the outside of the roof and the side wall of the compartment. The thermocouples were 1.6 mm diameter type K stainless steel clad thermocouples and were welded to the stainless steel structure and backed by a layer of 10mm Kaowool vacuum board.

3.3.3 Heat Flux Measurements

Gardon type water-cooled heat flux gauges were installed between the rear and centre pans and between the centre and front pans for measurement of the radiative heat flux at the floor. Due to the long durations of the experiments and the very high compartment temperatures, the heat flux gauges were damaged during the study and were not replaced.

Plate Thermocouples (PTC) were also installed in locations around the compartment predominantly relating to quarter points as can be seen by the black square areas in the photographs in Figure 3.2 and Figure 3.3. The PTC were installed to provide an inexpensive and simple method of measuring the heat flux at the floor, walls and ceiling around the compartment. The PTC consist of 150mm square stainless steel with a type-K thermocouple welded to the centre of the back and the exposed face painted with high temperature black paint. The plates were developed and calibrated following the principle present by Dillon [11] and Wickstrom [12]. Whilst the calibration of the thermocouple plates under the cone calorimeter and experiments undertaken by Yii [4], provided satisfactory results, early results in this experimental study indicated that the thermocouple plate results were not comparable with the heat flux measurements and that more development was required for use in a high temperature environment. Subsequently the measurements were not used.

3.3.4 Velocity Flow Measurements/Temperatures

Compartment pressures and vent flow velocities were monitored using the bi-directional probe developed by McCaffrey and Heskestad [13] and as discussed by Emmons [14]. This bi-directional probe consists of a 22mm diameter probe and is suitable for use in elevated temperature and situations in which high levels of soot can be expected. It is a robust, relatively simple probe and has an angular insensitivity to within about ±50° and an accuracy of about 5%. Each probe was connected to a differential pressure transducer with a pressure range of 0-25 Pa. Measurements of the local temperature was either by type K thermocouple or aspirated thermocouples.

Measurements of the temperature and differential pressure across the Bi-directional probe allow the local velocities to be determined by applying simple Bernoulli analysis as noted in the following expression [14].

$$V = 0.93\sqrt{\frac{2\Delta p}{\rho}} \qquad \textbf{where } \rho = \frac{352.8}{T}$$

3.3.4.a) Internal Instrumentation

Eight Bi-directional probes were installed within the compartment to investigate the behaviour between the pool fire pans at locations 1200mm from the rear wall and 2400mm from the rear wall. Three long probes were located along the centreline at the following heights measured from the ceiling; 25mm, 600mm (mid height of the enclosure), and 1175mm. Two sets of two probes were also installed 600mm from each of the side walls at 25mm from the ceiling and 1175mm from the ceiling. These locations are noted in detail in cross sectional sketch in Figure 3.14. All temperature measurements at these locations were taken using aspirated thermocouples.

The long bi-directional probes located along the centreline of the room required bracing to ensure their reading location was not significantly affected. Therefore they were supported on a counterweighted stainless steel wire system. This helped ensure that the stainless steel line was tight and reduced the sagging of the probes due to the high compartment temperatures. The shorter probes were considered to be less likely to be affected by the temperatures to the same extent as the longer centreline probes. This was observed to be the case during the experiments such that they had sufficient inherent strength and did not require any additional bracing.

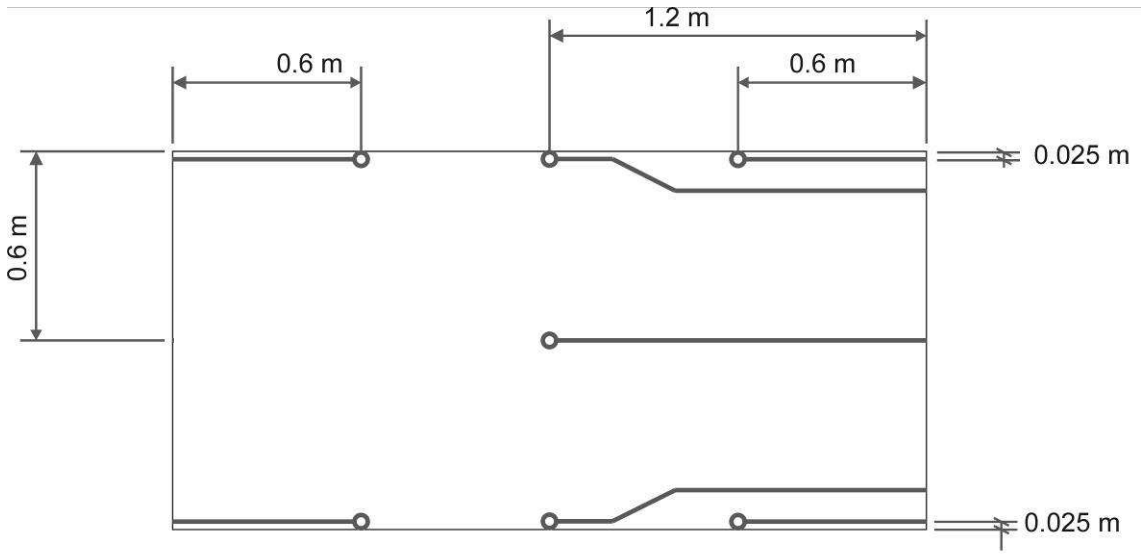

Figure 3.14: Cross-sectional sketch through the compartment showing the internal aspirated thermocouple and bi-directional probe locations

3.3.4.b) Vent Instrumentation

10 Bi-directional probes were also installed in the vent when the Full/Soffit/Door geometry was used, and 8 when the window/small window geometry was used. Details of the probe location for each of the ventilation scenarios, Full, Soffit/Door, and Window/Small Window are noted in the cross sectional sketch through the compartment in Figure 3.15.

Temperature measurements at these locations were taken using 1.6 mm diameter type K bare bead thermocouples, unless noted by * which indicated the use of aspirated thermocouples. The bi-directional probes and thermocouples were supported through a bracing system attached to the front of the compartment. It is noted that the thermocouple tree temperatures were not corrected for radiation and the aspirated thermocouples were not use in the reduction of vent velocities.

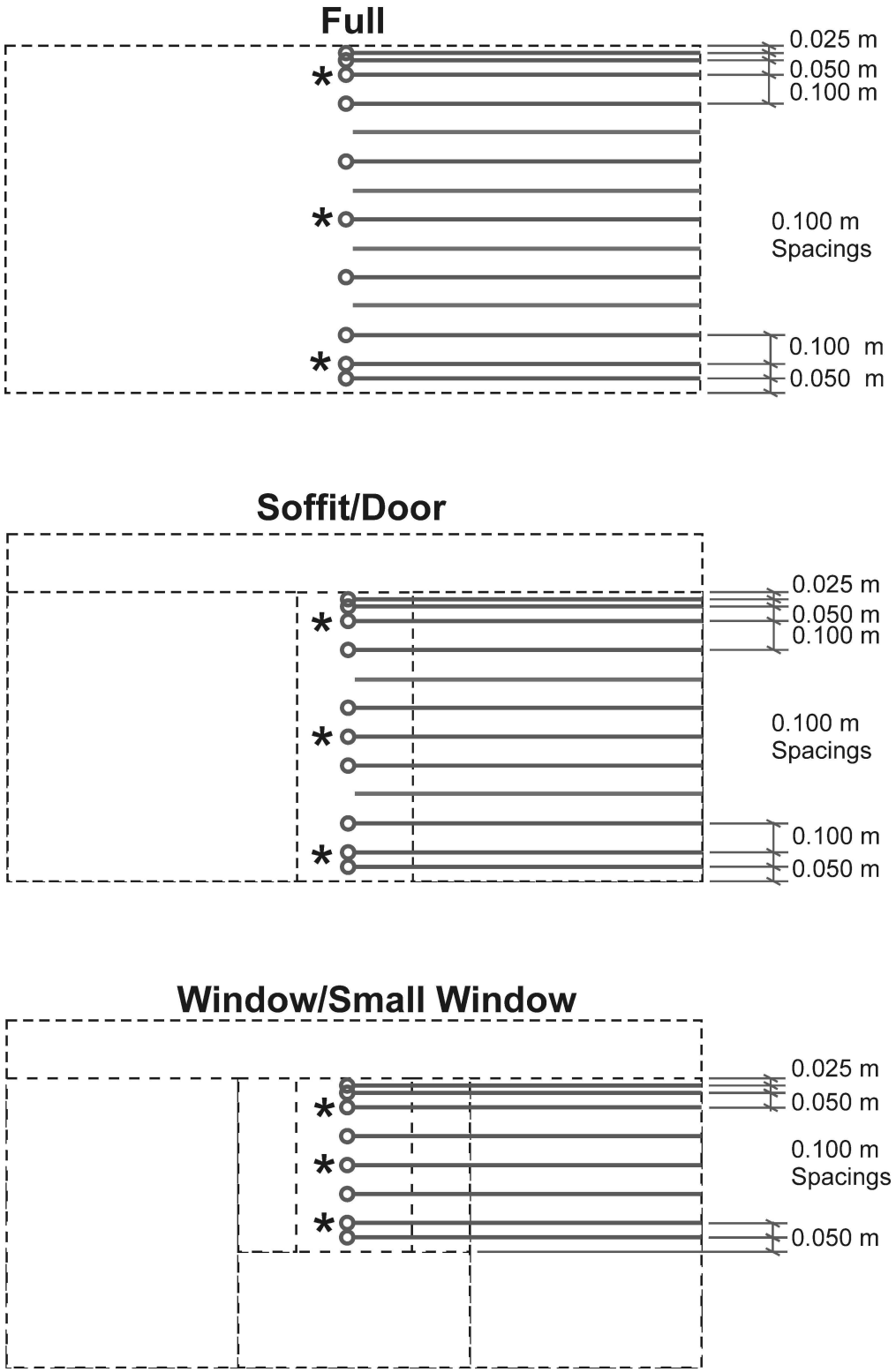

Figure 3.15: Cross sectional sketch of the vent thermocouple and bi-directional probe locations for the fully open, soffit, door, window and small window vent geometries. * indicates the locations of aspirated thermocouples.

3.3.5 Mass Loss

The mass loss of each individual pan was recorded on separate load cell platforms under each fuel tank. The load cells were calibrated and reported to have an accuracy of ±0.001kg. The initial mass was recorded at the start of each experiment for calibration and was continuously logged during each experiment.

3.3.6 Heat Release Rate

The heat release rate from each experiment was measured using oxygen depletion calorimetry and included O_2, CO_2, and CO species measurements with a Siemens Ultramat 6 Non Dispersive Infra Red (NDIR) analyser. The extraction system had a maximum flow rate of $4m^3/s$.

3.3.7 Combustion Species

After initial calibration experiments, nine sampling probes were installed round the base of each of the pans to sample combustion species at the base of each pool fire. The sampling probes were located 150mm from the front and side of each pan. This is shown in the photograph Figure 3.16.

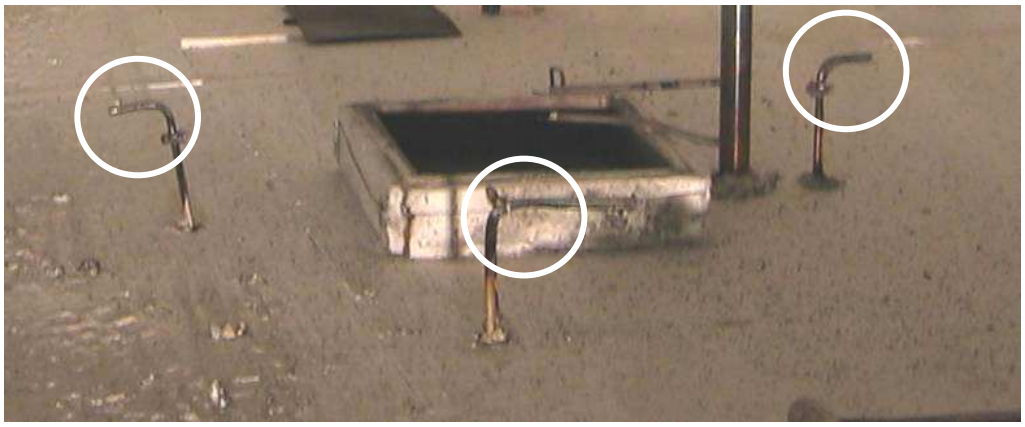

Figure 3.16: Photograph showing species sampling location at the base of the pans

All nine sampling tubes were connected to a multiple valve system leading to a Siemens Ultramat 6 O_2, CO_2, and CO analyser. Only one sample port could be sampled at any point in time and measurements were taken on a 5 minute revolving cycle bases. Temperatures were also measured at these locations using chromel-alumel thermocouples. As the experiments continued the sampling lines were susceptible to

blockage due to the sooty environment and the measurements were not continued. It would be recommended that any future use of these sampling probes would include the addition of an air pulse unit to enable periodic high pressure clearing of the sample lines.

3.4 Experimental Matrix and Procedure

The aim of this experimental study was to provide a set of pool fire enclosure experiments for five ventilation geometries, fully open , soffit, door, window and small window; with permutations of single and multiple pool fires in three different locations. Experiments with equivalent pan areas were also provided.

The completed matrix of 34 compartment experiments completed is detailed in Table 3.1. Three experiments were also conducted in the open under quiescent conditions to provide a base case comparison for the single 200mm square pan, the x2 equivalent area (283mm square) pan, and the x3 equivalent (346mm square) pan. All experiments were conducted in the fire laboratory at the University of Canterbury.

It should be noted that due to the excessively high temperatures achieved in the compartment experiments (up to 1200°C), and the long durations of the experiments (up to 2 hours), the compartment components (in particular the kaowool lining) were significantly affected. The initial set of experiments using fully open and soffit ventilation geometries provided significant ventilation into the compartment with no subsequent adverse effects on the compartment structure. However during the door and window ventilation geometries, extremely rapid fire growth and high temperatures were observed and it was decided to reduce the ventilation into a compartment to the small window geometry such that under-ventilated conditions could be achieved. This was expected to reduce the impact of the compartment fire on the structure. After the completion of the small window set of experiments the compartment was in poor condition to allow a complete set of door and window experiments to be performed. Hence a completed set of door and window experiments was not attained.

Table 3.1: Completed Experimental Matrix

		Opening Geometry				
		Full Open	*Soffit* 0.2m (downstand)	*Door* 1.0m x 0.4m	*Window* 0.6m x 0.8m	*Small Window* 0.6m x 0.4m
Pan Location	Rear Pan	×	×	×	×	×
	Centre Pan	×	×	×	×	×
	Front Pan	×	×	×	×	×
	Rear & Centre	×	×	×	-	×
	Rear & Front	×	×	-	-	×
	Centre & Front	×	×	-	-	×
	x2 Pan (Centre)	×	×	-	-	×
	All Pans	×	×	-	-	×
	x3 Pan (Centre)	×	×	-	-	×

3.4.1 Procedure

The typical pool fire does not reach a steady state condition instantaneously due to the transient effects of conduction losses into the liquid, pan edge and bottom heating effects, and the effect of the pan lip on the convective and radiative fluxes back to the pool surface. As the fire grows the radiative effects from the enclosure boundaries also provide enhancement effects. It is generally suggested as a guide that 10 minutes or more may be required before steady state burning is attained.

Each experiment involved calibration of the oxygen depletion calorimetry system before commencement. A three minute baseline was also taken to record the initial conditions, with ignition of the pan at three minutes. Each experiment was allowed to run for a duration of between 45 minutes to 120 minutes; dependent upon the size of the ventilation opening and fuel source. The experiment was stopped once compartment temperatures and oxygen depletion appeared to reach a quasi-steady state. Due to the high temperatures reached in the experiments, before each experiment the room was inspected to ensure correct placement of all measuring devices and the logging of channels were confirmed.

3.5 References

1 ISO 9705:1993, Fire Tests – Full Scale Room Test for Surface Producs, International Organisation for Standardization, 1993.

2 Karlsson, B and Quintiere, J., Enclosure Fire Dynamics, CRC Press, 2001

3 Parkes, A.R, "Underventilated Compartmetn Fires – A Precuser to Smoke Explosion", Master thesis, Univesity of Canternbury

4 Yii, E "Modelling the Effects of Fuel Types and Ventilation Openings on Post-Flashover Compartment Fires" PhD Thesis, University of Canterbury, 2002

5 Thomas, I., Moinuddin, K, Bennetts, I, "Fire Development In A Deep Enclosure, " Fire Safety Science -- Proceedings of the Eight International Symposium, International Association for Fire Safety Science, 2005, pp. 1277-1288

6 Thomas, I.R., Bennetts, I.D. "Fires In Enclosures With Single Ventilation Openings - Comparison Of Long And Wide Enclosures, " Fire Safety Science -- Proceedings of the Sixth International Symposium, International Association for Fire Safety Science, 2000, pp. 941-952

7 Blevins, L. "Behavior of Bare and Aspirated Thermocouples in Compartment Fires" Proceedings of the 33rd National Heat Transfer Conference August 15-17, 1999, Albuquerque, New Mexico, HTD99-280.

8 Blevins, L. G. and Pitts, W. M., "Modeling of Bare and Aspirated Thermocouples in Compartment Fires", Building and Fire Research Laboratory, National Institute of Standards and Technology, 1999, N1STIR 6310.

9 Blevins, L. and Pitts, W., "Modeling of Aspirated Thermocouples (Suction Pyrometers) for Fire Research", Building and Fire Research Laboratory, National Institute of Standards and Technology, 1997, N1STIR.

10 ASTM 603-98a, Standard Guide for Room Fire Experiments, Annual Book of ASTM Standards, Vol. 04.07.

11 Dillon, S. E, "Analysis of the Iso 9705 Room/Corner Test: Simulations, correlations and Heat Flux Measurements", NIST-GCR-98-756, 1998

12 Wickström, U., :The Plate Thermometer – A Simple Instrument for Reaching Harmonized Fire Resistance Tests:, Fire Technology, Second Quarter, pp 195-208, 1994

13 McCaffrey, B.J. and Heskestad, G., "Brief Communications: A Robust Bidirectional Low Velocity Probe for Flame and Fire Application," Combustion and Flame, Vol.26, 1976, pp.125 –127.

14 Emmons, H., "Vent Flows" SFPE Handbook of Fire Protection Engineering, 2nd Edn, National Fire Protection Association, Quincy, MA,1995.

Chapter 4: Equivalence Ratio 'Phi' Meter Development

This chapter is presented in the form of a paper submitted to a peer reviewed Journal describing the development, calibration, and experimental use of an enhanced Equivalence Ratio apparatus, 'Phi Meter'. The phi meter was developed to measure the time dependent equivalence ratio from enclosure fire experiments undertaken in conjunction with this research study as an aid to the classification of compartment fire behaviour. This enhanced phi meter was developed and configured on the principle of measuring O_2, CO_2 and CO combustion species and details of the formulation and derivation of the equivalence ratio equations is presented. A description of the apparatus and its calibration with propane and methane is detailed. The use of the phi meter in practical fire situations is also discussed along with practical considerations for continued use and future development.

The Development of the University of Canterbury Phi Meter

A. R. PARKES and C. M. FLEISCHMANN
University of Canterbury
Christchurch,
New Zealand

4.1 Abstract

This paper describes the development, calibration, experimental application of an enhanced Equivalence Ratio apparatus, or 'Phi Meter'. This phi meter was developed to measure the time dependent equivalence ratio from enclosure fire experiments. As with all combustion calorimetry, accuracy of the results increases with the number of species being measured and this phi meter was developed and configured to measure O2, CO2 and CO. The results indicate that the equivalence ratios measured for heptane pool fires range from 0.1 for oxygen rich conditions to 2.3 for fuel rich conditions.

KEYWORDS: equivalence ratio, phi meter, compartment fires, heptane

4.2 Introduction

The ventilation geometry of an enclosure during a fire is one of the most important variables governing the behaviour of a compartment fire. The amount of oxygen available for combustion influences the consequent production of combustion gases such as CO and CO_2. The equivalence ratio is a parameter that is becoming increasingly popular to describe the ventilation conditions during a fire. As part of a greater experimental pool fire study, an Equivalence Ratio (ϕ, phi) meter was designed and developed to aid in the analysis of the experimental results.

The phi meter apparatus measures the fuel/oxygen ratio compared with the stoichiometric fuel/oxygen ratio. The equation for the equivalence ratio is:

$$\phi = \frac{\left(\dot{m}_{fuel} / \dot{m}_{oxygen} \right)_{sample}}{\left(\dot{m}_{fuel} / \dot{m}_{oxygen} \right)_{Stoichiometry}} \qquad \textbf{(4.2-1)}$$

The equivalence ratio is an important parameter as it allows the determination of the level of oxygen available for combustion, and experimentally can indicate a measure of the level of ventilation during a compartment fire, e.g. fuel-rich or fuel-lean combustion. This can then indicate the production and composition of fire gases.

When $\phi<1$ this is considered an oxygen rich condition, which means that sufficient oxygen is theoretically available for complete combustion. When $\phi>1$ this indicates the regime when there is a fuel rich situation and there is not enough oxygen available for complete combustion. Subsequently as the ventilation geometry within the experimental enclosure is reduced, then the more un-pyrolysed products are formed and the more CO is expected to be produced. Studies indicate that the combustion yields are dependent upon the equivalence ratio [1,2] which are driven by ventilation.

The phi meter principle is based upon the oxygen consumption technique, the basis of which Thornton in 1917 [3] showed that for most organic liquids and gases that a more or less constant net amount of heat is released per unit mass of oxygen consumed for complete combustion [4]. This is of course also used to calculate the heat release rate during the compartment experiments.

The terms Global Equivalence Ratio (GER) and 'Local' Equivalence Ratio (ER) are used in this paper, and can be distinguished by the following difference. The GER is the equivalence ratio of the overall combustion process being measured. In the case of a compartment fire, the control volume is taken as the entire compartment. It does not account for any variation due to experimental sampling techniques such as single versus multiple sampling points, and sampling locations such as measurements in the compartment gas layer, vent, or in an exhaust hood [5]. The GER concept is discussed in detail by Pitts [6,7]. When the combustion process and sample flow mixture is taken

from a sampling probe then this is generally referred to as the equivalence ratio or local equivalence ratio as the result is dependent upon the sampling location and spatial variations. As the sampling probe used consists of a single point source this apparatus was considered to provide a local equivalence ratio, ER.

The original phi-meter was presented by Babrauskas et al. in 1994 [8]. This apparatus was further developed by Andersson et al [9,10]. Both phi-meters were designed to be a simple and versatile portable measuring device. Due to this simple nature, the apparatus' proposed to measure only the oxygen species with the CO_2 being removed by Ascarite chemical sorbant (active ingredient NaOH), and CO being re-combusted to CO_2 in the combustion process. H_2O was removed by either Drierite desiccant (active ingredient $CaSO_4$) and/or magnesium perchlorate. The sorbant media used for removing the CO_2 and H_2O in these phi-meters are a very important component, however they can be prone to clogging and can be expensive. Therefore it was considered beneficial to measure additional species if instrumentation were available. The accuracy of the phi-meter may also be expected to be improved by measuring the concentration of CO_2 and CO. As the analysers used are unable to handle wet gas mixtures, the O_2, CO_2 and CO are measured on a dry basis with the H_2O removed from the sample stream using (Drierite) desiccant.

4.3 The Phi Meter Concept

The concept behind the phi meter as presented by Babrauskas [8] and Lönnermark [11] is to sample the combustion gases from the enclosure, introduce oxygen whilst at the same time stimulating a combustion process. This combustion process burns all the remaining combustion gases and reduces the carbon atoms in the fuel to CO_2, and all of the hydrogen atoms to H_2O.

To stimulate combustion, the process must provide for two situations; the oxygen rich/fuel lean case and the fuel rich/oxygen lean case. In the first case sufficient oxygen is present in the sample mixture such that complete combustion is able to occur. However for the fuel rich case, sufficient oxygen is not present and complete combustion will not occur without assistance. In this instance a fixed amount of oxygen

is introduced into the sample flow to ensure that complete combustion occurs in such cases where the sample mixture is fuel rich.

The combustion gases are then past though a heated catalyst which combusts the gas stream leaving only CO_2, H_2O and O_2. The CO_2, and H_2O are removed leaving only oxygen to be analysed. Therefore to determine the original phi meter equivalence ratio the oxygen concentration is measured:

a). for the ambient air without oxygen added;

b). for ambient air with oxygen added, and

c). for the sampled combustion products with oxygen added.

In this study an enhanced Phi Meter was developed and configured to measure not only O_2 but CO_2 and CO as well. As the species instrumentation cannot handle H_2O in the sample flow, the water was removed from the sample by cooling the sample to condense the water and then passing the sample flow through Drierite desiccant (active ingredient $CaSO_4$) before measurements are made. Therefore all the O_2, CO_2 and CO measurements are taken on a dry basis.

The measurement of CO means that the resolution of complete combustion is not required to ensure the sample mixture reduces carbon atoms to CO_2. This means that a heated combustion catalyst as used in the phi meters by Babrauskas and Andersson was not required as the re-derived equations used to determine the ER used the measurements for the CO_2 and CO species. However the phi meter was designed to be used on compartment experiments using heptane pool fires, and as such a significant degree of soot was expected. Therefore a catalyst was used to ensure complete combustion whist limiting any carbon build up and any potential blockages in the sample lines.

Given therefore that the equivalence ratio relationship was based upon a simplified phi meter in which only oxygen was measured, the additional sampling of CO_2 and CO requires a re-evaluation of the equivalence ratio equations. The following relationship has been derived below to account for the additional species.

4.4 Phi Meter Equations

The original phi-meter apparatus sampled and measured only O_2 species, however in this study the CO_2 and CO species were left in the sample, therefore a new formulation was required. The following details the derivation of the equivalence ratio equations following the process described by Babrauskas [8] for use with sampling O_2, CO_2 and CO species.

The equivalence ratio is commonly defined as:

$$\phi = \frac{\left(\dot{m}_{fuel} / \dot{m}_{oxygen} \right)_{sample}}{\left(\dot{m}_{fuel} / \dot{m}_{oxygen} \right)_{Stoichiometry}}$$

This situation is the simplest form in which the sample flows are unburned prior to entering the tube furnace and that no additional oxygen added. This represents a well ventilated fire in which the equivalence ratio is considered to be less than 1.

where $\left(\dot{m}_{fuel}\right)_{sample} = \left(\dot{m}_{fuel}\right)_{stoicheometry}$

$$\phi = \frac{\left(\dot{m}_{oxygen} \right)_{Stoichiometry}}{\left(\dot{m}_{oxygen} \right)_{ambient}} \qquad \textbf{(4.4-1)}$$

Now the molar flow of oxygen required for complete combustion can be considered as:

$$\left(\dot{m}_{oxygen} \right)_{stoichiometry} = \left(\dot{m}_{oxygen} \right)_{ambient} - \left(\dot{m}_{oxygen} \right)_{sample} \qquad \textbf{(4.4-2)}$$

$$= \left(\dot{m}_{oxygen} \right)^{o} - \left(\dot{m}_{oxygen} \right)_{sample} \quad \textbf{(4.4-3)}$$

and substitution into equation (4.4-1) provides:

$$\phi = \frac{\left(\dot{m}_{oxygen} \right)^{o} - \left(\dot{m}_{oxygen} \right)_{sample}}{\left(\dot{m}_{oxygen} \right)^{o}} \quad \textbf{(4.4-4)}$$

And as the nitrogen does not participate in the combustion process, the mass flow rate of nitrogen is conserved into and out of the phi meter. Therefore dividing through by the Nitrogen flow rate where $\dot{m}^{o}_{N_2} = \dot{m}_{N_2}$ gives:

$$\phi = \frac{\frac{\dot{m}^{o}_{O_2}}{\dot{m}^{o}_{N_2}} - \frac{\dot{m}_{O_2}}{\dot{m}_{N_2}}}{\frac{\dot{m}^{o}_{O_2}}{\dot{m}^{o}_{N_2}}} \quad \textbf{(4.4-5)}$$

As the ratio of the molar flows is equal to the ratio of the mole fractions, the equivalence ratio can be expressed in terms of mole fractions.

Mole fractions are expressed as:

$$\mathrm{X}_i = \frac{n_i}{\sum n} \quad \textbf{(4.4-6)}$$

where

$$m_i = n_i M_i \quad \textbf{(4.4-7)}$$

Therefore the mole fraction can be expressed as:

$$X_i = \frac{\frac{m_i}{M_i}}{\sum \frac{m_i}{M_i}} \qquad \textbf{(4.4-8)}$$

and for the transient flow situation;

$$X_i = \frac{\frac{\dot{m}_i}{M_i}}{\sum \frac{\dot{m}_i}{M_i}} \qquad \textbf{(4.4-9)}$$

Therefore the mole fractions of oxygen as expressed in the phi meter relationship in equation (4.4-5) will be:

$X^o_{O_2}$ = mole fraction of the ambient case prior to the experiment, and

X_{O_2} = mole fraction during the experiment

The following relationship for mole fractions in the ambient case prior to the experiment can be expressed as:

$$X^o_{O_2} = \frac{\frac{\dot{m}^o_{O_2}}{M_{O_2}}}{\frac{\dot{m}^o_{O_2}}{M_{O_2}} + \frac{\dot{m}^o_{N_2}}{M_{N_2}} + \frac{\dot{m}^o_{CO_2}}{M_{CO_2}} + \frac{\dot{m}^o_{CO}}{M_{CO}}} \qquad \textbf{(4.4-10)}$$

and conversely during the experiment the mole fraction is represented as follows:

$$X_{O_2} = \frac{\frac{\dot{m}_{O_2}}{M_{O_2}}}{\frac{\dot{m}_{O_2}}{M_{O_2}} + \frac{\dot{m}_{N_2}}{M_{N_2}} + \frac{\dot{m}_{CO_2}}{M_{CO_2}} + \frac{\dot{m}_{CO}}{M_{CO}}} \qquad \textbf{(4.4-11)}$$

Rearranging the equations above gives the following expression for the ambient case prior to the experiment:

$$\frac{\dot{m}^o_{O_2}}{M_{O_2}} + \frac{\dot{m}^o_{N_2}}{M_{N_2}} + \frac{\dot{m}^o_{CO_2}}{M_{CO_2}} + \frac{\dot{m}^o_{CO}}{M_{CO}} = \frac{\frac{\dot{m}^o_{O_2}}{M_{O_2}}}{\mathrm{X}^o_{O_2}} \qquad \textbf{(4.4-12)}$$

and the corresponding expression during the experiment:

$$\frac{\dot{m}_{O_2}}{M_{O_2}} + \frac{\dot{m}_{N_2}}{M_{N_2}} + \frac{\dot{m}_{CO_2}}{M_{CO_2}} + \frac{\dot{m}_{CO}}{M_{CO}} = \frac{\frac{\dot{m}_{O_2}}{M_{O_2}}}{\mathrm{X}_{O_2}} \qquad \textbf{(4.4-13)}$$

Re-arranging the above in terms of the mass flow rate $\dot{m}^o_{O_2}$ where:

$$\mathrm{X}^o_{N_2} = 1 - \mathrm{X}^o_{O_2} - \mathrm{X}^o_{CO_2} - \mathrm{X}^o_{CO} = \frac{\frac{\dot{m}^o_{N_2}}{M_{N_2}}}{\frac{\dot{m}^o_{O_2}}{M_{O_2}} + \frac{\dot{m}^o_{N_2}}{M_{N_2}} + \frac{\dot{m}^o_{CO_2}}{M_{CO_2}} + \frac{\dot{m}^o_{CO}}{M_{CO}}} \qquad \textbf{(4.4-14)}$$

then the equation above becomes:

$$\frac{\dot{m}^o_{O_2}}{M_{O_2}} + \frac{\dot{m}^o_{N_2}}{M_{N_2}} + \frac{\dot{m}^o_{CO_2}}{M_{CO_2}} + \frac{\dot{m}^o_{CO}}{M_{CO}} = \frac{\dot{m}^o_{N_2}}{M_{N_2}}\left[\frac{1}{\left(1 - \mathrm{X}^o_{O_2} - \mathrm{X}^o_{CO_2} - \mathrm{X}^o_{CO}\right)}\right] \qquad \textbf{(4.4-15)}$$

And dividing through by $\frac{\dot{m}^o_{O_2}}{M_{O_2}}$ gives:

$$\frac{1}{\mathrm{X}^o_{O_2}} = \frac{M_{O_2}}{\dot{m}^o_{O_2}}\frac{\dot{m}^o_{N_2}}{M_{N_2}}\left[\frac{1}{\left(1 - \mathrm{X}^o_{O_2} - \mathrm{X}^o_{CO_2} - \mathrm{X}^o_{CO}\right)}\right] \qquad \textbf{(4.4-16)}$$

Therefore prior to the experiment to mass flow of oxygen is expressed as:

$$\dot{m}^{o}_{O_2} = \dot{m}^{o}_{N_2} \frac{M_{O_2}}{M_{N_2}} \left[\frac{\mathrm{X}^{o}_{O_2}}{\left(1 - \mathrm{X}^{o}_{O_2} - \mathrm{X}^{o}_{CO_2} - \mathrm{X}^{o}_{CO}\right)} \right] \quad \textbf{(4.4-17)}$$

and similarly during the experiment the mass flow:

$$\dot{m}_{O_2} = \dot{m}_{N_2} \frac{M_{O_2}}{M_{N_2}} \left[\frac{\mathrm{X}_{O_2}}{\left(1 - \mathrm{X}_{O_2} - \mathrm{X}_{CO_2} - \mathrm{X}_{CO}\right)} \right] \quad \textbf{(4.4-18)}$$

Substituting equations (4.4-17) and (4.4-18) into the initial equivalence ratio function in equation (4.4-1) gives:

$$\phi = \frac{m^{o}_{N_2} \frac{M_{O_2}}{M_{N_2}} \left[\frac{\mathrm{X}^{o}_{O_2}}{\left(1 - \mathrm{X}^{o}_{O_2} - \mathrm{X}^{o}_{CO_2} - \mathrm{X}^{o}_{CO}\right)} \right] - \dot{m}_{N_2} \frac{M_{O_2}}{M_{N_2}} \left[\frac{\mathrm{X}_{O_2}}{\left(1 - \mathrm{X}_{O_2} - \mathrm{X}_{CO_2} - \mathrm{X}_{CO}\right)} \right]}{m^{o}_{N_2} \frac{M_{O_2}}{M_{N_2}} \left[\frac{\mathrm{X}^{o}_{O_2}}{\left(1 - \mathrm{X}^{o}_{O_2} - \mathrm{X}^{o}_{CO_2} - \mathrm{X}^{o}_{CO}\right)} \right]} \quad \textbf{(4.4-19)}$$

It is assumed that as the mass flow rate of N_2 is conserved and does not participate in the combustion reactions, then $\dot{m}^{o}_{N_2} = \dot{m}_{N_2}$.

Subsequently rearranging the above in terms of $\dot{m}_{N_2}$ leads to:

$$\phi = \frac{\left[\frac{X^o_{O_2}}{\left(1 - X^o_{O_2} - X^o_{CO_2} - X^o_{CO}\right)}\right] - \left[\frac{X_{O_2}}{\left(1 - X_{O_2} - X_{CO_2} - X_{CO}\right)}\right]}{\left[\frac{X^o_{O_2}}{\left(1 - X^o_{O_2} - X^o_{CO_2} - X^o_{CO}\right)}\right]}$$

(4.4-20)

$$= \frac{\left[\frac{X^o_{O_2}\left(1 - X_{O_2} - X_{CO_2} - X_{CO}\right) - X_{O_2}\left(1 - X^o_{O_2} - X^o_{CO_2} - X^o_{CO}\right)}{\left(1 - X^o_{O_2} - X^o_{CO_2} - X^o_{CO}\right)\left(1 - X_{O_2} - X_{CO_2} - X_{CO}\right)}\right]}{\left[\frac{X^o_{O_2}}{\left(1 - X^o_{O_2} - X^o_{CO_2} - X^o_{CO}\right)}\right]}$$

(4.4-21)

Therefore the equivalence ratio term for the oxygen rich regime is represented by the following:

$$\phi = \frac{X^o_{O_2}\left(1 - X_{O_2} - X_{CO_2} - X_{CO}\right) - X_{O_2}\left(1 - X^o_{O_2} - X^o_{CO_2} - X^o_{CO}\right)}{X^o_{O_2}\left(1 - X_{O_2} - X_{CO_2} - X_{CO}\right)} \quad \text{for } \phi < 1$$

(4.4-22)

or

$$\phi = 1 - \frac{X_{O_2}}{X^o_{O_2}} \frac{\left(1 - X^o_{O_2} - X^o_{CO_2} - X^o_{CO}\right)}{\left(1 - X_{O_2} - X_{CO_2} - X_{CO}\right)} \quad \text{for } \phi < 1 \qquad \textbf{(4.4-23)}$$

As the term above represents the regime of no additional oxygen, this means that it is limited to the oxygen rich regime and cannot be used for the fuel rich regime.

To allow for the fuel rich case oxygen must be added to the gas flow stream. Therefore the molar flow of oxygen required for complete combustion including the added oxygen stream can be considered as:

$$\left(\dot{m}_{oxygen}\right)_{stoichiometry} = \left(\dot{m}_{oxygen}\right)_{added} + \left(\dot{m}_{oxygen}\right)^{o} - \left(\dot{m}_{oxygen}\right)_{sample} \qquad \textbf{(4.4-24)}$$

The added oxygen term can be expressed as:

$$\left(\dot{m}_{oxygen}\right)_{added} = \frac{\dot{m}_{added\,O_2}}{\dot{m}_{N_2}} \qquad \textbf{(4.4-25)}$$

Therefore from equation (4.4-5), the completed phi meter equation can be expressed below by including the added oxygen stream term above:

$$\phi = \frac{\dfrac{\dot{m}_{added\,O_2}}{\dot{m}_{N_2}} + \dfrac{\dot{m}^{o}_{O_2}}{\dot{m}^{o}_{N_2}} - \dfrac{\dot{m}_{O_2}}{\dot{m}_{N_2}}}{\dfrac{\dot{m}^{o}_{O_2}}{\dot{m}^{o}_{N_2}}} \qquad \textbf{(4.4-26)}$$

The first term of this equation is the added oxygen equivalence ratio term and is separately expressed as:

$$\phi_{added\,O_2} = \frac{\dfrac{\dot{m}_{added\,O_2}}{\dot{m}_{N_2}}}{\dfrac{\dot{m}^{o}_{O_2}}{\dot{m}^{o}_{N_2}}} \qquad \textbf{(4.4-27)}$$

Now the added oxygen flow stream can be represented in accordance with the ideal gas law where volumetric flow rate of the added oxygen stream $\dot{V}_{added}$ is evaluated with the volumetric flow rate of the total sample flow $\dot{V}$.

Therefore the molar flow of added oxygen can be expressed as:

$$\dot{m}_{added\,O_2} = \frac{\dot{V}_{added\,O_2} P_{added\,O_2}}{R \;\; T_{added\,O_2}} \tag{4.4-28}$$

And the molar flow of nitrogen can be expressed as:

$$\dot{m}_{N_2} = \frac{\dot{V}_{N_2} P}{R\,T} = \frac{\left(1 - \mathrm{X}_{O_2} - \mathrm{X}_{CO_2} - \mathrm{X}_{CO}\right) \dot{V}\,P}{R\,T} \tag{4.4-29}$$

and $\dot{V}_{N_2}$ can be expressed as;

$$\dot{V}_{N_2} = \dot{V}\left(1 - \mathrm{X}_{O_2} - \mathrm{X}_{CO_2} - \mathrm{X}_{CO}\right) \tag{4.4-30}$$

and from equation (4.4-20) where the denominator is:

$$\frac{\dot{m}^o_{O_2}}{\dot{m}^o_{N_2}} = \frac{\mathrm{X}^o_{O_2}}{\left(1 - \mathrm{X}^o_{O_2} - \mathrm{X}^o_{CO_2} - \mathrm{X}^o_{CO}\right)} \tag{4.4-31}$$

Then the added oxygen equivalence ratio term, can be expressed as:

$$\phi_{added\,O_2} = \frac{\left(1 - \mathrm{X}^o_{O_2} - \mathrm{X}^o_{CO_2} - \mathrm{X}^o_{CO}\right) \dot{V}_{added\,O_2} P_{added\,O_2} T}{\mathrm{X}^o_{O_2}\left(1 - \mathrm{X}_{O_2} - \mathrm{X}_{CO_2} - \mathrm{X}_{CO}\right) \dot{V}\,P T_{added\,O_2}} \tag{4.4-32}$$

Now given that the temperatures and the pressure are considered equal, and $X^{i}_{O_2}$ is the oxygen mole fraction of extra oxygen added, the volume flow of oxygen is:

$$\frac{\dot{V}_{added\,O_2}}{\dot{V}} = \frac{\left(X^{i}_{O_2} - X^{o}_{O_2} \right)}{\left(1 - X_{O_2} - X_{CO_2} - X_{CO} \right)} \qquad \textbf{(4.4-33)}$$

Therefore by substituting the above equations the added oxygen term becomes:

$$\phi_{addedO_2} = \frac{\left(1 - X^{o}_{O_2} - X^{o}_{CO_2} - X^{o}_{CO} \right)}{X^{o}_{O_2}\left(1 - X_{O_2} - X_{CO_2} - X_{CO} \right)} \frac{\left(X^{i}_{O_2} - X^{o}_{O_2} \right)}{\left(1 - X_{O_2} - X_{CO_2} - X_{CO} \right)} \qquad \textbf{(4.4-34)}$$

$$= \frac{\left(X^{i}_{O_2} - X^{o}_{O_2} \right)}{X^{o}_{O_2}\left(1 - X_{O_2} - X_{CO_2} - X_{CO} \right)} \qquad \textbf{(4.4-35)}$$

Thus the final equivalence meter equation that allows for all fuel regimes can be defined as follows:

$$\phi = 1 - \frac{X_{O_2}}{X^{o}_{O_2}} \frac{\left(1 - X^{o}_{O_2} - X^{o}_{CO_2} - X^{o}_{CO} \right)}{\left(1 - X_{O_2} - X_{CO_2} - X_{CO} \right)} + \frac{\left(X^{i}_{O_2} - X^{o}_{O_2} \right)}{X^{o}_{O_2}\left(1 - X_{O_2} - X_{CO_2} - X_{CO} \right)} \qquad \textbf{(4.4-36)}$$

This final equation is used to determine the equivalence ratio during the experiments. This formulation requires the following measurements:

$X^{o}_{O_2}$ = oxygen mole fraction at ambient air (without extra oxygen),

$X^{o}_{CO_2}$ = carbon dioxide mole fraction at ambient air,

X^{o}_{CO} = carbon monoxide mole fraction at ambient air,

$X^{i}_{O_2}$ = oxygen mole fraction with extra oxygen added prior to the experiment,

X_{O_2} = oxygen mole fraction during the experiment,

X_{CO_2} = carbon dioxide mole fraction during the experiment,

X_{CO} = carbon monoxide mole fraction during the experiment.

4.5 Construction of the Phi-meter

The phi-meter was developed part of a greater experimental enclosure pool fire study and utilises the oxygen consumption technique based upon the equations above. The phi meter used an existing electric quartz tube furnace through which the combustion gases were sampled, an additional sample stream of oxygen was added, and the mixture was re-combusted with reaction species measured and analysed. The experimental combustion gas mixture sample was drawn through the phi-meter by a 12 V DC pump. The sample passes from the experimental enclosure though a heated sample line consisting of a copper sample line within an insulated 20mm diameter stainless steel tube jacket. The sealed stainless steel jacket was pumped with Glycerine heated to 150°C to ensure that the temperature of the copper line was no less than 100°C to prevent condensation of the sample gases in the tube. The heater unit for the heated sample line was controlled by a thermocouple placed within the glycerine tank. The length of the sample line as used in the enclosure experiments was approximately 6m long.

In order to achieve complete combustion in the furnace, a sufficient supply of oxygen was provided to the furnace tube on the sampling side. Therefore prior to the sample

gas mixture entering the furnace, 1.0 l/min of oxygen was added with an MKS mass flow controller at the inlet to the tube furnace.

The sample was then drawn into the Electric Tube furnace. This furnace had an existing quartz tube was 100mm length 15mm in diameter tapering to the main chamber 300mm long with a diameter of 30mm. The quartz tube was sealed at each end by a two part metal screw cap fitting which seals tightly on a high temperature rubber gasket. The quartz tube was also filled with a metal oxide catalyst to aid in the combustion process. Metal oxide granules filled approximately ¾ of the tube.

The quartz tube was then supported by the end fittings within the electric tube furnace. As noted in the Andersson [9] the temperature of the furnace was required to be hot enough to provide complete combustion, and furnace temperatures of 300°C to 800°C were used. Therefore a temperature range of 800°C to 1000°C was selected for the furnace temperature of the phi meter and during calibration and the experiments the CO was monitored to confirm the temperature was high enough to ensure oxidation to CO_2. Control of the furnace temperature was provided by two thermocouples located within the quartz tube catalyst. One thermocouple was located in the lower half of the catalyst and the other at the top half of the catalyst. Both thermocouples were monitored to observe any localised effects. It was observed that were there any breakages or loss of pressure to the quartz tube this was reflected by a sudden temperature drop in the furnace temperature.

The photograph on the left in Figure 4.1 shows the dimensions of the quartz tube with oxygen/sample inlet fittings at the bottom and outlet fitting to the top to the tube. The right hand photograph shows the completed furnace unit with quartz tube installed.

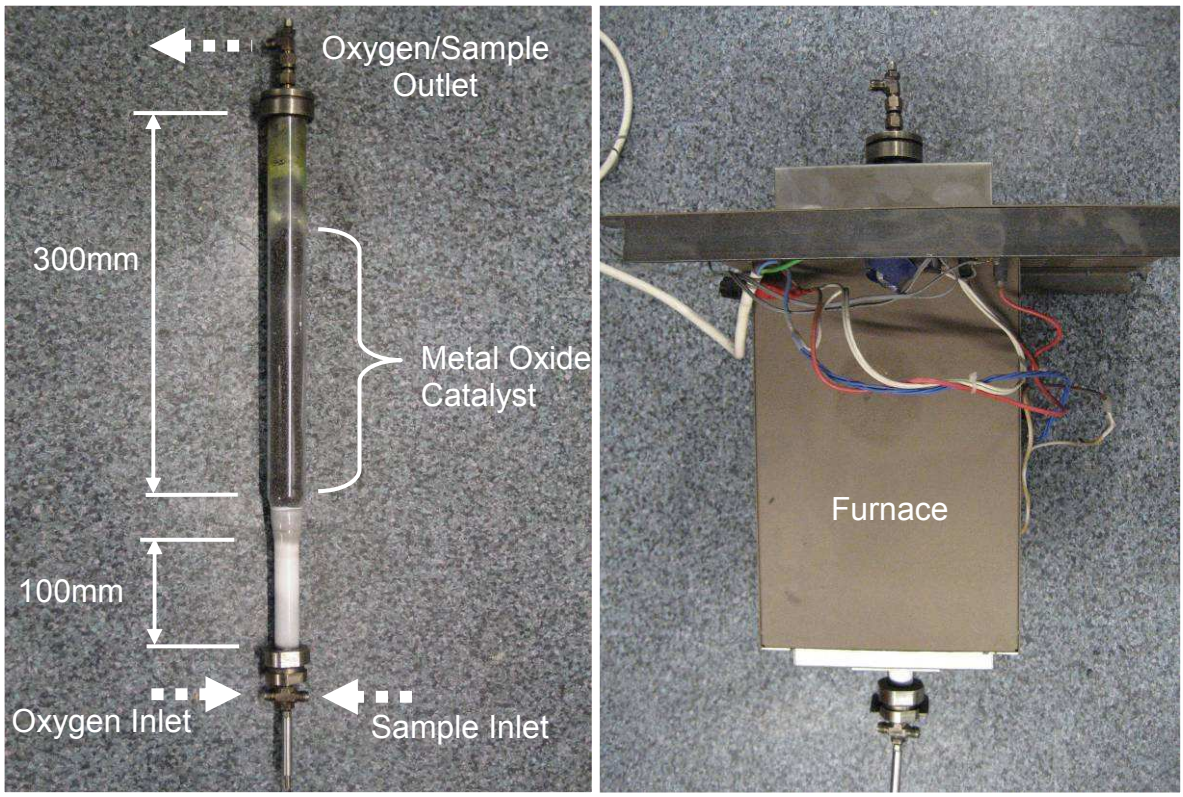

Figure 4.1: Photographs showing the dimensions of the quartz tube with inlet and outlet fittings to the left, and the completed furnace unit with installed quartz tube on the right

After combustion within the furnace the sample passes through a 7µm soot filter to remove any excess carbon. The filter was routinely checked during the experiments and it is noted that it was clean at all times and did not need to be replaced. The sample was then past through Drierite desiccant to remove water before passing through the pump and a cold trap to lower the sample temperature before entering the O_2, CO_2 and CO analysers'.

Based upon the requirement for added oxygen and an equivalence ratio range of 0 to 3, the oxygen level was set to approximately 60% therefore the oxygen analyser was required to have the capability to measure in the operating range of 0 to 70%. The analyser used was a Servomex Paramagnetic Oxygen analyser. The CO and CO_2 measurements were provided by a Siemens Ultramat 6 Non Dispersive Infra Red (NDIR) analyser with operating ranges of 0 to 30%. The analysis of the equivalence ratio was based upon oxygen consumption using equation (4.4-36) above. A schematic diagram of the completed phi meter apparatus is given in Figure 4.2 showing the heated sample line and instrumentation layout.

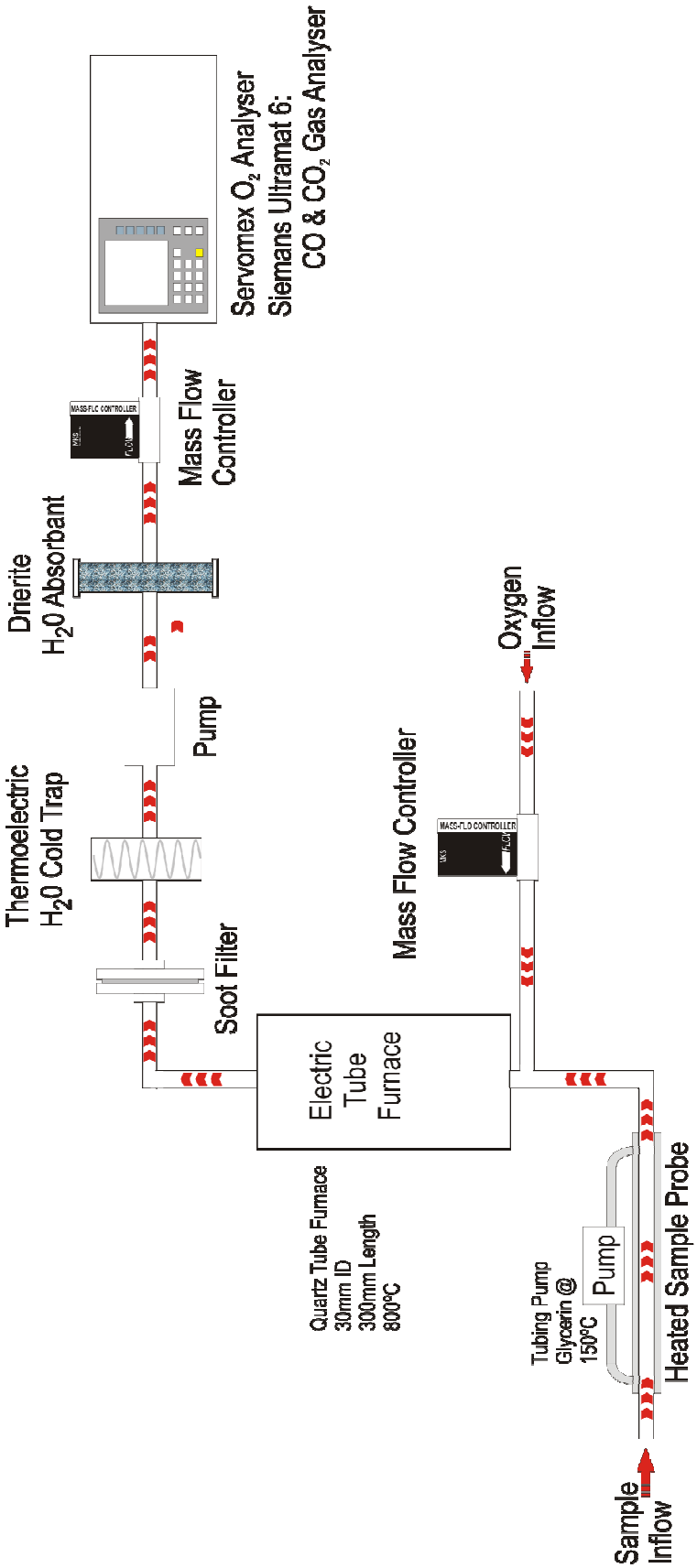

Figure 4.2: Sketch of the completed Phi Meter Layout showing the heated sample line and instrumentation layout

An initial investigation and layout was also trialled with a secondary set of analysers measuring the time dependent O_2, CO_2 and CO species for the combustion mixture without the added oxygen. The heated sampling line was split to provide one flow path to a set of O_2, CO_2 and CO analysers measuring the direct compartment sample gas mixture, whist the other sampling line provided the phi meter process. Due to the complexity with sampling line structure and flows, this approach was not continued but is considered to be worth further investigation.

4.6 Calibration Experiments

Numerous experiments were performed in order to calibrate and evaluate the performance of the phi-meter. Propane and Methane were used as the combustion gas sources due to ready availability. Experiments were carried out by sampling varying proportions of a propane/methane air fuel mixture. A partial amount of propane or methane was introduced into the sample line using a mass flow controller along with air. At the furnace a fixed level of oxygen was introduced. The flows were mixed prior to entering the furnace and combustion took place within the tube furnace. Measurements of both the total sample gas flow and the added oxygen were recorded and the theoretically calculated equivalence ratio was resolved from the combustion equation for Propane C_3H_8 and Methane CH_4 and compared to that measured by the phi meter.

Initial calibration experiments focused on the equivalence ratios less than 1.0. This first set of experiments used methane in the sample gas flow, and the results detailed in Figure 4.3 shows that a good agreement was achieved between the actual equivalence ratio and the values predicated by the phi meter.

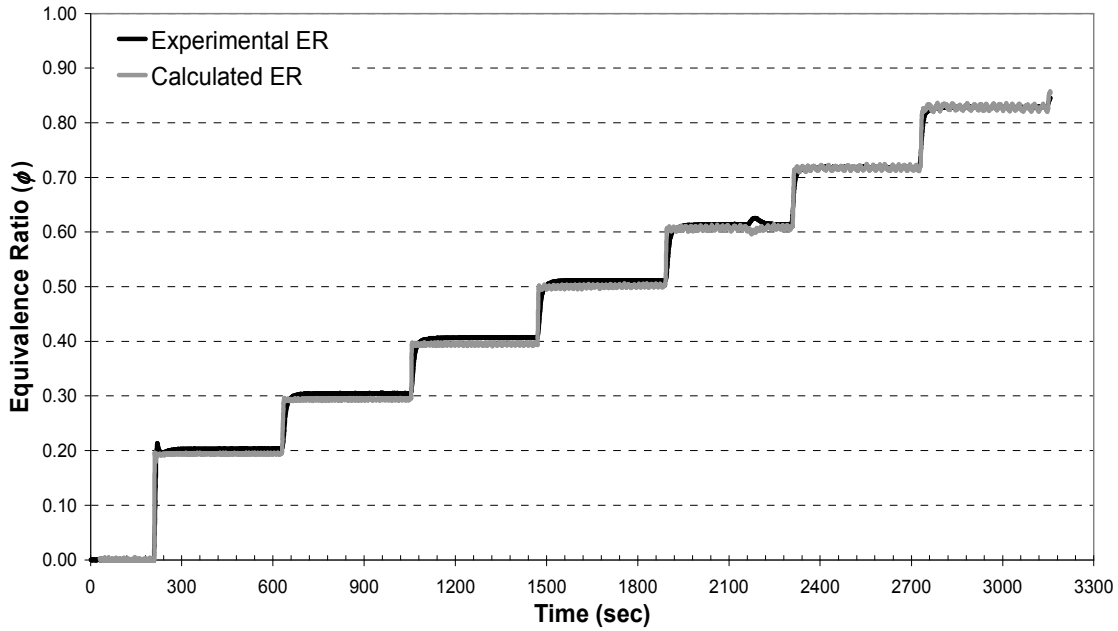

Figure 4.3: Measured and calculated phi values from a calibration experiment on the combustion of methane.

After calibration for phi < 1.0 the phi meter was then used to determine the accuracy for equivalence ratios greater than 1.0. The example shown below in Figure 4.4 present the results from a methane experiment in which the equivalence ratio was varied from 0.5 to 4.0 and Figure 4.5 shows the results from a propane methane experiments in which the equivalence ratio was varied from 0.5 to 3.5. The gas flows were measured by mass flow controllers and from this the calculated equivalence ratio was determined based upon the chemical composition of the fuel.

The experiments provided good agreement between the measured and calculated values. It was noted during the experiments that flashes within the quartz furnace tube indicated combustion and this was prevalent in the higher air fuel mixtures. The experiments involving higher equivalence ratios were noisy, and the experimental equivalence ratio results less than 0.5 are lower than the calculated phi meter values. This was due to the fluctuations in the sampling flow rate as a result of controlling small gas flows with a mass flow controller having a large flow range. For the calibration series the mass flow controller used was 20l/s while the sampling flow rate was of the order of 4l/s. This sampling control issue was remedied for the compartment experiments mass flow controllers with ranges from 1l/s to 5l/s were used which allowed better control of the gas flows.

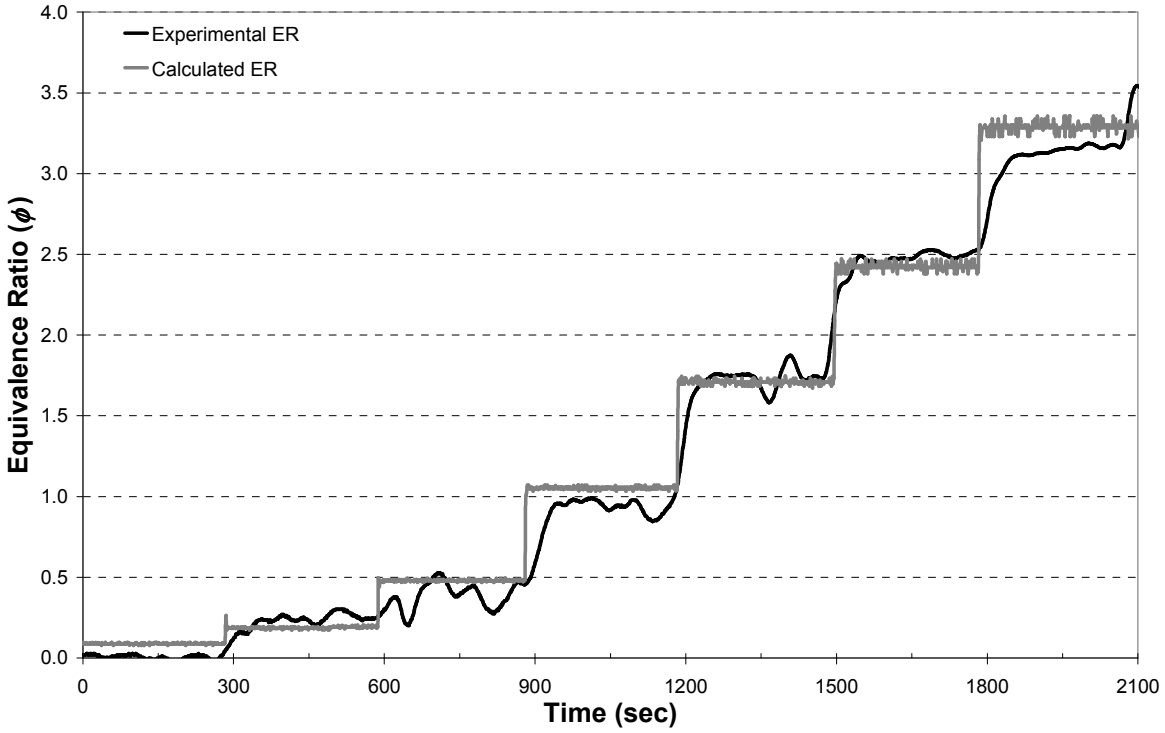

Figure 4.4: Measured and calculated phi values from a calibration experiment on the combustion of methane.

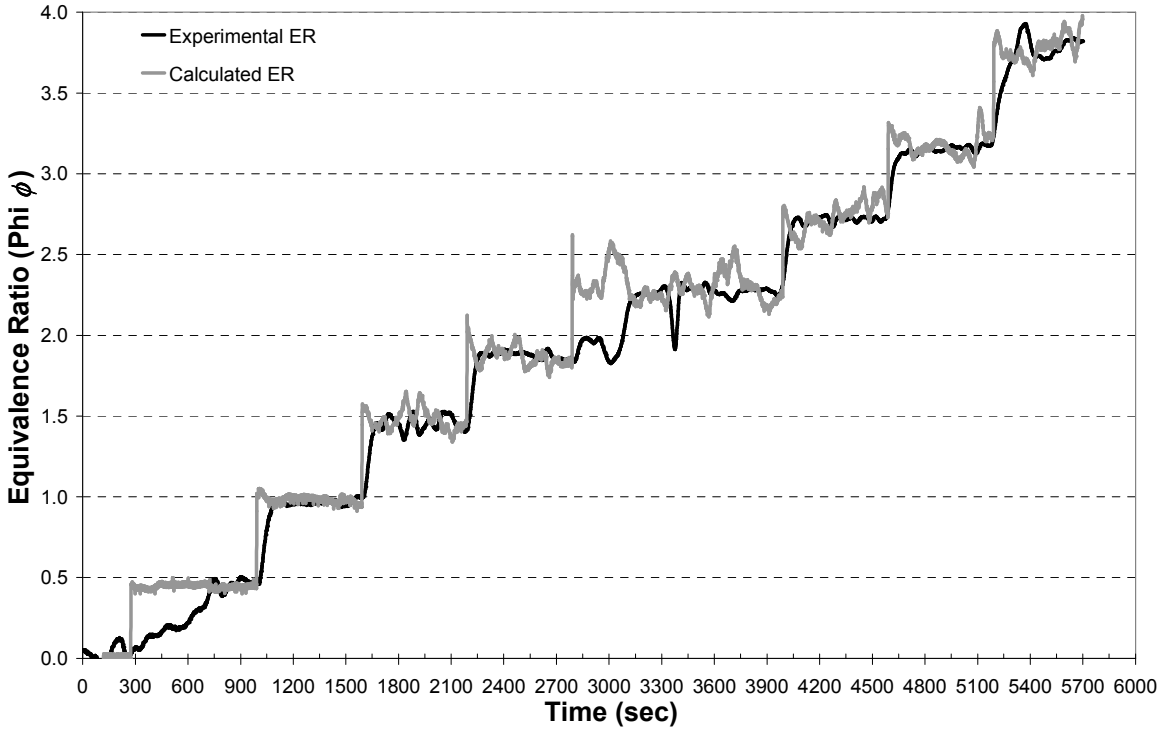

Figure 4.5: Measured and calculated phi values from a calibration experiment on the combustion of propane.

The completed series of experiments carried out using the variations in the fuel gas and air mixture are detailed in Figure 4.6 and show a very good agreement of the measured versus calculated values for the equivalence ratio. The solid straight line represents the ideal result of equality when the measured and calculated values are compared.

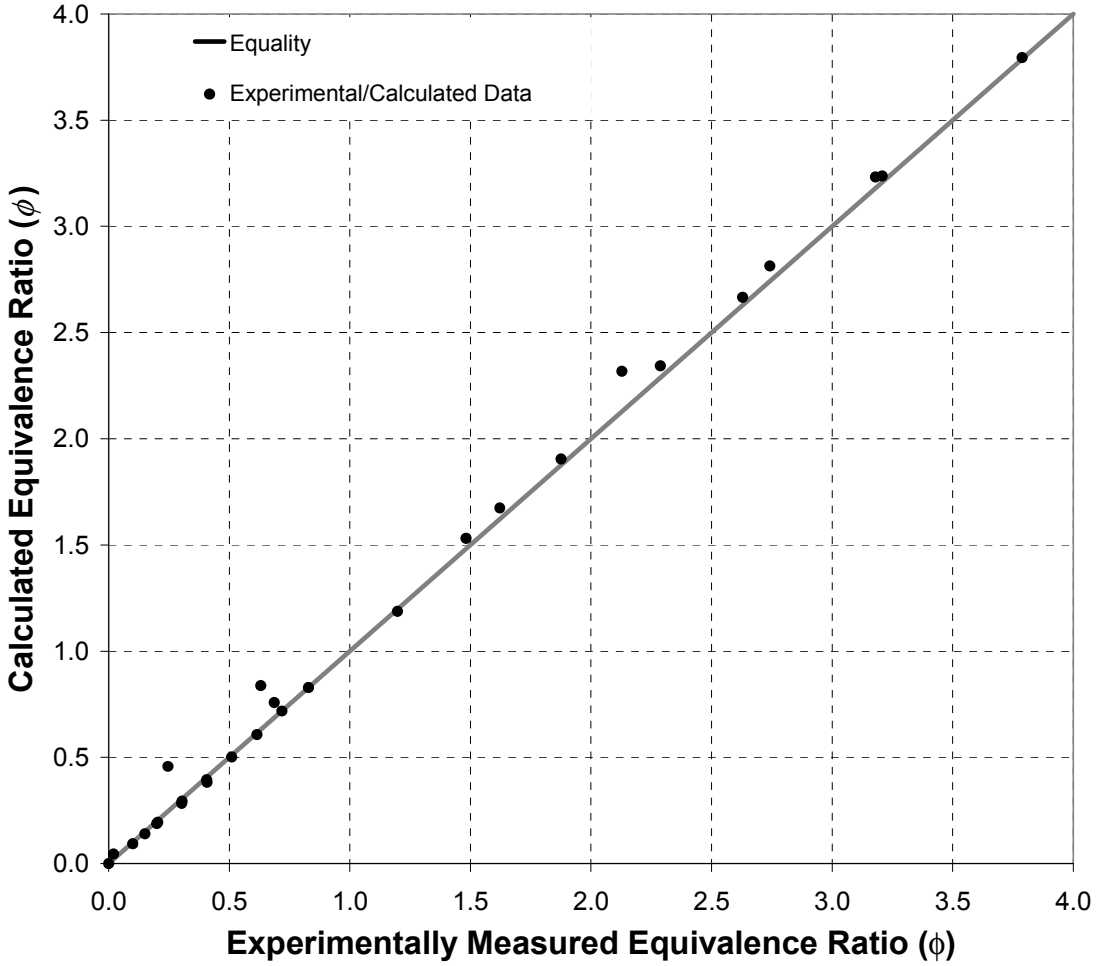

Figure 4.6: Measured versus calculated phi value for experiments with propane.

4.6.1 Response Time

It was noted that during the phi meter operation there was a delay at each point the air fuel mixture was modified. This was due to the time taken to travel from the far end of the heated sampling line, through the adsorbent, combustion within the reactor and analysis. This delay time was investigated by introducing an amount of nitrogen into the sample line and determining the time taken to be analysed. The delay time was calculated to be approximately 40 seconds.

The delay time is required to be of sufficient length such that complete combustion occurs within the furnace. The species remaining after combustion were evaluated and it was noted that as no CO was found within the post furnace sample flow, it can be assumed that it was oxidised to CO_2. It is noted that blockages that occurred in the system during the experiments are likely to have affected the response time of the phi meter although this was not able to be quantified.

4.7 Compartment Experiments

The enhanced phi meter was used in the compartment experimental study described in this work and the description for the experimental enclosure and instrumentation as detailed in *Chapter 3: Experimental Setup and Procedure.* Thirty nine experiments were conducted in a 2.4m wide by 3.6m long by 1.2m high compartment constructed from stainless steel. The walls, ceiling and floor of the compartment were lined with two layers of 10mm ceramic fibre board. Ventilation into the compartment was designed to be easily modified using panel construction to enable the ventilation geometry to be changed from fully open, to a soffit, and to a door. These panels when connected to the compartment are also lined with two layers of 10mm ceramic fibre board. The dimensions of the various ventilation geometries are as follow:

1. ***Full*** – 2.4m wide x 1.2m high (Unrestricted), ($A_v\sqrt{H_v} = 3.155$)
2. ***Soffit*** – 2.4m wide x 1.0m high (0.2m downstand), ($A_v\sqrt{H_v} = 2.4$).
3. ***Door*** – 0.4 m wide by 1.0 m high, ($A_v\sqrt{H_v} = 0.4$).
4. ***Window*** – 0.8 m wide by 0.6 m high (0.2m sill), ($A_v\sqrt{H_v} = 0.372$).
5. ***Small-window*** – 0.4 m wide by 0.6 m high (0.2m sill), ($A_v\sqrt{H_v} = 0.186$).

Constant head heptane pool fires were used in the experiments, with a 200mm square pans, 50mm high. The perimeter of the pan was insulated with 20 mm thick ceramic fibre board. The pan was able to be positioned in three different locations within the room for every corresponding change in ventilation opening. These locations were as follow (based upon pan centreline dimensions);

a) Rear location: The pan in the rear position was located 3.0m from the front of the compartment.

b) Centre location: The pan in the centre location position was located 1.8m from the front of the compartment.

c) Front location: The pan in the front location position was located 0.6m from the front of the compartment.

Figure 4.7 is a sketch of the compartment showing the three pan locations, fully open ventilation, and notable instrumentation.

Heptane fuel is pumped from 40-litre pre fabricated stainless steel fuel tanks using a tubing pump connected to individual header tanks. From the header tank the pan was gravity fed allowing a constant fuel surface height. Ignition was by a series of sparkplug electrodes connected to two 15000 volt transformers.

The phi meter apparatus developed for this experimental study aimed to evaluate the species at the exit plane of the compartment. As the combustion gasses were expected to be well mixed at this point a copper tube sampling port was installed located approximately 25mm below the top of the centre of the ventilation geometry. This is also consistent with ASTM 603-98a [12] which notes that additional measurements of carbon monoxide and carbon dioxide in a test room, may yield useful information if sampled 25mm below the top of the doorway.

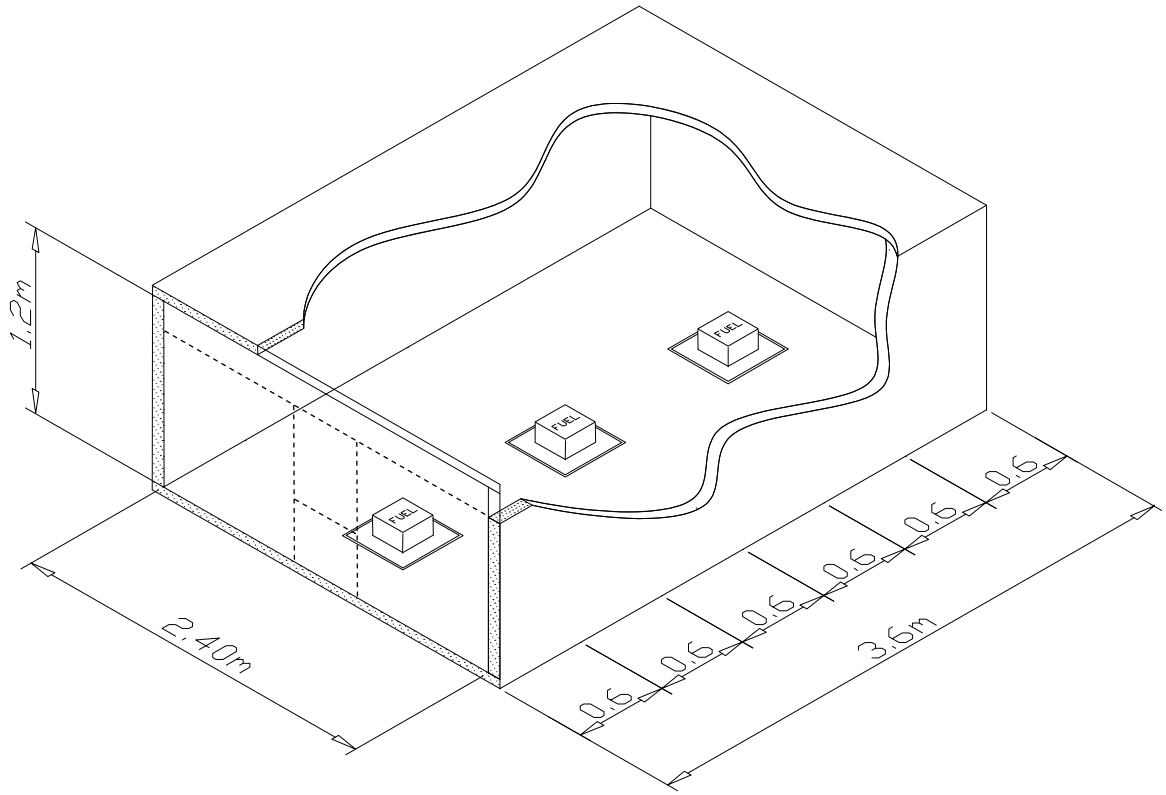

Figure 4.7: Sketch of the experimental compartment showing the three pool fire locations. The ventilation geometries are indicated by the dotted lines.

Results from the compartment experiments indicated that the equivalence ratios measured for heptane pool fires range from 0.1 for oxygen rich conditions and 2.3 for fuel rich conditions. Two examples of the use of the phi meter in this real fire compartment study are detailed below. The first example in Figure 4.8 shows the time dependent results of a compartment experiment with all three 200mm square pans located in the rear, centre and front pan locations in the enclosure using the soffit ventilation geometry. In this experiment sufficient ventilation is available such that the combustion behaviour is considered oxygen rich. This is confirmed by an equivalence ratio of less than 1.

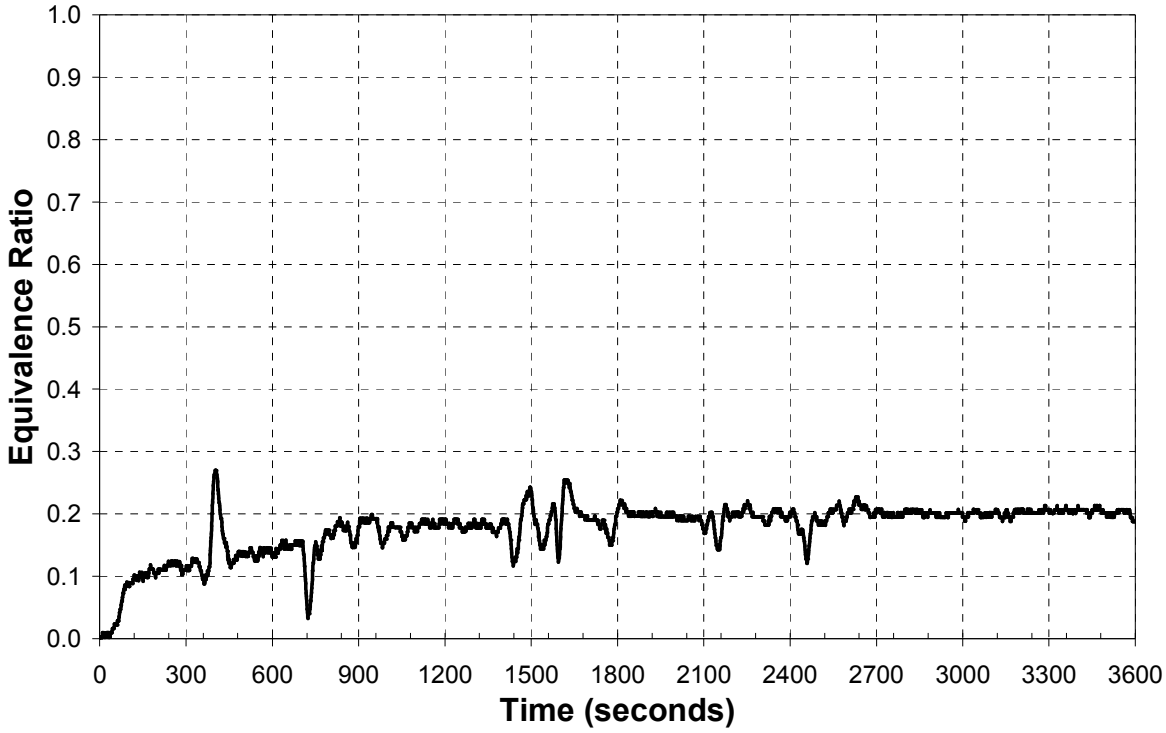

Figure 4.8: Equivalence ratio time history for the compartment experiment using three 200mm square pans in the rear, centre and front location with the soffit ventilation geometry

Figure 4.9 shows the experiment with all three 200mm square pans located in the rear, centre and front pan locations using the small window geometry. In this experiment the compartment was an under-ventilated and combustion behaviour fuel rich. This provided post flashover compartment behaviour which was ventilation limited, and is confirmed by the equivalence ratio of greater than 1.

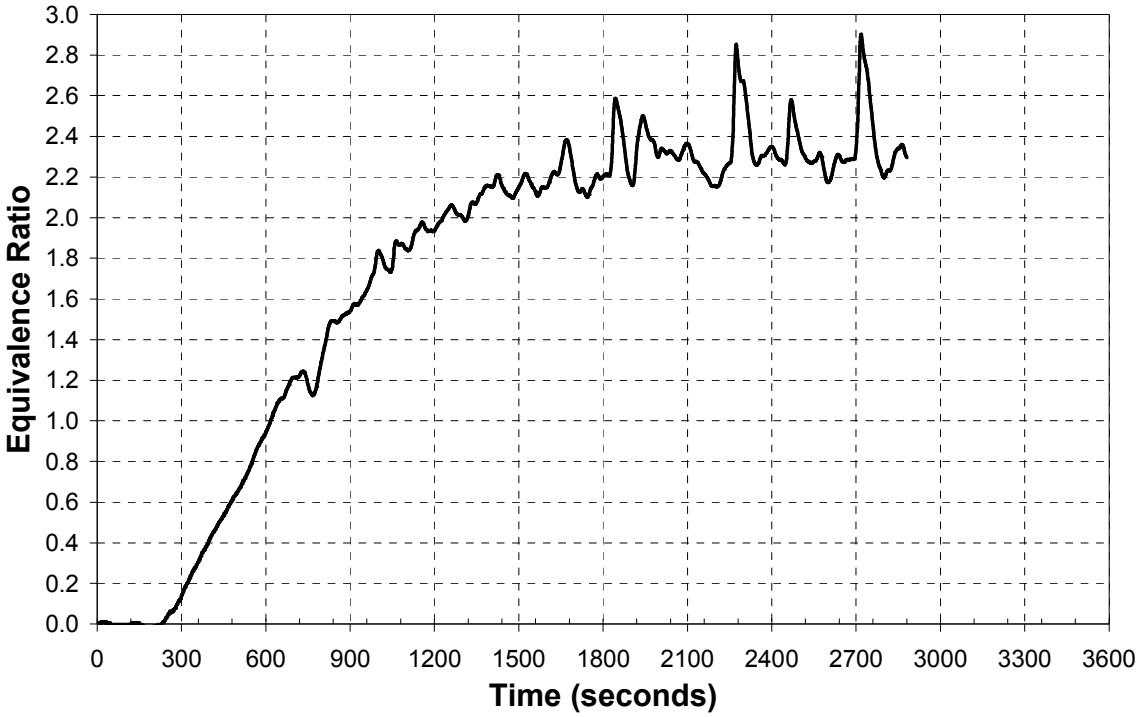

Figure 4.9: Equivalence ratio time history for the compartment experiment using three 200mm square pans in the rear centre and front location with the small window ventilation geometry

It is noted that although the time history equivalence ratios verge toward a quasi-steady average value, there are times at which the equivalence ratio spikes. These were identified during the experiments by an increase in the furnace temperature indicating a reduction in flow due to a temporary blockage of the sample line or in the catalyst.

Although in this instance the phi meter was use to provide an equivalence ratio for a compartment fire which had reached a quasi-steady state, it was also developed to investigate any time dependent changes. The response of the phi meter to determine the time dependent changes in the equivalence ratio has been compared with the heat release rate and upper layer temperatures for the rear, centre and front experiment (Figure 4.10) with the small window geometry. The equivalence ratio time scale has been adapted to allow for the 40 second response time (assuming no delay by a blockage).

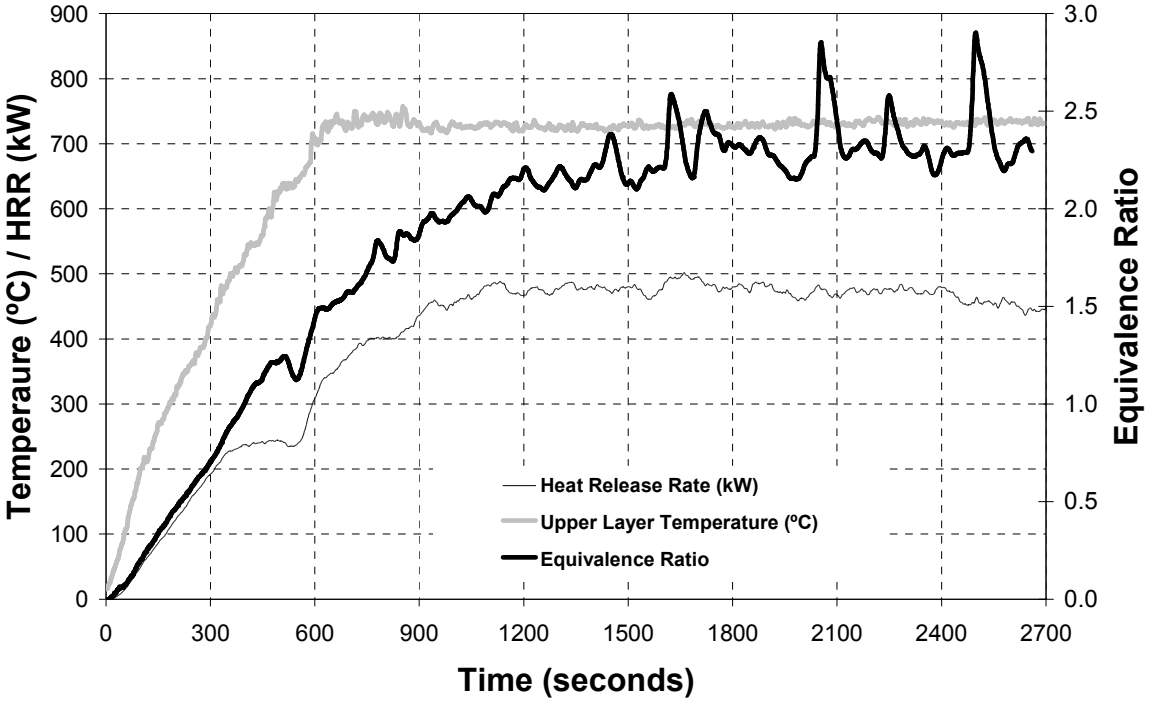

Figure 4.10: Equivalence ratio comparison with upper layer temperature and heat release rate for the rear, centre & front individual pan experiment with the small window geometry.

The phi meter was able to distinguish reasonable time dependent changes during the enclosure fire experiments. Even with the measurement of three combustion species the phi meter was considered a fairly compact device and could be moved to remote locations for use.

The combustion catalyst provided in the tube furnace to ensure complete combustion during the heptane pool fire proved to be effective as it was noted that in all of the experiments the CO was completely resolved e.g. no CO remained in the system. Even though this is that case the use of additional species analysers is still considered beneficial to allow better accuracy of the results.

4.8 Conclusions and Future Research

The ventilation conditions of an enclosure fire are one of the most important variables as this influences the combustion and the consequent production of combustion gases such as CO and CO_2. As part of a greater experimental compartment pool fire study

conducted at the University of Canterbury, an Equivalence Ratio (ϕ, phi) meter was designed and developed to aid in the classification of the compartment fire behaviour. A new version of a phi meter was developed and configured on the principle of measuring O_2, CO_2 and CO combustion species with from the existing theory. The analysing of CO_2 and CO had the advantage of not requiring the removal by chemical means of CO_2 from the sample flow. The measuring of CO also provided confirmation that the entire CO was combusted in the furnace.

The experimental results presented for the calibration of the phi meter provide very good agreement with the theoretically calculated values for propane and methane and the time dependent results for each of the compartments experiments indicated good sensitivity in the results. The results indicate that the equivalence ratios measured for heptane pool fires range from 0.1 for oxygen rich conditions and 2.3 for fuel rich conditions.

The use of a quartz tube as a combustion reactor in the furnace provided a number of problematic experimental issues. Firstly the stainless steel screw fittings at each end of the quartz tube required careful attention to ensure an air tight seal without the risk of over tighting and breaking the quartz. The gasket seals were also temperamental due to the heat, so pressure gauges were installed on the system to ensure pressure/vacuum checks could easily be accomplished to confirm no leakage. Initially the furnace was heated and cooled at the end of experiment, however this had a tendency to affect the seals at either end of the tube furnace, and required constant attention. Given the nature of a quartz tube, there were a number of breakages when handling the tube. Future development would recommend the use of metal tube within the furnace.

The following are suggested for future development of the phi meter.

- Further use of the phi meter is required over a wider range of equivalence ratio values in particular from 1.5 to 3.0.
- Given the measurement of CO, the phi meter apparatus could be configured without the use of a catalyst. The catalyst was provided as a check to ensure complete combustion. This was successful however there were a number of blockages in the

sample line inlet and also within the furnace tube. Future development without the catalyst would limit potential blockages.

- Although the phi meter was developed to sample continuously and measure the time-dependent compartment equivalence ratio, a quasi-steady state equivalence ratio was reached at the end of the experiments. Due to difficulties with blockages of the sample line inlet and furnace tube, it is expected that sampling at selected time intervals may be beneficial to limit potential blockages. This would also ensure no response time delays as a result of a blockage.
- If used with fuel producing high soot content then air pulse cleaning of the sample line and inlet is suggested during testing.
- The sampling port could be revised to use a probe with equally spaced sampling holes to thereby remove any spatial variation in the vent opening.
- The phi meter should be developed using a high temperature metal alloy tube (such as Inconel) in the furnace and not the quartz tube.

4.9 References

1 Blomqvist, P., Lönnermark, A., "Characterisation of the Combustion Products in Large-scale Fire Tests: Comparison of Three Experimental Configurations" Fire and Materials, 25, pp. 71-81, 2001.

2 Wieczorek, C. J., Vandsbuger, U., McKay, C, and Sathyamoorthy, S., "The applicability of Correlations Between the Species Formation and the Global Equivalence Ratio in a ½-Scaled Iso Compartment with Nongaseous Fuel" Fire Safety Science Proceedings of the Sixth International Symposium, pp 965-976.

3 Thornton, W. M, "The Relation of Oxygen to the Heat of Combustion of Organic Compounds", Philosophical Magazine and Journal of Science, Vol.33, No. 196: 196-203 (1917).

4 Janssens, M. L. “Measuring Rate of Heat Release by Oxygen Consumption” Fire Technology, August 1991, pp234-249

5 Wieczorek, C. J., Vandsbuger, U. and Floyd, J., “An Evaluation of the Global Equivalence Ration Concept for Compartment Fire: Data Analysis Methods” Journal of Fire Protection Engineering, Vol. 14, pp 9-34, February 2004.

6 Pitts, W. M., “The Global Equivalence Ratio Concept and the Prediction of Carbon Monoxide Formation in Enclosure Fires”, National Institute of Standards and Technology Monograph 179, Gaithersburg, MD, 1994, p 171.

7 Pitts, W. M., “Limitations of the Global Equivalence Ratio Concept for Predicting CO Formation in Room Fires”, Proceedings of 12th Joint Panel Meeting of the UJNR Panel of Fire Research and Safety, Oct.27-Nov.2 1992 Produced by: Building Research Institute, Tsukuba, Ibaraki and the Fire Research Institute, Mitaka, Tokyo, 1994.

8 Babrauskas, V., Parker, W. J, Mullholland, G., and Twilley, W. H, “The phi meter: A simple, fuel-independent instrument for monitoring combustion equivalence ratio” Rev. Sci. Instrum. Vol 65, No 7, pp. 2367-2375, July 1994.

9 Andersson, B., Holmstedt, G., and Dagneryd, A. “Determination of the equivalence ratio during fire, comparison of techniques” Fire Safety Science – Proceedings of the Seventh International Symposium, pp. 295-308, 2002.

10 Lönnermark, A., Blomqvist, P., Mansson, M. and Persson, H., “TOXFIRE – Fire Characteristics and Smoke Gas Analysis in Under-Ventilated Large-Scale Combustion Experiments: Tests in the ISO 9705 Room” SP Swedish National Testing and Research Institute, SP REPORT 1996:45, 1996.

11 Lönnermark, A., and Babrauskas, V., “TOXFIRE – Fire Characteristics and Smoke Gas Analyses in Under-ventilated Large-Scale Combustion Experiments: Theoretical

Background and Calculations" SP Swedish National Testing and Research Institute, SP REPORT 1996:49, 1996.

12 ASTM 603-98a, Standard Guide for Room Fire Experiments, Annual Book of ASTM Standards, Vol. 04.07.

Chapter 5: Single Pan Experimental Results

The following chapter details the results from the experimental series using a single 200mm square heptane pan in three independent locations (rear, centre and front) within the experimental compartment. This series of experiments used the five different ventilation geometries of fully open, soffit, door, window, and small window.

This chapter is presented in the form of the paper submitted and presented at the Eighth International Symposium, International Association for Fire Safety Science, Beijing China titled "*The Impact of Location and Ventilation on Pool Fire in a Compartment*". The paper has been modified in the section from the original paper to include the results from the window and small window experiments which were not completed at the submission for the IAFSS paper.

The paper provides an introduction and brief background on pool fires and a general overview of the experimental apparatus and instrumentation. For a full description of the experimental apparatus and instrumentation refer should be made to *Chapter 3: Experimental Setup and Procedure*.

Results of measurements recorded during the experiments are presented, including heat release rate, heat flux, compartment temperatures and vent velocities. Visual observations are also discussed. A detailed account of compartment observation for the compartment experiments is provided in Appendix B.

The Impact of Location and Ventilation on Pool Fire in a Compartment

A. R. PARKES and C. M. FLEISCHMANN
University of Canterbury
Christchurch,
New Zealand

5.1 Abstract

This paper describes recent experiments to investigate the effects that the location of a fire within an enclosure has upon the rate of heat release. A series of pool fire experiments were conducted in a ½ domestic scale compartment using five ventilation geometries (*fully open, soffit, door, window and small window*), and heptane pool fires located in three evenly distributed locations within the compartment (rear, centre and front). The primary goal of this work is to demonstrate the impact that the fire location within a compartment can have on the heat release rate and subsequent compartment conditions. Results indicate that the fire location and ventilation can significantly impact the heat release rate of the fire. In most cases the fire will have a larger heat release rate than under free burning conditions however, when the fire is near the opening the heat release rate is actually less than the free burning value.

KEYWORDS: compartment fires, fire growth, fire location, heat release rate, mass loss rate, pool fires, flashover

5.2 Introduction

The practicing fire engineer in today's performance based environment evaluates the life safety risk to occupant with respect to the fire conditions developing within a room. The use of fire and evacuation modelling is often employed to assess the fire conditions in conjunction with the fire protection measures provided. It should be noted however that these evaluative tools are only as accurate as the limitations of the models used and input fire scenarios assessed by the engineer.

With the advancement of computational fire modelling, the current computer models are able to provide greater accuracy with which a fire scenario can be simulated. However an increased level of analysis also requires an increased level of understanding as to requirements of the input parameters.

The common computational tool used by the practising engineer is that of a zone model due to the low cost, availability and ease of use. Zone models rely on the user to input an expected fire scenario and by default this is generally located in the centre of the input room geometry. Based upon the engineer specifying a time dependent fire growth rate using engineering judgement (typically the fire growth rates are based upon the idealised t^2 fire growth rates), the output of the analysis is regarded as a '*credible design fire scenario*'. Generally, corner and wall fire scenarios are neglected and other locations within the room are not expected to result in significantly different behaviour to that of the centrally located scenario. Hence location of the fire source is not deemed important and is not accounted for.

Computational Fluid Dynamic (CFD) models are less commonly used as a consultancy tool due to their cost and time consuming use. However the results from these models can provide significant advantages, although the model will still be bound by the user input and general scenarios as mentioned above.

Generally the factors that influence the development of a fire in an enclosure are: fuel type, enclosure geometry and properties, and ventilation. Given the use of pool fires in this study, it is recognised that compartment effects due to radiation and ventilation play as significant role in the burning rate of the pool fire. This has a considerable effect on the heat release rate and the fire dynamics within enclosures. Although the location of a fire can also have a distinct effect on the fire development, this specifically relates to wall and corner fires. Typically if a fuel package is located away from the bounding walls, air is able to be entrained into the plume from all directions. Therefore the location of a fire away from the walls is not considered a significant factor and credible design fire scenarios are developed considering fire located in the centre of an enclosure.

This paper describes recent experiments at the University of Canterbury to investigate the effect that the location of a fire within an enclosure has upon the mass loss rate and rate of heat release. A series of compartment fires using five typical ventilation geometries (*fully open, soffit, door, window and small window*), and heptane pool fires located in three evenly distributed locations within the compartment (rear, centre and front) are discussed and the results presented. The primary goal of this work is to demonstrate that location of the fire within a compartment can play a significant role in compartment fires.

5.3 Background

Burning liquid fires have been studied extensively. It has long been known that the burning rate of pool fires is controlled by the heat transfer back to the surface. For pool fire sizes of interest to fire engineers, i.e. diameters greater than 0.2 m, the heat transfer is governed by the radiation back to the surface. For pools fire with diameters between 0.2m and 1m the flame is considered to be optically thin whereas for pools fire greater than 1m in diameter the flame is optically thick [1]. The burning rate for pool fires greater than 0.2 m can be estimated using the following semi-theoretical expression [2]

$$\dot{q} = \Delta h_c \ \dot{m}_f \ = \ \Delta h_c \ \dot{m}''_\infty \left[1 - \exp\left(-k\beta \ D\right)\right] A_p \qquad \textbf{(5.3-1)}$$

For heptane in a 0.2m square pan the free burning heat release rate is expected to be 100kW using typical values for heptane ($\dot{m}''_\infty = 0.101$ kg/s.m² , $\kappa\beta$=1.1m^{-1}, Δh_c=44.6MW) taken from reference [1].

A pool fire geometry represents a worse case in terms of radiation enhanced mass loss rate. The entire fuel surface sees the hot upper layer and bounding surfaces. Thomas and Bennetts, have studied large pool fires in a deep narrow compartment with different opening geometries [3]. In their study, the entire floor of the compartment was covered with fuel pans. Results highlighted the importance of ventilation geometry on the burning rate of the pools.

More complex wood cribs fuels in large narrow enclosures have been studied at BRE [4,5]. In the BRE study, wood cribs were placed over the entire floor of a long narrow compartment with a single vent at the opposite end of the enclosure. The importance of the fire location relative to the opening was also identified in this work as the fire ignited in the rear, spread quickly to the front of the enclosure and then spread more slowly into the compartment as the fuel was consumed, thus demonstrating the importance of the fire location relative to the ventilation opening.

The expected heat release rate within an enclosure sufficient to cause flashover can also be calculated using the following expression derived by Babrauskas [6].

$$\dot{Q} = 600\, A_v \sqrt{H_v} \qquad \textbf{(5.3-2)}$$

For the different ventilation geometries represented in this study the most severe ventilation limited case is that of the small window opening of 0.4m wide by 0.6m high. This has an $A_v\sqrt{H_v}$ = 0.186, providing a predicted heat release rate of 112kW for flashover.

The pool fire geometry represents a worse case in terms of radiation enhanced mass loss rate. The entire fuel surface sees the hot upper layer and bounding surfaces. More complex fuels such as furniture or wood cribs will be partially shielded from the compartment environment and therefore less radiation will reach the fuel surface.

5.4 Experimental Apparatus and Procedure

5.4.1 Apparatus

Fifteen experiments were conducted in a 2.4m wide by 3.6m long by 1.2m high compartment constructed from stainless steel. Figure 1 is a sketch of the compartment showing the three pan locations, fully open ventilation, and notable instrumentation. The walls, ceiling and floor of the compartment were lined with two layers of 10mm ceramic fibre board. For visual observations, five windows were located on one side of the compartment, four at lower half of the compartment with the fifth located at the upper level near at the front of the room.

Ventilation into the compartment was designed to be easily modified using panel construction to enable the ventilation geometry to be changed from fully open, to a soffit, and to a door. These panels when connected to the compartment are also lined with two layers of 10mm ceramic fibre board. The dimensions of the various ventilation geometries are as follow:

1. ***Full*** – 2.4m wide x 1.2m high (Unrestricted), ($A_v\sqrt{H_v} = 3.155$)
2. ***Soffit*** – 2.4m wide x 1.0m high (0.2m downstand), ($A_v\sqrt{H_v} = 2.4$).
3. ***Door*** – 0.4 m wide by 1.0 m high, ($A_v\sqrt{H_v} = 0.4$).
4. ***Window*** – 0.8 m wide by 0.6 m high (0.2m sill), ($A_v\sqrt{H_v} = 0.372$).
5. ***Small-window*** – 0.4 m wide by 0.6 m high (0.2m sill), ($A_v\sqrt{H_v} = 0.186$).

Heptane pool fires were used in all experiments, with a 200mm square pan 50mm high. The perimeter of the pan was insulated with 20 mm thick ceramic fibre board. The pan is able to be positioned in three different locations within the room for every corresponding change in ventilation opening. These locations are as follow (based upon pan centreline dimensions);

a) *Rear location*: The pan in the rear position was located 3.0m from the front of the compartment.

b) *Centre location*: The pan in the centre location position was located 1.8m from the front of the compartment.

c) *Front location*: The pan in the front location position was located 0.6m from the front of the compartment.

Heptane fuel is pumped from 40-litre pre fabricated stainless steel fuel tanks using a tubing pump connected to individual header tanks. From the header tank the pan was gravity fed allowing a constant fuel surface height. Ignition was by a series of sparkplug electrodes connected to two 15000 volt transformers.

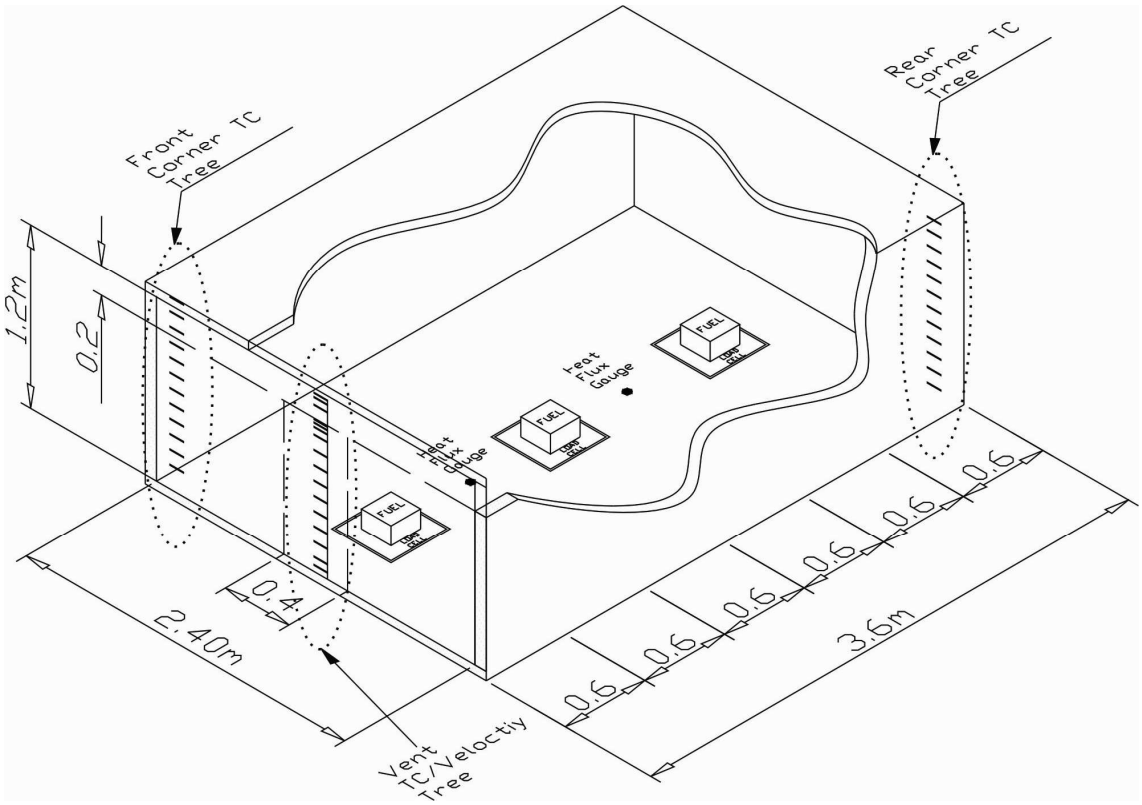

Figure 5.1: Sketch of the experimental compartment showing all three pool fire locations, *full* ventilation condition and relevant instrumentation.

5.4.2 Instrumentation

Compartment Temperatures: To measure the compartment gas temperatures, vertical thermocouple trees were installed at the front and rear of the enclosure (see Figure 1). Two sets of 15, 1.6 mm diameter type K thermocouples were used and positioned at spacings of generally 100mm vertically between the floor and ceiling. To avoid effects from the boundary layer, the thermocouples were installed 150 mm off the rear wall, 100mm off the side walls, and 25 mm from the floor/roof.

Vent Temperatures/Pressures: A thermocouple tree was installed within the vent to record the vent temperatures. 14, 1.6 mm diameter type K thermocouples at a spacing of 100mm were used, with this being reduced to 12 when the soffit/door geometry was used, and 8 when the *window/small-window* geometry was used. 10 Bi-directional probes were also installed in the vent when the *full/soffit/door* geometry was used, and 8 when the *window/small-window* geometry was used. These were used for measurements of vent velocities and were connected to pressure transducers with a pressure range of 0-25 Pa.

Heat Flux: Two Gardon type water-cooled heat flux gauges were installed between each of the separate pan locations e.g. 600mm from the centre of each pan. The heat flux gauge at location 1 is 2400mm from the front opening (between the rear and centre pans) and location 2 is 1200mm from the front opening (between the centre and front pans). These were used to measure the radiation heat flux at the floor during each experiment.

Mass Loss: The mass loss of the fuel was recorded on a load cell upon which the fuel tanks sit.

Heat Release Rate: The heat release rate from each experiment was measured using oxygen depletion calorimetery and included O_2, CO_2, and CO species measurements. The extraction system had a maximum flow rate of 4 m^3/s.

Data Acquisition: A Universal Data Logging (UDL) system developed at the University of Canterbury is used to log voltages from the above instrumentation through software and hardware interfaces. The hardware consists of serial boxes for each different sensing device which is then calibrated with the UDL programme and an associated calibration and offset factors. The sampling rate for the UDL program was 1 sample per second using a Pentium P4 computer.

5.5 Procedure

Sixteen experiments were conducted in this series including one experiment of a single pan in the open under quiescent conditions to provide a base case for comparison. Table 5.1 summarizes the ventilation geometry and pan locations for the fifteen compartment experiments.

Table 5.1: Experimental Matrix for the fifteen compartment experiments showing the pan location and ventilation geometry.

		Opening Geometry				
		Full Open	*Soffit* 0.2m (downstand)	*Door* 1.0m x 0.4m	*Window* 0.6m x 0.8m	*Small-window* 0.6m x 0.4m
Pan Location	Rear Pan	**x**	**x**	**x**	**x**	**x**
	Centre Pan	**x**	**x**	**x**	**x**	**x**
	Front Pan	**x**	**x**	**x**	**x**	**x**

Each experiment involved calibration of the oxygen depletion calorimetery system before commencement. A three minute baseline is also taken to record the initial conditions, before ignition of the pan. Each experiment was allowed to run for a total duration after ignition of at least 60 minutes.

5.6 Experiment Results

Summary: The results of the 15 single pans experiments are summarised in Table 5.2. Column 1 gives the location of the pan within the compartment (**Open** – free-burning in open, **Rear** – 3.0 m from opening, **Centre** - 1.8 m from opening, **Front** - 0.6 m from front). Columns 2 and 3 are the ventilation configurations and corresponding ventilation factors (***Full*** – 1.2 m by 2.4 m wall fully open $(A_v\sqrt{H_v} = 3.155)$, ***Soffit*** – 2.4 m wide by 1.0 m high $(A_v\sqrt{H_v} = 2.4)$, ***Door*** – 0.4 m wide by 1.0 m high $(A_v\sqrt{H_v} = 0.4)$, ***Window*** – 0.8 m wide by 0.6 m high $(A_v\sqrt{H_v} = 0.372)$, ***Small-window*** – 0.4 m wide by 0.6 m high $(A_v\sqrt{H_v} = 0.186)$). Column 4 & 5 is the total heat (energy) released and total mass loss, respectively, during the last 1200 seconds of the fully developed phase of burning. Column 6 is the effective heat of combustion, respectively, calculated from columns 4 & 5. Columns 7 to 9 are the layer height, upper layer temperature, and lower layer temperature based on maximum slope of the temperature profile at TC tree #2 in the corner nearest the opening. Column 10 and 11 are the average heat flux measurements 1.2 m from the front opening and 1.2 m from the rear wall, respectively, averaged over the last 300 seconds. Column 12 and 13 is the mass loss rate, MLR, and heat release rate, respectively, averaged over the last 1200 seconds of the experiment.

Table 5.2: Summary of data from single pan experiments and the single free-burning pool fire.

Pan Location	Vent Config.	$A_v\sqrt{H_v}$	Total Energy Last 1200 sec (MJ)	Total Mass Loss (kg)	ΔH_c (kJ/kg)	Layer Height, HL (mm)	T_{Ave} Upper Layer (°C)	T_{Ave} Lower Layer (°C)	Ave. Heat Flux #1 Last 300 sec (kW/m²)	Ave. Heat Flux #2 Last 300 sec (kW/m²)	Ave. MLR Last 1200 sec (kg/s)	Ave. HRR Last 1200 sec (kW)
Freeburn	-	-	104.9	2.29	45785						0.00191	87.4
Rear	Full	3.155	201.4	4.46	45181	1000	169	38	4.7	2.5	0.00371	111.8
	Soffit	2.400	132.8	3.02	43945	700	177	33	5.3	3.0	0.00252	110.6
	Door	0.400	327.2	7.49	43690	0	681		65.4	46.0	0.00624	272.4
	Window	0.372	267.0	6.59	40536	300	617	476	40.8	40.9	0.00549	222.3
	S Window	0.186	306.4	7.67	39942	0	779		27.4	40.6	0.00639	255.1
Centre	Full	3.155	102.3	2.21	46235	1000	140	31	7.4	3.1	0.00184	85.2
	Soffit	2.400	113.9	2.41	47246	700	158	35	11.3	3.9	0.00201	94.8
	Door	0.400	267.7	6.45	41507	300	635	491	96.4	54.7	0.00538	222.9
	Window	0.372	181.7	4.02	45203	300	463	327	-	22.6	0.00335	151.3
	S Window	0.186	291.2	6.64	43850	0	785		-	-	0.00553	242.5
Front	Full	3.155	113.0	2.50	45204	1000	163	55	1.7	7.8	0.00208	94.1
	Soffit	2.400	112.9	2.59	43618	800	194	51	2.6	9.2	0.00216	94.0
	Door	0.400	65.0	1.52	42847	400	236	121	3.4	13.0	0.00126	54.2
	Window	0.372	100.4	2.47	40575	400	325	184	-	26.5	0.00206	83.6
	S Window	0.186	274.1	8.15	33644	0	858		-	-	0.00679	228.2

Figure 5.2 to Figure 5.6 compare the heat release rate histories for the each of the three different single individual pan locations; *rear*, *centre* and *front*, with the different ventilation openings; *full*, *soffit*, *door*, *window* and *small window*. Each of the plots also includes the single free-burning pool fire heat release rate history for further comparison.

The free-burning fire shows a steady heat release rate of 87 kW after the initial growth phase of approximately 3 minutes. This is 15% lower than the predicted value given in equation (5.3-1). This reduction is believed to be due to the constant fuel surface height and insulated pan walls.

Both the *full* and *soffit* geometry results (Figure 5.2 and Figure 5.3 respectively) are similar and hence the addition of the soffit has little effect. The heat release rates for each of individual pan locations are similar with a slight increase in the HRR for the rear pan which is considered a result of radiation feedback from the rear compartment wall.

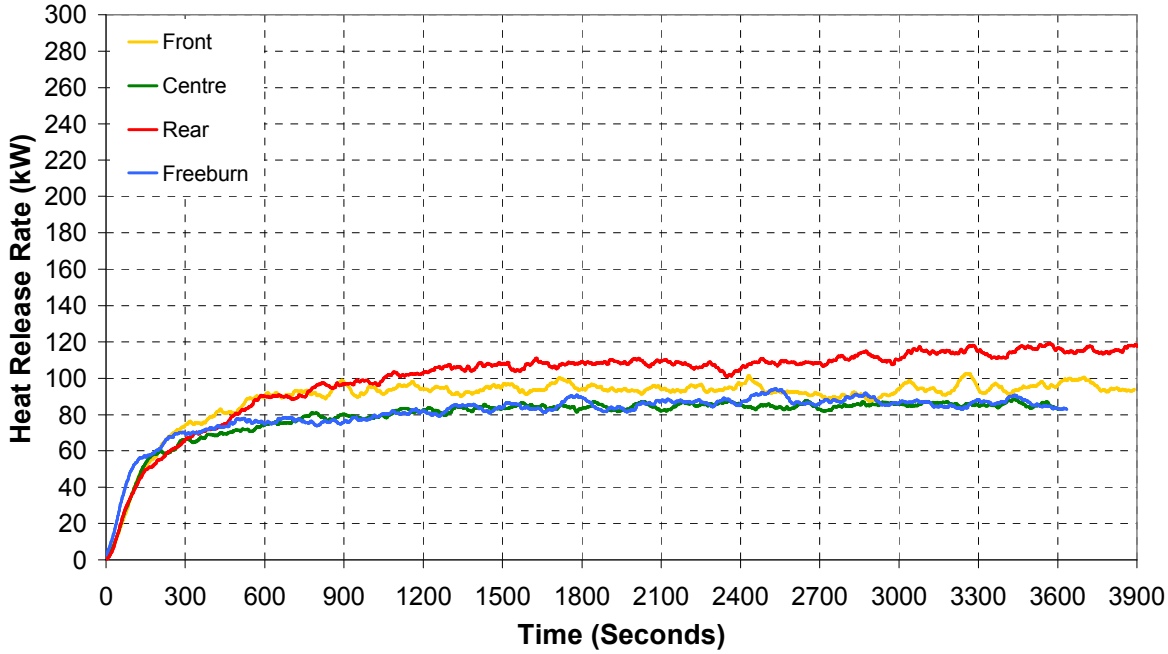

Figure 5.2: Comparison of the heat release rate histories for the each of the three pan locations with a vent *full* open 2.4 m wide and 1.2 m height along with the free-burning pool.

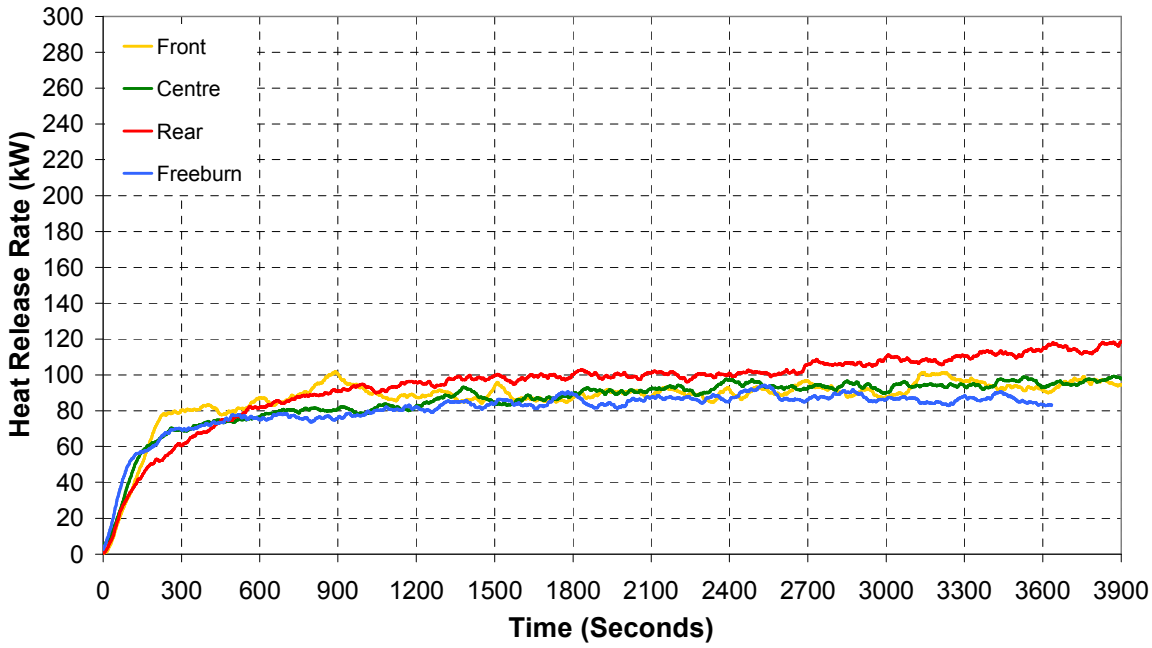

Figure 5.3: Comparison of the heat release rate histories for the each of the three pan locations with a single *soffit* vent 2.4 m wide and 1.0 m height along with the free-burning pool.

Both the rear and centre pan experiments with the *door* and *window* vent geometries (Figure 5.4 and Figure 5.5 respectively), show significant enhancement to the fire due to radiation feedback from the compartment.

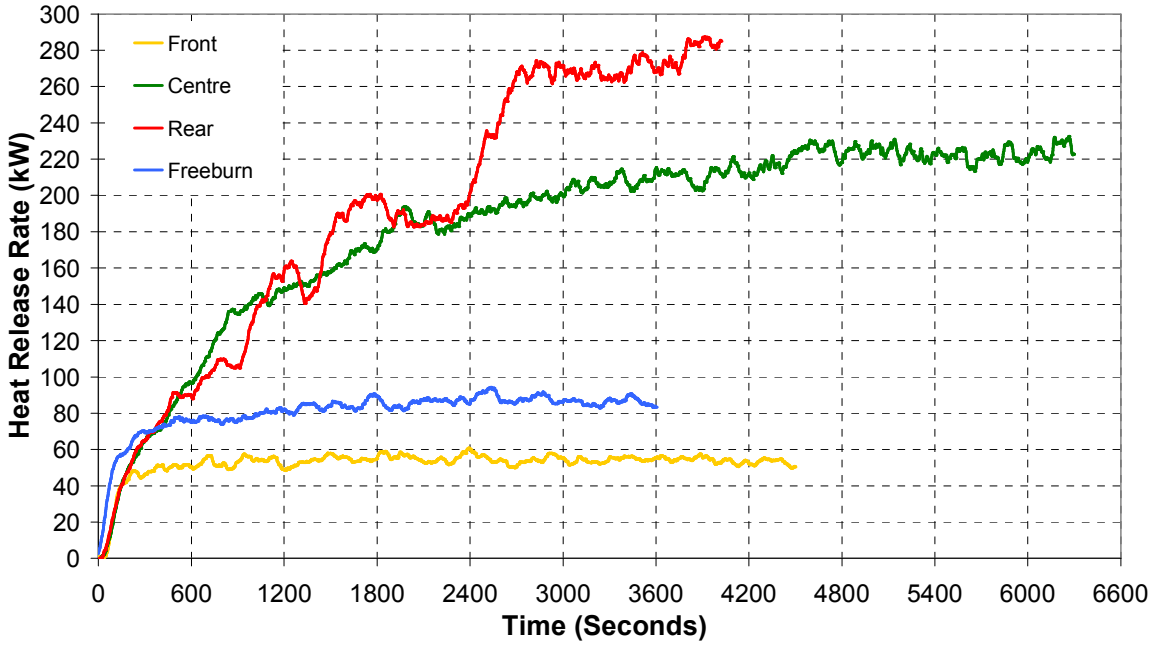

Figure 5.4: Comparison of the heat release rate histories for the each of the three pan locations with a single *door* vent 0.4 m wide and 1.0 m height along with the free-burning pool.

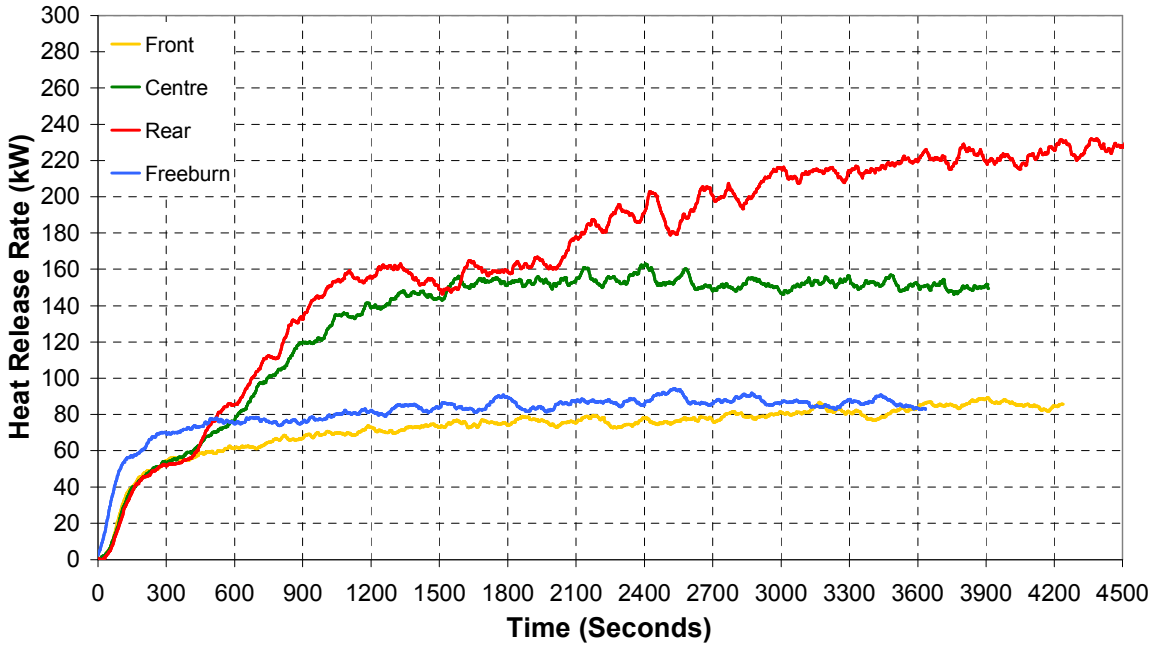

Figure 5.5: Comparison of the heat release rate histories for the each of the three pan locations with a single *window* vent 0.8 m wide and 0.6 m height along with the free-burning pool.

For the *door* geometry, Figure 5.4 shows the average heat release rate during the last 1200 seconds of the experiment as of 223 kW for the centre location and 272 kW when the pan was placed in the rear of the compartment which is a 162% and 211% increase respectively over the free burning heat release rate. For the *window* geometry, the average heat release rate is 151 kW for the centre location and 222 kW when the pan

was placed in the rear of the compartment. This is a 73% and 154% increase respectively over the free burning heat release rate.

These values when compared with equation (5.3-2), shows that the placement of the pan from the centre to the rear causes a transition from pre-flashover to the predicted post-flashover phase. This is in sharp contrast to the pan placed near the front opening. For the *door* geometry, the average heat release rate during the last 1200 seconds of the experiment was 54 kW and for the window geometry of 84 kW. This represents a 38% and a 4% decrease respectively compared to the free-burning value.

For the *small-window* vent geometry (Figure 5.6) there is considerable enhancement to the fire due to radiation feedback from the compartment for all pan location, Table 5.2 shows the average heat release rate during the last 1200 seconds of the experiment as of 228 kW for the front location, 242 kW for the centre location, and 255 kW when the pan was placed in the rear of the compartment. This is a 160%, 177%, and 192% increase respectively over the free burning heat release rate. All of the *small-window* experiments these approach or exceed the predicted heat release rate of 240kW for flashover as noted from equation (5.3-2).

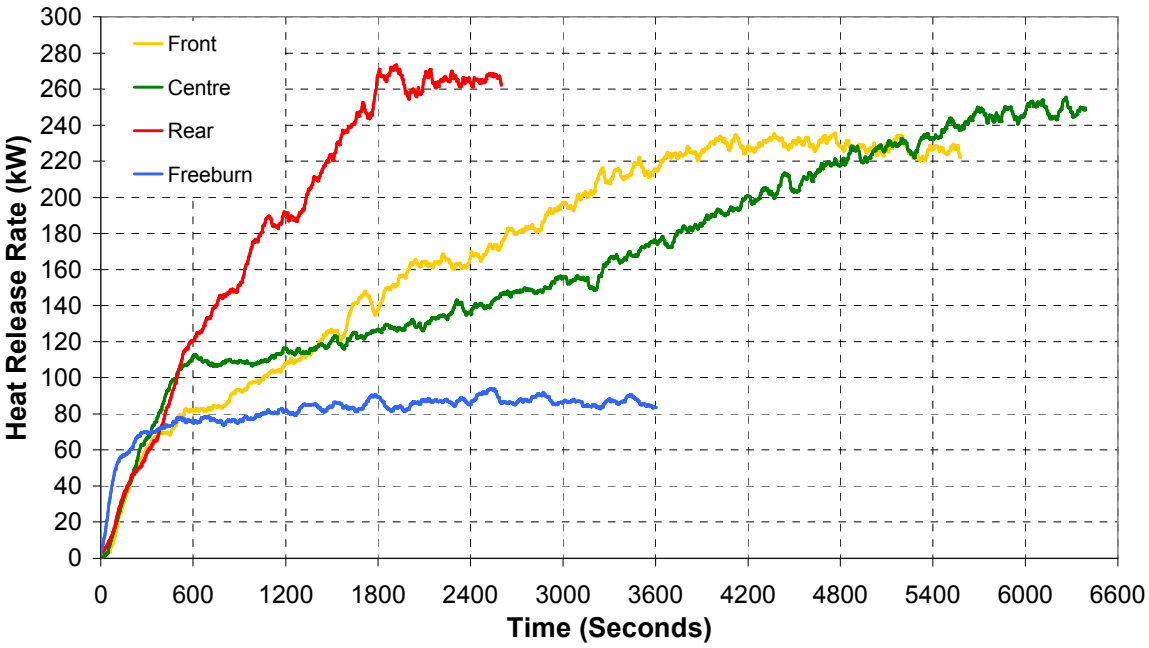

Figure 5.6: Comparison of the heat release rate histories for the each of the three pan locations with a single *small-window* vent 0.4 m wide and 0.6 m height along with the free-burning pool.

The reduction in heat release rate for the door (front pan) experiment when compared to the free-burning case is due to the flame leaning over as a result of the incoming air through the vent. Figure 5.7 shows one for each pan location and vent configuration. The flames structures for each of the single pan experiments are very different. The *full*, *soffit*, *door* and *window* experiments provide pre-flashover compartment behaviour, whereas the *small-window* experiments near flashover conditions.

Figure 5.7 shows a set of photographs for the flame profiles for the *full*, *soffit*, *door*, *window* experiments. The *small-window* experiment profiles are not shown in this set as the compartment conditions meant that visual observations through the windows were limited due to turbulent and sooty compartment conditions obscuring the windows.

The *full* vent (Figure 5.7 A-C) and *soffit* vent (Figure 5.7 D-F) had relatively minor leaning flame structure, but the *door* vent (Figure 5.7 I) had the most severe lean which was significant enough to reduce the radiation feedback to the fuel surface. The *window* front pan location (Figure 5.7 L) also had a major flame lean but this did not significantly reduce the heat release rate. For the centre pan location the flame (Figure 5.7 H) structure was also forced to lean over but not as severely as the front location, although there is significant burning around the base of each of the pans. The *door* (Figure 5.7 G) and *window* vent (Figure 5.7 J) for the rear pan location show a lean and significant burning around the base of the pan with the flame structure leaning horizontally to the rear of the compartment such that it in contact with the wall.

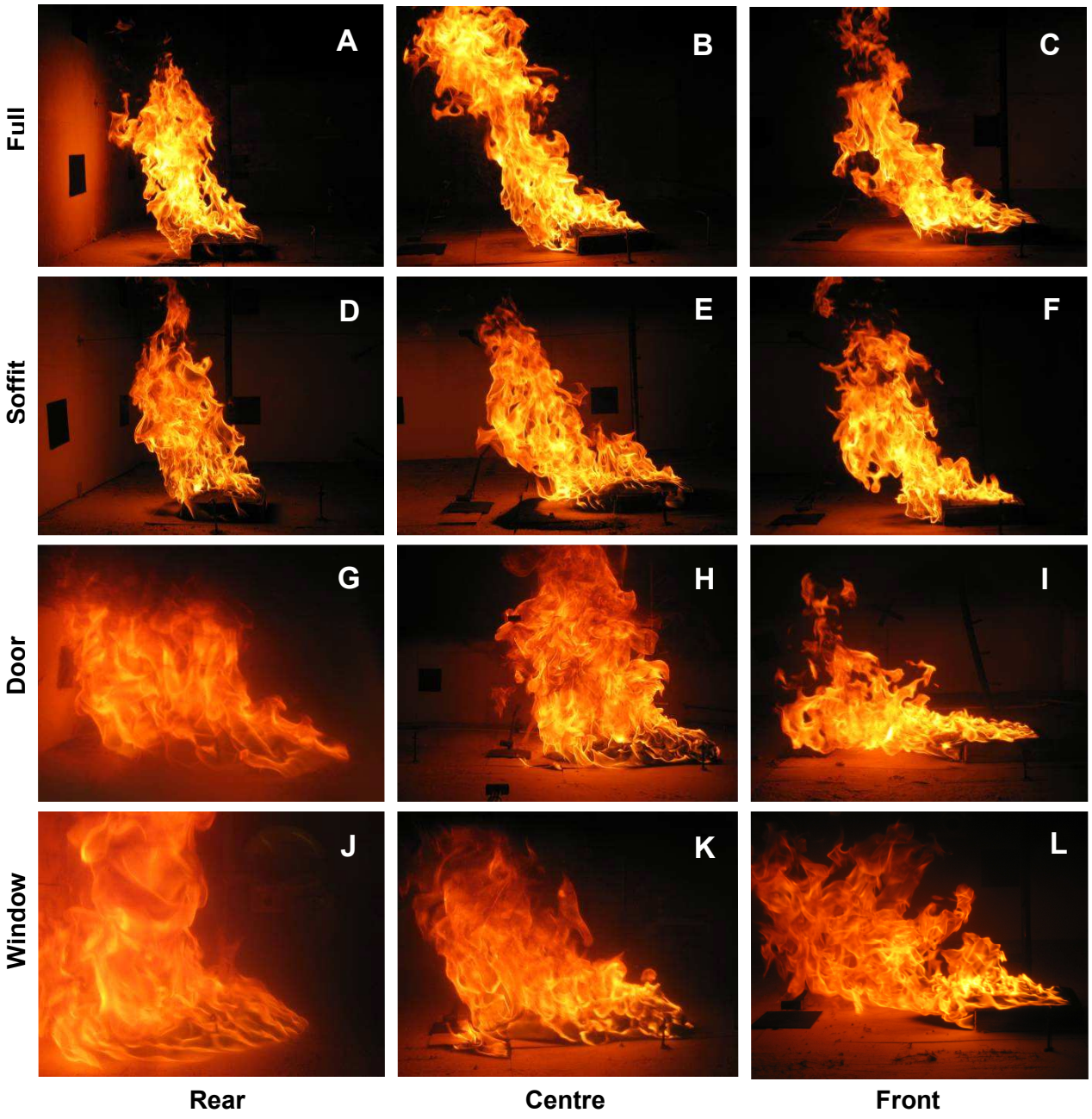

Figure 5.7: Photographs taken for each pan location showing the internal flame structure for the *full*, *soffit*, *door*, *window* vent geometries. Photographs of the *small-window* flame profile are not available due to no visibility from the turbulent and sooty compartment environment.

For the *small-window* experiments, the compartment fires initially displayed similar appearance to that of the *window* geometry, however as they developed the flame leaning and flame extension along the floor was significant. In the case of the front pan the flame front extended along the floor toward the rear of the compartment. This is shown in the photograph in Figure 5.8 in which the fire location in the front pan is blown along the floor past the centre pan location.

Figure 5.8: Photographs showing the flame lean and flame extension along the floor with the front pan for the *small-window* vent geometry.

This floor driven fire behaviour was consistent for all pan locations. As the fires developed the flow is driven along the floor to the rear of the compartment, returning in a turbulent circular nature as it rebounds of the rear wall. Due to internal observations being unavailable for the turbulent sooty small window experiments, Figure 5.9 M to O shows the external flaming indicating near post flashover venting.

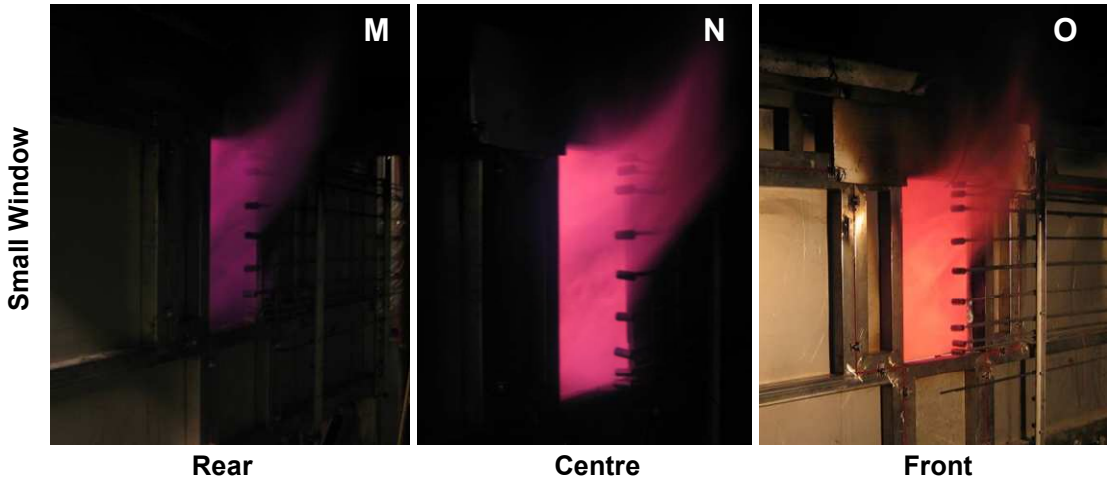

Figure 5.9: Photographs taken for each pan location showing the external flame structure for the *small-window* vent geometries.

For the single pan experiments the rear pan location provides the highest heat release rate for each ventilation geometry as a result of the enhancement provided by the rear compartment wall. Figure 5.10, Figure 5.11, and Figure 5.12 compare the heat release rate histories for the five different ventilation openings with the fire in the rear, centre and front of the compartment along with the free-burning pool fire heat release rate history for further comparison.

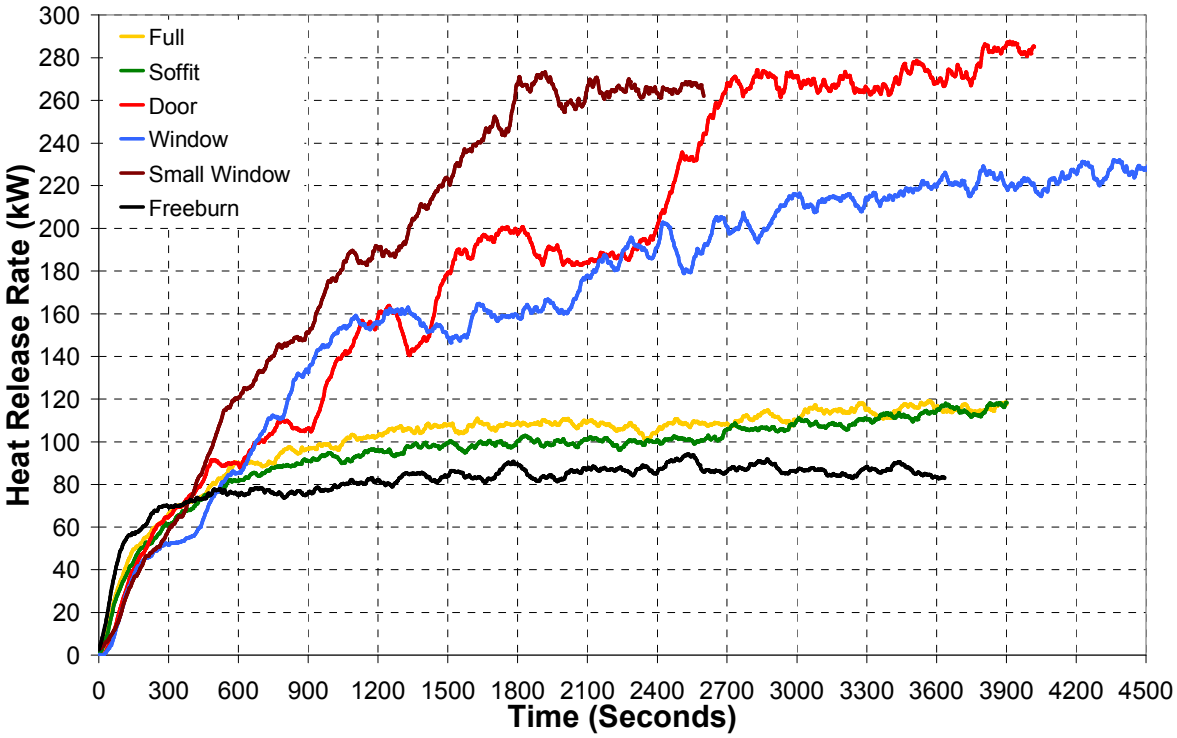

Figure 5.10: Comparison of the heat release rate histories for the pan in the rear of the compartment for each of the five ventilation openings along with the freeburn pool.

Figure 5.10 and Figure 5.11 show that the *door* and *small-window* geometries provide the highest heat release rate for the rear and centre location respectively in the single pan series, and these also exceed the predicted heat release rates required for flashover. The small window also provides the greatest heat release rate for the front pan location, however the front pan with the door geometry provides a heat release rate that was less than the free burning rate. It can be seen in Table 5.2 that the mass loss rate of the front pan is approximately 65% of the free burning rate and this is as a result of the leaning over effect of the flame in the pan reducing the enhancement to the pool fire.

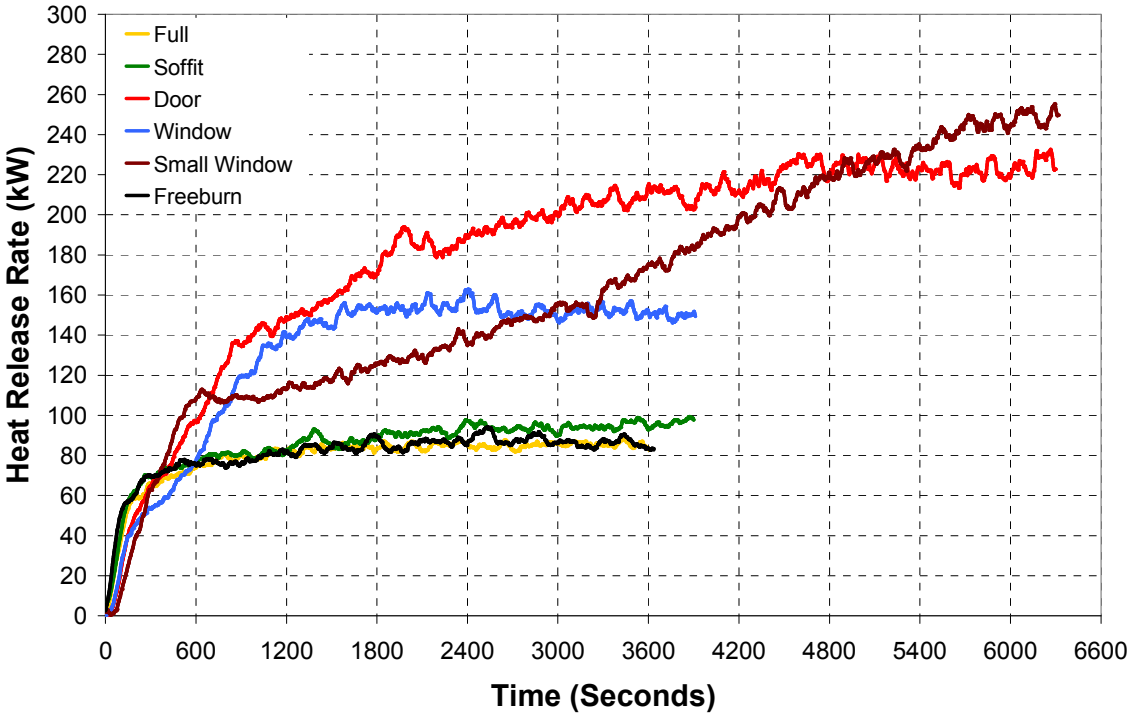

Figure 5.11: Comparison of the heat release rate histories for the pan in the centre of the compartment for each of the five ventilation openings along with the freeburn pool.

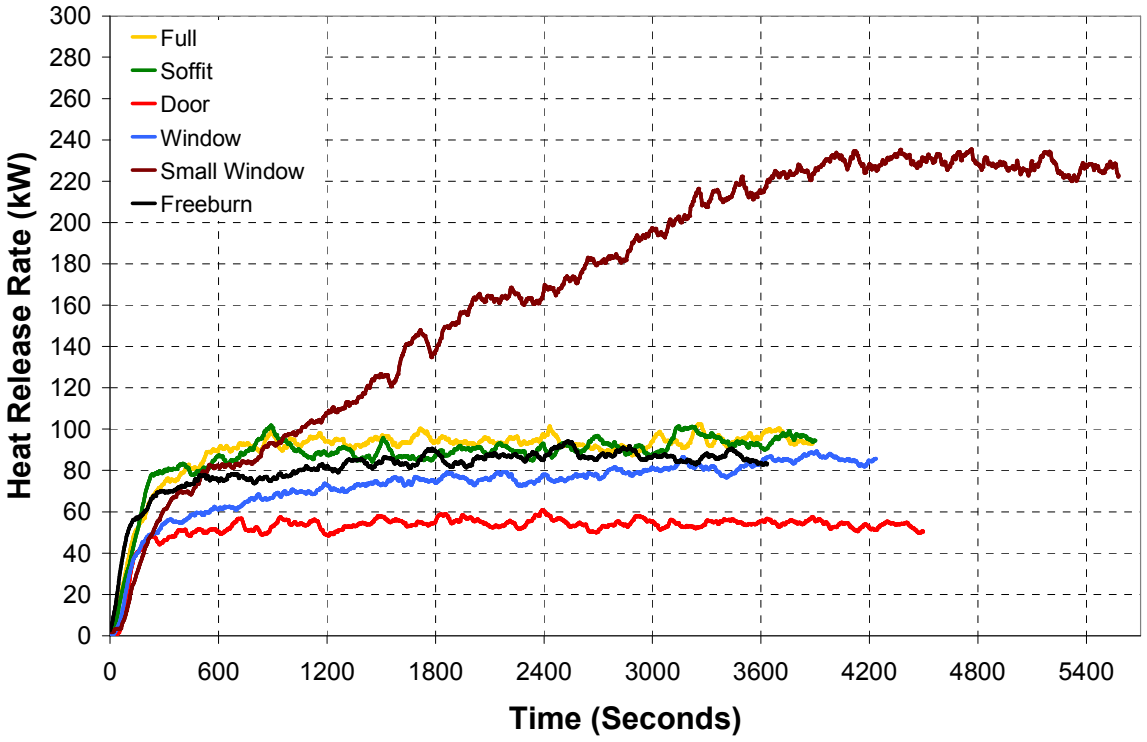

Figure 5.12: Comparison of the heat release rate histories for the pan in the front of the compartment for each of the five ventilation openings along with the freeburn pool.

Figure 5.13 and Figure 5.14 compare the average aspirated thermocouple temperatures (25mm below ceiling located 1.2 m from the front opening and 1.2 m from rear wall) in the ceiling jet and the Gardon gauge heat flux history measurements with the fire at the rear of the compartment respectively. It can be seen that a reduction in ventilation provided by either of the *door*, *window* or *small-window* vent geometries provides significant radiation enhancement to the fire from the compartment in comparison with the *full* and *soffit* vents. In both the *full* and *soffit* vent geometry experiments, the ceiling jet temperatures do not exceed 300ºC, whilst in the *door* and *window* experiments the temperatures are approximately 800ºC, and the *small-window* experiments ceiling jet temperatures approach 1000ºC. Table 5.2 also shows that the conditions within the compartment are representative of a post-flashover situation considering typical post-flashover conditions of temperatures >600 ºC [6] and heat flux values at the floor >20kW/m² [7].

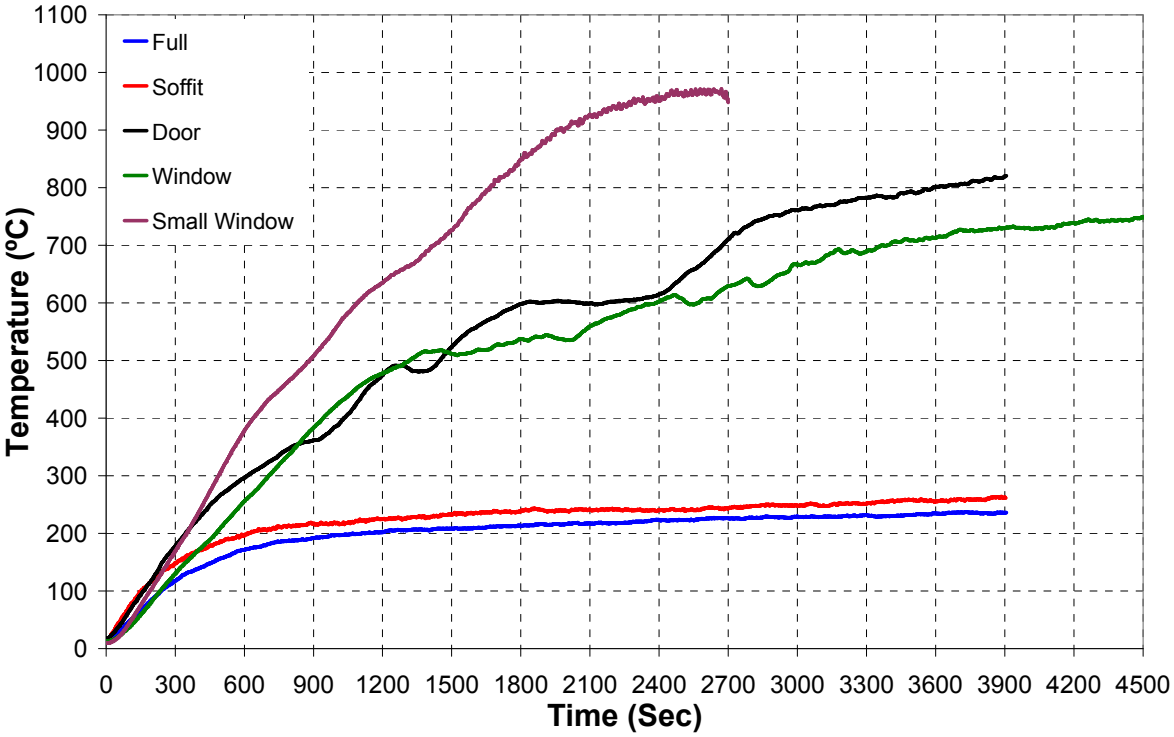

Figure 5.13: Average temperature histories for the two aspirated thermocouple 25mm below ceiling located 1.2 m from the front opening and 1.2 m from rear wall of the compartment for each of the five ventilation openings.

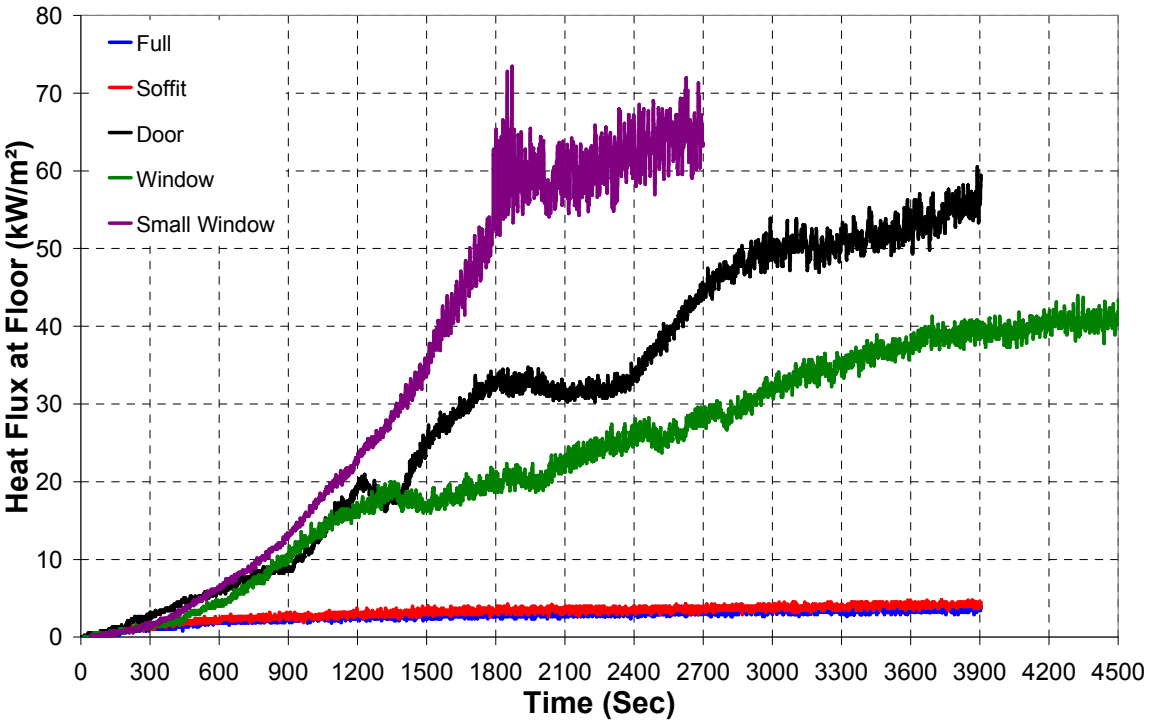

Figure 5.14: Average heat flux histories received at floor level, 1.2 m from the front opening and 1.2 m from rear wall of the compartment for each of the five ventilation openings.

Figure 5.15, Figure 5.16 and Figure 5.17 show the temperature profile from the thermocouple tree located in the corner closest to the ventilation opening (refer to Figure 3.1.1) for the rear, centre and front pans respectively at the completion of each experiment. The profiles for the *full* opening show a typical profile expected for a ceiling jet flow with the high temperatures near the ceiling and a rapid drop in temperature moving toward the floor. This profile was consistent for all of the pan locations with the *full* vent opening. For *soffit* openings the profile is also the traditional two layer pre-flashover profile. This was also consistent for all the other pan locations with the *soffit* ventilation opening with the average upper layer temperature being of the order of 200ºC, as seen in Table 2.

In the experiments with the *door* and *window* vents, the profiles were less consistent or predictable. For the front pan *door* and *window* experiments the profile is a typical two layer pre-flashover profile with an upper layer temperature of 236ºC and 325ºC respectively. When the pan is moved to the centre the upper layer temperatures increase to 635ºC and 463ºC. However, when the same pan is moved to the rear of the compartment the temperature profile is more uniform from floor to ceiling as expected in a fully developed post-flashover fire. In this case the average temperature was 681ºC for the *door* vent and 617ºC for the *window* vent, well within the expected post-flashover temperatures. For the fire in the centre of the compartment with the *door* and *window* openings there is a more transitional profile between pre-flashover and post-flashover with an average upper layer temperature of 635ºC but reducing to less than 490ºC near the floor for the *door* vent and an average upper layer temperature of 463ºC, reducing to 327ºC near the floor for the *window* vent.

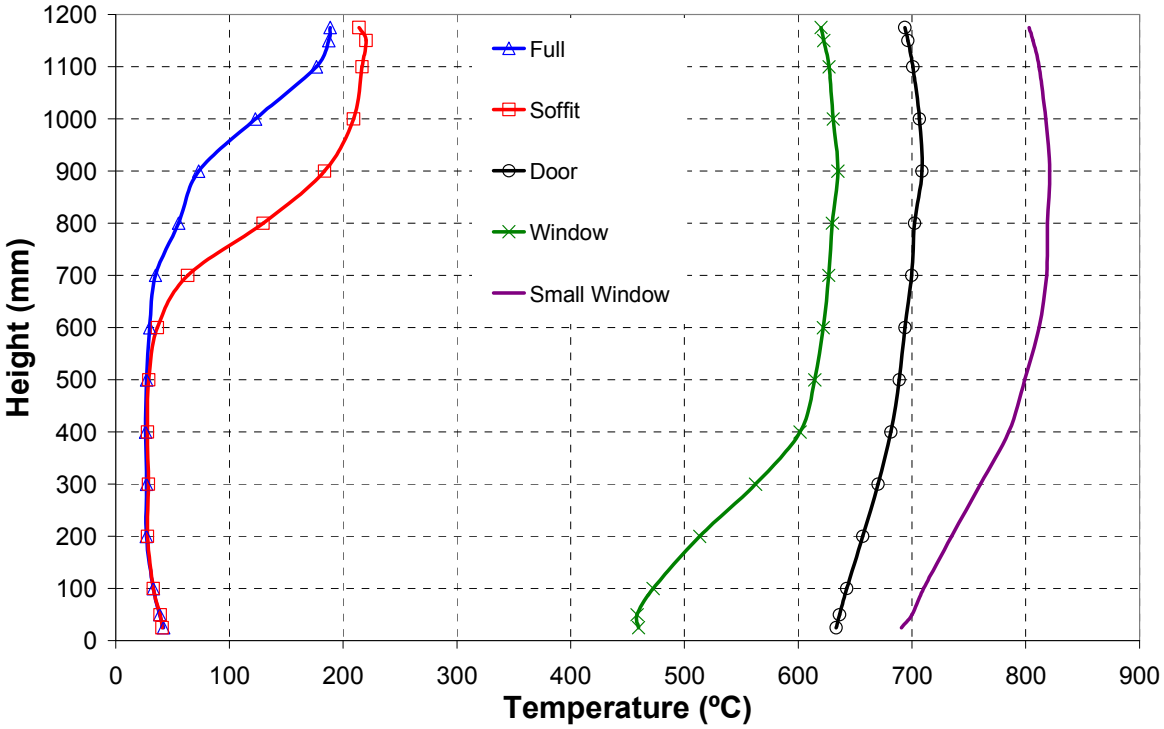

Figure 5.15: Temperature profiles at the thermocouple tree in the compartment corner closest to the vent from the rear pan experiments for all five ventilation openings, at the completion of the each experiment.

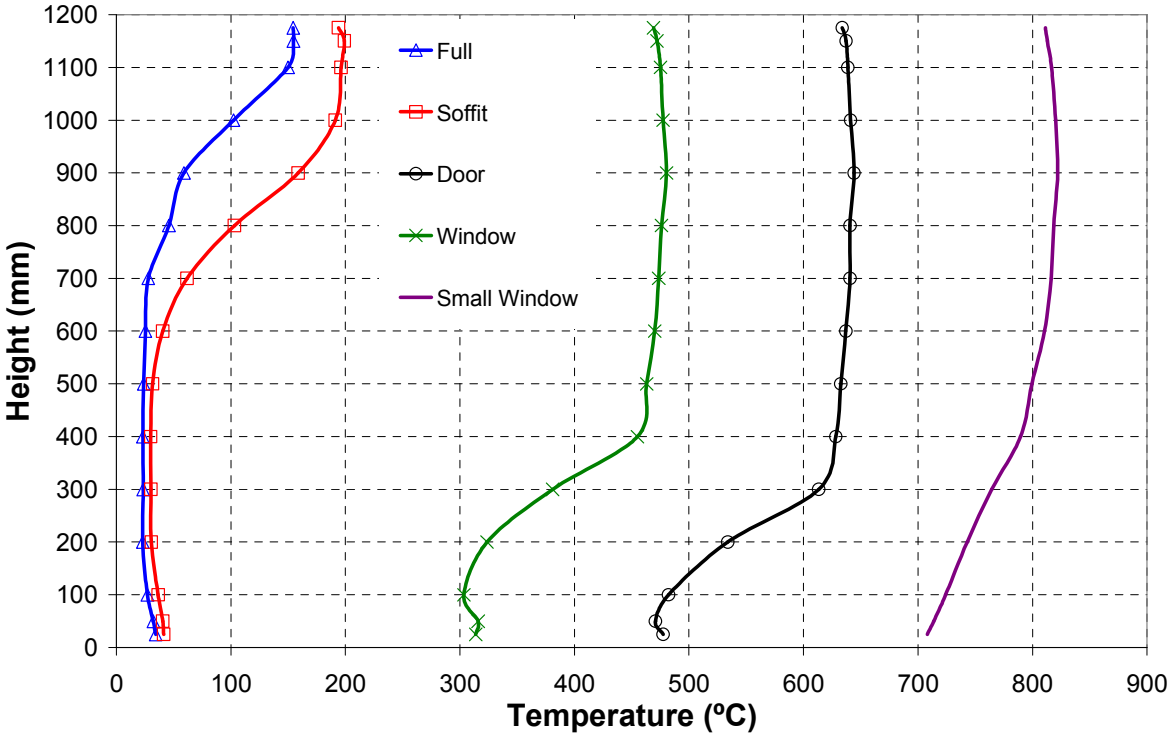

Figure 5.16: Temperature profiles at the thermocouple tree in the compartment corner closest to the vent from the centre pan experiments for all five ventilation openings, at the completion of the each experiment.

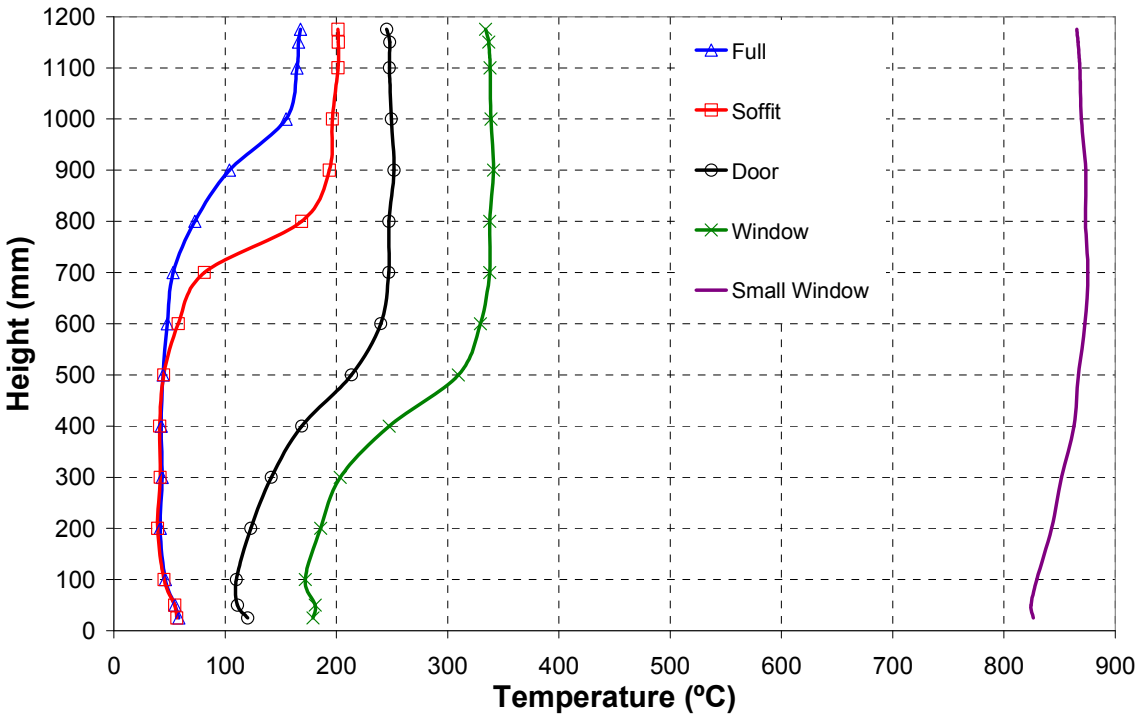

Figure 5.17: Temperature profiles at the thermocouple tree in the compartment corner closest to the vent from the front pan experiments for all five ventilation openings, at the completion of the each experiment.

Figure 5.18, Figure 5.19, and Figure 5.20 show the velocity profile for the bi-directional probes located in the centre of the vent opening.

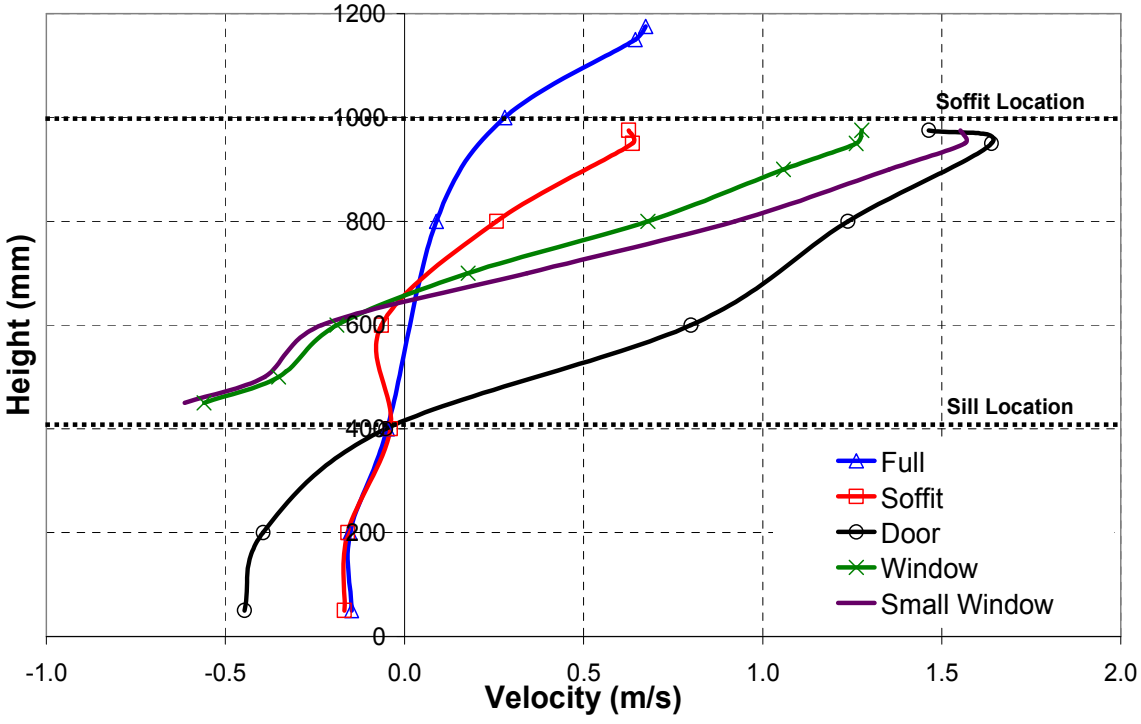

Figure 5.18: Velocity profiles at the bi-directional probes in the centre of the vent opening from the rear pan experiments for all five ventilation openings, at the completion of the each experiment

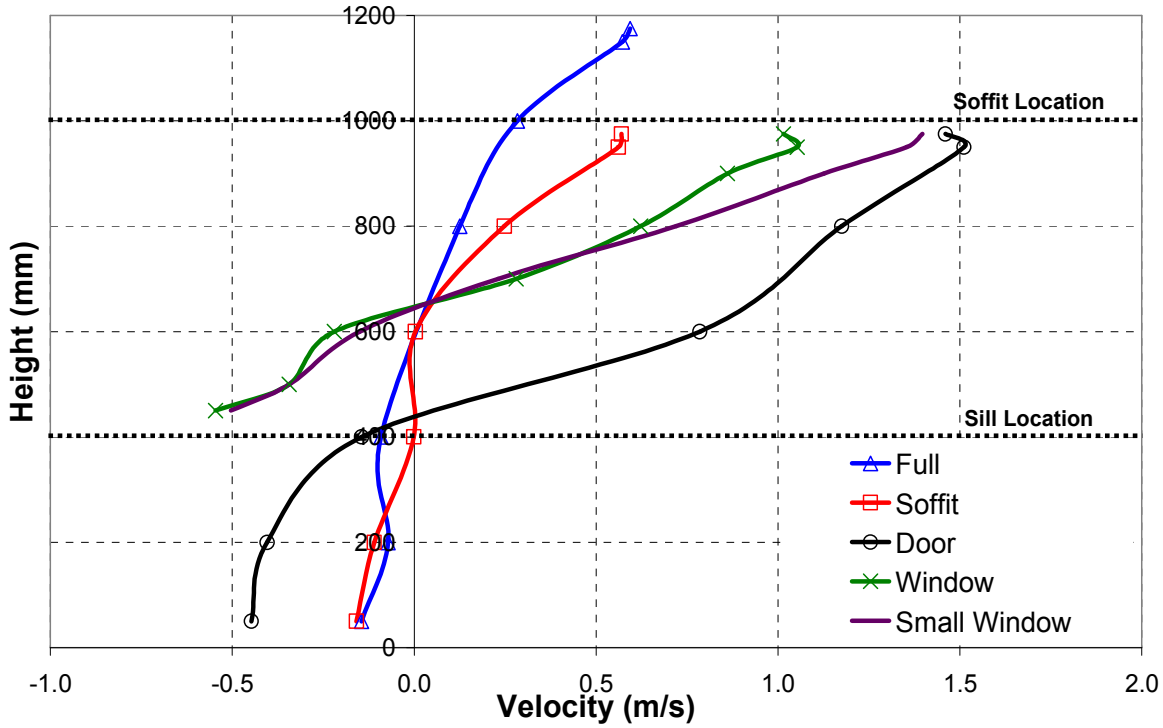

Figure 5.19: Velocity profiles at the bi-directional probes in the centre of the vent opening from the centre pan experiments for all five ventilation openings, at the completion of the each experiment

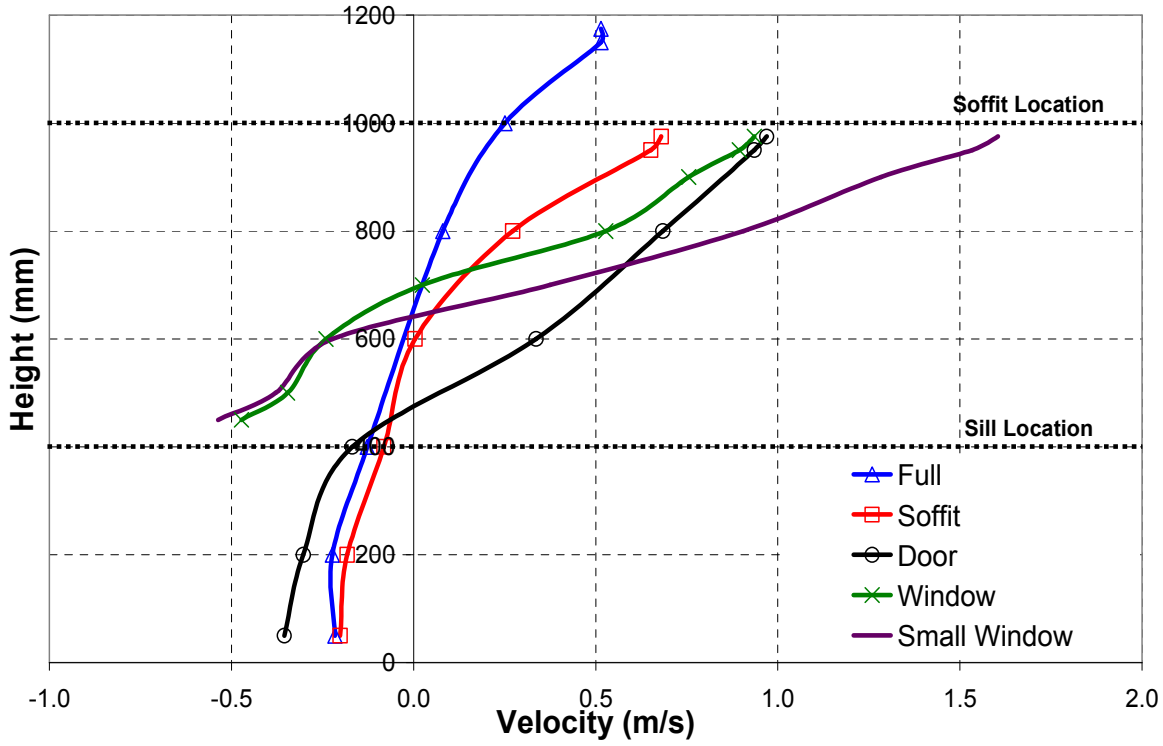

Figure 5.20: Velocity profiles at the bi-directional probes in the centre of the vent opening from the front pan experiments for all five ventilation openings, at the completion of the each experiment

In the experiments for both the *full* and *soffit* opening the velocities near the floor are less than 0.2 m/s which caused the flame in the pan to tip approximately 30º off the vertical axis as seen in Figure 5.7. However, for the *door*, *window* and *small-window* experiments the velocities were much higher ranging from 0.37 m/s for the front location with the *door* to 0.61 m/s for the rear location with the *small-window*. The affect on the flame shape can be seen in Figure 5.7 and Figure 5.8 which shows the flame leaning over significantly enough that the flame is in contact with the floor on the leeward side of the pan.

It is observed that the outflow velocity decreases as the pan is moved towards the front of room. This can be attributed to a reduction in mass loss rates at the front pan location. Table 5.2 details the average mass loss rate of all of the pans, and it can be seen that as the pan location is moved to the front of the compartment the MLR is less than those of the centre and rear locations.

5.7 Conclusions

- The results of this research clearly show that the location of the fire can have a pronounced effect on pool fires. This can be seen in the experiments with the *door*, and *window*, geometries, where a transitional phase between a pre-flashover fire and a post flashover fire occurs when the pan is moved progressively from the front to the rear of the compartment.

- The heat release rate for the pool fire is a function of the fire location and can be significantly greater than the predicted free burning rate and even greater than the maximum free burning rate for an optically thick pool fire.

- The shape of the flame is greatly impacted by the velocity through the vent and can lean significantly over by the incoming airflow such that the flame is in contact with the floor on the leeward side of the pan. In some cases the incoming air can actually reduce the heat release rate below the free-burning heat release rate.

- The *small-window* vent provides uniform post flashover conditions and velocities flows drive the flame structure along the entire length of the compartment floor before reaching the flashover transition.

5.8 Future Research

- Further research should include multiple fires in multiple locations to assess the impact on the compartment environment when compared to a single fire of equal surface area.
- Additional work is needed using different size vents over a range of opening factors in order to further quantify the heat release rate versus ventilation factor.
- More experimental work is required to quantify the effect of fire location when the fire is not located along the centreline of the ventilation opening including along sidewalls and in corners.
- The results given here should be modelled in field models such as FDS to validate the model for use in fire location studies such as this. Many of the recommendations given above could be tested numerically to reduce the size of the experimental work required.

5.9 Acknowledgements

The authors would like to acknowledge the financial support provided by the New Zealand Fire Service Commission and the Foundation of Research Science and Technology (FRST).

5.10 References

---

1 Babrauskas, V, “Heat Release Rates”, The SFPE Handbook of Fire Protection Engineering, Section 3/Chapter 1, 3rd edition, 2002.

2 Babrauskas, V., Estimating Large Pool Fire Burning Rates, Fire Technology 19, 251-261 (1983).

3 Thomas, I. R., and Bennetts, I D., "Fires in Enclosures with Single Ventilation Openings – Comparison of Long and Wide Enclosures", Fire Safety Science – Proceedings of the Sixth International Symposium, 941-952, 1999.

4 Kirby, B. R., Wainman, D. E., Tomlinson, L. N., Kay, T. R. and Peacock, B. N., Natural Fires in Large Scale Compartments, A British Steel Technical, Fire Research Station Collaborative Project, BSC, 1994.

5 Cooke, G. M. E., "Tests to Determine the Behaviour of Fully Developed Natural Fires in a Large Compartment", Fire Note 4, BRE, 1998.

6 Walton, W.D and Thomas, P. H, "Estimating Temperatures in Compartment Fires", The SFPE Handbook of Fire Protection Engineering, Section 3/Chapter 6, 3rd edition, 2002

7 Drysdale, D, An Introduction to Fire Dynamics, 2nd Edition, John Wiley & Sons, New York, 1998.

Chapter 6: Multiple Pan Experimental Results

This chapter details results from the experimental series using multiple 200mm square heptane pans in various permutations of three pan locations (rear, centre and front) within the experimental compartment. This series of experiments used five different ventilation geometries; fully open, soffit, door, window, and small window. The chapter is presented in the form of the paper submitted to Fire & Materials and follows on from the work described in the paper published and presented at the Eighth International Symposium, International Association for Fire Safety Science, Beijing China titled "*The Impact of Location and Ventilation on Pool Fire in a Compartment*" [1].

The paper is divided into two sections detailing the experimental results from;

- Double multiple pan experiments in which two 200mm square pans are located in combination within the enclosure. Results from experiments with a x2 pan e.g. a pan having the equivalent area to that of two 200mm square pans (283mm square) located in the centre of the room, are also detailed.
- Triple multiple pan experiments in which three 200mm square pans are located simultaneously in the enclosure. Results from experiments with a x3 pan e.g. a pan having the equivalent area to that of three 200mm square pans (346mm square) located in the centre of the room are also detailed.

The paper provides an introduction and brief background on pool fires and a general overview of the experimental apparatus and instrumentation. For a full description of the experimental apparatus and instrumentation, refer to *Chapter 3: Experimental Setup and Procedure*. Results of measurements recorded during the experiments are presented, including heat release rate, heat flux, compartment temperatures, and vent velocities. Visual observations are also discussed, however a detailed account of visual observations from all experiments is provided in Appendix B.

The Impact of Size, Location and Ventilation on Multiple Pool Fires in a Compartment

A. R. PARKES and C. M. FLEISCHMANN
University of Canterbury
Christchurch,
New Zealand

6.1 Abstract

This paper describes recent experiments to investigate the impact that the size and location of multiple fires within an enclosure have upon the rate of heat release. A series of pool fire experiments were conducted in a ½ domestic scale compartment using five typical ventilation geometries (fully open, soffit, door, window and small window). Multiple heptane pool fires were located in permutations of three evenly distributed locations within the compartment (rear, centre and front) as well as larger equivalent area pans located only in the centre. The primary goal of this work is to demonstrate that the fire location within a compartment can have a more significant impact upon the heat release rate and subsequent compartment conditions than that of an equivalent sized fire located in the centre. Results show that the fire location and ventilation significantly impact the heat release rate of the fire and that multiple fires with a pan located near the ventilation opening can have a larger heat release rate than a fire with a larger equivalent area located in the centre of the compartment.

KEYWORDS: compartment fires, fire growth, fire size, fire location, heat release rate, mass loss rate, pool fires, flashover

6.2 Introduction

The work detailed in this study continues the previous work by Parkes et.al [1] and describes subsequent experiments at the University of Canterbury to investigate the effect that the size and location of a fire within an enclosure has upon the mass loss rate and rate of heat release. It is recognised that compartment effects due to radiation and ventilation play a significant role in the burning rate of the pool fire. The ventilation geometry of the enclosure affects the fire behaviour by increasing the impact of the

upper layer and the subsequent radiation feedback to the fuel surface. The ventilation also modifies the combustion behaviour of a fire, and this of course has a considerable effect on the heat release rate.

The use of computer models as part of fire engineering design is common practise. The models are used to develop performance based designs to show that the impact of a fire does not affect the building's occupant(s). Although these models do have limitations it is not uncommon to see them being misused. Many are also limited to evaluating single prescribed burning items, and the behaviour of a multi-packaged fuel source within a compartment cannot be accurately determined [2,3]. This is due to objects burning at different rates as a result of the interaction of each object and the interaction with the surrounding environment.

As calculations of fire behaviour in buildings are not possible unless the heat release rate of the fire is known, research into the behaviour of these multi-packaged fuel sources is required. The use of the heat release rate of a design fire is the key characteristic that describes quantitatively how "big" a fire is. In a fire engineering design the heat release rate is therefore the most important variable in evaluating the fire hazard [4]. The location of the fire can also have a distinct affect on the fire development, and it is noted that performance based design fire scenarios typically consider a fire located in the centre of an enclosure. Therefore the fire engineering design premise that a '*credible design fire scenario*' can consist of one centrally non-wall bounded fire was investigated in this study.

A series of compartment fires using five typical ventilation geometries (fully open, soffit, door, window and small window) were conducted. The results of heptane pool fires located in multiple locations within the compartment (*rear-centre*, *rear-front*, *centre-front*, *rear-centre-front*) as well as pool fires of equivalent area to two and three pans located in the centre of the compartment are discussed and the results presented.

The primary goal of this work is to demonstrate that the location of multiple fires within a compartment can play a significant role in compartment fires and improve the understanding of the interaction of these characteristics upon fire behaviour.

6.3 Background

Burning liquid fires have been studied extensively. It has long been known that the burning rate of pool fires is controlled by the heat transfer back to the surface. For pool fire sizes of interest to fire engineers, i.e. diameters greater than 0.2 m, the heat transfer is governed by the radiation back to the surface. For pools fire with diameters between 0.2m and 1m the flame is considered to be optically thin whereas for pools fire greater than 1m in diameter the flame is optically thick [5]. The burning rate for pool fires greater than 0.2 m can be estimated using the following semi-theoretical expression [6]

$$\dot{q} = \Delta h_c \ \dot{m}_f \ = \ \Delta h_c \ \dot{m}''_\infty \left[1 - \exp\left(-k\beta \ D\right)\right] A_p \qquad \textbf{(6.3-1)}$$

For heptane in a 0.2m square pan the free burning heat release rate is expected to be 100kW using typical values for heptane ($\dot{m}''_\infty = 0.101$ kg/s.m² , $\kappa\beta$=1.1m^{-1}, Δh_c=44.6MW) taken from reference [1].

A pool fire geometry represents a worse case in terms of radiation enhanced mass loss rate. The entire fuel surface sees the hot upper layer and bounding surfaces. Thomas and Bennetts, have studied large pool fires in a deep narrow compartment with different opening geometries [7]. In their study, the entire floor of the compartment was covered with fuel pans. Results highlighted the importance of ventilation geometry on the burning rate of the pools.

More complex wood cribs fuels in large narrow enclosures have been studied at BRE [8,9]. In the BRE study, wood cribs were placed over the entire floor of a long narrow compartment with a single vent at the opposite end of the enclosure. The importance of the fire location relative to the opening was also identified in this work as the fire ignited in the rear, spread quickly to the front of the enclosure and then spread more slowly into the compartment as the fuel was consumed, thus demonstrating the importance of the fire location relative to the ventilation opening.

It has long been observed that pool fires can burn in a high fuel rich manner. Babrauskas [10] has also shown that the ventilation limited stoichiometric fuel pyrolysis rate can be estimated as;

$$\dot{m}_f(st) = \frac{0.5}{r} A_v \sqrt{H_v} \qquad \textbf{(6.3-2)}$$

Where :

r = stoichiometric air/mass ratio = 15.1 for heptane

A_o = vent area (m^2)

h_o = vent height (m)

With the heat of combustion of heptane, 44600 kJ/kg [11], this estimates a heat release rate of 274kW for the small window ventilation controlled conditions.

The expected heat release rate within an enclosure sufficient to cause flashover can also be calculated using the following expression derived by Babrauskas [12].

$$\dot{Q} = 600\, A_v \sqrt{H_v} \qquad \textbf{(6.3-3)}$$

For the different ventilation geometries represented in this study the predicted heat release rates for flashover are; *Full* (1893kW), *Soffit* (1440kW), *Door* (240kW), *Window* (223kW), and *Small Window*, (112kW).

The pool fire geometry represents a worse case in terms of radiation enhanced mass loss rate. The entire fuel surface sees the hot upper layer and bounding surfaces. More complex fuels such as furniture or wood cribs will be partially shielded from the compartment environment and therefore less radiation will reach the fuel surface.

6.4 Experimental Apparatus and Procedure

6.4.1 Apparatus

Nineteen experiments were conducted in a 2.4m wide by 3.6m long by 1.2m high compartment constructed from stainless steel. Figure 6.1 is a sketch of the compartment

showing the multiple pan locations, fully open ventilation, and notable instrumentation. The walls, ceiling and floor of the compartment were lined with two layers of 10mm ceramic fibre board. For visual observations, five windows were located on one side of the compartment, four in the lower half of the compartment with the fifth located at the upper level near at the front of the room as shown in Figure 6.1.

Ventilation into the compartment was designed to be easily modified using panel construction to enable the ventilation geometry to be changed from fully open, to a soffit, and to a door. These panels when connected to the compartment were also lined with two layers of 10mm ceramic fibre board. The dimensions of the various ventilation geometries were:

1. ***Full*** – 2.4m wide x 1.2m high (Unrestricted), ($A_v\sqrt{H_v} = 3.155$)
2. ***Soffit*** – 2.4m wide x 1.0m high (0.2m downstand), ($A_v\sqrt{H_v} = 2.4$).
3. ***Door*** – 0.4 m wide by 1.0 m high, ($A_v\sqrt{H_v} = 0.4$).
4. ***Window*** – 0.8 m wide by 0.6 m high (0.2m Sill), ($A_v\sqrt{H_v} = 0.372$).
5. ***Small-window*** – 0.4 m wide by 0.6 m high (0.2m Sill), ($A_v\sqrt{H_v} = 0.186$).

Heptane pool fires were used in all experiments, with a 200mm square pan 50mm high. The perimeter of the pan was insulated with 20 mm thick ceramic fibre board. The pans were able to be positioned in various permutations of three locations within the compartment, for every corresponding change in ventilation opening. These locations are noted below, based upon pan centreline dimensions;

a) Rear location: The pan in the rear position was located 3.0m from the front wall of the compartment.
b) Centre location: The pan in the centre location position was located 1.8m from the front wall of the compartment.
c) Front location: The pan in the front location position was located 0.6m from the front wall of the compartment.

The equivalent area pans (*x2* and *x3* sized pans) were located in the centre of the compartment only, e.g. centre 1.8m from the ventilation opening and rear compartment wall. Heptane fuel was pumped from 40-litre pre-fabricated stainless steel fuel tanks using a tubing pump connected to individual header tanks. From the header tank the pan

was gravity fed allowing a constant fuel surface height. Ignition was by a series of electrodes connected to two 15000 volt transformers.

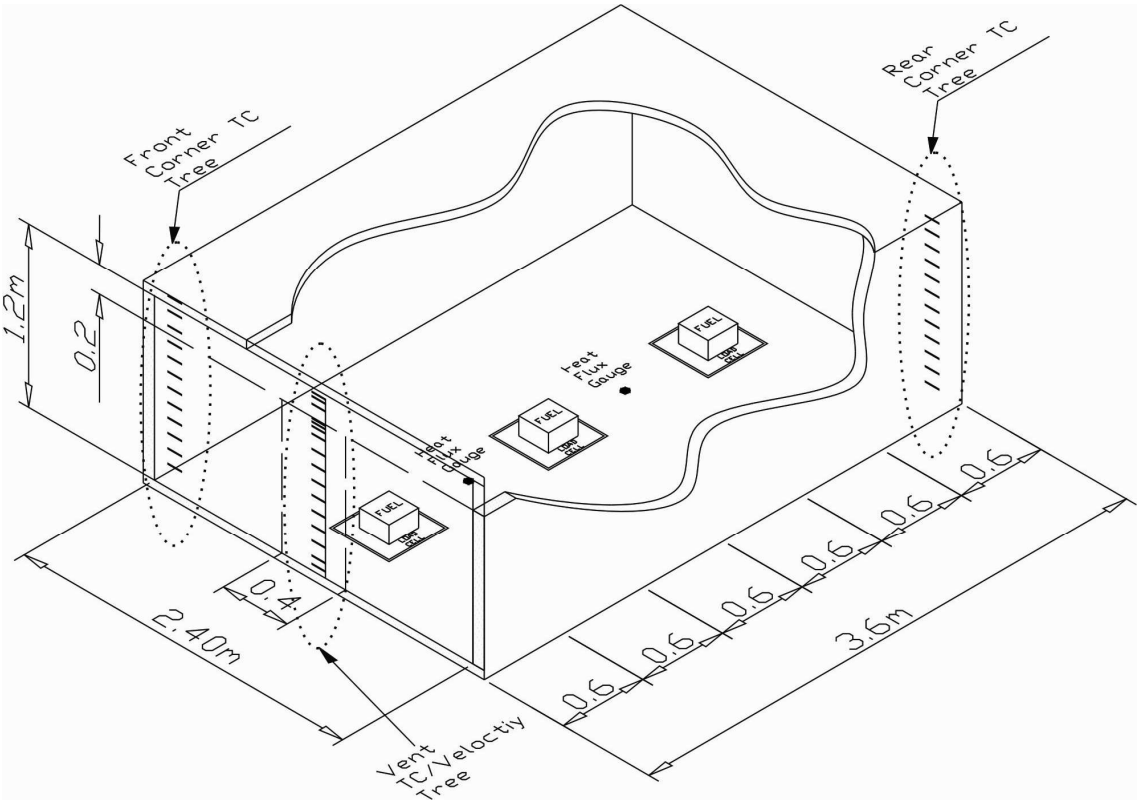

Figure 6.1: Sketch of the experimental compartment showing all three pool fire locations, fully open ventilation condition and relevant instrumentation.

6.4.2 Instrumentation

Compartment Temperatures: To measure the compartment gas temperatures, vertical thermocouple trees were installed at the front and rear of the enclosure (see Figure 1). Two sets of 15, 1.6 mm diameter type K thermocouples were used and positioned at spacings of generally 100mm vertically between the floor and ceiling. To avoid effects from the boundary layer, the thermocouples were installed 150 mm off the rear wall, 100mm off the side walls, and 25 mm from the floor/roof.

Vent Temperatures/Pressures: A thermocouple tree was installed within the vent to record the vent temperatures. 14, 1.6 mm diameter type K thermocouples at a spacing of 100mm were used, with this being reduced to 12 for the *soffit/door* geometry, and 8

for the *window/small-window* geometry. 10 Bi-directional probes were also installed in the vent when the *full/soffit/door* geometry was used, and 8 when the *window/small-window* geometry was used. These were used for measurements of vent velocities and were connected to pressure transducers with a pressure range of 0-25 Pa.

Heat Flux: Two Gardon type water-cooled heat flux gauges were installed between each of the separate pan locations e.g. 600mm from the centre of each pan. The heat flux gauge at location 1 is 2400mm from the front opening (between the rear and centre pans) and location 2 is 1200mm from the front opening (between the centre and front pans). These were used to measure the radiation heat flux at the floor during each experiment.

Mass Loss: The mass loss of the fuel was recorded on a load cell upon which the fuel tanks are positioned.

Heat Release Rate: The heat release rate from each experiment was measured using oxygen depletion calorimetery and included O_2, CO_2, and CO species measurements. The extraction system had a maximum flow rate of 4 m^3/s.

Data Acquisition: A Universal Data Logging (UDL) system developed at the University of Canterbury is used to log voltages from the above instrumentation through software and hardware interfaces. The hardware consists of serial boxes for each different sensing device which is then calibrated with the UDL programme and an associated calibration and offset factors. The sampling rate for the UDL program was 1 sample per second using a Pentium P4 computer.

6.5 Procedure

Twenty one experiments were conducted in total including two experiments with a x2 and x3 equivalent area pan in the open under quiescent conditions to provide a base case for comparison. Table 6.1 summarizes the ventilation geometries and pan locations for the completed matrix of 19 multiple pan and equivalent pan freeburn experiments. It is noted that due to the excessively high temperatures achieved in the compartment and the long durations of the experiments (up to 2 hours), the compartment construction was significantly effected. Therefore a complete set of door and window experiments were not able to be completed due to the damage to the compartment.

Table 6.1: Completed Experimental Matrix

		Opening Geometry				
		Full Open	*Soffit* 0.2m (downstand)	*Door* 1.0m x 0.4m	*Window* 0.6m x 0.8m	*Small Window* 0.6m x 0.4m
Pan Location	**Double Pan Experiments**					
	Rear & Centre	×	×	×	-	×
	Rear & Front	×	×	-	-	×
	Centre & Front	×	×	-	-	×
	x2 Pan (Centre)	×	×	-	-	×
	Triple Pan Experiments					
	All Pans (rear, centre & front)	×	×	-	-	×
	x3 Pan (Centre)	×	×	-	-	×

Each experiment involved calibration of the oxygen depletion calorimetry system before commencement. A three minute baseline was taken to record the initial ambient conditions, with ignition of the pan at three minutes. Each experiment was allowed to run for a total duration after ignition of at least 60 minutes.

6.6 Summary Results

The experimental results from the multiple pan experiments are divided into the following two sections:

1. ***Double Pan Experiments;*** This section details the results from all experiments involving two individual 200mm square pans in the three permutation locations (rear-centre, rear- front, centre-front) and the x2 equivalent area pan located in the centre of the room. Results are detailed in Table 6.2.

2. ***Triple Pan Experiments;*** This section details the results from the experiments involving three individual 200mm square pans in the rear, centre and front locations, and the x3 equivalent area pan located in the centre of the room. Results are detailed in Table 6.3.

Each of the tabulated summaries in Table 6.2 and Table 6.3 is presented in the following layout. The first column specifies the location of the pool fire pans with respect to the experiment. This details multiple locations using permutations of the rear (3.0 m from the compartment ventilation opening), centre (1.8 m from the compartment ventilation opening), and front (0.6 m from the compartment ventilation opening) locations within the compartment as well as larger equivalent free burning pool fires (refer to Figure 3.8 showing pan sizes and locations). The tabulated locations are detailed as, **x2 freeburn** (free-burning pool fire in the open with an equivalent area of two 200mm pans), **x3 freeburn** (free-burning pool fire in the open with an equivalent area of three 200mm pans), **Rear-Centre** (200mm square pans located in the rear and centre), **Rear-Front** (200mm square pans located in the rear and front), **Centre-Front** (200mm square pans located in the centre and front), **x2 centre** (pan of equivalent area to two 200mm pans located in the centre), **x3 centre** (pan of equivalent area to three 200mm pans located in the centre). The second and third columns specify the configuration type of the ventilation geometry and their associated ventilation factors [13]. Five different ventilation geometries were provided; ***Full*** (2.4m wide x 1.2m high), ***Soffit*** (2.4m wide x 1.0m high), ***Door*** (0.4 m wide by 1.0 m high), ***Window*** (0.8 m wide by 0.6 m high), ***Small-window*** (0.4 m wide by 0.6 m high). The fourth column is the total heat (energy) released during the fully developed phase of burning for the

last 1200seconds of each experiment. The fifth column specifies the mass loss (kg) of the pans for the last 1200seconds of each experiment. The total mass loss of all pans is listed first followed by the individual mass loss associated with the rear, centre and front pan locations for experiments with multiple pans. The sixth column details the effective heat of combustion, calculated from columns four and five. Columns seven to nine detail the layer height, upper layer temperature, and lower layer temperature based on maximum slope of the temperature profile at the front corner TC tree nearest the opening. It is noted that if only one temperature term is stated then the compartment conditions are represented by a single zone with a uniform temperature. Columns 10 and 11 are the average heat flux measurements 1.2 m from the front opening (between the centre and front pans) and 2.4 m from the front opening (between the rear and centre pans), respectively. The results are averaged over the last 300 seconds of the experiment. Column 12 is the mass loss rate, MLR, averaged over the last 1200seconds of the experiment. The averaged total mass loss is stated first followed by the individual mass loss rates associated with the rear, centre and front pan locations for those experiments with multiple pans. Column 13 is the heat release rate, averaged over the last 1200seconds of the experiment.

6.6.1 *Double Pan Summary*

The results of the 14 double pan experiments are summarised in Table 6.2 below.

Table 6.2: Summary of data from double pan experiments and the x2 free-burning pool fire.

Pan Location	Vent Config.	Av√Hv	Total Energy last 1200 sec (MJ)	Mass Loss				ΔHc (kJ/kg)	Layer Height, HL (mm)	T_{Ave} Upper Layer (°C)	T_{Ave} Lower Layer (°C)	Ave. Heat Flux #1 Last 300 sec (kW/m²)	Ave. Heat Flux #2 Last 300 sec (kW/m²)	Average MLR (last 1200 sec)				Ave. HRR Last 1200 sec (kW)
				Total (kg)	Rear Pan (kg)	Centre Pan (kg)	Front Pan (kg)							Total (kg/s)	Rear Pan (kg/s)	Centre Pan (kg/s)	Front Pan (kg/s)	
x2 Freeburn			261.4	5.7				45494						0.00479				217.8
Rear Centre	Full	3.155	249.2	5.8	3.3	2.5	-	42971	800	212	62	17.2	6.2	0.00487	0.00278	0.00209	-	206.0
	Soffit	2.400	336.6	7.7	4.6	3.1	-	43846	700	342	104	31.4	12.1	0.00640	0.00385	0.00255	-	278.1
	Door	0.400	544.4	14.8	7.9	6.9		36795	0	849		60.9	42.5	0.01233	0.00661	0.00572	-	453.7
	Window	0.372																
	Small Window	0.186	300.4	9.7	4.9	4.8	-	30993	0	902		-	33.84	0.00808	0.00409	0.00399	-	250.1
Rear Front	Full	3.155	241.2	5.7	2.9	-	2.8	42172	800	219	61	7.4	11.7	0.00480	0.00245	-	0.00235	199.4
	Soffit	2.400	277.6	6.1	3.5	-	2.6	45789	700	279	74	10.2	17.3	0.00505	0.00289	-	0.00216	229.4
	Door	0.400																
	Window	0.372																
	Small Window	0.186	509.4	12.4	3.5		8.9	40932	0	776		23.1	30.5	0.01037	0.00295	-	0.00742	424.5
Centre Front	Full	3.155	222.8	5.2	-	2.5	2.6	43015	800	215	60	12.5	13.0	0.00433	-	0.00212	0.00221	184.1
	Soffit	2.400	247.5	5.7	-	3.3	2.4	43208	700	285	84	20.1	21.1	0.00477	-	0.00275	0.00202	204.6
	Door	0.400																
	Window	0.372																
	Small Window	0.186	465.6	12.1	-	3.5	8.6	38379	0	763		-	-	0.01010	-	0.00293	0.00717	387.7
x2 Centre	Full	3.155	270.7	6.3	-	-	-	43090	800	237	69	27.0	11.5	0.00524	-	-	-	225.4
	Soffit	2.400	324.1	7.3	-	-	-	44548	700	330	109	-	-	0.00606	-	-	-	269.8
	Door	0.400																
	Window	0.372																
	Small Window	0.186	298.3	8.6	-	-	-	34714	0	875		-	-	0.00716	-	-	-	248.4

Note: Shaded Rows indicate those experiments not completed due to damaging compartment conditions

6.6.2 Triple Pan Summary

The results of the 7 triple pans experiments are summarised in Table 6.3.

Table 6.3: Summary of the data from the triple pan experiments and the x3 free-burning pool fire.

Pan Location		Vent Config.	Av√Hv	Total Energy last 1200 sec (MJ)	Mass Loss				ΔHc (kJ/kg)	Layer Height, HL (mm)	T_{Ave} Upper Layer (°C)	T_{Ave} Lower Layer (°C)	Ave. Heat Flux #1 last 300 sec (kW/m²)	Ave. Heat Flux #2 last 300 sec (kW/m²)	Average MLR (last 1200 sec)				Ave. HRR Last 1200 sec (kW)
					Total (kg)	Rear Pan (kg)	Centre Pan (kg)	Front Pan (kg)							Total (kg/s)	Rear Pan (kg/s)	Centre Pan (kg/s)	Front Pan (kg/s)	
x3 Freeburn				420.2	8.7				48121						0.00728	-	-	-	350.2
Rear	Full		3.155	337.7	9.2	3.6	2.8	2.7	36839	700	265	79	4.5	2.4	0.00764	0.00301	0.00234	0.00229	281.2
Centre	Soffit		2.400	533.0	12.6	6.1	3.5	3.0	42320	600	411	151	5.1	2.8	0.01050	0.00510	0.00290	0.00249	443.8
Front	Door		0.400																
	Window		0.372																
	Small Window		0.186	566.2	14.6	2.9	3.0	8.6	38906	0	726		60.4	41.5	0.01213	0.00244	0.00253	0.00716	464.6
x3 Centre	Full		3.155	628.9	14.3	-	-	-	43875	700	422	167	90.5	35.5	0.01195	-	-	-	523.7
	Soffit		2.400	873.4	21.5	-	-	-	40701	600	639	335	-	-	0.01788	-	-	-	727.2
	Door		0.400																
	Window		0.372																
	Small Window		0.186	294.2	9.3	-	-	-	31569	0	1039		-	-	0.00777	-	-	-	245.0

Note: Shaded Rows indicate those experiments not completed due to damaging compartment conditions

6.7 Double Pan Experimental Results

6.7.1 Heat Release Rate

Figure 6.2 through to Figure 6.5 compare the heat release rate histories for each of the three different double pan locations; *rear-centre*, *centre-front*, *rear-front*, and the *x2 centre* pan with each of the different ventilation openings; *full*, *soffit*, *door*, *window* and *small window*. The experimental series using the door and window ventilation geometries were not completed due to damage to the compartment from the high temperatures and long durations of the experiments. However the result from the door experiment with the Rear-Centre pan locations was completed and is shown in Figure 6.4. To allow for further comparison, each of the plots includes the single x2 free-burning pool fire heat release rate history, and the scale provided is based upon the maximum heat release rate achieved.

Both the full and soffit geometry results (Figure 6.2 and Figure 6.3 respectively) are similar and indicate a slight increase in the heat release rate as result of the soffit downstand. The x2 centre pan shows a slightly higher heat release rate which is attributed to the radiative feedback to the larger pool surface area, and the increased optical thickness of the larger flame.

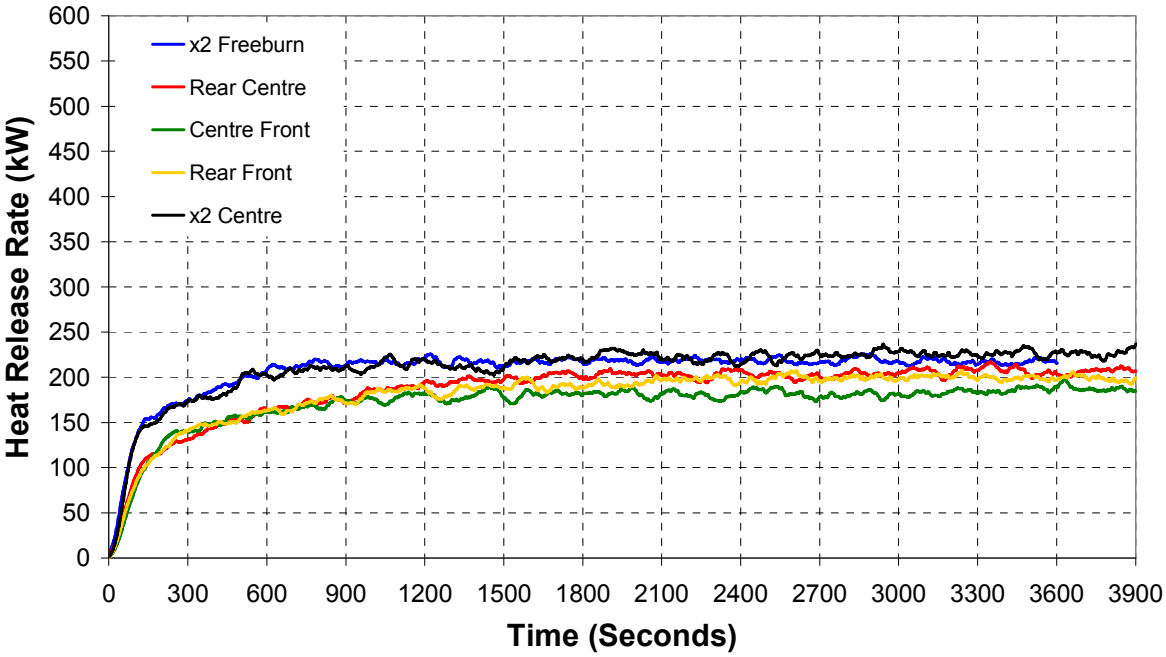

Figure 6.2: Comparison of the heat release rate histories for the each of the double pan locations with a *full* vent (2.4 m wide and 1.2 m high) along with x2 centre pan and the x2 free-burning pool.

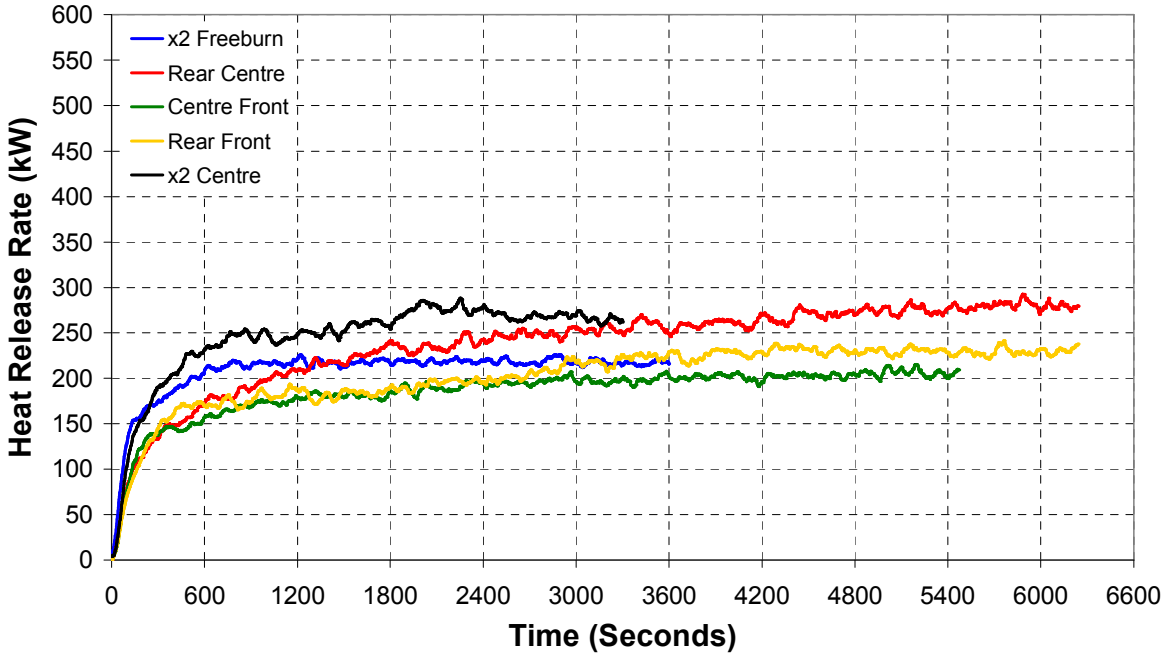

Figure 6.3: Comparison of the heat release rate histories for the each of the double pan locations with a *soffit* vent (2.4 m wide and 1.0 m high) along with x2 centre pan and the x2 free-burning pool.

The experiment with the door geometry (Figure 6.4) shows significant enhancement to the fire due to radiation feedback from the compartment. Table 6.2 shows the average heat release rate during the last 1200 seconds of the experiment is 454 kW for the rear-centre pans, which is a 108% increase over the free burning heat release rate. It is noted that the rear centre experiment was stopped at approximately 1500 seconds as quasi steady state conditions were achieved.

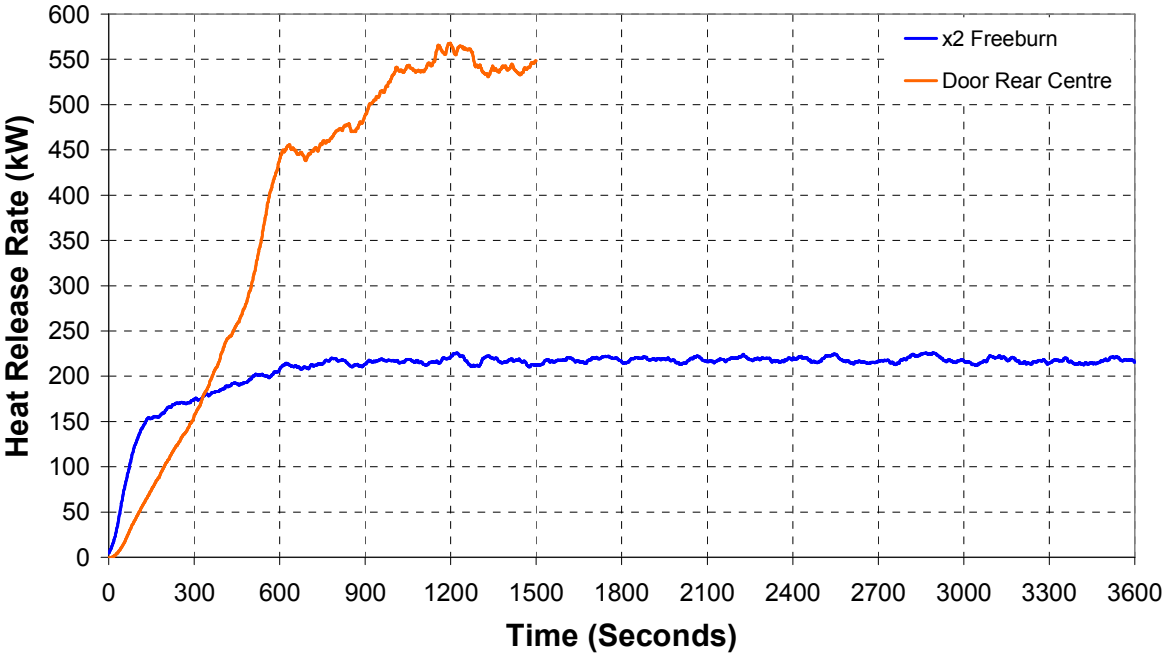

Figure 6.4: Comparison of the heat release rate histories for the each of the double pan locations with a single *door/window* vent along with the x2 free-burning pool.

For the small window geometry (Figure 6.5), the average heat release rate is 250 kW for the rear-centre location, 424 kW for the rear-front location, and 388kW for the centre-front location. This is a 14%, 95%, and 78% increase respectively over the free burning heat release rate. The average x2 centre pan heat release rate is 249kw which is 14% increase over the free burning rate.

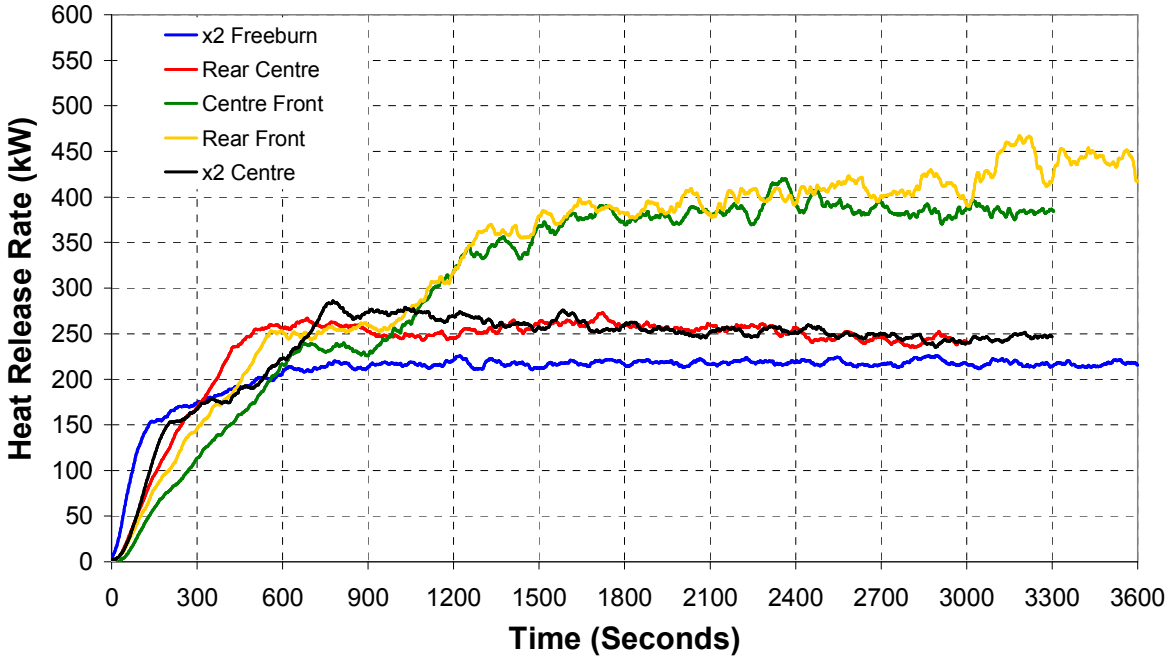

Figure 6.5: Comparison of the heat release rate histories for the each of the three pan locations with a single *small-window* vent 0.4 m wide and 0.6 m height along with the x2 free-burning pool.

These values when compared with Equation (6.3-3) shows that all pan locations with the small window geometry provide post-flashover conditions. However in particular it is noticed that although the post-flashover regime is present for all small window experiments, the experiments involving a front pan in conjunction with another pan provide a heat release rate that is at least 53% higher than the experiments without the front pan. This increase in HRR is discussed further in section 6.9.1.

6.7.2 Vent Flows

The effect of a pan located at the front of the compartment can also be seen in Figure 6.6 which shows a set of photographs of the post-flashover external flaming for the small window geometry experiments. The photographs show a significant increase in the visible external burning when the front pan is included (bottom photographs). This suggests that when the front pan is provided there is a significant increase in the production of un-pyrolysed fuel which then burns externally.

Figure 6.6: Photographs taken showing the external flaming profiles for the small window vent geometries

6.7.3 Temperatures

The rear-centre pan locations provide the highest compartment temperatures of all the double pan experiments completed, although it should be noted that the window experiments are not included and only the door rear-centre experiment was completed. Figure 6.7, Figure 6.8, and Figure 6.11 compare the average aspirated thermocouple temperatures in the ceiling jet with the rear-centre, centre-front and rear-front pan location in the compartment respectively. The time-temperature histories show the full and soffit experiments are similar for all the pan location experiments, and the small

window time-temperature histories for the centre-front and the rear-front cases were at least 100ºC less than the rear-centre location.

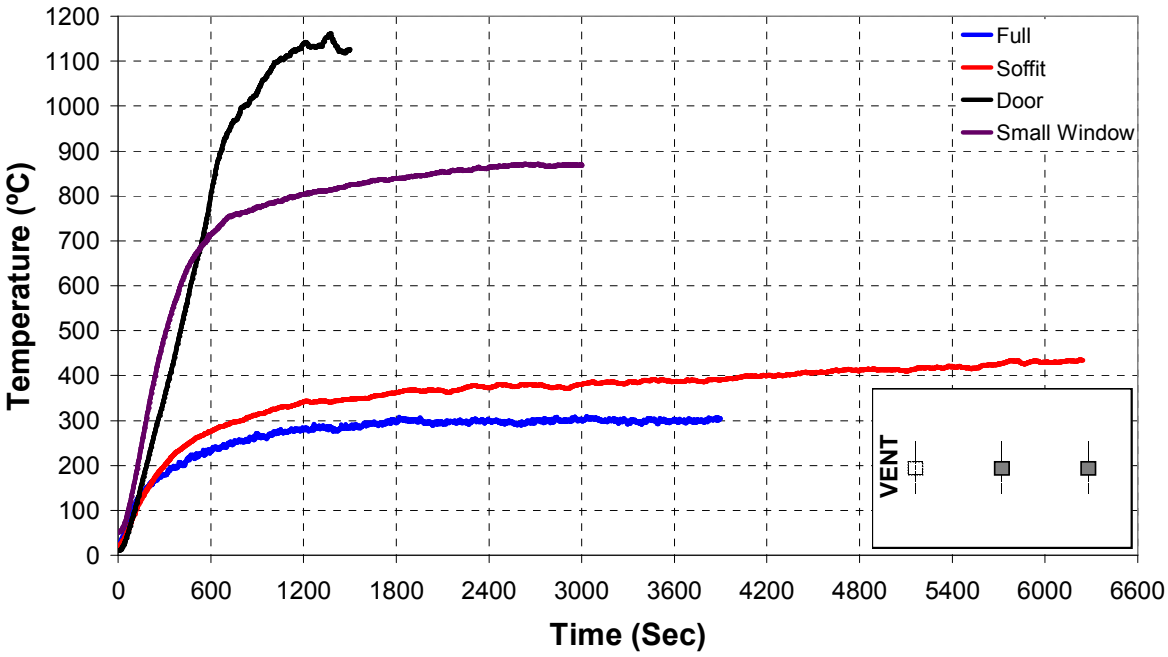

Figure 6.7: Average temperature histories for the two aspirated thermocouple 25mm below ceiling located 1.2 m from the front opening and 1.2 m from rear wall of the compartment for the rear-centre pan locations.

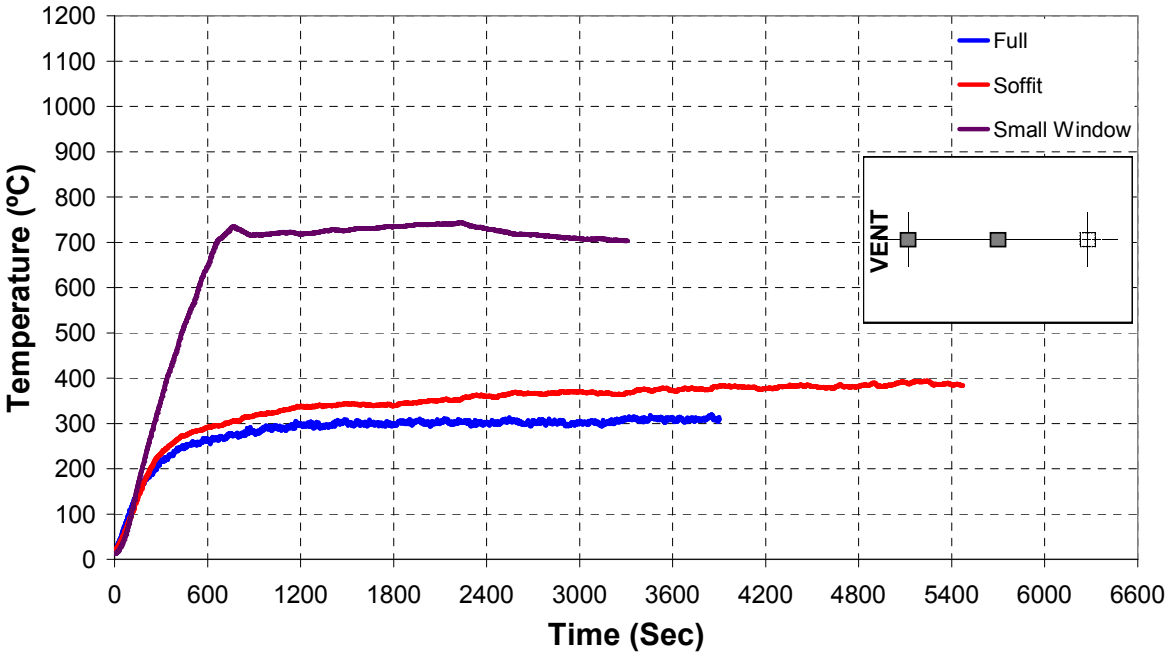

Figure 6.8: Average temperature histories for the two aspirated thermocouple 25mm below ceiling located 1.2 m from the front opening and 1.2 m from rear wall of the compartment for the centre-front pan locations.

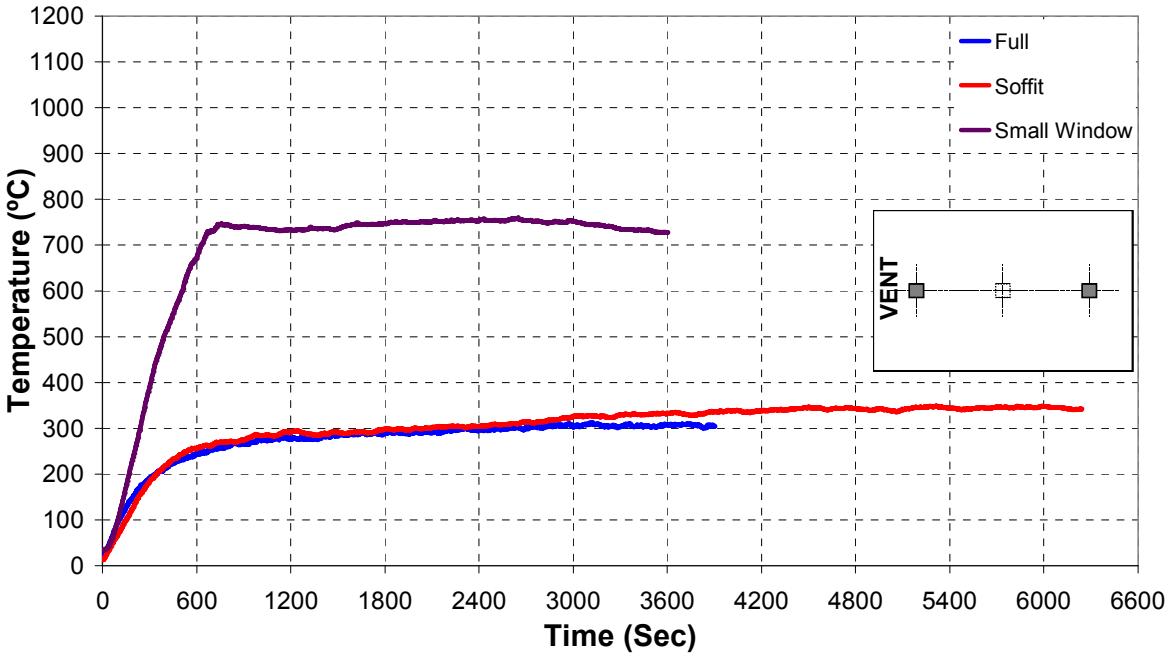

Figure 6.9: Average temperature histories for the two aspirated thermocouple 25mm below ceiling located 1.2 m from the front opening and 1.2 m from rear wall of the compartment for the rear-front pan locations.

As expected a reduction in ventilation provided by either of the door or small window vent geometries provides significant radiation enhancement to the fire from the compartment in comparison with the full and soffit vents. In both the full and soffit geometries the ceiling jet temperatures do not exceed 450ºC while the door geometry temperature exceeds 1100ºC, and the small window geometry approaches 900ºC.

Figure 6.10 shows the compartment temperatures for the x2 centre pan. When compared with the rear-centre time-temperature histories in Figure 6.7, it can be seen that whilst compartment temperatures are greater by approximately 100ºC for the full and soffit experiments, they are similar for the small window case. Table 6.2 also shows that the conditions within the compartment are representative of a post-flashover situation considering typical post-flashover conditions of temperatures >600ºC [14].

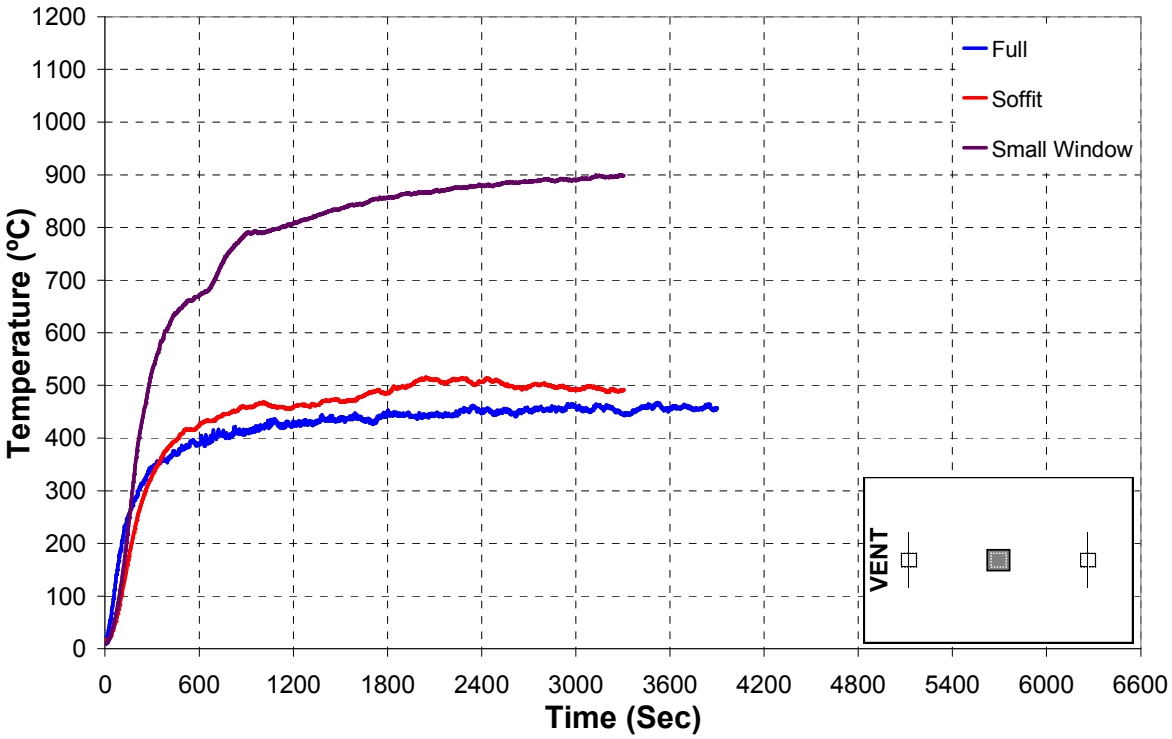

Figure 6.10: Average temperature histories for the two aspirated thermocouple 25mm below ceiling located 1.2 m from the front opening and 1.2 m from rear wall of the compartment for the x2 pan locations.

Figure 6.11, to Figure 6.14 show the temperature profiles from the thermocouple tree located in the corner closest to the ventilation opening for the rear-centre, rear-front, centre-front, and x2 centre pans respectively at the completion of each experiment. The profiles for the full opening show the typical profile expected for a ceiling jet flow with the high temperatures near the ceiling and a rapid drop in temperature moving toward the floor. This profile was consistent for all of the double pan locations with the full vent opening. For the soffit opening the profile is also the typical two layer pre-flashover profile with a deeper upper hot layer than that of the full opening. This was also consistent for all the other pan locations with the soffit ventilation opening with the average upper layer temperature being on the order of 300ºC. The experiments with the door and small window vents provided consistently uniform temperature profiles from floor to ceiling, as expected in a fully a developed post-flashover fire. In general the average temperature was of the order of 750ºC well above the expected post-flashover temperatures, however the rear-centre location provided the highest temperature of 849ºC for the door vent and 902ºC for the small window vent. Typically it is noted that there are no significant difference in the temperature profiles for all the experiments.

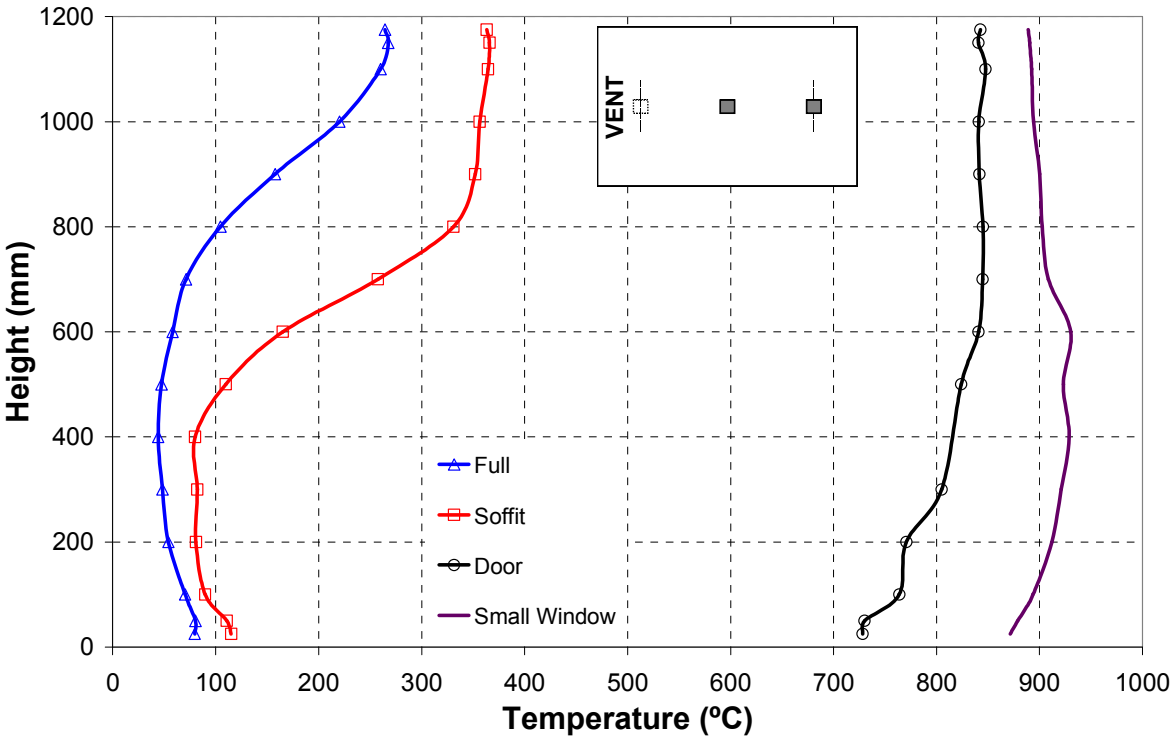

Figure 6.11: Temperature profiles at the thermocouple tree in the compartment corner closest to the vent from the rear-centre pan experiments, at the experiment completion.

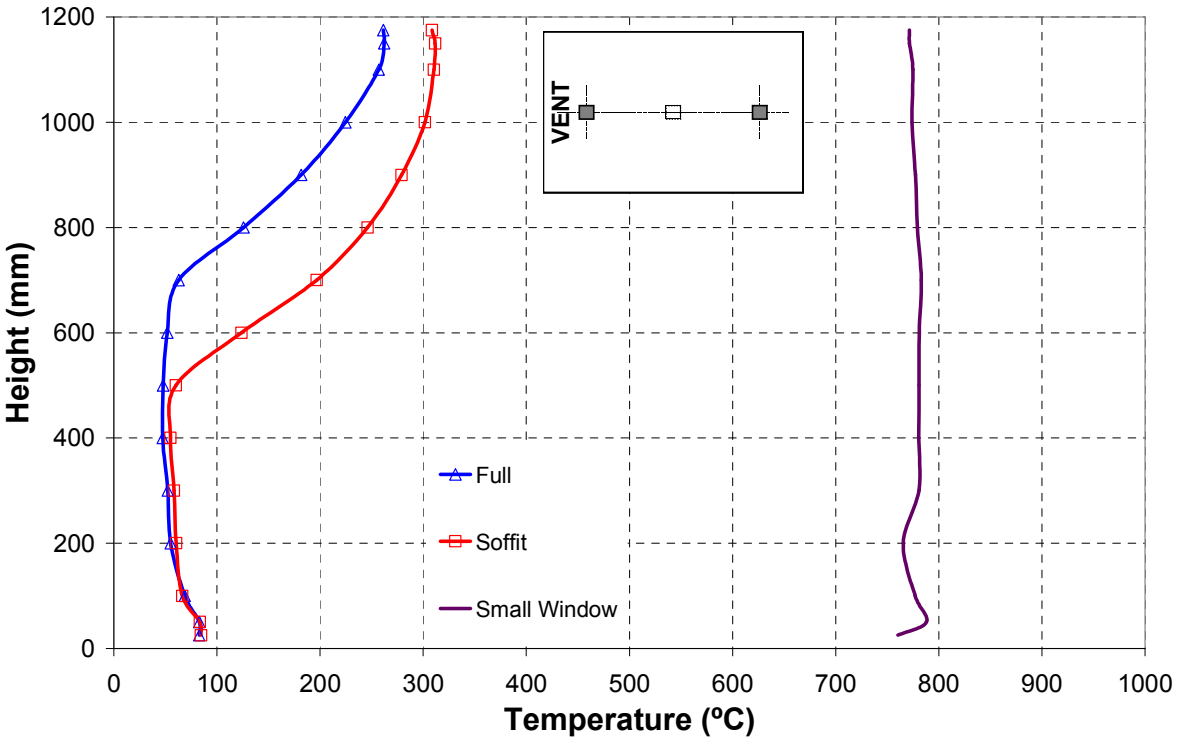

Figure 6.12: Temperature profiles at the thermocouple tree in the compartment corner closest to the vent from the rear-front pan experiments, at the experiment completion

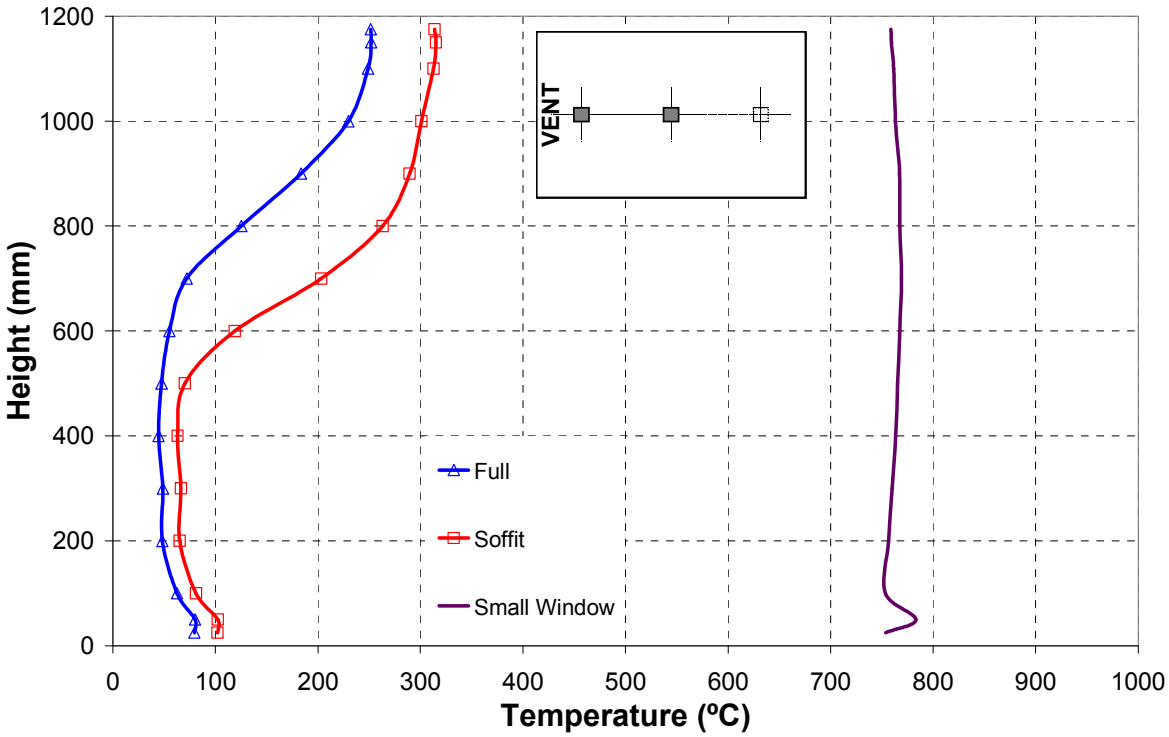

Figure 6.13: Temperature profiles at the thermocouple tree in the compartment corner closest to the vent from the centre-front pan experiments, at the experiment completion

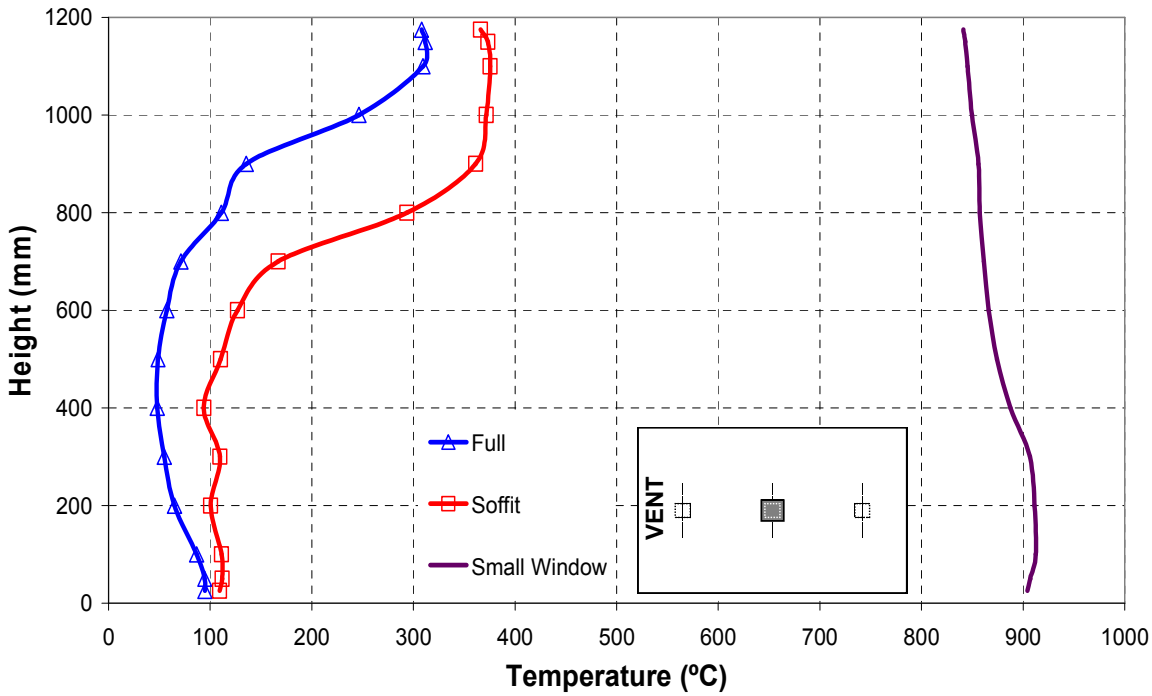

Figure 6.14: Temperature profiles at the thermocouple tree in the compartment corner closest to the vent from the x2 sized centre pan experiments, at the experiment completion

6.7.4 Vent Velocity Profiles

Figure 6.15, Figure 6.16, and Figure 6.17 shows the velocity profile for the bi-directional probes located in the centre of the vent opening. In the experiments for both the full and soffit opening the velocities near the floor are approximately 0.25 m/s. In the developmental stages of the fire this causes the flame to lean in similar manner to that reported in the single pan series of experiments [1]. However, for the door and small window experiments the velocities were much higher ranging from 0.46 m/s to 0.62 m/s for the rear location with the small window.

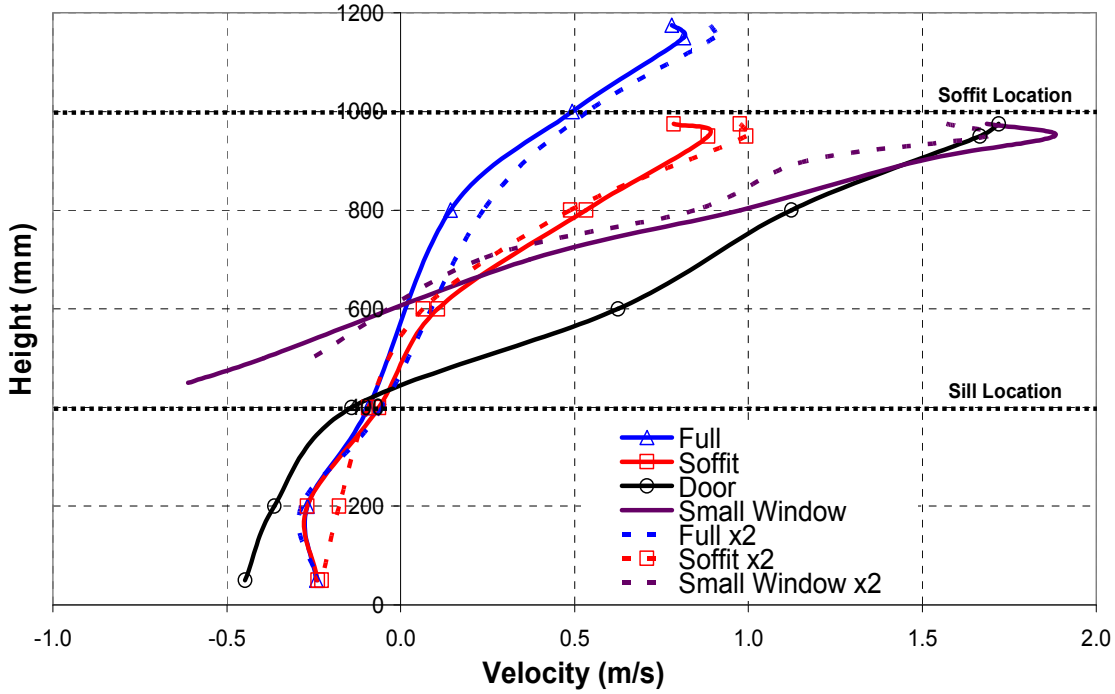

Figure 6.15: Velocity profiles in the centre of the vent opening from the rear-centre pan experiments and the x2 centre pans, at the experiment completion

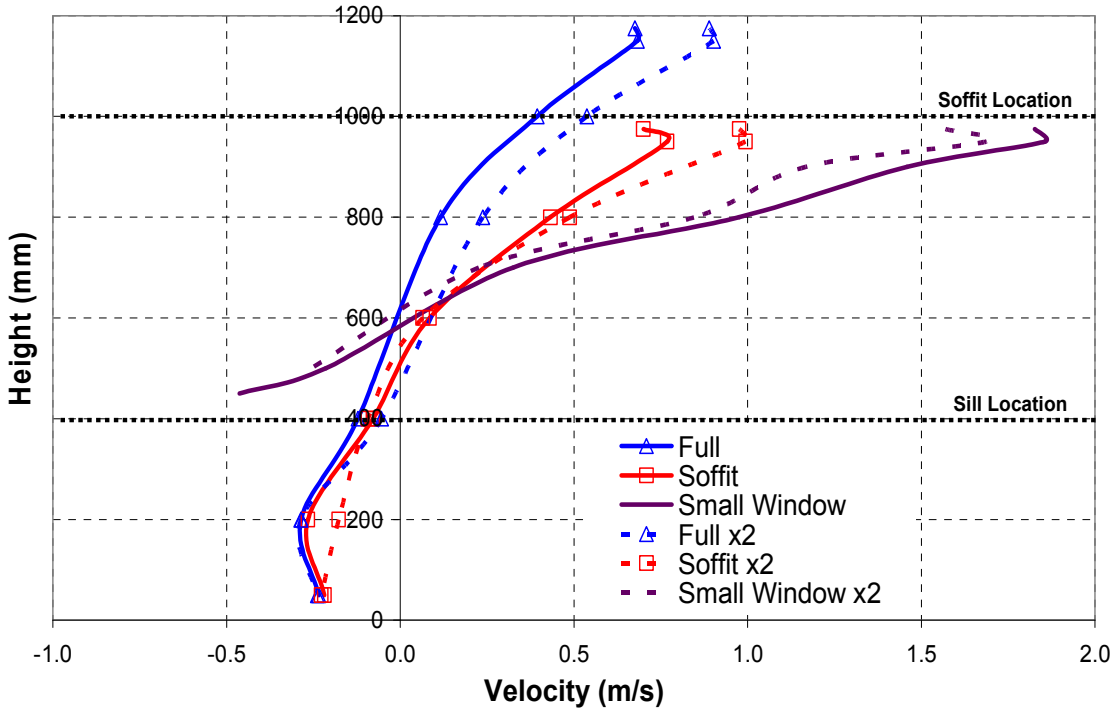

Figure 6.16: Velocity profiles in the centre of the vent opening from the centre-front pan experiments and the x2 centre pans, at the experiment completion.

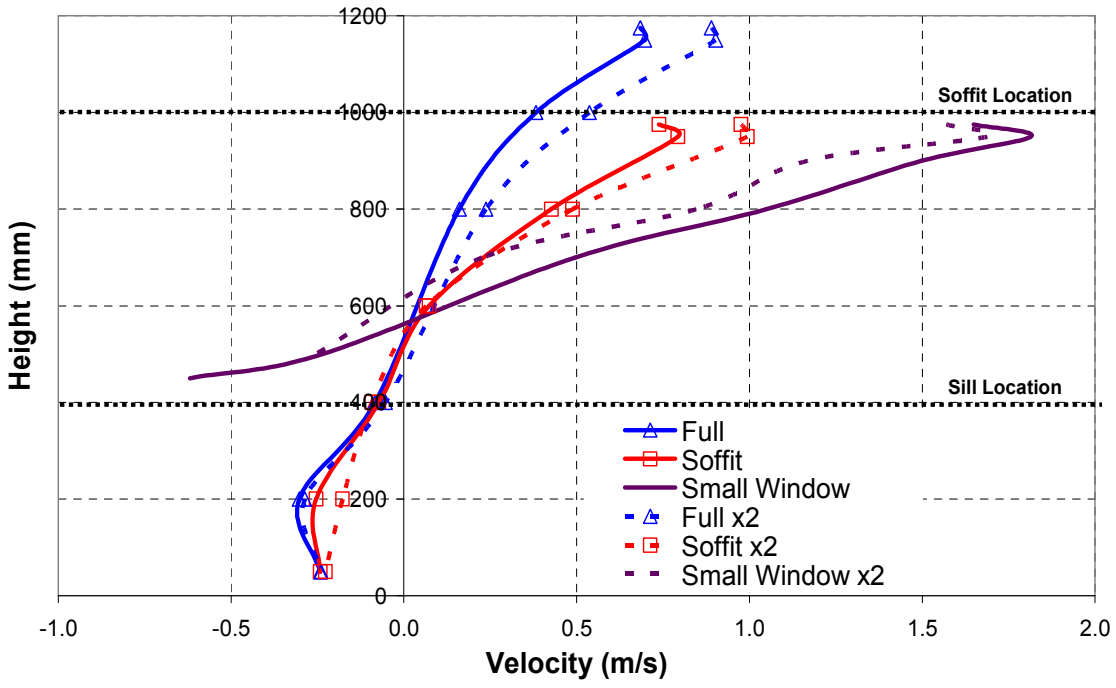

Figure 6.17: Velocity profiles in the centre of the vent opening from the rear-front pan experiments and the x2 centre pans, at the experiment completion

The effect on the flame shape can be seen in the photographs of the rear-centre pan experiment with the door geometry (Figure 6.18), which shows the centre flame blown over significantly such that the flame is in contact with the floor on the leeward side of the pan. This has the effect of providing additional radiation enhancement to the rear pan.

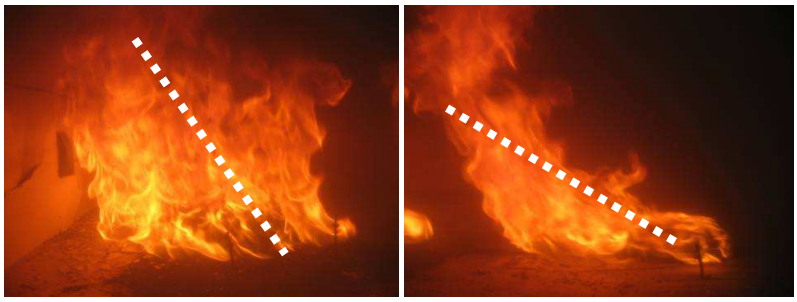

Figure 6.18: Rear and Centre double pan profiles; Door Vent

The vent velocities in the small window experiments also provided significant impact in the developing stages and caused the flame from the pan located near the vent to blow over horizontally such that the flame extended along the floor toward the rear of the compartment as shown in Figure 6.19. As the fire reached a quasi-steady state the compartment behaviour changed to a complex well mixed post flashover environment.

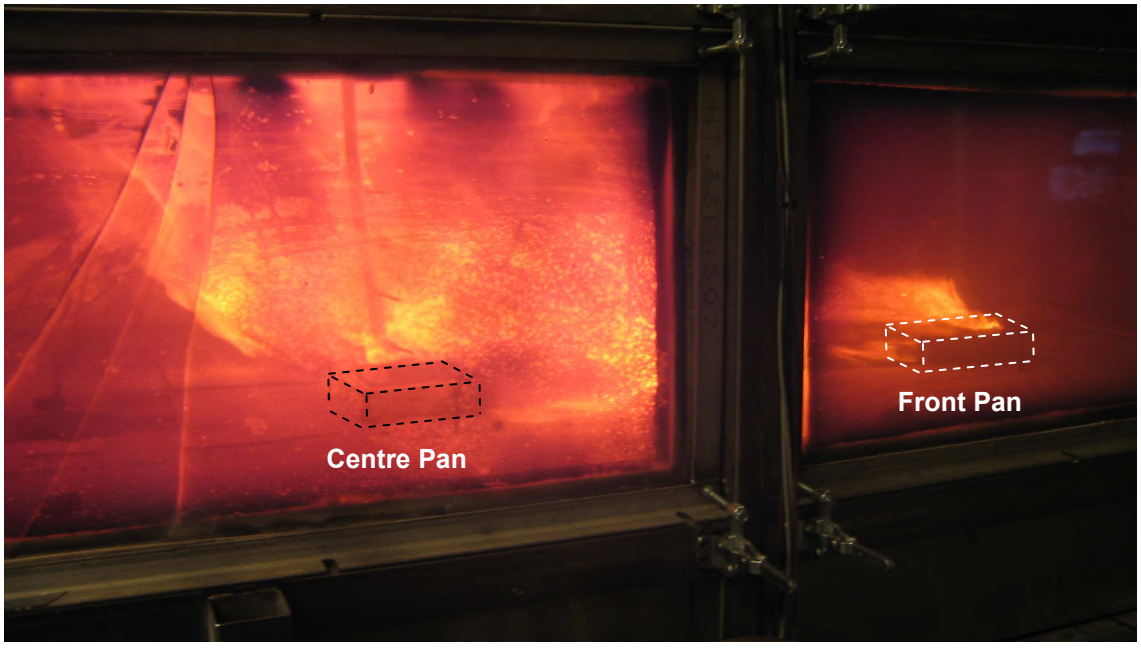

Figure 6.19: Centre/Front pan burning profile; Small window vent

6.8 Triple Pan Experimental Results

6.8.1 Heat Release Rate

Figure 6.20 and Figure 6.21 compare the heat release rate histories for the triple pan location; *rear-centre-front*, and the *x3 centre* pan with the different ventilation openings; *full*, *soffit*, *door*, *window* and *small window*. The experimental series of the door and window ventilation geometries were not completed due to damage to the compartment from the high temperatures and long durations of the experiments.

Both the full and soffit geometry results in Figure 6.20 and Figure 6.21 respectively, show significant increases as a result of the soffit downstand. For the rear-centre-front location with the full geometry the average heat release rate is 281kW and for the soffit geometry the average heat release rate is 444kW, an increase of 58%. For the x3 centre pan location with the full geometry the average heat release rate is 524kW, and for the soffit geometry the average heat release rate is 727kW, an increase of 39%. It is noted in Figure 6.21 with the x3 centre pan soffit experiment, a decrease in the HRR which was a result of a change over in the fuel reservoirs allowing the fuel height to drop momentarily in the pan. In the rear-centre-front pan location experiment with the full geometry (Figure 6.20), it can be seen that the heat release rate is lower than the freeburn heat release rate for an x3 equivalent area pan. The higher heat release of the larger x3 freeburn pan is considered to be a result of a greater level of radiation feedback provided to the pool surface and the optical thickness of the flame. It is noted that in the rear-centre-front compartment experiment there was no interaction between adjacent pans therefore the burning behaviour is similar to the cumulative effect of a single pan multiplied three times. This behaviour is confirmed when the total heat release rate of 281kW from the rear-centre-front experiment is compared with the cumulative 290kW obtained in the single pan series for the rear, centre and front single pans [1].

For the small window geometry, the average heat release rate for the x3 centre pan is also noted to be less than the x3 free burn case due to ventilation controlled conditions and is controlled. This is as a result of a ventilation limited conditions as noted in equation (6.3-2).

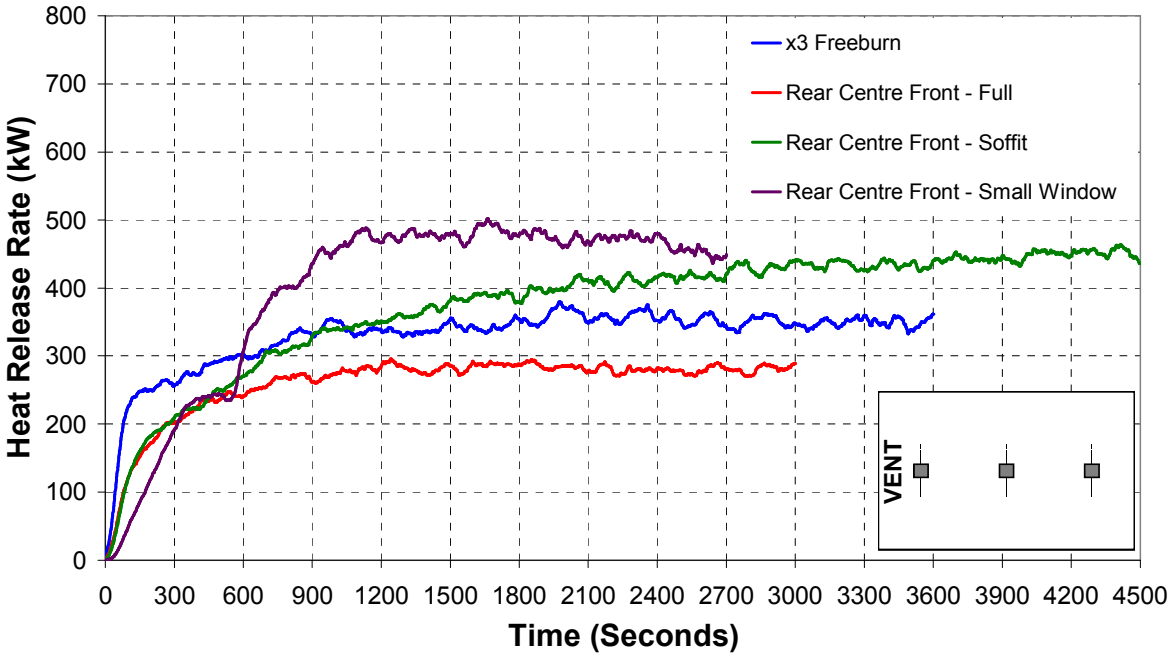

Figure 6.20: Comparison of the heat release rate histories for the each of the rear-centre-front pan experiments with a *full, soffit* and *small window* vent, along with the x3 free-burning pool.

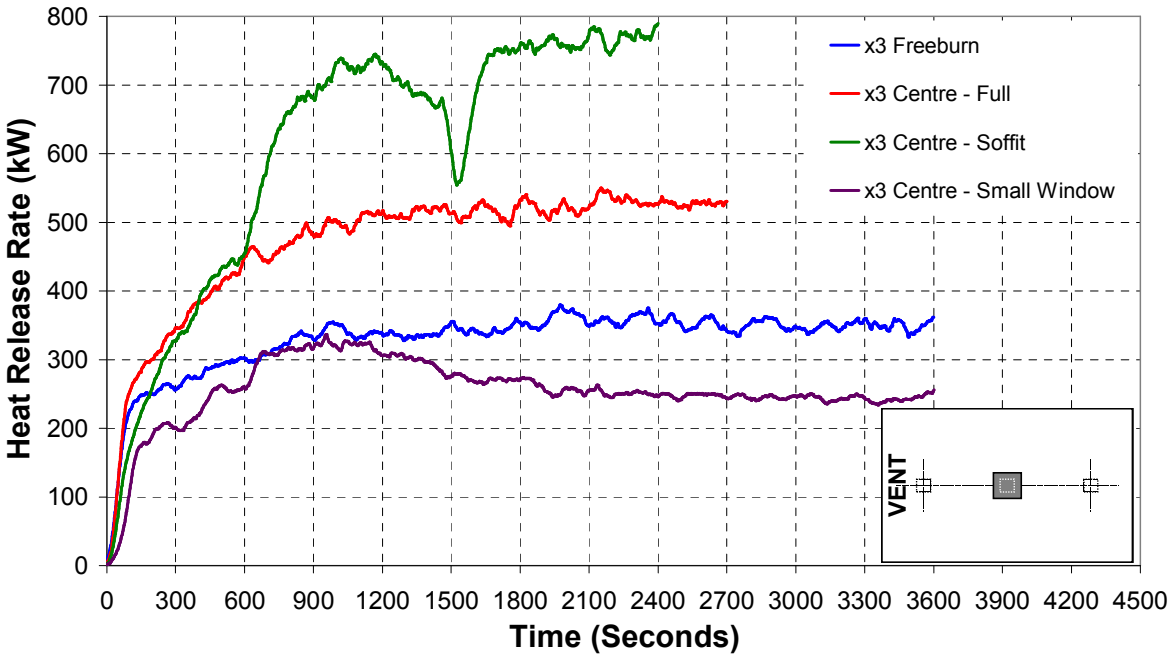

Figure 6.21: Comparison of the heat release rate histories for the each of the x3 centre pan experiments with a *full*, *soffit* and *small-window* vent, along with the x3 free-burning pool.

6.8.2 Vent Flows

The difference between the singular x3 centre pan and the rear-centre-front pans can be seen in Figure 6.22 which shows a set of photographs of the post flashover external flaming profiles for the *small window* geometry experiments. As shown, there is a significant increase in the external burning with the rear-centre-front pans.

Figure 6.22: External flaming profiles from small window geometry compartment experiments

Figure 6.23 and Figure 6.24 compare the average aspirated thermocouple temperatures in the ceiling jet for the rear-centre-front and the x3 centre pans respectively. The time temperature histories show that the x3 centre experiment provided higher ceiling jet temperatures than the three individual pans. The rear-centre-front temperatures range between 400-700ºC while the x3 centre temperatures are representative of a post-flashover situation with temperatures between 700-1000ºC.

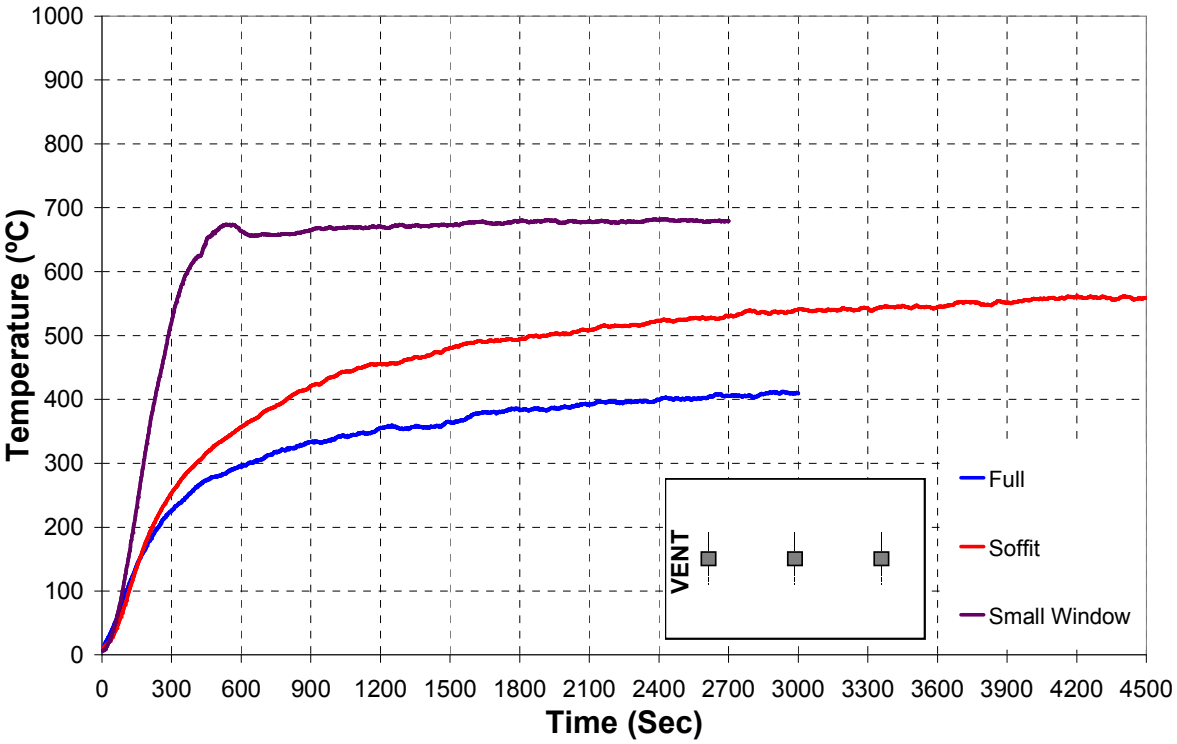

Figure 6.23: Average temperature histories for the two aspirated thermocouple 25mm below ceiling located 1.2 m from the front opening and 1.2 m from rear wall of the compartment for the rear-centre-front pan experiments with the full, soffit and small window geometries.

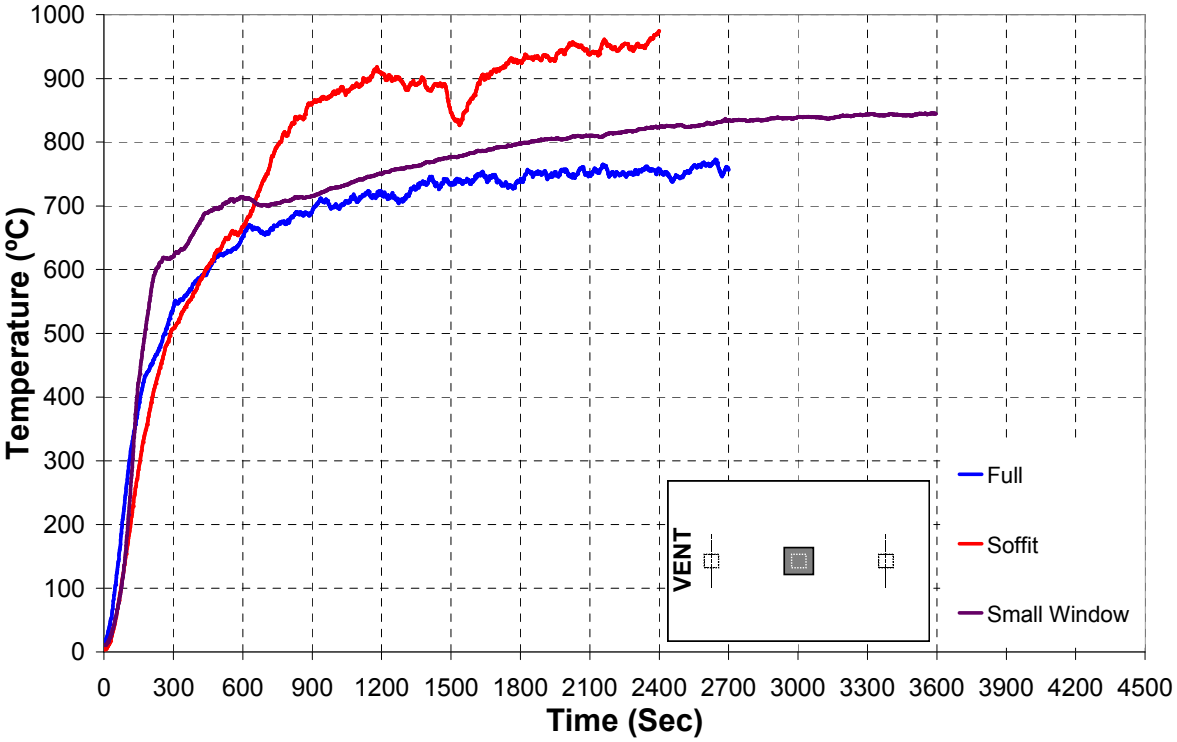

Figure 6.24: Average temperature histories for the two aspirated thermocouple 25mm below ceiling located 1.2 m from the front opening and 1.2 m from rear wall of the compartment for the x3 centre pan experiments with the full, soffit and small window geometries.

6.8.3 Temperatures

Figure 6.25 and Figure 6.26, show the temperature profiles from the thermocouple tree located in the corner closest to the ventilation opening for the rear-centre-front and x3 centre, experiments. The profiles for the full and soffit openings again show the typical pre-flashover profile expected with high temperatures near the ceiling and a drop in temperature toward the floor. When compared with the heat release rate time-temperature histories in Figure 6.20 and Figure 6.21 it can be seen that the experiments with the single x3 pan in the centre of the room provide significantly higher compartment temperatures than three individual pans for the full and soffit ventilation. Subsequently this results in a higher heat release rate. For the small window geometry the single x3 pan in the centre of the room also has significantly higher compartment temperatures than three individual pans. However this does not result in a corresponding increase in the heat release rate due to the combustion behaviour. The combustion zone for both cases occurs within the compartment just inside the vent and this provides significant radiation feedback to the front pan located just inside the vent, but as the x3 centre pan is located away from the opening it does not receive the same level of radiation enhancement.

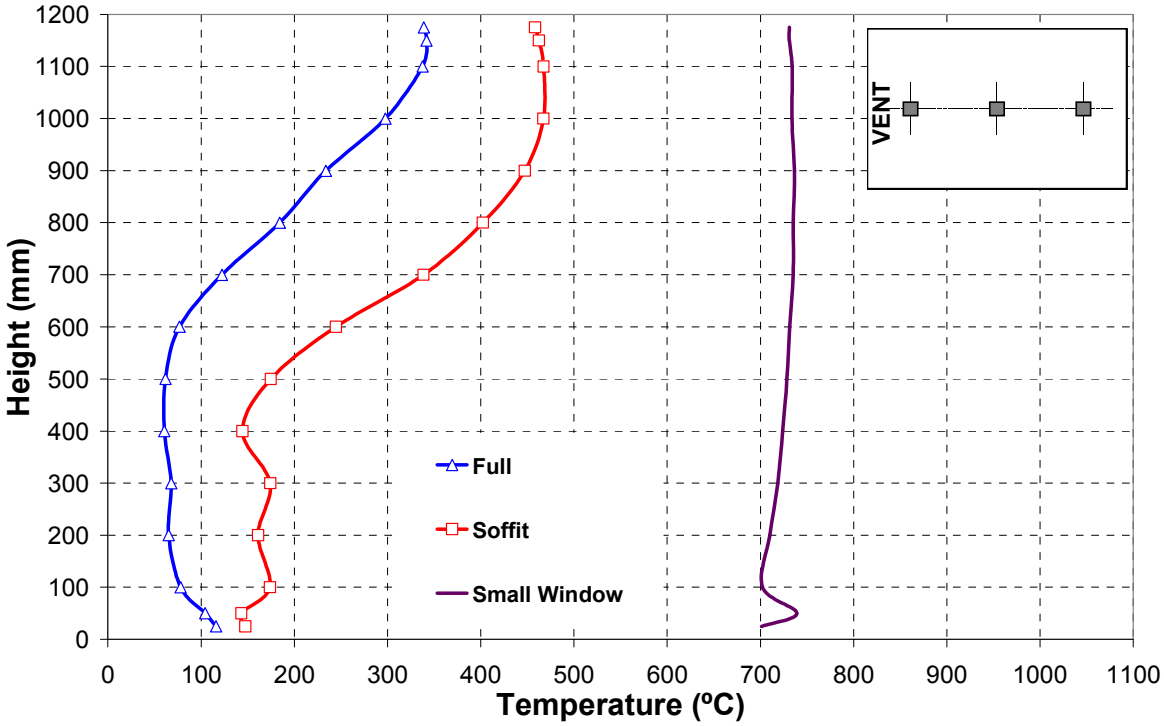

Figure 6.25: Temperature profiles at the thermocouple tree in the compartment corner closest to the vent from the rear-centre-front pan experiments, at the experiment completion.

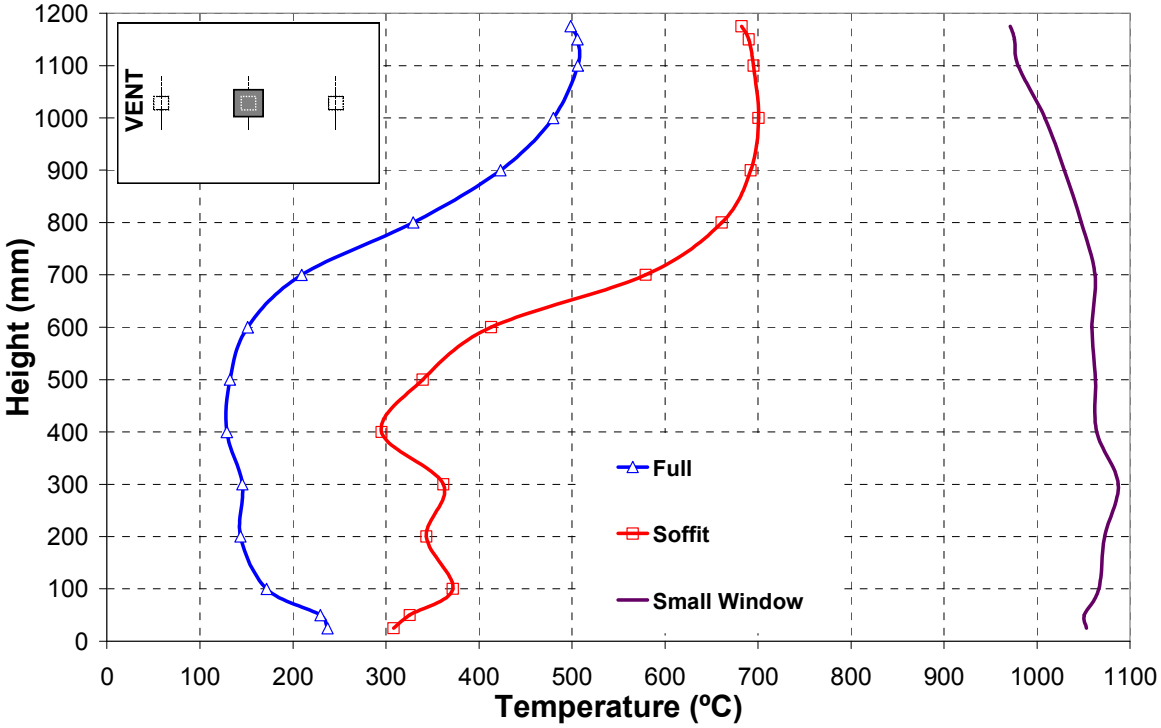

Figure 6.26: Temperature profiles at the thermocouple tree in the compartment corner closest to the vent from the x3 sized centre pan experiments for the ventilation openings, at the completion of the each experiment.

6.8.4 Vent Velocity Profiles

Figure 6.27, shows the velocity profile for the bi-directional probes located in the centre of the vent opening. In these experiments the velocities near the floor range from 0.27m/s for the small window to 0.41m/s for the soffit geometry. In the developing stages of the rear-centre-front pan (full and soffit) experiments the vent velocities cause the flame to lean over in similar manner to that reported in the double pan series, however this forced lean over effect is not significant and there was no interaction of the fire plumes. The velocities for the small window geometry provided a significant impact in the early stages with horizontal flames extending along the floor toward the rear of the compartment, but this quickly develops into a post flashover environment with external flaming.

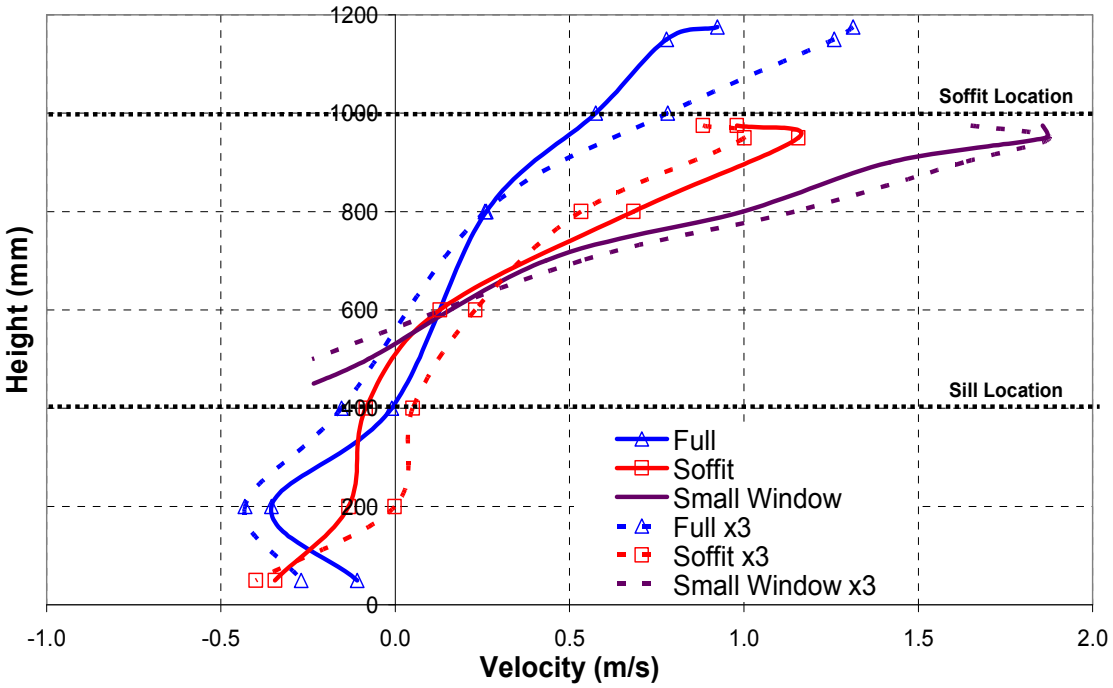

Figure 6.27: Velocity profiles at the bi-directional probes in the centre of the vent opening from the rear-centre-front pan experiments and the x3 centre pans, at the completion of the each experiment

6.9 Discussion of Results

6.9.1 Double Pan Experiments

The double pan experiments show that there is no significant increase in compartment fire behaviour between the full and soffit geometries. Although there is some enhancement as a result of an increase in the upper hot layer depth and higher temperatures which is expected, the heat release rates are not significantly greater than the equivalent area free burning heat release rate. Enhancement is noted only with the experiments involving the rear pan location which can be attributed to an increase in radiation to the fuel surface from the rear wall. There is also enhancement in the experiments involving the x2 centre pan which is a result of an increase in the upper layer temperatures. The full and soffit ventilation openings are not ventilation limited and provide the typical compartment behaviour of a two layered pre-flashover regime.

As the ventilation is reduced the significance of the compartment effects becomes apparent and there is a significant increase in compartment temperatures with typical compartment behaviour of a single zone post-flashover regime. For the door geometry the increase in compartment temperatures equates to a significant increase in the heat release rate, 108% greater than the x2 free burning rate. The small window geometry is ventilation limited and subsequently the heat release rate is driven by ventilation into the room and compartment effects. The heat release rate is ventilation limited in all cases except those involving a pan located near the vent opening. In these instances the heat release rates are 95% greater than the free-burning case and 53% greater than any other orientation. This is a result of the contributing factor of the front pan. The combustion zone is located within the vent opening area and the increase in radiation to the front pan increases the mass loss rate. Subsequently the instance the heat release rate of two individual pans can be 71% greater than that of the x2 equivalent area pan located in the centre of the room. This can be seen by comparison of the mass loss rate of the front pan and the x2 centre pan as detailed in Table 6.2. In the experiments with the rear-front and centre-front pan the mass loss rate of the front pan is at least equivalent to or greater than the mass loss rate of the x2 centre pan.

6.9.2 Triple Pan Experiments

The triple pans experiments show that due to an increase fire size (pool area) the impact of compartment effects can be significant. A significant difference in the compartment fire behaviour between the full and soffit geometries is noted. For the fully open geometry, compartment enhancement is significant only in the x3 centre pan experiment which provides a heat release rate 50% greater than the x3 freeburn pan. This is due to an increase in radiation feedback to the larger x3 pan area as a result of high compartment temperatures (over 400ºC) and the optical thickness of the flame. The heat release rate for the rear-centre-front experiment was found to be 20% less than the x3 freeburn pan. This was a result of each of the pans burning similar to single isolated pans. Each pan was not significantly affected by the fire plume from any adjacent pan and with compartment temperatures less than 265ºC there was little radiation enhancement.

With the soffit opening compartment enhancement occurs as a result of the deeper upper layer and increasing the compartment temperatures and this was consistent for both the rear-centre-front and x3 centre pan experiments. It is also noted that the full and soffit openings are not ventilation limited and provide the typical compartment behaviour of a two layered pre-flashover regime.

As the opening geometry is reduced the *small-window* generates ventilation limited conditions in which there is a significant increase in compartment temperatures yielding typical a single zone post-flashover regime. Subsequently the heat release rate is driven by the ventilation into the room and compartment effects. The heat release rate is ventilation limited for the x3 centre pan experiment, but the rear-centre-front experiment again provides the catalyst of a front pan location which increases the heat release rate. Again with the combustion zone located within the vent opening area the increase in radiation to the front pan drives the heat release rate 32% greater than the x3 free-burning case. In the instance the heat release rate of three individual pans is greater than that of the x3 equivalent area pan located in the centre of the room by 90%. This can be seen by comparison of the mass loss rate of the front pan and the x3 centre pan as detailed in Table 6.3. In this instance the front pan has a similar mass loss rate to that of the x3 centre pan when excluding the rear and centre pans.

6.10 Conclusions

The results of this research clearly show that the size and location of a multiple fires can have a pronounced effect on compartment fire behaviour. The following concepts have been identified;

- The results show that the number of pans and location of the fires can have a pronounced effect on compartment behaviour. This can be seen in the under-ventilated compartment small window experiments which involve a front pan in co-ordination with a rear and/or centre pan in the compartment. In these experiments the heat release rate can be approximately 50% greater than any other orientation.
- The heat release rate for a compartment pool fire is a function of the fire location and can be significantly greater than the predicted free burning rate and even greater than the maximum free burning rate for an optically thick pool fire.
- The heat release rate for the pool fire is a function of the size of the fire.

  - For pre-flashover fires a single pan located in the centre of the room generally provides the highest heat release rate for compartment conditions This is relevant to the fire design for life safety conditions.
  - For post-flashover fires the single pan located in the centre of the room does not generally provide the highest heat release rate compartment conditions This is relevant to the fire design for fire spread and structural stability.
- Experiments with the full and soffit openings display distinct upper and lower layer temperature pre-flashover profiles.
- The under ventilated fire with a small window vent provides uniform post flashover conditions which is consistent with the single zone well stirred post-flashover assumption.
- An assumption that a fire located away from the wall boundaries will behave like an asymmetric plume is not valid. Vent velocities into a compartment can drive the fire plume into the adjacent wall reducing entrainment and it behaves like a wall adjacent fire.
- When a compartment is well ventilated there is little effect on the heat release rate from the compartment environment. Compartment effects become more pronounced with respect to the size of the fire such as large pool fires with flame heights directly impinging upon the ceiling of the compartment.

6.11 Future Research

- Further research should include multiple fires in multiple locations to assess the impact on the compartment environment when compared to a single fire of equal surface area.
- Additional work is needed using different size vents over a range of opening factors in order to further quantify the heat release rate versus ventilation factor.
- More experimental work is required to quantify the effect of fire location when the fire is not located along the centreline of the ventilation opening including along sidewalls and in corners.

- More experimental work is required to quantify the effect of fire size in locations other that the centre of the compartment such as the rear and front locations.
- The results given here should be modelled in field models such as FDS to validate the model for use in fire location studies such as this. Many of the recommendations given above could be tested numerically to reduce the size of the experimental work required.

6.12 References

1 Parkes, A. R, Fleischmann, C. M. The Impact of Location and Ventilation on Pool Fire in a Compartment" Fire Safety Science -- Proceedings of the Eight International Symposium, International Association for Fire Safety Science, 2005, pp. 1289-1300

2 Wade, C.A., "BRANZFIRE Technical Reference Guide" Study Report No. 92 (revised), Building Research Association of New Zealand, Judgeford, 2004.

3 Peacock, R.D, Jones, W. J, Reneke, P. A, Forney, G. P, "CFAST – Consolidated Model of Fire Growth and Smoke Transport (Version 6) User's Guide", NIST Special Publication 1041, National Institute of Standards and Technology, U.S. Department of Commerce, Gaithersburg, December 2005.

4 Babrauskas, V., and Peacock, R. D., Heat Release Rate: The Single Most Important Variable in Fire Hazard, Fire Safety J. 18, 255-272 (1992).

5 Babrauskas, V, "Heat Release Rates", The SFPE Handbook of Fire Protection Engineering, Section 3/Chapter 1, 3rd edition, 2002.

6 Babrauskas, V., Estimating Large Pool Fire Burning Rates, Fire Technology 19, 251-261 (1983).

7 Thomas, I. R., and Bennetts, I D., "Fires in Enclosures with Single Ventilation Openings – Comparison of Long and Wide Enclosures", Fire Safety Science – Proceedings of the Sixth International Symposium, 941-952, 1999.

8 Kirby, B. R., Wainman, D. E., Tomlinson, L. N., Kay, T. R. and Peacock, B. N., Natural Fires in Large Scale Compartments, A British Steel Technical, Fire Research Station Collaborative Project, BSC, 1994.

9 Cooke, G. M. E., "Tests to Determine the Behaviour of Fully Developed Natural Fires in a Large Compartment", Fire Note 4, BRE, 1998.

10 Babrauskas, V., and Wickström, U. G., Thermoplastic Pool Compartment Fires, Combustion and Flame 34, pp. 195-201 (1979).

11 Babrauskas, V, "Heat Release Rates", The SFPE Handbook of Fire Protection Engineering, Section 3/Chapter 1, 3rd edition, 2002

12 Walton, W.D and Thomas, P. H, "Estimating Temperatures in Compartment Fires", The SFPE Handbook of Fire Protection Engineering, Section 3/Chapter 6, 3rd edition, 2002

13 Karlsson, B and Quintiere, J., Enclosure Fire Dynamics, CRC Press, 2001

14 Drysdale, D, An Introduction to Fire Dynamics, 2nd Edition, John Wiley & Sons, New York, 1998.

Chapter 7: Experimental Analysis

This chapter details further analysis of the experimental results from both the single pan and multiple pan experiments to help quantify the observed and recorded compartment behaviour. Ventilation is perhaps the most important factor in determining compartment pool fire behaviour, as the reduction of ventilation into a compartment can either limit the growth of a fire or induce high compartment temperatures leading to the onset of flashover should sufficient fuel be available. As the rate of burning of the enclosure fire is assumed proportional to the ventilation factor, the following observed and measured results are generally analysed in terms of the ventilation geometry:

- Observed Flame Behaviour and Vent Flows,
- Heat Release Rate,
- Mass Loss Rate,
- Equivalence Ratio,
- Combustion Efficiency,
- Compartment Temperatures.

7.1 Observed Flame Behaviour and Vent Flows

One of the main observations taken during the experiments was that of the leaning over behaviour of the pool fires located toward the rear of the compartment and a detailed account of compartment observation for the compartment experiments is provided in Appendix B. As the ventilation into the compartment is reduced in size, the magnitude of the velocities across the vent interface will naturally increase. The range of vent velocities for all experiments based upon each ventilation geometry are shown in Figure 7.1. This shows that the inflow velocity the bottom edge of the vent opening ranges from 0.45m/s for the full and soffit openings to approximately 0.62m/s for the small window ventilation geometry.

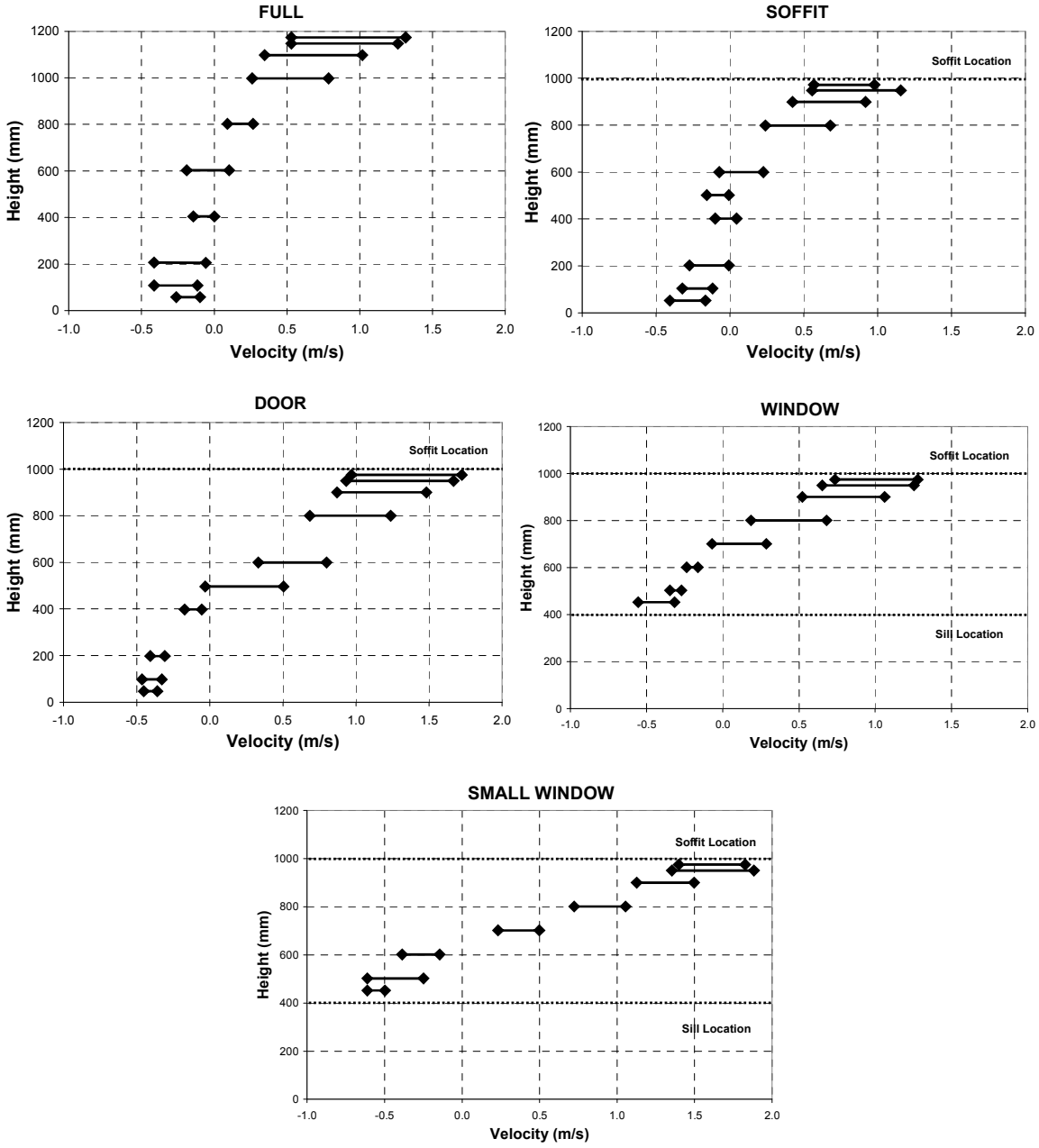

Figure 7.1: Vent velocities recorded for all experiments with respect to each ventilation geometry

The effect of these velocities causes the pool fire flame orientation within the space to lean over toward the rear of the room. While leaning fire plumes have been investigated in forest fires, tunnels and other external conditions, in internal spaces it is not a well quantified phenomenon. The experiments conducted in this study confirm that the flows into the compartment as a result of the ventilation opening can be significant enough to alter the fire behaviour.

With the fully unrestricted and soffit ventilation openings to the compartment, the leaning angle was noted as approximately 45 degrees from the vertical as is seen Figure 5.7. As the ventilation was decreased thru the *door*, *window* and *small-window* geometry experiments, the vent velocity increased and the flame leaning was noted at a maximum of 60 degrees from the vertical plane. As the fire continues to develop in the *small-window* experiments, the leaning angle becomes horizontal and the flame was observed to extend along the entire length of the enclosure floor. This horizontal flame was only observed in the fire growth stages of the under ventilated (*small-window*) experiments and this stage quickly transitions to a well stirred post-flashover regime.

The pan location in the front of the compartment was observed to have the most significant flame lean, and in the under ventilated experiments also exhibited a pulsing phenomenon before reaching quasi-steady state conditions. The leaning-over effect with the rear pan was noted to push the flame into the rear wall such that the fire plume hugs the rear wall. This has implications on the design aspects of near-wall fires as the assumption that the fire can entrain air on all sides is not valid. In the case of the window and door geometries the flame lean was sufficient to reduce the plume feedback to the pool surface and the heat release rate was less than that for the free burn case.

7.2 Heat Release Rate

In general the heat release rate, HRR, follows expected trends for the simple compartment series involving the single pan and double pan series. This is detailed in the HRR comparisons shown in Figure 7.2 which show that as the ventilation was decreased the HRR increased. The exception to this occurred in the triple pan series in which the small vent opening had a lower HRR than that of the full and soffit opening, although this is a result of the post-flashover ventilation limited regime.

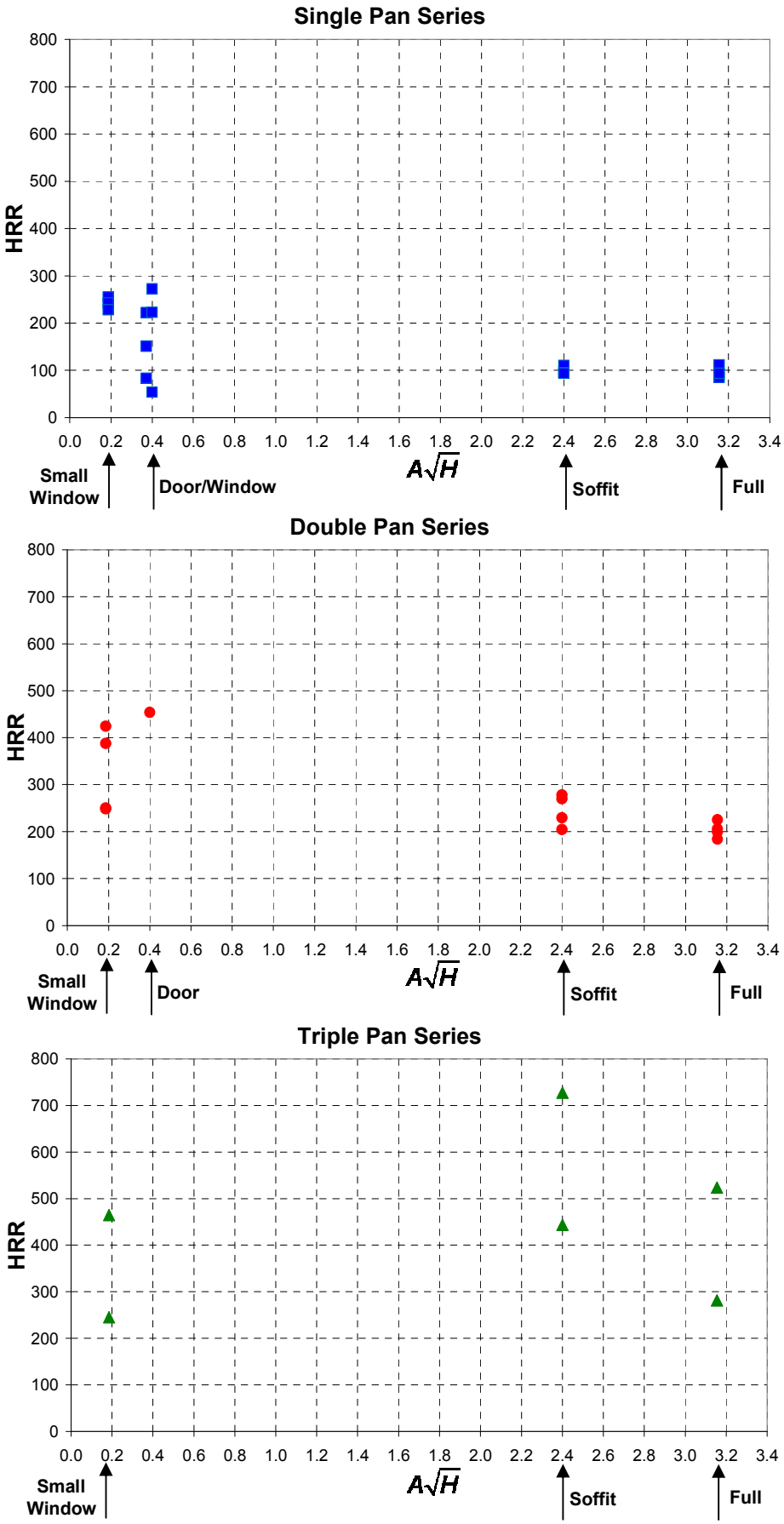

Figure 7.2: Comparison of the HRR with the ventilation factor for all experiments

The heat release rate comparison for all of the experiments is shown below in the heat release profiles for the full vent (Figure 7.3), soffit vent (Figure 7.4), door vent (Figure 7.5), window vent (Figure 7.6) and small window vent (Figure 7.7) and confirms the impact upon the location of the front pan in the experiments.

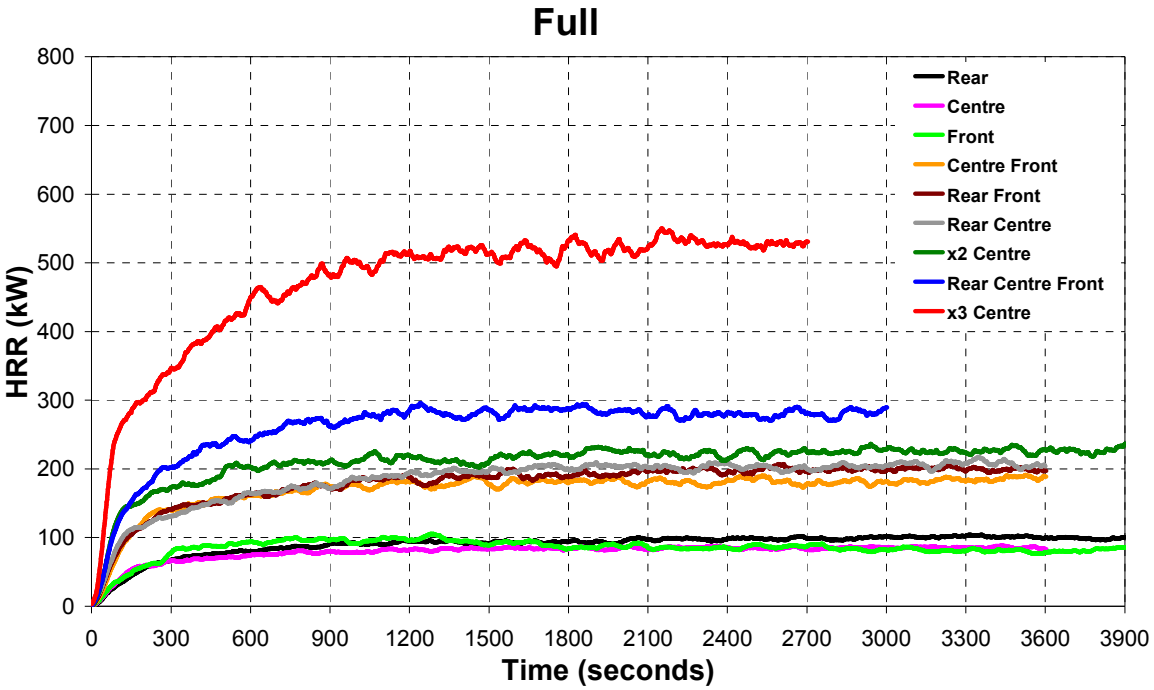

Figure 7.3: Full vent geometry HRR profiles – all nine compartment experiments

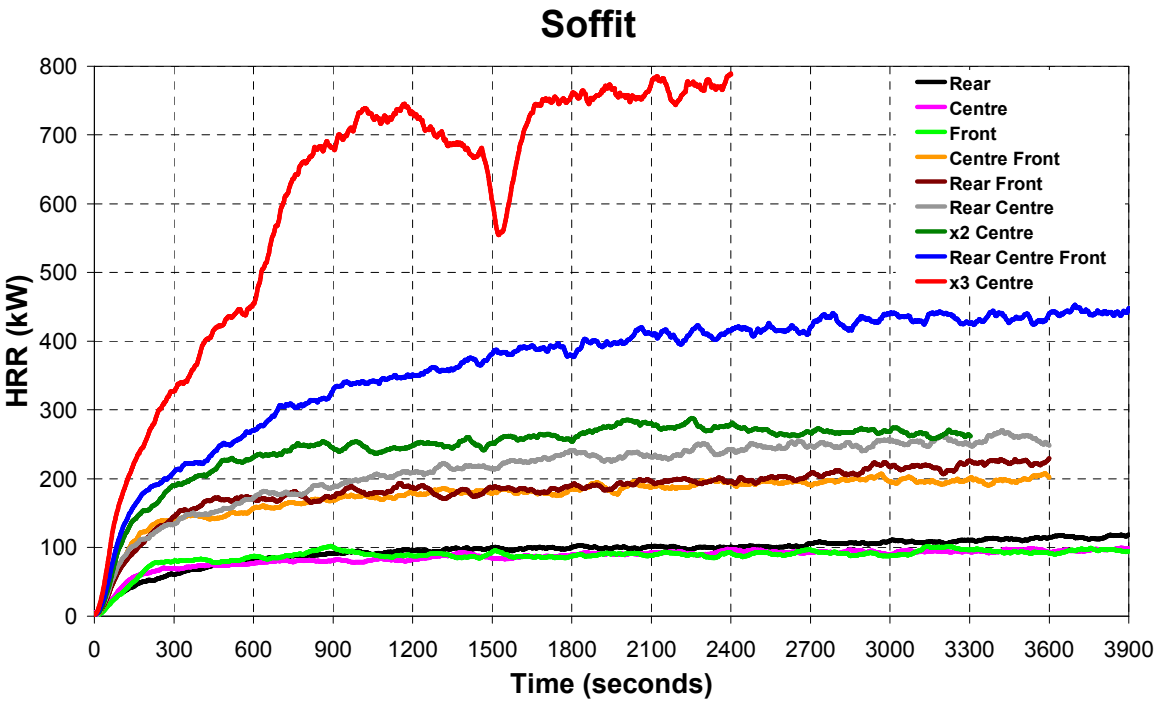

Figure 7.4: Soffit vent geometry HRR profiles – all nine compartment experiments

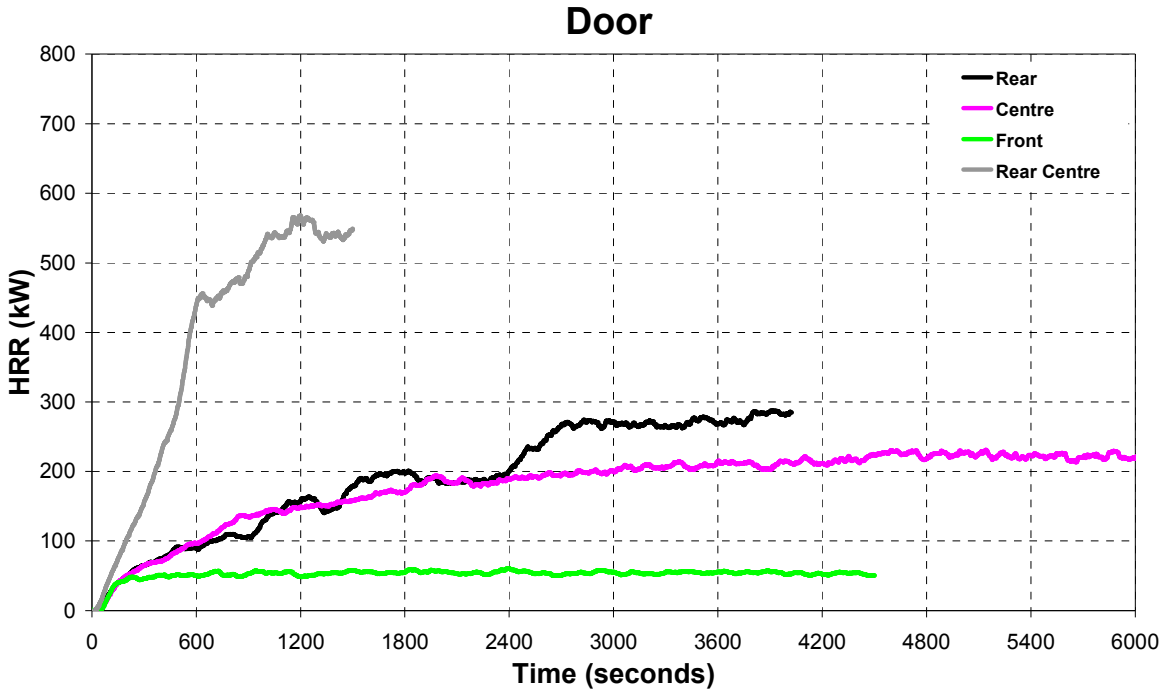

Figure 7.5: Door vent geometry HRR profiles – all four compartment experiments

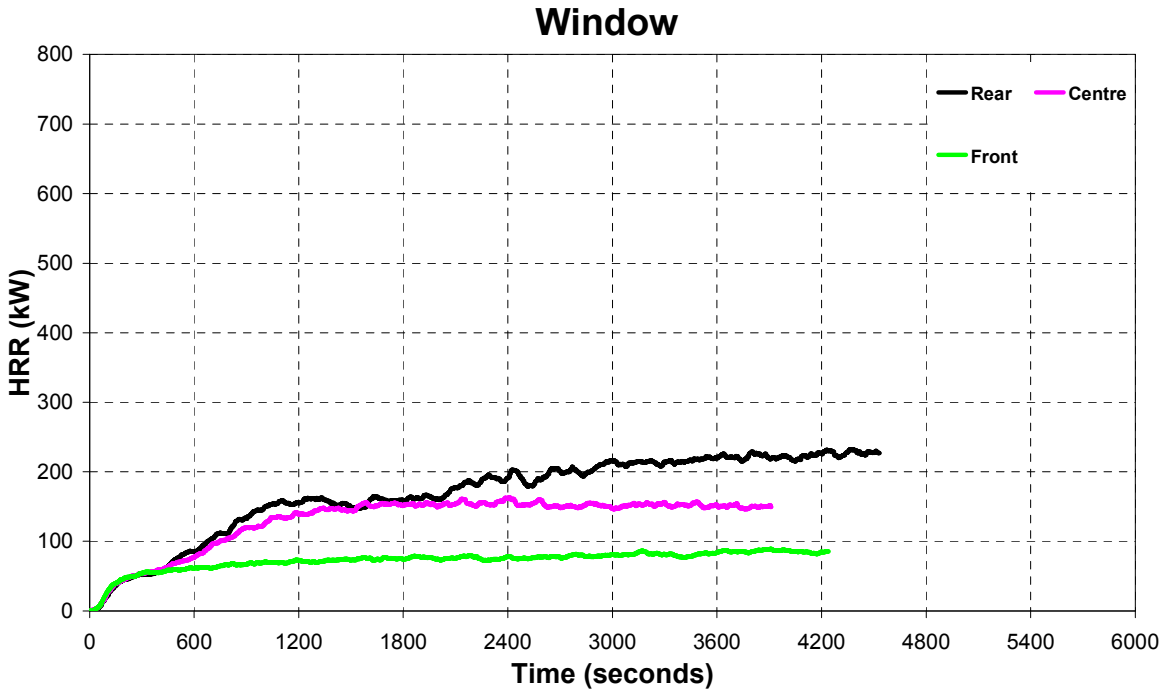

Figure 7.6: Window vent geometry HRR profiles – all 3 compartment experiments

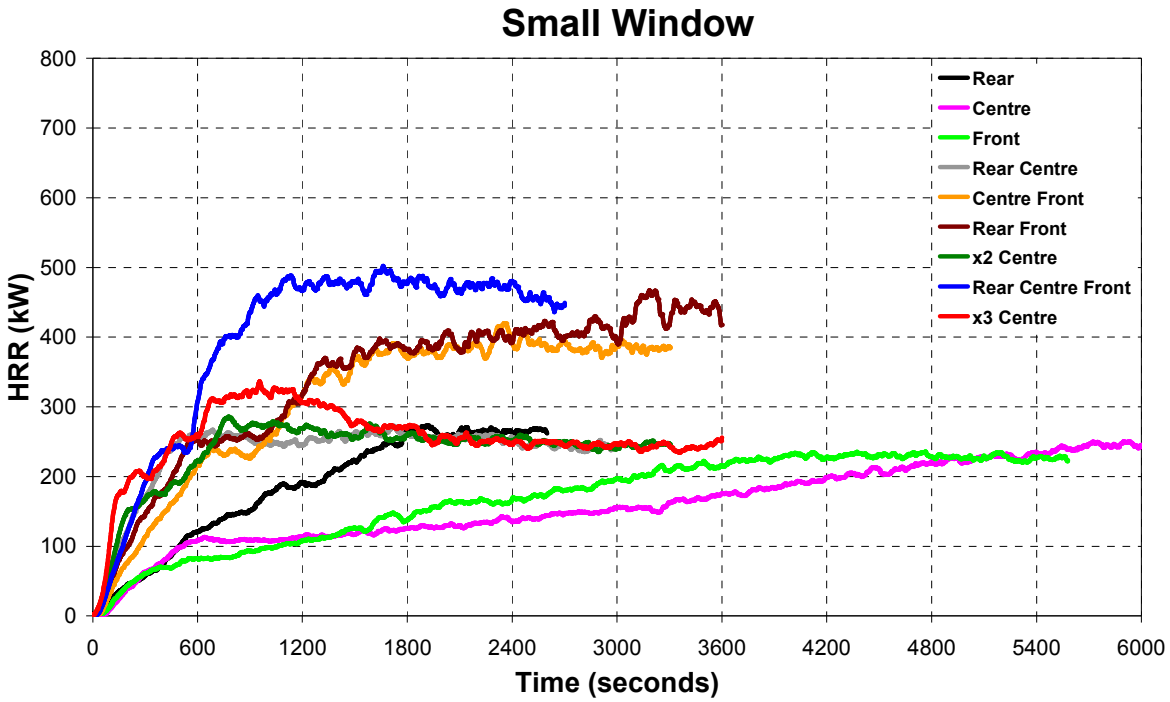

Figure 7.7: Small vent geometry HRR profiles – all nine compartment experiments

For the well ventilated enclosure with the full and soffit geometries (Figure 7.3 and Figure 7.4) the single pan located in the centre of the room provides the highest heat release rate when compared to any other equivalent fire loading layout. This is shown by the greater heat release rates for the x2 and x3 centre pans when compared to equivalent area multiple pan experiments.

However for ventilation limited enclosure using the small window (Figure 7.7) the presence of a pan near the ventilation opening provides a complex combustion regime in which the front pan drives a heat release rate that is significantly greater that any equivalent set or singular larger area pool fire. It is noted that the ventilation limited stoichiometric fuel pyrolysis rate can be estimated by equation (2.3-5);

$$\dot{m}_p(st) = \frac{0.5}{r} A_v \sqrt{H_v}$$

Where :

r = stoichiometric air/mass ratio = 15.1 for heptane

A_v = vent area (m^2)

H_v = vent height (m)

Multiplication by the heat of combustion of heptane, 44600 kJ/kg [1], yields a heat release rate of 274kW for ventilation controlled conditions. As shown in Figure 7.7, the HRR of all pool fire orientations approach this value, excluding the multiple pan experiments involving a front pan. Therefore the addition of the front pan is noted as the driving mechanism for the heat release rate due to significant radiation enhancement to the pool surface from the combustion zone in the vent.

This is significant as multiple fires with an aggregate pan size less than that of the large centrally located fire can provide a 73% greater heat release rate. In the experiments with the small window opening, the single large x3 pan located in the centre of the room had a heat release rate lower than that of two small pans (a combined area of $^2/_3$ of the x3 pan).

7.3 Mass Loss Rate

The mass loss rates (MLR) per unit area for all the experiments are detailed in Table 7.1 to compare the significance of the contribution of each pan location with respect to compartment fire behaviour. The total mass loss rate per unit is detailed in the forth column with the individual mass loss rate for the individual pan locations, *rear*, *centre* and *front* shown in columns five to seven.

Table 7.1: Mass Loss Rate per unit area for all 34 compartment experiments and 3 freeburn experiments.

Pan Location	Vent Configuration	Av√Hv	Average MLR per unit area (last 1200 sec)			
			Total (kg m²/s)	Rear Pan (kg m²/s)	Centre Pan (kg m²/s)	Front Pan (kg m²/s)
Freeburn		-	0.048			
Rear	Full	3.155	0.093	0.093	-	-
	Soffit	2.400	0.063	0.063	-	-
	Door	0.400	0.156	0.156	-	-
	Window	0.372	0.137	0.137	-	-
	S Window	0.186	0.160	0.160	-	-
Centre	Full	3.155	0.046	-	0.046	-
	Soffit	2.400	0.050	-	0.050	-
	Door	0.400	0.134	-	0.134	-
	Window	0.372	0.084	-	0.084	-
	S Window	0.186	0.138	-	0.138	-
Front	Full	3.155	0.052	-	-	0.052
	Soffit	2.400	0.054	-	-	0.054
	Door	0.400	0.032	-	-	0.032
	Window	0.372	0.052	-	-	0.052
	S Window	0.186	0.170	-	-	0.170
x2 Freeburn			0.060			
Rear Centre	Full	3.155	0.061	0.070	0.052	-
	Soffit	2.400	0.080	0.096	0.064	-
	Door	0.400	0.154	0.165	0.143	-
	Small Window	0.186	0.101	0.102	0.100	-
Rear Front	Full	3.155	0.060	0.061	-	0.059
	Soffit	2.400	0.063	0.072	-	0.054
	Small Window	0.186	0.130	0.074	-	0.186
Centre Front	Full	3.155	0.054	-	0.053	0.055
	Soffit	2.400	0.060	-	0.069	0.051
	Small Window	0.186	0.126	-	0.073	0.179
x2 Centre	Full	3.155	0.065	-	-	-
	Soffit	2.400	0.076	-	-	-
	Small Window	0.186	0.090	-	-	-
x3 Freeburn			0.061	-	-	-
Rear Centre Front	Full	3.155	0.064	0.075	0.059	0.057
	Soffit	2.400	0.087	0.128	0.073	0.062
	Small Window	0.186	0.101	0.061	0.063	0.179
x3 Centre	Full	3.155	0.100	-	-	-
	Soffit	2.400	0.149	-	-	-
	Small Window	0.186	0.065	-	-	-

It is generally observed that for the single pan series as the pan is moved from the front to the rear of the compartment the MLR and heat release rates increase. This is a result of radiation enhancement from the rear wall to the pool surface. This is shown in the comparison of the MLR for each pool location in the single pan series as a function of the ventilation factor in Figure 7.8. The exception to this is the under-ventilated small window experiment in which the front pan has a marginally greater mass loss rate than either of the other pans. Conversely it is also noted that the HRR of the front pan is very similar to that of the free burning heat release rate. This is expected as there is less radiation enhancement to the pool fire as a result of compartment effects.

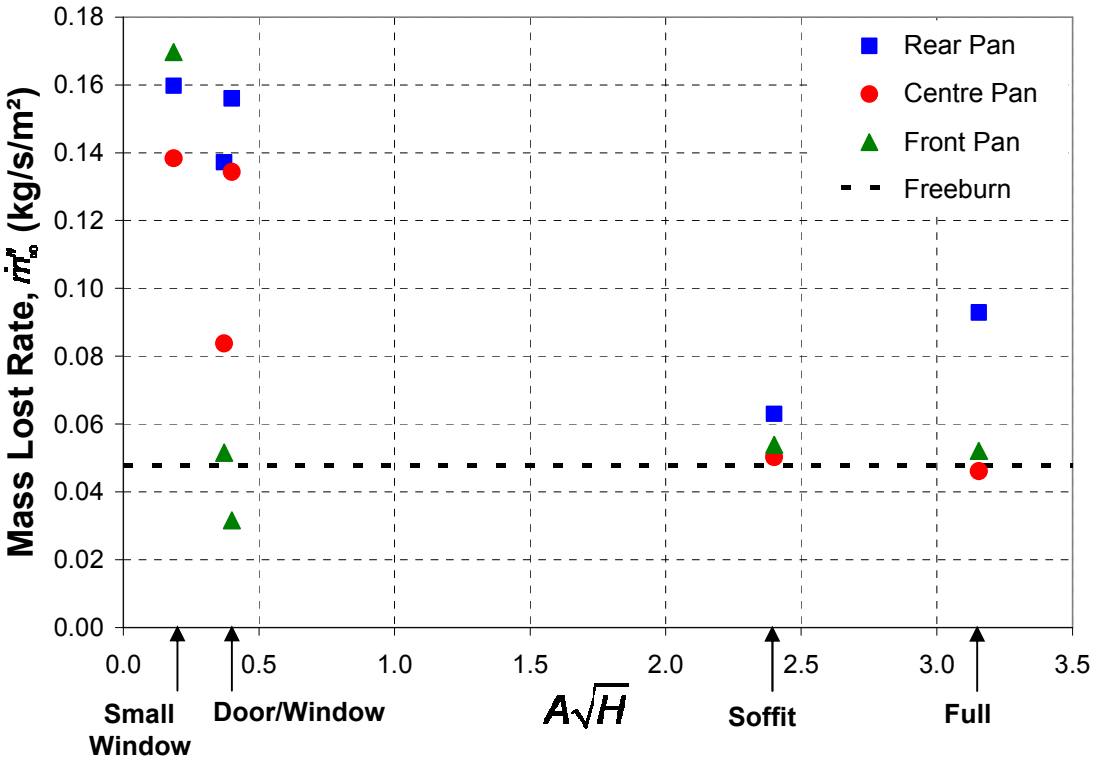

Figure 7.8: Comparison of the mass loss rates for each pool location in the single pan series as a function of the ventilation factor

The double pan series also notes a significant increase in the mass loss rate of the front pan as part of multiple location series. This is shown in the mass loss rates comparison for the double pan series in Figure 7.9 in which the mass loss rate of the front pan in the centre front (CF) series and rear front (RF) have mass loss rates that are;

- 3.7 times that of the free burn mass loss rate of a single pan, and

- 2.0 times the mass loss rate of the single x2 equivalent sized pan located in the centre of the compartment.

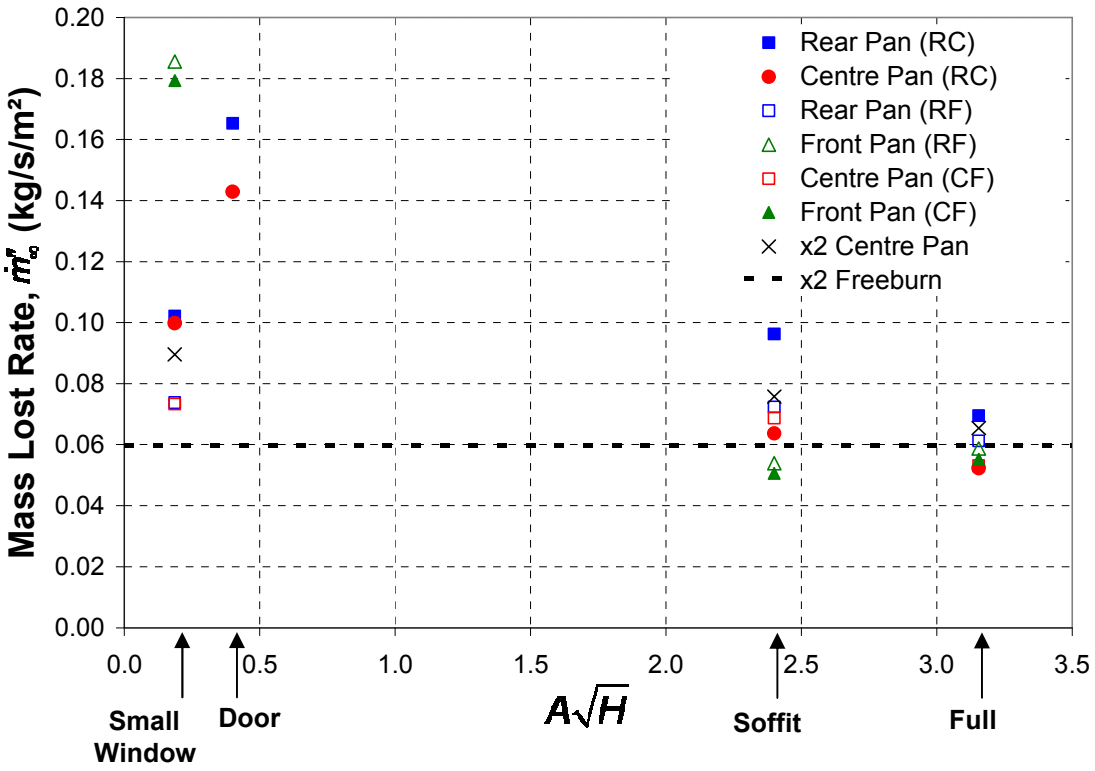

Figure 7.9: Comparison of the mass loss rates for each pool location in the double pan series as a function of the ventilation factor

The triple pan series mass loss rate comparisons are shown in Figure 7.10 and continue to reflect the trend of the enhanced burning in the front pan location.

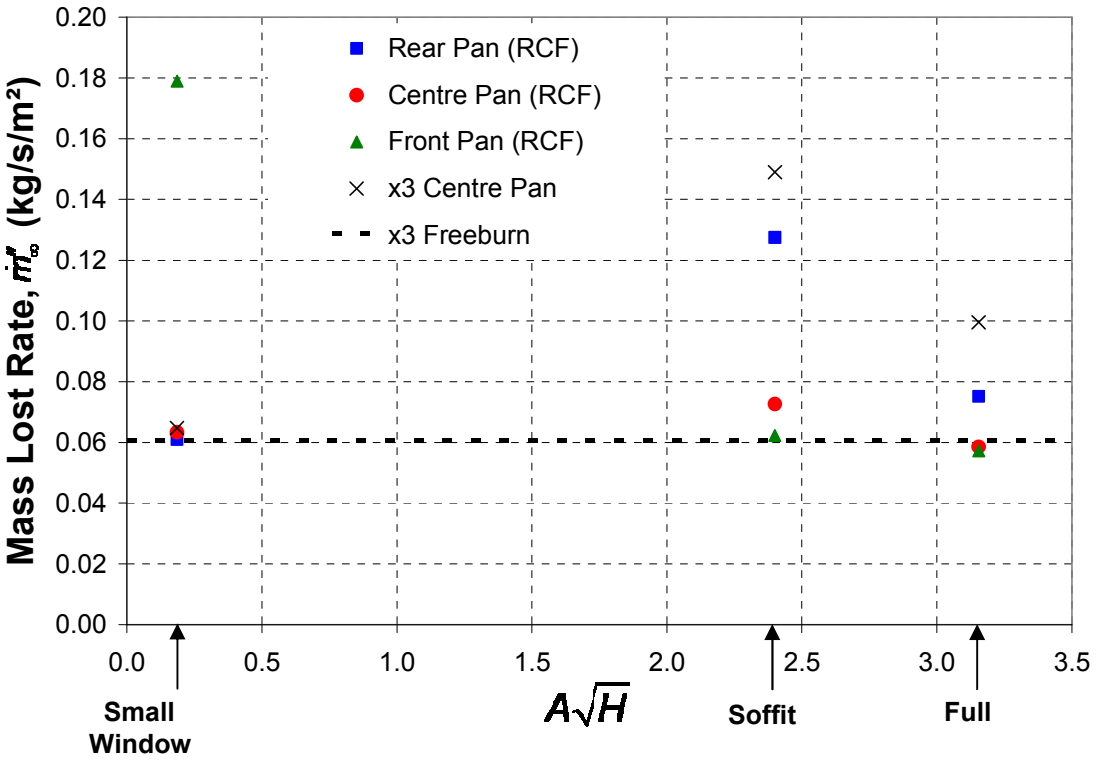

Figure 7.10: Comparison of the mass loss rates for each pool location in the triple pan series as a function of the ventilation factor

For the ventilated experiments the larger pan in the centre of the room provides the greatest mass loss rate. However for the under ventilated small window experiment the front pan again is significantly greater than any of the other pan locations. In this instance the mass loss rate of the front pan in the rear centre front (RCF) series has a mass loss rates that is;

- 3.7 times that of the free burn mass loss rate of a single pan, and
- 2.8 times the mass loss rate of the single x3 equivalent sized pan located in the centre of the compartment.

7.4 Equivalence Ratio, ϕ

The phi meter developed as part of this experimental study was used to categorise fire behaviour and development in terms of actual the fuel/oxygen ratio compared with the stoichiometric fuel/oxygen ratio. The Equivalence Ratio (ER) provides a measure of the level of ventilation during a compartment fire, e.g. fuel-rich or fuel-lean combustion and in this study was measured at 25mm below the top of the centre of the vent (refer

page 4-24). When $\phi<1$ it is considered an oxygen rich condition, which means that sufficient oxygen is available for combustion. When $\phi>1$ this indicates the regime when there is a fuel rich situation and there is not enough oxygen available for complete combustion. Therefore as the ventilation into an enclosure is reduced the ER is expected to increase which is shown in the results in Table 7.2.

The experimental results for the 34 compartment experiments completed are summarised in Table 7.2. The forth and fifth columns detail the total heat released (energy) and total mass loss, respectively, during the fully developed phase of burning which occurs in the last 1200 seconds of an experiment. The six and seventh columns are the ER values measured by the phi meter (approximated average value during the quasi-steady state period), and whether or not visual confirmation of external flaming occurred respectively. It is noted that for all but the small window and the door geometry scenario with the rear and centre pans together, no visible flaming occurred outside the vent opening.

Table 7.2: Phi meter experimental results

Pan Location	Vent Configuration	Av√Hv	Total Energy last 1200 sec (MJ)	Ave. HRR Last 1200 sec (kW)	Equivalence Ratio (ϕ)	Visible External Flaming
Rear	Full	3.155	201.4	111.8	0.1	no
	Soffit	2.400	132.8	110.6	0.1	no
	Door	0.400	327.2	272.4	0.35	no
	Window	0.372	267.0	222.3	0.4	no
	S Window	0.186	306.4	255.1	0.95	YES
Centre	Full #1	3.155	102.3	85.2	0.05	no
	Soffit	2.400	113.9	94.8	0.1	no
	Door	0.400	267.7	222.9	0.15	no
	Window	0.372	181.7	151.3	0.25	no
	S Window	0.186	291.2	242.5	0.90	YES
Front	Full	3.155	113.0	94.1	0.05	no
	Soffit	2.400	112.9	94.0	0.05	no
	Door	0.400	65.0	54.2	0.2	no
	Window	0.372	128.6	83.6	0.16	no
	S Window	0.186	274.1	228.2	1.15	YES
Rear Centre	Full	3.155	245.8	204.8	0.06	no
	Soffit	2.400	302.5	252.1	0.15	no
	Door	0.400	544.4	453.7	1.06	YES
	Window	Not completed				
	Small Window	0.186	300.4	250.1	1.20	YES
Rear Front	Full	3.155	239.4	199.5	0.10	no
	Soffit	2.400	255.5	212.9	0.10	no
	Door	Not completed				
	Window	Not completed				
	Small Window	0.186	509.4	424.5	1.90	YES
Centre Front	Full	3.155	219.7	183.1	0.05	no
	Soffit	2.400	236.2	196.8	0.10	no
	Door	Not completed				
	Window	Not completed				
	Small Window	0.186	465.6	387.7	1.70	YES
x2 Centre	Full	3.155	270.7	225.4	0.14	no
	Soffit	2.400	324.1	269.8	0.16	no
	Door	Not completed				
	Window	Not completed				
	Small Window	0.186	298.3	248.4	1.15	YES
Rear Centre Front	Full	3.155	337.7	281.2	0.15	no
	Soffit	2.400	533.0	443.8	0.2	no
	Door	Not completed				
	Window	Not completed				
	Small Window	0.186	566.2	464.6	2.30	YES
x3 Centre	Full	3.155	628.9	523.7	0.05	no
	Soffit	2.400	873.4	727.2	0.45	no
	Door	Not completed				
	Window	Not completed				
	Small Window	0.186	294.2	245.0	1.30	YES

Note: Shaded Rows indicate those experiments not completed due to damaging compartment conditions

As noted in Table 7.2 all but the small window and door (rear centre) experiments yielded an ER of less than 1 indicating sufficient ventilation was available for the full, soffit, window and remaining door experiments.

In both the full and soffit ventilation geometries, the upper layer temperatures do not exceed 300ºC and as expected the ER is significantly less than 1. For the fully open case the ER ranged from 0.05 to 0.15 and for the soffit ventilation case the ER ranged from 0.05 to 0.45. Two typical examples of ER time histories measure by the phi meter for these well ventilated compartment conditions are shown in Figure 7.11. Both of these examples are from experiments using the x2 equivalent pan located in the centre of the compartment. The fully open vent time history is shown to the left with the soffit vent shown to the right.

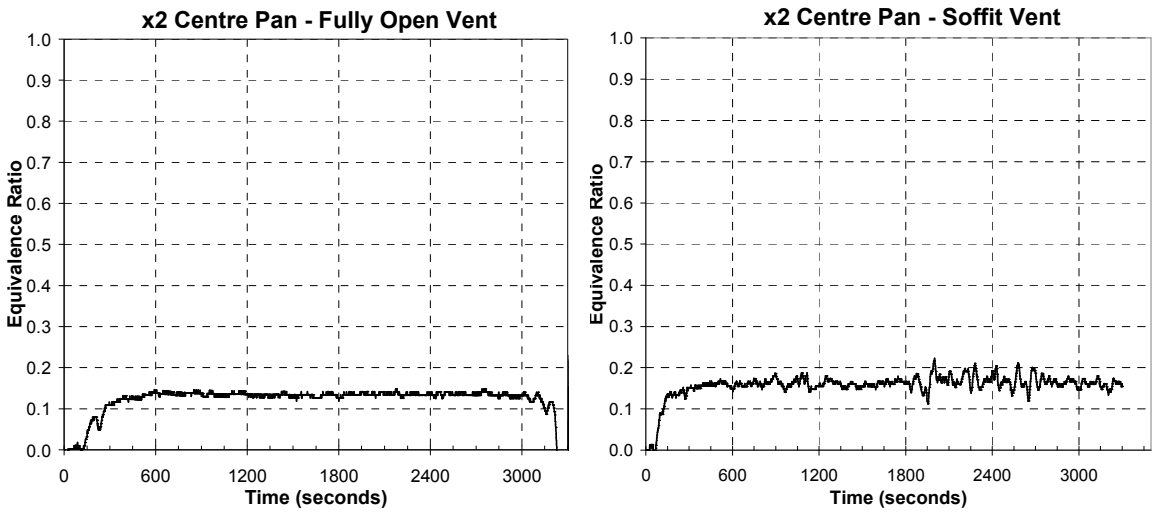

Figure 7.11: Typical equivalence ratio time history results with the full and soffit ventilation geometries.

As the ventilation into the enclosure was reduced by the door and window restrictions, all pans show an increase in the fuel mass loss rate from that in the full and soffit cases. This was indicated by burning around the base of the pans, upper layer temperatures approaching 600ºC, and an increase in the ER, although still less than 1.0. This indicates sufficient oxygen was still available such that combustion was not considered ventilation limited. For the single pan door ventilation case the ER ranged from 0.2 to 0.65 and for the window ventilation case the ER ranged from 0.16 to 0.4. An example of door and window ER time histories is shown in Figure 7.12. Both of these examples are from experiments using a single 200mm square pan located in the rear of the

compartment. The door vent time history is shown to the left with the window vent shown to the right.

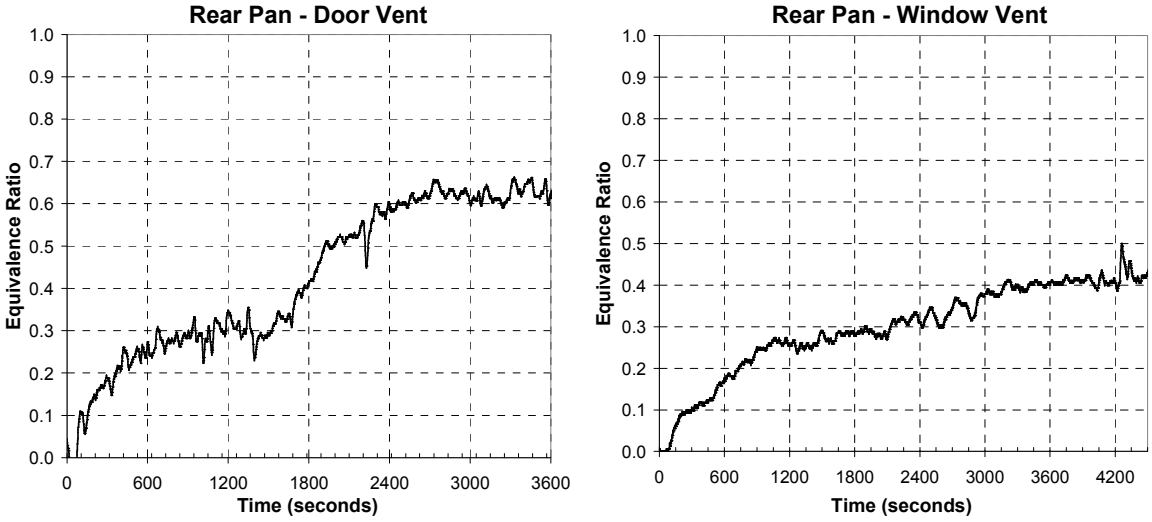

Figure 7.12: Typical equivalence ratio time histories for the full and soffit ventilation.

Theoretically external flaming is expected to occur at an equivalence ratio of 1.0, as at this level the combustion regime transitions from oxygen rich to fuel rich. This requires the fire to source oxygen from outside the enclosure at which point projection flaming will occur. It has also been known that flashover may occur at an equivalence ratio below 1 [2], depending on the size of the ventilation opening.

One experiment with the rear-centre pan with the door geometry was completed with compartment temperatures exceeding 800ºC, and the equivalence ratio was measured to be 1.05. Along with external flaming in the vent this indicated flashover had occurred. For the small window geometry, temperatures approached or exceeded 800ºC and the conditions within the compartment were representative of a post-flashover situation considering typical post-flashover conditions of temperatures >600 ºC [3]. In these experiments, the beginning of external flaming occurred at a measured equivalence ratio of 1.0 or greater. The photographs in Figure 7.13 detail the small window experiments post-flashover behaviour with sustained external flaming profiles and the associated measured ER.

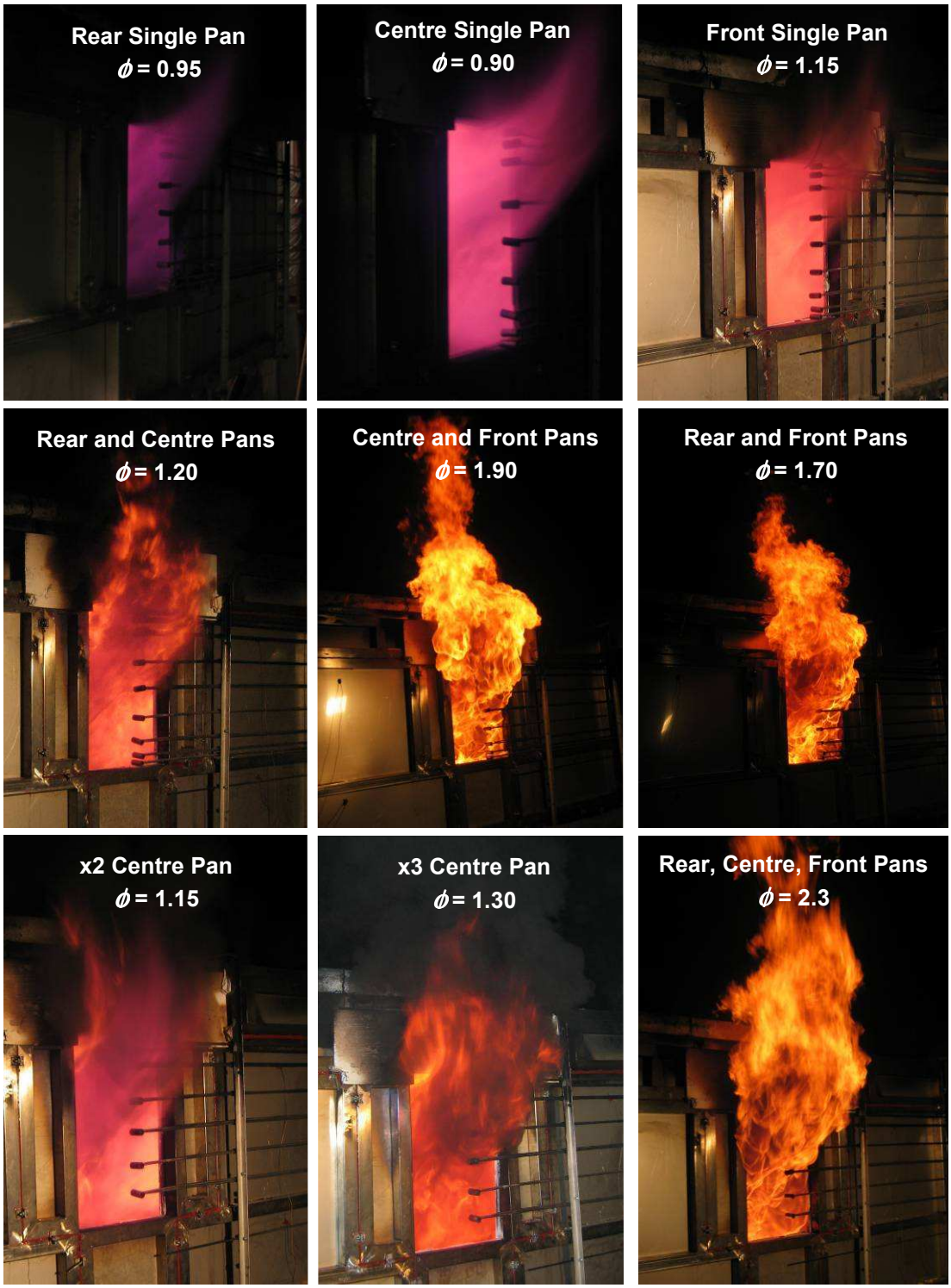

Figure 7.13: External flaming from small window geometry compartment experiments with associated equivalence ratio values

The individual equivalence ratio time histories for these small window experiments are further detailed in Figure 7.14 for the single pan series, in Figure 7.15 for the double pan series, and Figure 7.16 for the triple pan series.

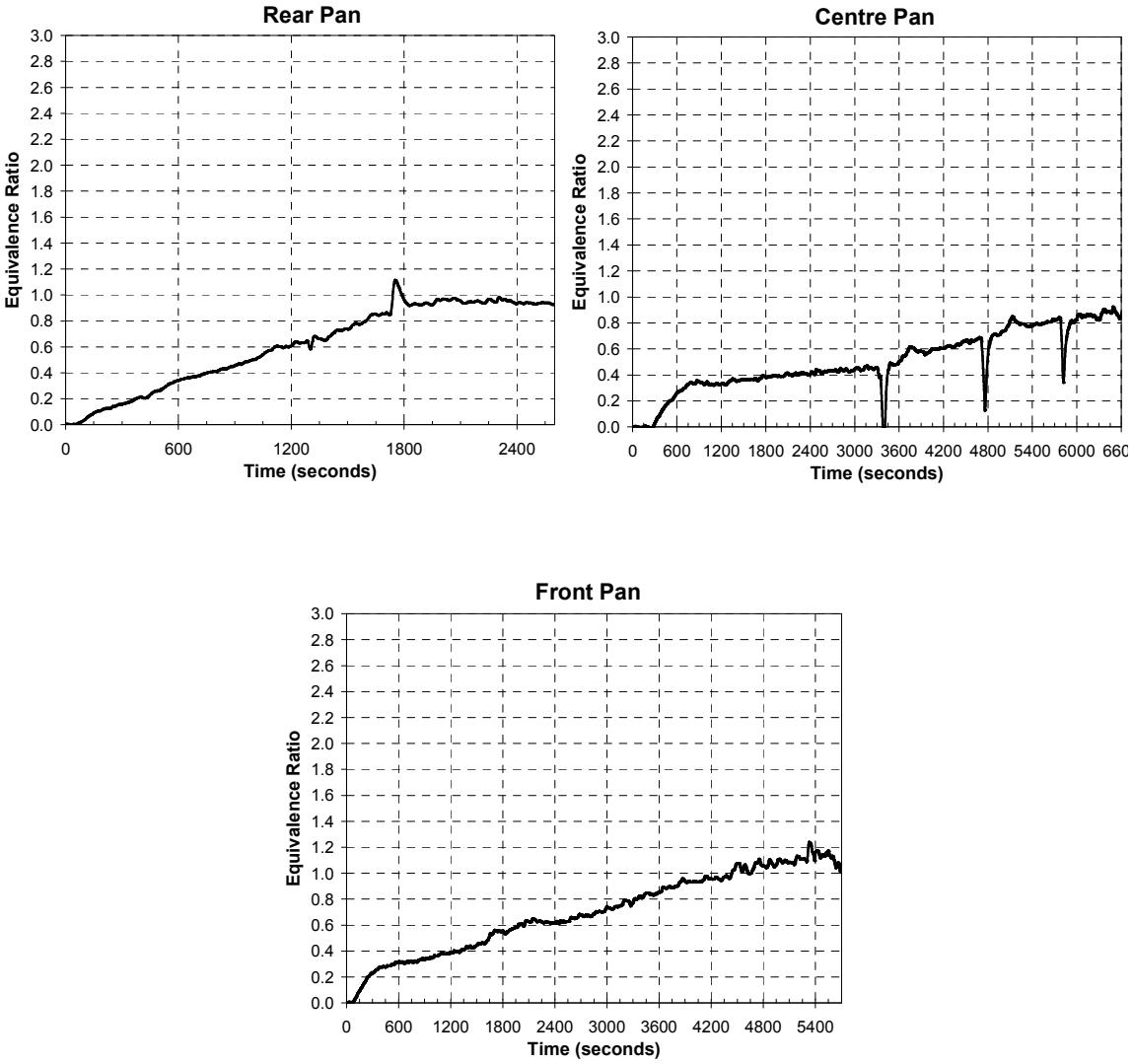

Figure 7.14: Single pan equivalence ratio time histories for the small window vent showing measurements rear, centre and front pan location experiments

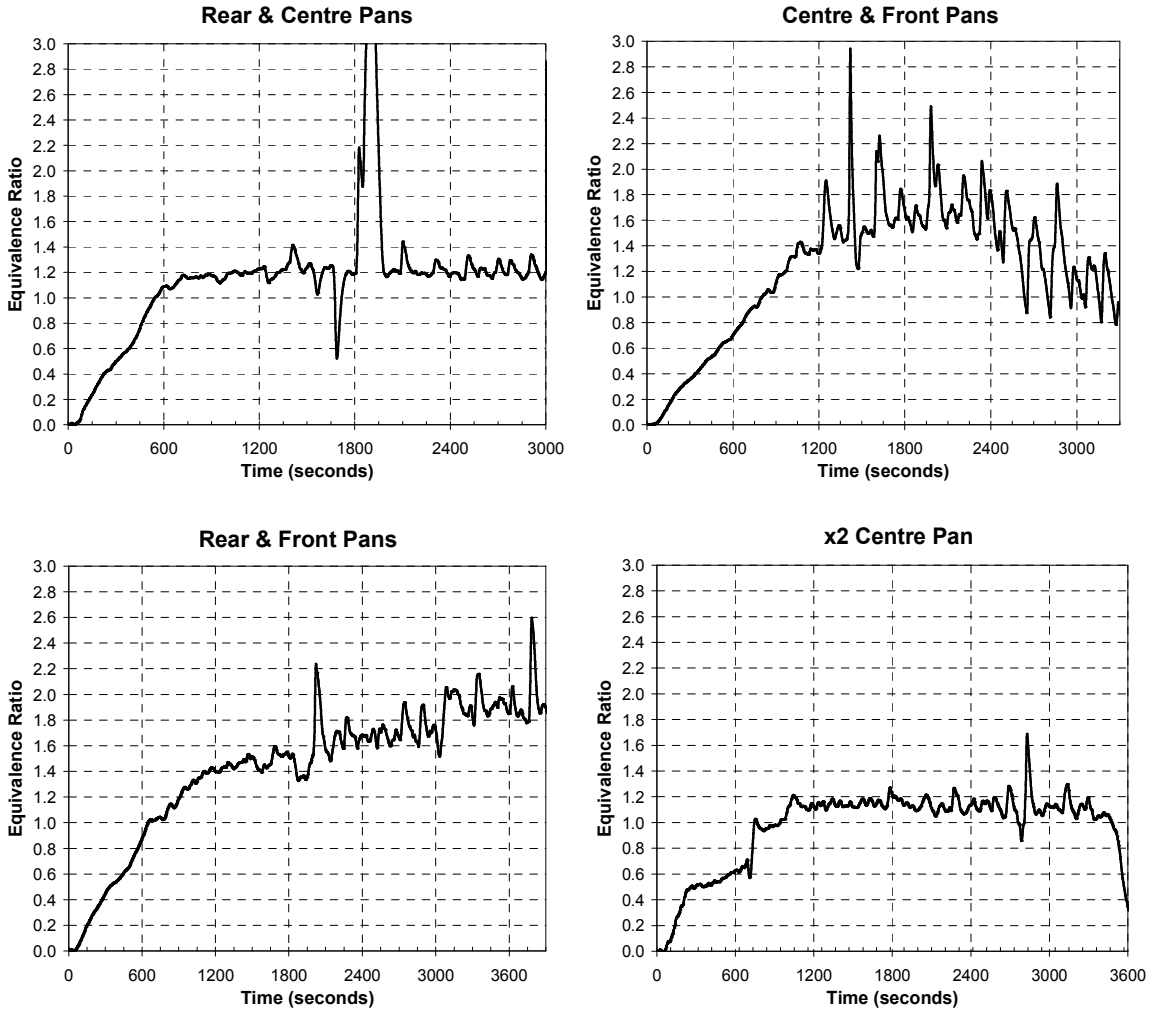

Figure 7.15: Double pan equivalence ratio time histories for the small window vent showing measurements from the rear-centre, centre-front, rear-front and x2 equivalent centre pan experiments

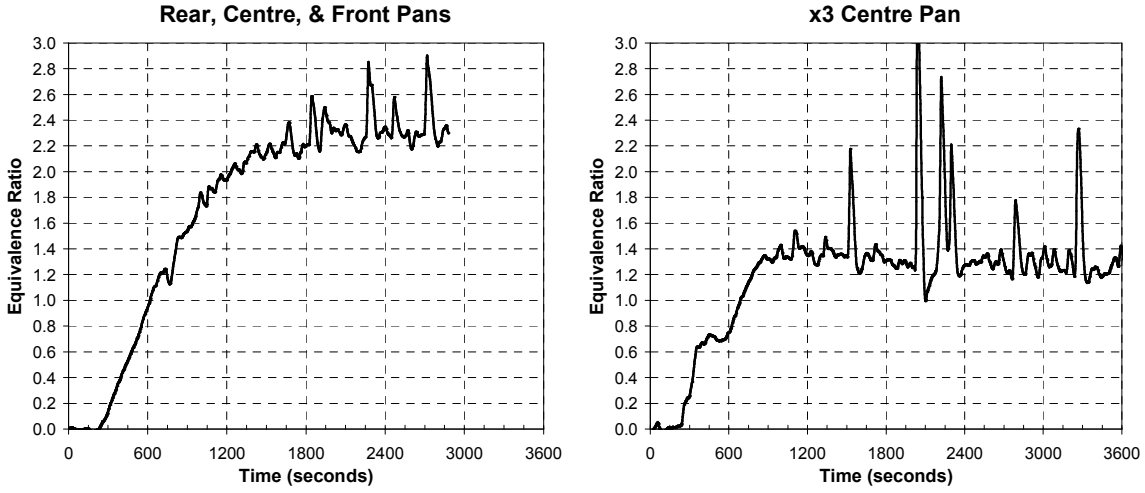

Figure 7.16: Triple pan equivalence ratio time histories for the small window vent showing measurements from the rear-centre-front and x3 equivalent centre pan experiments

Although the time history equivalence ratios verge toward a steady value at the end of the experiment at which point a quasi-steady state was deemed to have been achieved there are times at which the equivalence ratio spikes. These were identified during the experiments by an increase in the furnace temperature indicating a reduction in flow due to a blockage. The temporary blockages occur due to a build up of soot at the sampling port and also within the furnace catalyst.

The quasi-steady state equivalence ratios for all 34 experiments are shown relative to the ventilation factor in Figure 7.17 for the single pan series, Figure 7.18 for the double pan series, and Figure 7.19 for the triple pan series.

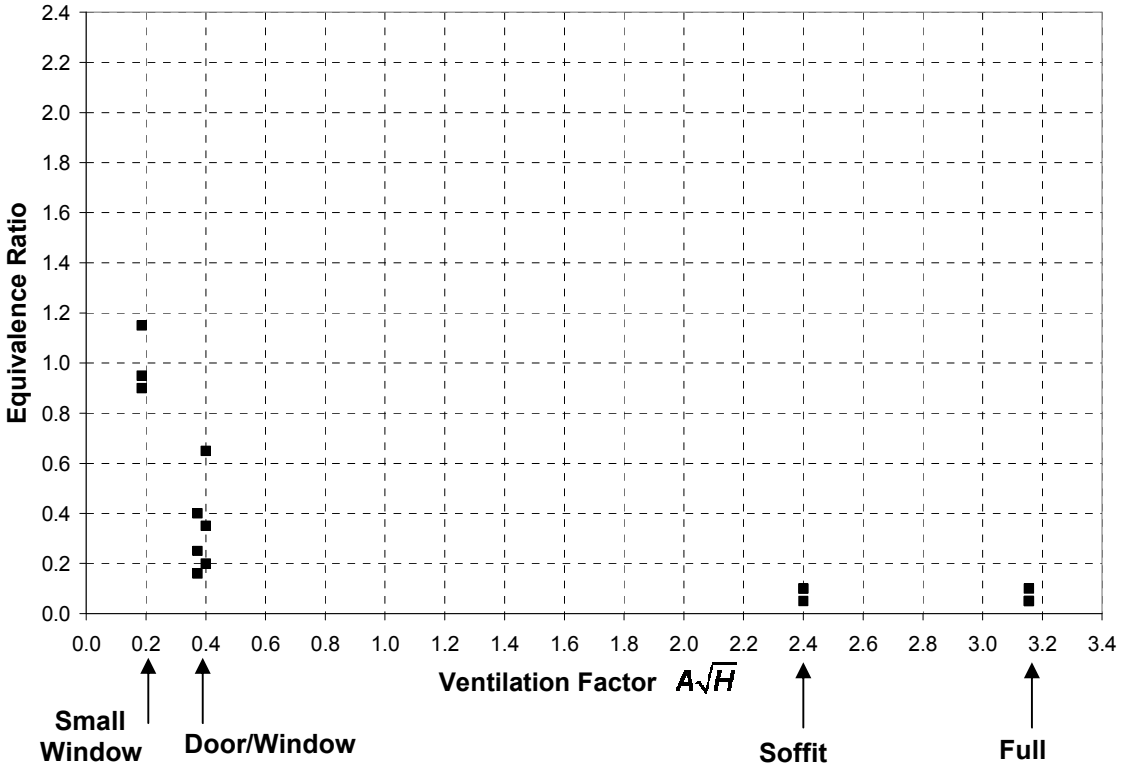

Figure 7.17: Equivalence ratio versus ventilation factor for the individual single pan series

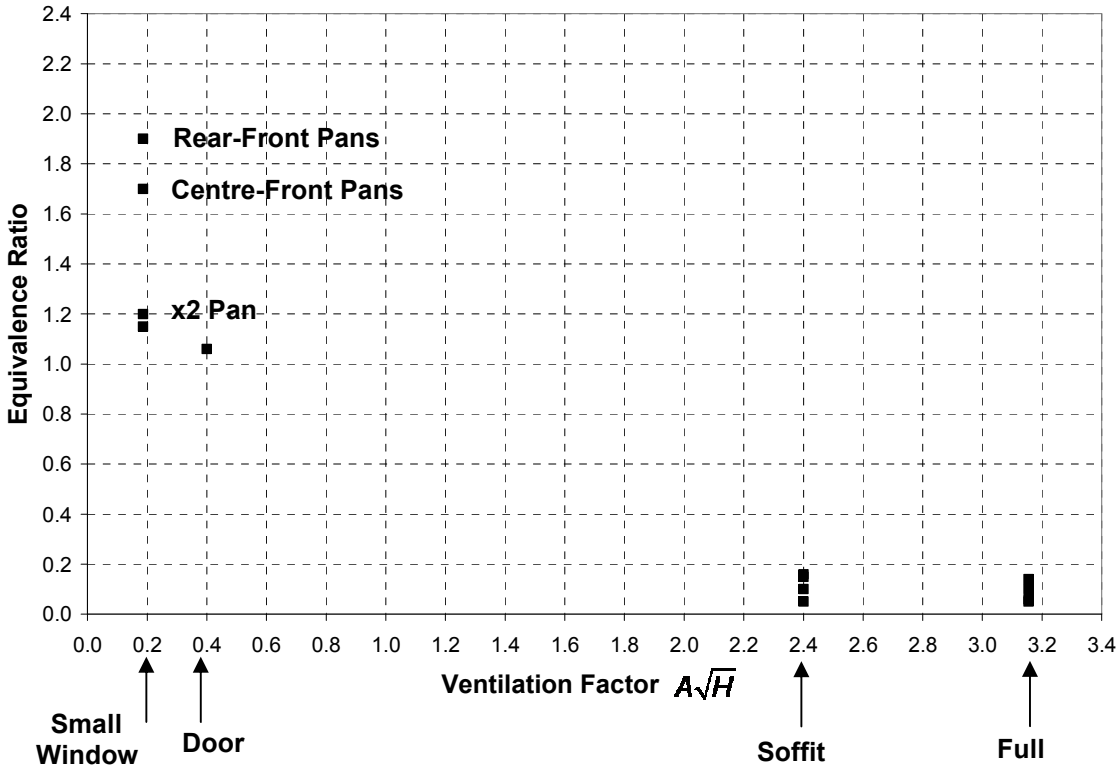

Figure 7.18: Equivalence ratio versus ventilation factor for the double pan series

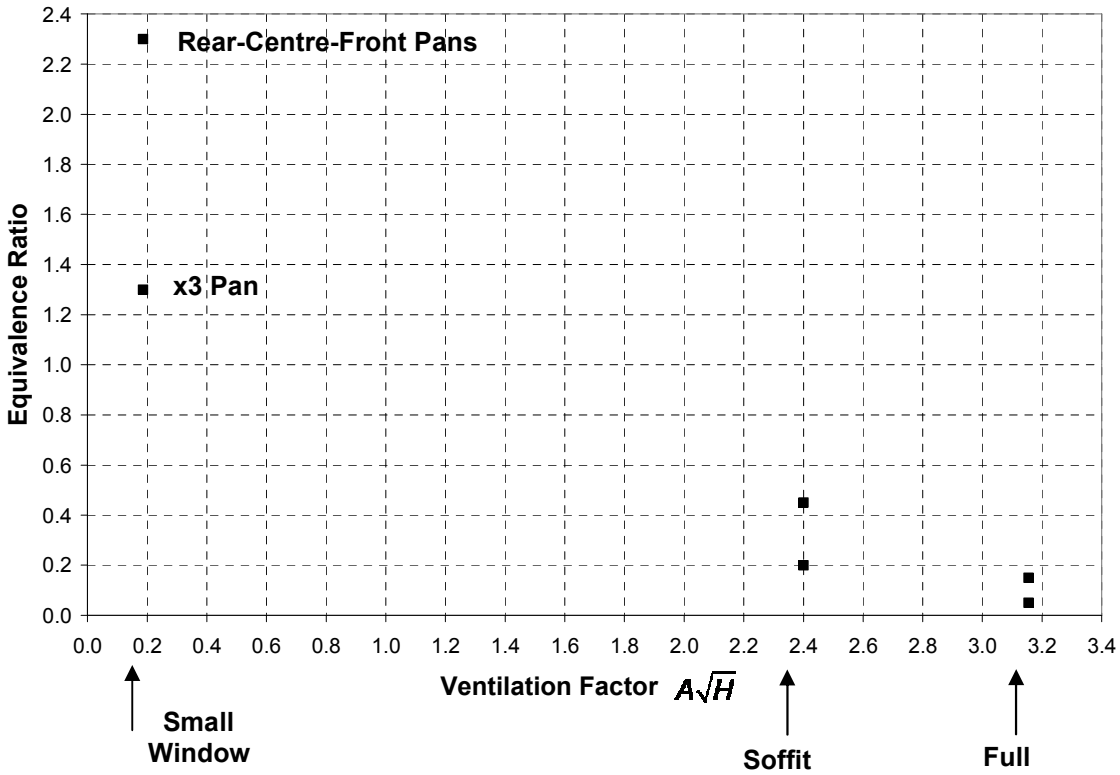

Figure 7.19: Equivalence ratio versus ventilation factor for the triple pan series

As expected as the ventilation is reduced the equivalence ratio increases. However Figure 7.18 and Figure 7.19 show that the equivalence ratios for the small window experiments provide for a large variation. The effect of fire location is also noted with the ER for the experiment using the x2 pan in the centre of the room measured at 1.15, and when the enclosure was provide with two individual single pans in either the centre-front location or the rear-front location, the ER was measured to be 1.7 and 1.9 respectively. The ER for the experiment using the x3 pan in the centre of the room was also measured to be 1.3, however when the enclosure was provide with three individual single pans in rear-centre-front locations, the ER was measured to be 2.3. This is a result of compartment behaviour due to the specific location of the front pan near the vent opening.

The equivalence ratio was also calculated from the mass relationship between the stoichiometric mass loss rate and air consumption. This was compared with the measurements from the phi meter and is detailed in Figure 7.20.

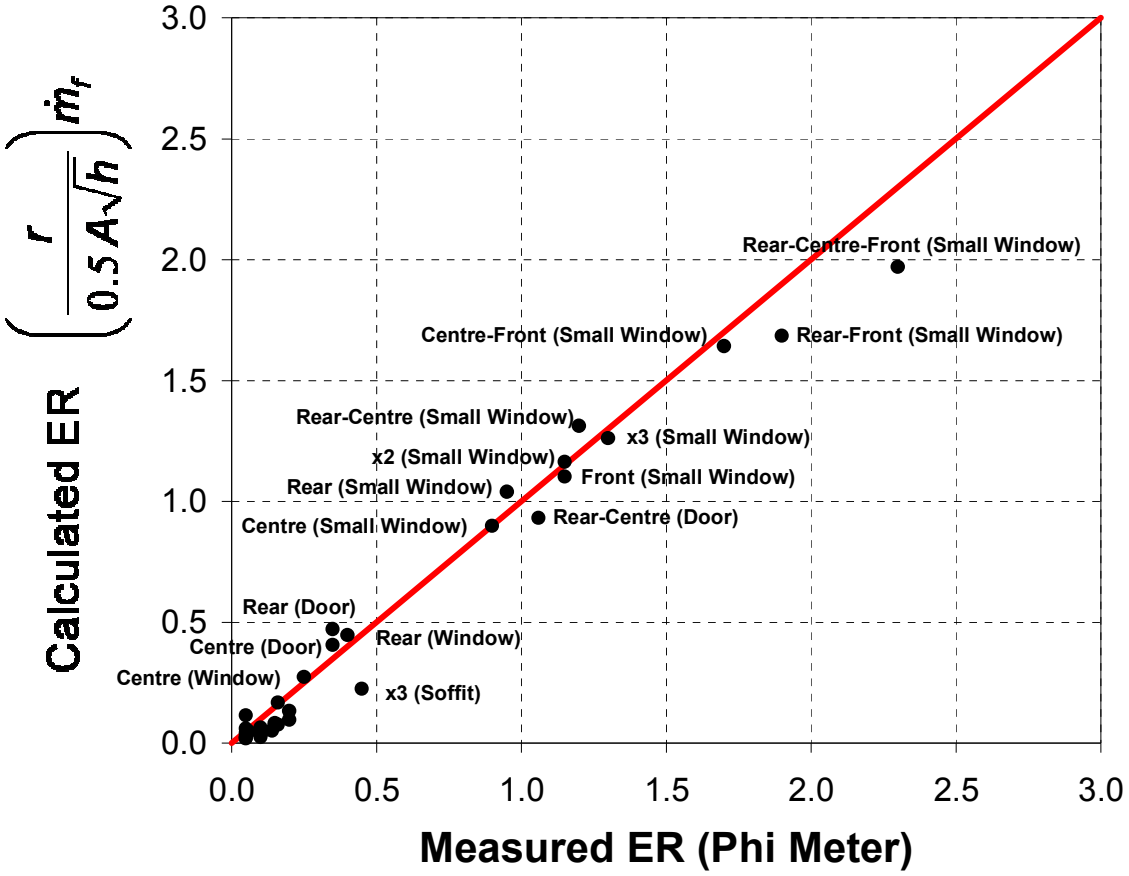

Figure 7.20: Comparison of the calculated global equivalence ratio and the measure equivalence ratio from the phi meter

Therefore the phi meter provides a good comparison with the calculated ER. Given the higher measured ER values for the experiments with the front pan location, this indicates the production of unburnt fuel which has a significant impact upon the combustion behaviour.

7.5 Combustion Efficiency

The combustion efficiency is the ratio between the actual heat release rate and the heat release rate required for complete combustion. The heat release rate for complete combustion can be expressed in the following form:

$$\left(\dot{Q}\right)_{stoichiometry} = \dot{m}_{fuel}\left(\Delta h_c\right)$$

Therefore using this term in conjunction with the measured actual heat release rate, the combustion efficiency can be calculated as follows:

$$\chi = \frac{\left(\dot{Q}\right)_{measured}}{\dot{m}_{fuel}\left(\Delta h_c\right)}$$

The MLR of the fuel has been used to evaluate the combustion efficiency for the experiments. The value for the heat of combustion is taken as 44600 MJ/kg. Results of the combustion efficiencies are tabulated in Table 7.3.

Table 7.3: Combustion efficiency results for all 34 compartment experiments

Pan Location	Vent Configuration	Av√Hv	Ave. MLR Last 1200 sec (kg/s)	Q_{actual} (kW)	Q_{stoich} (kW)	Combustion Effciency
Rear	Full	3.155	0.00371	111.8	165.7	0.67
	Soffit	2.400	0.00252	110.6	112.4	0.98
	Door	0.400	0.00624	272.4	278.4	0.98
	Window	0.372	0.00549	222.3	244.8	0.91
	S Window	0.186	0.00639	255.1	285.1	0.89
Centre	Full	3.155	0.00184	85.2	82.2	1.04
	Soffit	2.400	0.00201	94.8	89.6	1.06
	Door	0.400	0.00538	222.9	239.7	0.93
	Window	0.372	0.00335	151.3	149.4	1.01
	S Window	0.186	0.00553	242.5	246.9	0.98
Front	Full	3.155	0.00208	94.1	92.9	1.01
	Soffit	2.400	0.00216	94.0	96.2	0.98
	Door	0.400	0.00126	54.2	56.4	0.96
	Window	0.372	0.00206	83.6	92.0	0.91
	S Window	0.186	0.00679	228.2	302.8	0.75
Rear Centre	Full	3.155	0.00487	206.0	217.4	0.95
	Soffit	2.400	0.00640	278.1	285.3	0.97
	Door	0.400	0.01233	453.7	549.9	0.83
	Small Window	0.186	0.00808	250.1	360.3	0.69
Rear Front	Full	3.155	0.00480	199.4	214.1	0.93
	Soffit	2.400	0.00505	229.4	225.3	1.02
	Small Window	0.186	0.01037	424.5	462.6	0.92
Centre Front	Full	3.155	0.00433	184.1	193.2	0.95
	Soffit	2.400	0.00477	204.6	212.9	0.96
	Small Window	0.186	0.01010	387.7	450.6	0.86
x2 Centre	Full	3.155	0.00524	225.4	233.5	0.97
	Soffit	2.400	0.00606	269.8	270.4	1.00
	Small Window	0.186	0.00716	248.4	319.4	0.78
Rear Centre Front	Full	3.155	0.00764	281.2	340.7	0.83
	Soffit	2.400	0.01050	443.8	468.1	0.95
	Small Window	0.186	0.01213	464.6	540.9	0.86
x3 Centre	Full	3.155	0.01195	523.7	532.8	0.98
	Soffit	2.400	0.01788	727.2	797.5	0.91
	Small Window	0.186	0.00777	245.0	346.4	0.71

In a fire the combustion efficiency is expected to decrease as a function of the ventilation into the compartment and this is reflected in this experimental study and as detailed in Figure 4.4 in which the combustion efficiency drops as the ventilation within the enclosure is reduced.

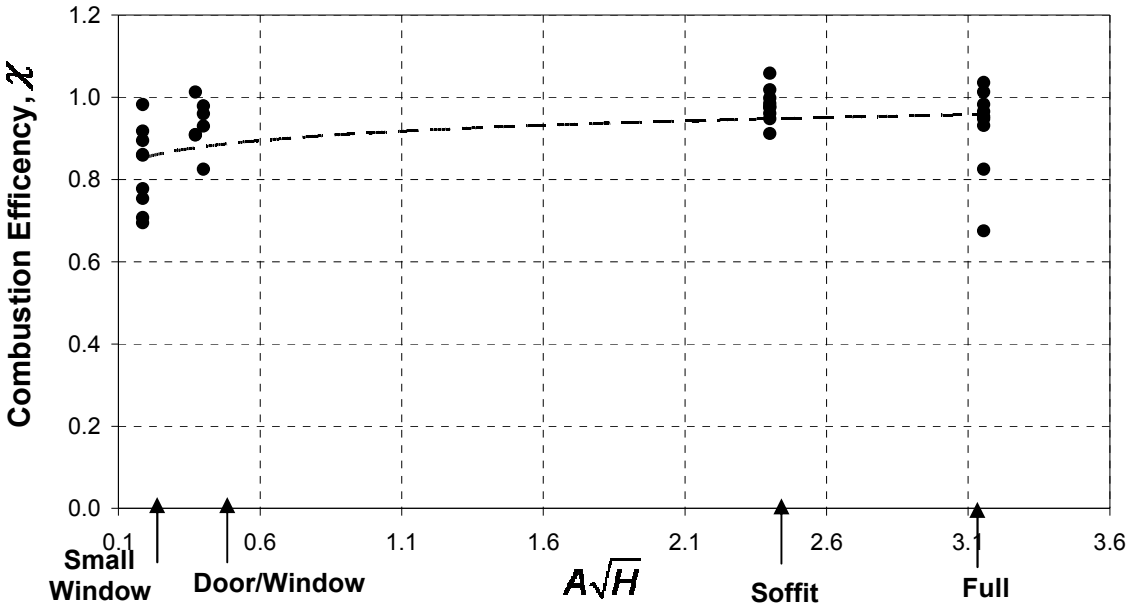

Figure 7.21: Comparison of the combustion efficiency with the ventilation factor.

The average combustion efficiencies for each ventilation geometry were calculated to be 0.93 (fully open), 0.98 (soffit), 0.92 (door), 0.94 (window), and 0.83 (small window).

7.6 Compartment Temperatures

Upper layer temperatures are plotted in as a function of the ventilation factor in Figure 7.22 and it can be seen that as expected the temperatures within the compartment increase as the ventilation is reduced and are a function of the fire size. It can be seen that the compartment larger single centrally located x3 pan provide the highest compartment temperature followed by the rear-centre and front pans. It is noted that for all small window experiments the temperatures within the compartment reflect that of a single zone post-flashover profile regime, whilst all other geometries typically displayed pre-flashover upper and lower layer profile.

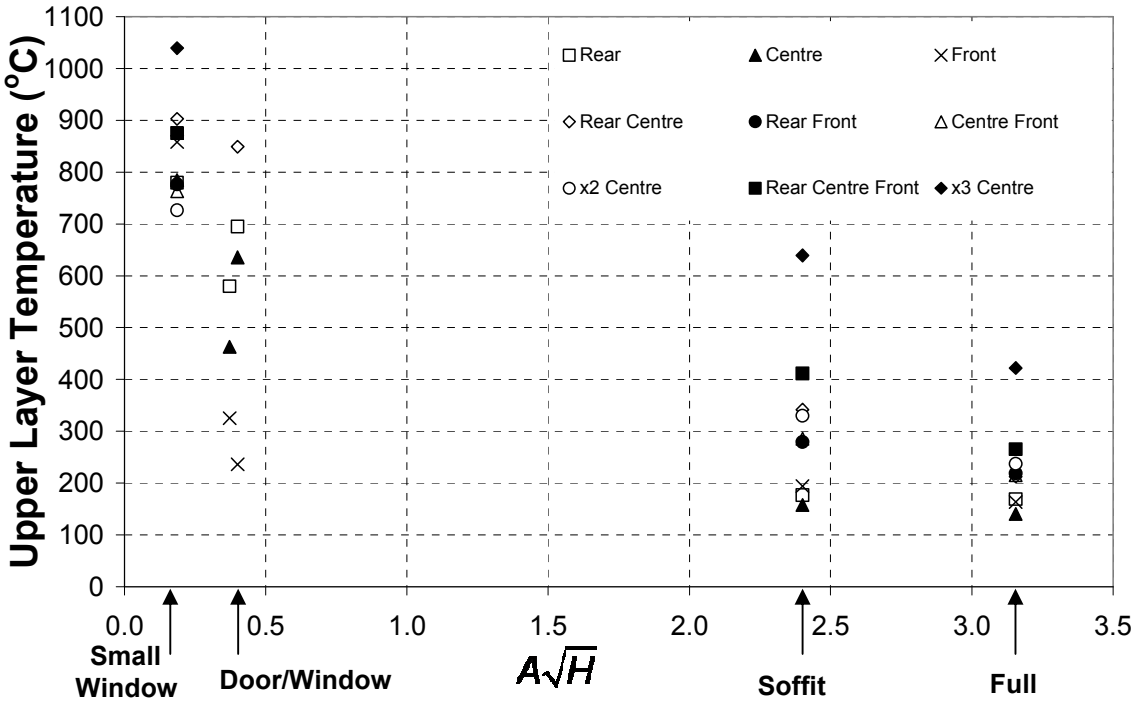

Figure 7.22: Comparison of the upper layer compartment temperatures with the ventilation factor.

7.7 Summary

The impact of compartment ventilation geometries and pool fire characteristics have identified that the inclusion of a pan in front of a room provides for complex combustion behaviour particularly when included with other pans in multiple locations.

The generalised approach that a fire located in the centre of the room which is considered by practising engineers to be a '*credible design fire scenario'* is valid only during pre-flashover when sufficient ventilation is provided e.g. the full and soffit geometries. The full and soffit openings are provided with sufficient ventilation such that there fire behaviour is consistent with a pre-flashover regime. It is also noted that the MLR HRR of the front pan is very similar to that of the free burning heat release rate. This is expected as there is less radiation enhancement to the pool fire as a result of compartment effects.

This is not however the case for under-ventilated fires. The under-ventilated post-flashover fire provides a combustion zone at the vent which extends into the

compartment surrounding a pan located at the front of the room. This combustion zone provides significant radiation enhancement to the front pan which significantly increases the mass loss rate, and un-pyrolysed products and subsequently increases the heat release rate. A large centrally located pan is located at a distance from this vent combustion zone and is not affected to the same extent by the radiation enhancement. This means that a large single pan located in the centre of a room does not provide the highest HRR, and multiple pans distributed in the compartment can provide a significantly greater HRR of the order of 50% on the provision that one of the single pans is located adjacent to the ventilation opening.

The ventilation into the enclosure also impacts upon the incoming vent flows and a leaning-over effect of the pool fires is noted. For the rear pan location the flame can be pushed into the rear wall such that the assumption that fire is separated from the wall and entrainment from all sides is available is not valid. The lean on the front flame can also be significant enough to decrease the heat release rate due to a reduction in flame feedback to the pool surface. This occurred predominately in the door vent experiment in which the mass loss rate was 66% of the free burn MLR.

7.8 References

1 Babrauskas, V, "Heat Release Rates", The SFPE Handbook of Fire Protection Engineering, Section 3/Chapter 1, 3rd edition, 2002

2 Wieczorek, C. J., Vandsbuger, U. and Floyd, J., "An Evaluation of the Global Equivalence Ration Concept for Compartment Fire: Data Analysis Methods" Journal of Fire Protection Engineering, Vol. 14, pp 9-34, February 2004.

3 Drysdale, D, An Introduction to Fire Dynamics, 2nd Edition, John Wiley & Sons, New York, 1998.

Chapter 8: FDS Analysis

This chapter serves the purpose of providing background information on the work completed using Fire Dynamics Simulator, FDS, to model the compartment fire experiments presented in this study. It is noted that during this experimental study the continued development of FDS has meant that although a significant amount of work was completed on FDS4 [1], and the current version of the model now available is version 5 [2].

There has been a significant change in the application of liquid fuels between these versions and this chapter will briefly discuss these and some of the general results of the work completed. It is noted for reference that the grid size of all of the results cited here is 50mm. Detailed background on FDS is not provided and the reader should consult the technical reference guide [3] for details about the model.

8.1 FDS Version 4

Version 4 of FDS provided a pyrolysis model to specify a liquid fuel. In this instance the surface line of the pool fire is specified as 'Liquid' and the thermal properties are similar to those of a solid material. The evaporation rate of the fuel is governed by the Clausius-Clapeyron equation and the fuel gases burn regardless of any ignition source. The thermal conductivity, density and specific heat are used to compute the loss of heat into the liquid via conduction using the same one-dimensional heat transfer equation that is used for solids.

The specification of a maximum burning rate could be provided on the surface input line, however the applicability of this was investigated and noted that suggest maximum burning rates are less than that obtained experimentally. An example input line for the pool fire is noted below;

```
&REAC ID='HEPTANE'
      FYI='Heptane, C_7 H_16'
      MW_FUEL=100.
      NU_O2=11.
      NU_CO2=7.
      NU_H2O=8.
      CO_YIELD=0.006
      SOOT_YIELD=0.015 /

&SURF ID= 'HEPTANE'
      RGB= 0.40,0.40,0.40
      HEAT_OF_VAPORIZATION= 316.
      HEAT_OF_COMBUSTION= 46112.
      PHASE= 'LIQUID'
      DELTA= 1.5
      KS= 0.16
      C_P= 2.24
      DENSITY= 800.
      TMPIGN= 98. /
```

Results from the modelling of both the free burn and compartment case indicate that the burning rate and subsequent heat release rate reach maximum point even when no maximum burning rate is specified. This is noted in Figure 8.1 showing the results from the free burning experiments and compartment experiments with full, soffit and small window geometries.

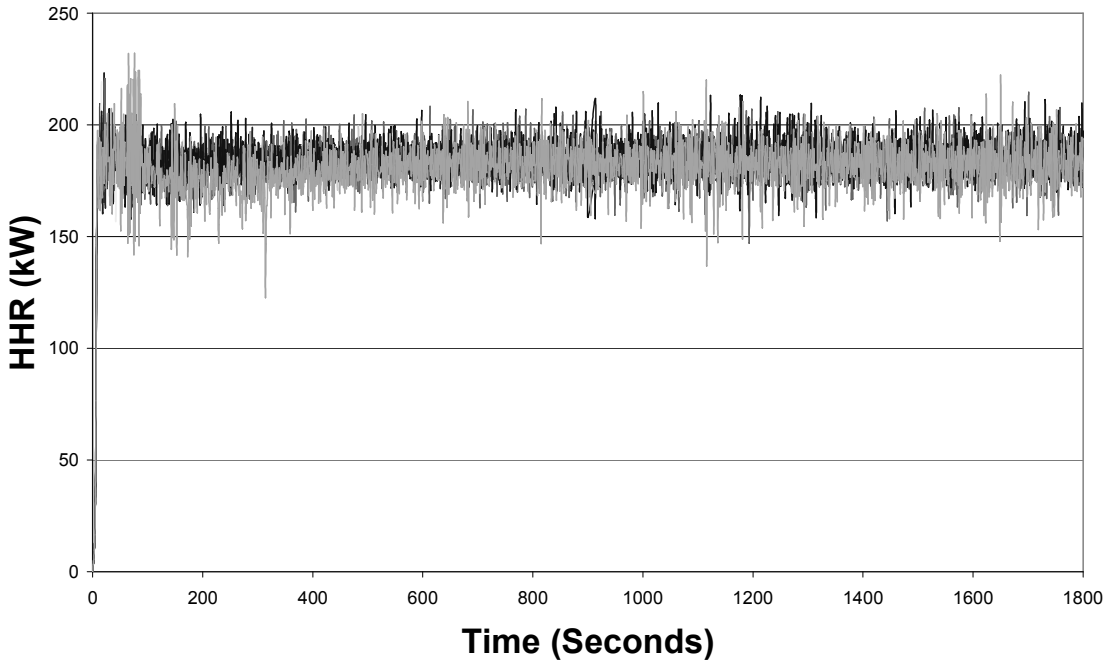

Figure 8.1: Comparison of the FDS4 heat release rate histories for free burning, and compartment experiments with full, soffit, small window vent with a single pool fire in the rear centre and front locations.

The liquid phase results were also checked by specifying the surface as a solid with a heat of vaporisation; however the resulting heat release rate was as noted for the liquid phase case. These results indicate that the radiative fraction to the fuel may be limited and that this would require further investigation. Visually however it was noted that FDS 4 did identify the flame lean-over as experienced in the compartment fire experiments as shown in Figure 8.2.

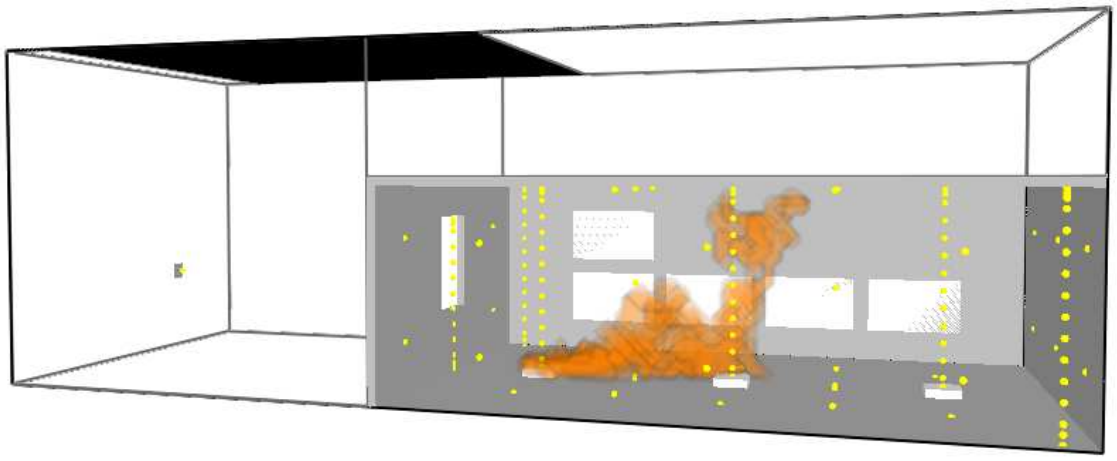

Figure 8.2: Flame lean-over in FDS 4 modelling.

Although the results indicated that FDS4 under-predicted the behaviour of pool fires, any further work using this version was superseded by the development of FDS 5.

8.2 FDS Version 5

Version 5 of FDS has made changes to the way that materials specified deal with radiation. In the previous versions thermal radiation from the gas space was absorbed at the surface of the material, and the emission to the gas space took place on the surface. FDS 5 allows a material to be designated an absorption coefficient (l/m) that will allow the radiation to penetrate and be absorb into the solid. Correspondingly, the emission of the material is based on the internal temperatures, not just the surface. This is critical for pool fires as the radiation received from the surrounding environment effect the burning rate.

To determine the appropriate absorption coefficient for heptane for the application of the liquid pyrolysis model within FDS 5 the experimental data for the single pan free burning pool fire is to be used as the base reference case. FDS 5 is then used to model

the free burning pool fire with different absorption coefficients in order to determine the correct value for application for modelling of the compartment fire experiments.

The liquid pool fire is modelled by specifying its relevant properties via the MATL namelist group and it is the inclusion of a boiling temperature that defines the use of the liquid pyrolysis model. Typical input for the free burning case is detailed below;

```
&REAC ID='HEPTANE'
     FYI='Heptane, C_7 H_16'
     HEAT_OF_COMBUSTION = 44500.
     C=7.
     H=16.
     CO_YIELD=0.006
     SOOT_YIELD=0.015 /

&MATL ID='HEPTANE'
     EMISSIVITY = 1.0
     NU_FUEL =0.97
     HEAT_OF_REACTION=315.
     CONDUCTIVITY=0.8
     SPECIFIC_HEAT= 2.00
     DENSITY= 711.
     ABSORPTION_COEFFICIENT = 40.
     BOILING_TEMPERATURE=98. /

&SURF ID='HEPTANE POOL'
     MATL_ID = 'HEPTANE','KAOWOOL VB'
     THICKNESS=2.500,0.020
     TMP_INNER = 18. /

&MATL ID='KAOWOOL VB'
     SPECIFIC_HEAT=1.090
     DENSITY=250.
     CONDUCTIVITY_RAMP = 'k_ramp' /
&RAMP ID='k_ramp',T= 400.0, F=0.090 /
&RAMP ID='k_ramp',T= 600.0, F=0.150 /
&RAMP ID='k_ramp',T= 800.0, F=0.155 /
&RAMP ID='k_ramp',T=1000.0, F=0.195 /

&SURF ID='KAOWOOL'
     MATL_ID='KAOWOOL VB'
     THICKNESS=0.020
     BACKING='EXPOSED'/

&OBST  XB=0.4,0.6,  0.4,0.6,  0.0,0.05,  SURF_IDS='HEPTANE  POOL',  'KAOWOOL',
'KAOWOOL' / HEPTANE PAN
```

Results from the modelling are shown in Figure 8.3 and have been time averaged over 30 seconds to enable clarity.

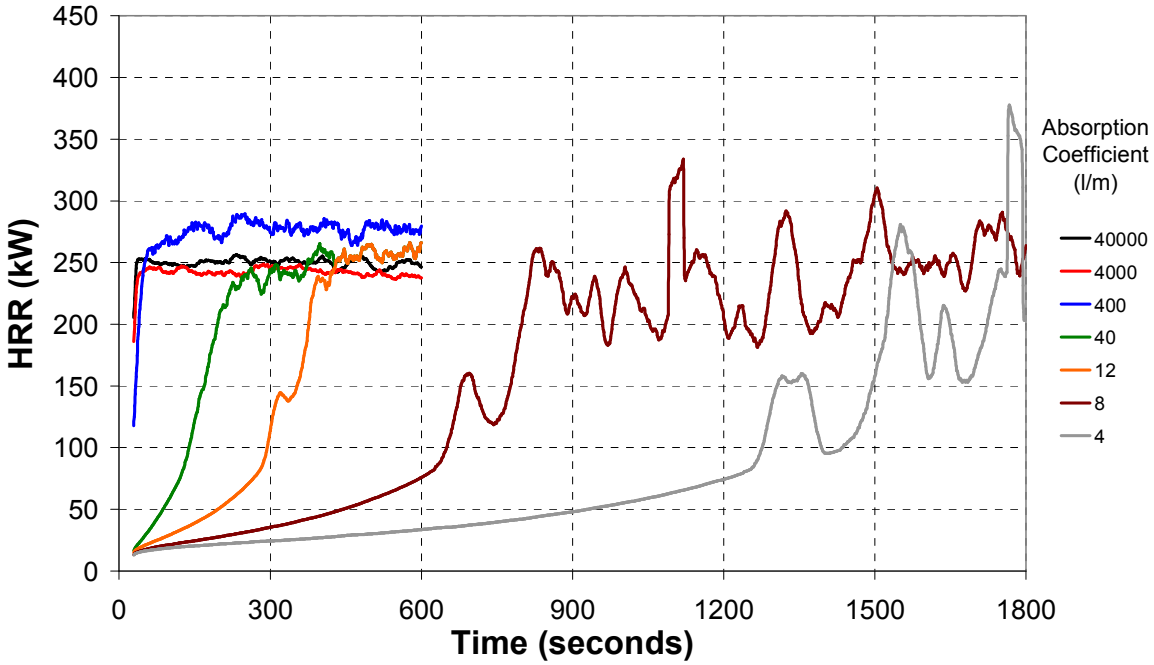

Figure 8.3: Heat Release Rate profiles for free burning pool fires as a function of the absorption coefficient.

It is noted that whilst the absorption coefficient has an effect upon the behaviour of the HRR of the pool fire this is only limited to a delay in the growth. The HRR achieved by the pool fire is of the order of 250kW which is well above that of 87kW obtained in the free burn experiments. Comparison by using the fuel source as a solid was also completed and had the same results as the pool fire.

8.3 Summary

From the modelling completed to date, it has been identified that further development is required for FDS 5 on the prediction of liquid pool fires. The current version of the model provides for liquid fuel and radiation predictions however the results indicate that these parts of the program are not currently able to model the complex situation provided in this experimental study.

8.4 References

1 McGrattan, K, Forney, G., "Fire Dynamics Simulator (Version 4) User's Guide" NIST Special Publication 1019, National Institute of Standards and Technology, U.S. Department of Commerce, Gaithersburg, March 2006.

2 McGrattan, K.B, Klein, B., Hostikka, S., Floyd, J. "Fire Dynamics Simulator (Version 5) Users Guide" NIST Special Publication 1019-5, National Institute of Standards and Technology, U.S. Department of Commerce, Gaithersburg, February 2008

3 McGrattan, K.B, Hostikka, S., Floyd, J., Baum, H., Rehm, R. "Fire Dynamics Simulator (Version 5) Technical Reference Guide" NIST Special Publication 1018-5, National Institute of Standards and Technology, U.S. Department of Commerce, Gaithersburg, January 2008

Chapter 9: Conclusions and Recommendations

This chapter summarises and concludes the experimental compartment fire study. The conclusions and recommendations from the aim of the research are presented and divided into three categories; Compartment Fire Behaviour, Equivalence Ratio 'Phi' Meter and Computer Modelling.

9.1 General

Thirty four fire experiments were conducted in a reduced scale compartment (½ height) with dimensions of 3.6m long by 2.4m wide by 1.2m high using five typical ventilation geometries (fully open, soffit, door, window and small window). Heptane pool fires were used, located in permutations of three evenly distributed locations within the compartment (rear, centre and front) as well as larger equivalent area pans located only in the centre.

It is noted that this experimental work studied half scale residential compartment fires and encountered conditions in which temperatures exceeded 1200°C. In conjunction with the long duration of the experiments, compartment fire temperatures of this magnitude cause the physical boundaries of the compartment to become unstable and material failure was imminent. For the enclosure used in this experimental study, the windows and internal lining materials were subject to either partial or total failure. In the process of investigating compartment fire conditions, the behavioural properties of various building materials and their limitations showed testament to the difficulties that arise when attempting compartment fire experiments.

9.2 Compartment Fire Behaviour

The results of this experimental study were found to have significant implications for Fire Safety Engineering assumptions and these are described below.

9.2.1 Effect of Ventilation on Temperatures and Compartment Behaviour

The experimental study has confirmed many of the previously identified compartment fire behavioural aspects such as pre-flashover and post flashover temperatures. In particular the following is noted:

- Experiments with the fully open and soffit ventilation openings exhibit pre-flashover compartment behaviour with distinct upper and lower layer temperature profiles.
- Door and window ventilation opening experiments also generally provide a two zone pre-flashover profile however tend toward a single zone post-flashover assumption.
- Small window opening experiments were under-ventilated with uniform conditions consistent with the single zone well stirred post-flashover assumption.
- The single pan fires with the door and window ventilation geometries exhibit a transitional phase between a pre-flashover fire and a post-flashover fire with the regime being dependent upon the location of the fire. As the single pan location is moved progressively from the front to the rear of the compartment the compartment behaviour changes from a pre-flashover fire to a post-flashover fire. This is as a result of the increase in compartment effects on the fire located at the rear of the compartment.

9.2.2 Effect of Ventilation on the Shape of Fire Plume

The impact of the ventilation opening on compartment behaviour identified the following:

- The magnitude of incoming ventilation velocities range from 0.45m/s to 0.62m/s and induce a leaning of the fire plume. The shape of the flame is greatly impacted by the velocity through the vent and can be pushed over by the incoming airflow such that the flame is in contact with the floor on the leeward side of the pan.
- The incoming vent velocity flows can have an impact upon the heat release rate. In some cases when the fire is located near the vent opening the incoming air can actually reduce the heat release rate below the free-burning heat release rate. This is

due to the flame leaning over to near horizontal and reducing the radiation feedback from the fire plume to the surface of the pool fire.

- An assumption that a fire located away from the wall boundaries will always behave like an asymmetric plume is not valid for small compartments in which conditions reaching flashover can occur. Vent velocities into a compartment can drive the fire plume into the adjacent wall reducing entrainment and behaves like a fire located adjacent to the wall.

9.2.3 Effect of Multiple Fires Compared with a Single Fire

The considered assumption that a single centrally located fire is considered the credible design fire scenario was investigated and the following conclusions noted:

- The comparison of multiple fires compared to a single fire located in the centre of the room shows that the assumption that a fire located in the centre of the room can be considered the 'credible design fire scenario'. However this is valid only for well ventilated pre-flashover compartment fires and not to under-ventilated post-flashover compartment fires.
- When comparing compartment fire behaviour, the fuel source (pan) size is not as significant as the location of the fuel source. The effect of a fire near the vent opening has been shown to have a significant impact on compartment fire behaviour. Whilst a larger sized centrally located pan provides a more optically thick profile than that of multiple small pans of equivalent area, the additional radiative feedback to the fuel surface by a fire located near the vent opening can provide a heat release rate greater than a larger equivalent area centrally located fire. In this instance the mass loss rate of the front pan is at least equivalent to that of the larger centrally located pan. The results have shown that:
    - The heat release rate of two individual pans can be 71% greater than that of the x2 equivalent area pan located in the centre of the room.
    - The heat release rate of three individual pans is greater than that of the x3 equivalent area pan located in the centre of the room by 90%.

9.2.4 Effect of Pan Size

When considering the effect of pan size on a fire in the centre of a compartment the following compartment behaviour is noted:

- When a compartment is well ventilated there is little effect from the compartment environment on a small pan. As the pan size increases the compartment effects become more pronounced. Large pool fires have a more optically thick profile and flame heights directly impinge upon the ceiling of the compartment, which increases the compartment temperatures more rapidly than that for smaller fires. The radiative feedback to the pan subsequently increases as does the heat release rate.
- When a compartment is under-ventilated, the post-flashover combustion behaviour is ventilation limited. Although the compartment temperatures are higher for the larger pans sizes, the ventilation limited heat release rates are similar.

9.2.5 Effect of Fire Location

This research has identified that heat release rate of compartment pool fires is a function of the fire location and can be significantly greater than the predicted free burning rate and greater than for a large centrally located fire. The following compartment fire behaviour aspects dependent upon the location of the fuel source have been identified.

- Depending upon the degree of ventilation into an enclosure a transitional phase from a pre-flashover fire to a post-flashover fire can occur when the pan location is moved from the front to the rear of the compartment.
- For well ventilated compartment fire the MLR is similar to that for the free burning fire.
- Under-ventilated post-flashover compartment fires provide a combustion zone within the vent which also extends into the compartment and surrounds a pan located at the front of the room. This combustion zone provides significant radiation enhancement to the front pan and can increase the mass loss rate to 3.7 times the free burning rate. At the same time the high temperatures continue to volatise the fuel in other locations. This behaviour increases the production of un-pyrolysed products and subsequently the heat release rate. A pan is located at a distance from this vent combustion zone and is not affected to the same extent by the radiation enhancement. This means that a large single pan located in the centre of a room does not provide the highest HRR scenario. Multiple pans distributed in the compartment with an aggregate pan size of less than that of a large centrally located fire can even provide a 73% greater heat release rate. In the experiments with the small window opening, the single large x3 pan located in the centre of the

room had a heat release rate lower than that of two small pans (a combined area of $^{2}/_{3}$ of the x3 pan).

- An assumption that a fire located away from the wall boundaries will always behave like an axisymetric plume is not valid for small compartments in which conditions reaching flashover can occur. Vent velocities into a compartment can drive the fire plume into the adjacent wall and impact upon the flame behaviour.

9.2.6 Design Assumptions

The assumption that the credible design fire scenario is a centrally located non-wall bounded was investigated with the following recommendations made:

- The assumption that a fire located in the centre of the room provides the highest heat release rate is valid for well ventilated pre-flashover compartment fires. Whilst for most designers the design of a building based upon the timeline prior to flashover the general concept of a centrally located fire is considered appropriate.
- The assumption that a fire located in the centre of the room provides the highest heat release rate is not valid for under-ventilated post-flashover compartment fires.

9.2.7 Recommendations and Future Work

This thesis has revealed a number of important of considerations for the improvement in understanding into compartment behaviour. This can impact upon the application of fire safety assumptions when applied to computer fire models.

The most significant finding is the impact of the vent located fuel source and its compartment enhancement effect. Therefore further research is recommended to determine the flow characterises surrounding a fire close to the vent opening. It is therefore recommend that further research be undertaken to determine the impact that the size of a fire close to the vent has upon the compartment behaviour. The incoming vent velocity has also be identified as increasing around a fire located close to the vent opening and detailed study is recommended to investigate this velocity flow regime.

As compartment fire severity is fuel location dependent and this work focused on one dimensional pool locations, further research is also recommended to investigate multiple fire location including along sidewalls and in corners.

9.3 Equivalence Ratio 'Phi' Meter

9.3.1 Enhanced Design

As part of the experimental compartment pool fire study an enhanced Equivalence Ratio apparatus, 'Phi' meter, was successfully designed and developed to aid in the analysis of the experimental results by measuring concentrations of combustion gases at a single point in the vent opening. The Phi meter was developed to sample continuously and measure a time dependent equivalence ratio based upon the oxygen consumption technique. The measurement of the equivalence ratio helps to categorise the combustion behaviour of a compartment fire. The enhanced phi meter differed from those previously developed as it not only measured the oxygen concentration but included CO_2 and CO. The analysing of CO_2 and CO had the advantage of not requiring the removal of CO_2 by chemical means from the sample flow and the measurement of zero CO also provided confirmation that the entire CO was combusted in the furnace.

9.3.2 Revised Equations

The equations for calculating the equivalence ratio were a revised formulation derived from the existing theory to allow for the measurement of CO_2 and CO in addition to O_2. The experimental results presented for the calibration of the phi meter provide very good agreement with the theoretically calculated values for small scale propane and methane gas streams. The phi meter was used as a measurement tool in the real fire experiments as part of this study to provide a compartment equivalence ratio. The many results were plotted and were found to provide good agreement with the equivalence ratio calculated from total compartment mass loss rates.

9.3.3 Experimental Results

When used to categorise compartment fire behaviour the measurements from the phi meter was found to accurately indicate the onset of flashover, which is considered when the equivalence ratio exceeds a value of 1. The results indicate that the equivalence ratios measured for heptane pool fires range from 0.1 for oxygen rich conditions and 2.3 for fuel rich conditions. The time dependent results for each of the compartments experiments indicated good sensitivity in the results.

9.3.4 Recommendations and Future Work

The following are suggested as improvements and for future development of the phi meter.

- Further use of the phi meter is required over a wider range of equivalence ratio values in particular from 1.5 to 3.0.
- Given the measurement of CO, the phi meter apparatus could be configured without the use of a catalyst. The catalyst was provided to ensure complete combustion given the proposed high carbon environment for heptane pool fires. This was generally successful; however there were a number of blockages in the some experiments as a result of both a blockage in the sample line inlet and also within the furnace tube.
- Although the phi meter was developed to sample continuously and measure the time-dependent compartment equivalence ratio, the experiments reached a quasi-steady state equivalence ratio at the end of the experiments. Due to difficulties with blockages of the sample line inlet and furnace tube, it is expected that selective sampling may also be beneficial to limit blockages.
- If used with fuel producing high soot content then air pulse cleaning of the sample line and inlet is suggested during testing.
- The sampling port could be revised to use a probe with equally spaced sampling holes to thereby remove any special variation in the vent opening.
- The phi meter is developed with a metal tube in the furnace and not a quartz tube.

9.4 Computer Modelling

The results of the FDS modelling have indicated that the use of the model in its current form can not be applied to predict pool fires. Although the model provides both liquid fuel and radiation predictions, the model did not accurately predict even the simplest geometry of a pool fire burning in the open air. Subsequently the simulation of the compartment fire experiments as presented in this work is outside the capability of the model and future development work is recommended to improve both the pool behaviour and radiative aspects of the model.